THÈSE

En vue de l'obtention du

DOCTORAT DE L'UNIVERSITÉ DE TOULOUSE

Délivré par
L'université Toulouse III - Paul Sabatier

Discipline ou spécialité :
Chimie Moléculaire

Présentée et soutenue par *Juan Manuel GARCIA*

Le *17 octobre 2011*

Diallylphosphines and phosphine-stabilized germylenes as versatile ligands for transition metal complexes

---

JURY

Dr. **J.-M. Sotiropoulos**	Université de Pau	*Rapporteur*
Dr. **R. Dorta**	Université Simon Bolivar	*Rapporteur*
Pr. **M. Gomez**	Université Paul Sabatier	
Dr. **A. Arce**	IVIC - Caracas	
Dr. **A. Briceño**	IVIC – Caracas	
Dr. **E. Ocando**	IVIC - Caracas	
Dr. **A. Baceiredo**	CNRS, Université Paul Sabatier	

Ecole doctorale : *Ecole Doctorale Sciences de la matière*

Unités de recherche : *LHFA (Toulouse) – LFQO-IVIC (Caracas)*

Directeurs de Thèse : *Edgar Ocando*, *Antoine Baceiredo, Tsuyoshi Kato*

A mis padres y hermanos

A mi amor Yennifer

Acknowledgements

A mi tutor Dr. Edgar Ocando por darme la oportunidad de trabajar en su laboratorio y por su colaboración en la conducción de esta tesis de grado. A todos los amigos que durante estos años han formado parte del LFQO. Un especial agradecimiento a todos los buenos amigos del centro de Química (IVIC), Maria Cristina Goite, Yomaira Otero, Deisy Peña, Yokoy León, Lenin Díaz, María Liliana Ospino, Lizaira Bello, Iruany Boyer, Vanessa Hernan, Barbara Rodríguez y James Posada, por todos los buenos momentos compartidos.

Al Dr. Antoine Baceiredo y Dr. Tsuyoshi Kato por darme la confianza y la oportunidad de trabajar en su laboratorio, por su gran apoyo en el desarrollo de esta tesis de grado. Un especial agradecimiento a todos los amigos del LHFA por todos esos buenos momentos que compartimos juntos.

Al Instituto Venezolano de Investigaciones Científicas, por todo el apoyo financiero e institucional prestado. Al FONACIT por el soporte económico brindado a través de la Beca Misión Ciencias y del proyecto G-2005000433, G-2005000447. Al programa de cooperación PCP y al CNRS, por todo el apoyo financiamiento y institucional prestado para mi estancia en Toulouse/Francia.

Al Laboratorio Nacional de Resonancia Magnética Nuclear (RMN), en especial al Sr. Alberto Fuentes, Lic. Liz Cubillan y MSc. Ligia Llovera, por ser personas altamente serviciales que siempre me ayudaron en esta ardua tarea.

A mis buenos amigos Magaly Henríquez, Gerardo Velásquez, José Biomorgi, Rawad Tadmouri, Aracelys Marcano, Ninoska Martinez, Dayana Martín por su gran apoyo en los momentos difíciles, por todos esos buenos momentos que compartimos durante mi estancia en Toulouse.

Por último, esta tesis no hubiese sido posible sin el apoyo incondicional de mis padres y hermanos, gracias por ayudarme y animarme a lograr mis metas. Igualmente, a Yennifer Hill por ser mi gran apoyo en estos últimos años, por ser la compañera incondicional, por estar siempre a mi lado en los momentos de felicidad y tristeza.

Abstract

Ligand hybrid design is becoming an increasingly important area of the synthetic activity in organometallic chemistry. The coordination chemistry of diallylphosphines and phosphine-stabilized germylenes has been studied in this thesis. In particular, phosphine-stabilized germylenes have not only been studied by its potential use as ligands for transition metals, but also as possible synthetic tools in organic chemistry.

Diallylphosphine behave as bidentate ligands to stabilize cationic rhodium species of type $[Rh(COD)\{\eta^3(P,C,C)RP(CH_2CH{=}CH_2)_2\}][BF_4]$ [R= $^{i}Pr_2N$, ^{t}Bu and Ph]. Hemilabile properties of diallylphosphine ligands have been demonstrated by ligand exchange reactions. In solution, a dynamic equilibrium of exchange between the two allylic double bonds was detected by low temperature NMR analysis. In the same way, the reversible displacement of coordinated allylic double bond by acetonitrile could be observed. Theoretical calculations have been performed to explain the experimental results for the order of reactivity on removing the acetonitrile under vacuum.

Germylenes stabilized by coordination of a phosphine ligand have been synthesized and fully characterized. Reactivity studies showed that phosphine-stabilized germylenes are unreactive toward unsaturated compounds, such as: alkyne, alkene and carbonyl derivatives, but reactive toward 2,3-dimethylbutadiene. The reactivity of phosphonium-stabilized germylenes toward transition metal complexes have been studied by reaction with the dimer complex $[Rh_2(\mu\text{-}Cl_2)(COD)_2]$**,** demonstrating that phosphine-stabilized germylenes are useful ligands with high potential in organometallic chemistry. The first isolable germanium analogue of alkynes, known as germyne, stabilized by coordination of a phosphine ligand has been synthesized and fully characterized. Synthesized germynes rearrange at RT affording a phosphaalkene and a new stable *N*-heterocyclic germylene.

Keywords: Hybrid ligands, hemilabile properties, phosphine-stabilized germylene, germyne, coordination chemistry.

Contents

Abbreviations and Symbols

COD	1,5-Cyclooctadiene
MeCN	Acetonitrile
Å	Angstrom
BCP	Bond critical point
br	Broad
cm	Centimeter
δ	Chemical shift in ppm
J	Coupling constant
Cy	Cyclohexane
COE	Cyclooctene
deg	Degree
°C	Degree Celsius
K	Degree Kelvin
DAP	Diacetylpyridine
Et_2O	Diethyl ether
$^{i}Pr_2N$	di-isopropylamine
DIPP	Diisopropylethylenediamine-phosphine
d	Doublet
v	Frequency in cm^{-1}
g	Grams
Hz	Hertz
h	Hours
^{i}Pr	*iso*-propyl
MHz	Megahertz
mp	Melting point
OMe	Methoxy
Me	Methyl
MAO	Methylaluminoxane
μL	Microliter
mg	Milligrams
mL	Milliliter
mmol	Millimol
min	Minutes
m	Multiplet
nm	Nanometer
^{n}Bu	*n*-Butyl
NMR	Nuclear magnetic resonance
O-Tol	*orto*-toluene
ppm	Part per million
OPh	Phenoxy
Ph	Phenyl
RT	Room temperature
s	Singlet
IR	Spectroscopy infrared
^{t}Bu	*tert*-Butyl
THF	Tetrahydrofuran

Introduction

The organometallic chemistry plays an increasingly important role in the modern organic synthesis. In effect, the search of new, faster, more efficient, selective and environmentally friendly synthetic methods has led to growing development of the homogeneous catalysis, in which, the synthesis of catalysts capable of inducing chemo, stereo and enantio-selectivity in the catalytic reactions comprises an important area. In this way, the design of hybrid ligands, characterized for containing at least two different chemical functionalities, capable to exert a subtle control on the metal center, modulating the nature of the catalytically active species, has been subject of study for many researchers.[1-10]

In this sense, the synthesis of functionalized phosphine has constituted one of the main axes of research in our laboratory (LFQO-IVIC) and a particular interest have been focused on the diallylphosphine ligands, due its potential hemilabile properties, which are considered of great important in the homogenous catalysis.

Complementing the study of the interaction of polydentate phosphine ligands on metal centers and the modulation of this influence, new ligands, as phosphine-stabilized germylene derivatives, have been synthesized. These heavier homologues of carbenes have attracted our interest not only as possible synthetic tools in organic chemistry but also for their potential use as ligands for transition metals. The interaction of both families of potential bidentate ligands with some rhodium complexes has been started.

In this manuscript, we report results concerning the study of the ligating properties of the diallylphosphine ligands, as well as, the synthesis and reactivity of germanium(II) species stabilized by coordination of a phosphine ligand. This research work demonstrates that diallylphosphines and phosphine-stabilized germylenes are versatile ligands with high potential in organometallic chemistry.

In the first chapter, a bibliographic review concerning definition of hybrid ligands and, more specifically, the coordination behavior of the allylphosphine as ligands is presented. Chapters 2 ad 3 will concern the study of coordination chemistry of diallylphosphine ligand, as well as, the evaluation of its properties hemilabile.

Chapter 4 refers to the synthesis and reactivity of germylene derivatives stabilized by a ligand phosphine and, in chapter 5, the study of the ligating properties of the phosphine-stabilized germylenes is presented.

Owing the growing interest that has aroused the germanium compounds analogue of alkyne, the last chapter is dedicated to the synthesis of germynes stabilized by coordination of a phosphine ligand.

Chapter I

Hemilability of hybrid ligands and the coordination chemistry of allylphosphine ligands

I.1. Hybrid Ligands

Hybrid ligands are polydentate ligands that contain at least two different types of chemical functionality capable of bonding to metal centers (Figure I.1).[8,9]

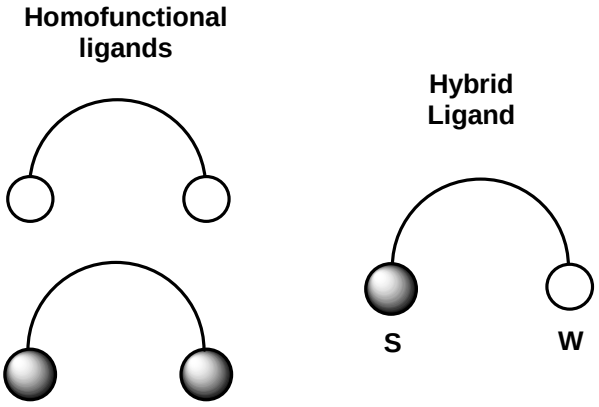

Figure I.1. A Hybrid ligand contains two chemically different donor functions.

These functionalities are often very different from each other to increase the difference in the coordination mode with the metal center and therefore their chemoselectivity (Figure I.2). In turn, these features influence coordination/reactivity of other ligands coordinated to the metal, in particular those in the *trans* position.[8,10]

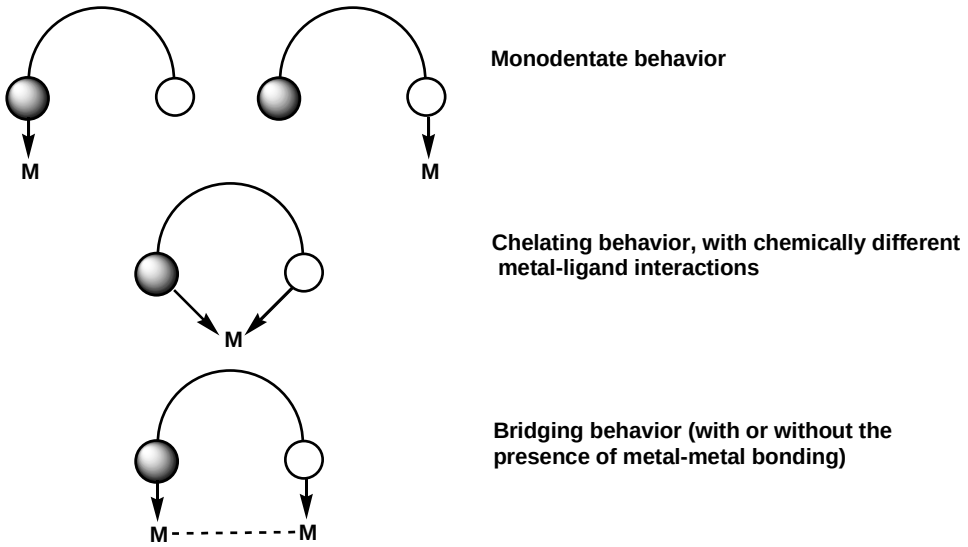

Figure I.2. Coordination modes of hybrid ligands.

I.2. Hemilability

The term "hemilabile" was introduced by J. C. Jeffrey and T. B. Rauchfuss [11] about 25 years ago, but the phenomenon itself had been observed earlier by P. Braunstein [12]. Hybrid ligands with hemilabile character have one group (**S**) bound strongly to metal center while other group (**W**) is weakly bonding and therefore can be easily displaced by coordinating ligands or molecules of solvent (**L**), remaining available for recoordination to the metal center (Figure I.3).[1,3,8-10,13] Hemilability was first investigated in mononuclear complexes, but this concept can be easily extended to dinuclear complexes [14] and metal clusters,[15,16] where the labile coordination site does not need to be at the metal attached by strong donor group (**S**), but could be at an adjacent metal (Figure I.3).[10]

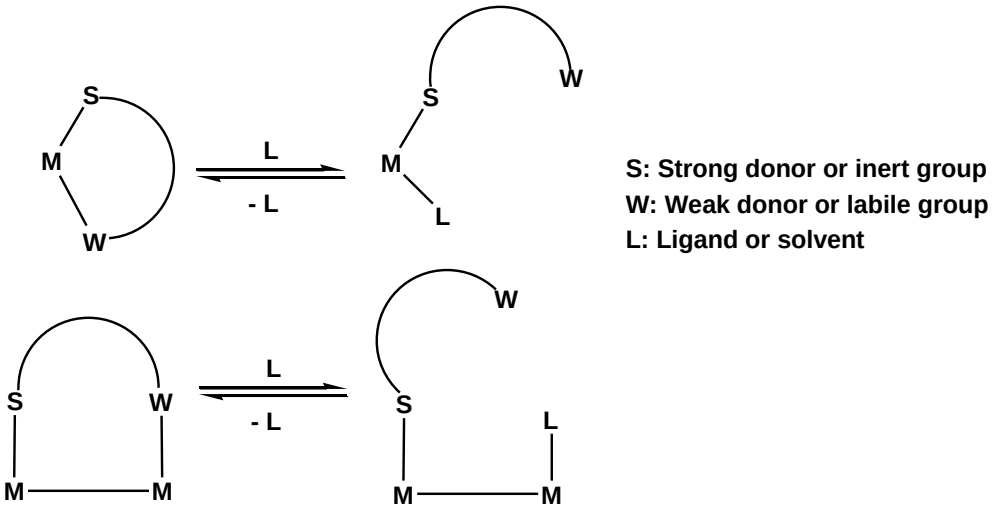

Figure I.3. Hemilability of hybrid ligands.

The hemilabile nature of hybrid ligands can be observed in several ways. The hemilability of a chelate ligand can be observed as a fluxional process that involves the dissociation and recoordination of the weakly bonding moiety by intramolecular ligand exchange processes. The exchange involves a transient species which is either coordinatively unsaturated if formed from a dissociative pathway or saturated by solvent molecules. The exchange process can involve two or more hemilabile ligands on a single transition metal center. In addition, there are examples in which complexes formed from hemilabile ligands that contain two or more weakly bonding groups per ligand undergo intermolecular ligand exchange reactions.

A second important feature that may arise from hemilability in the metal complex is the facility to undergo ligand interchange reactions that involve an equilibrium between weakly bonding groups of hemilabile ligand and external molecules, such as a monodentate ligands, a small molecules, or an organic substrates. The hemilabile character for a ligand is the reversibility of the formation/displacement of the **W→M** interaction. The irreversibility opening or closing of a chelate with or without participation of an external reagent is considered a sign of reactivity, but not of hemilability (Figure I.4).

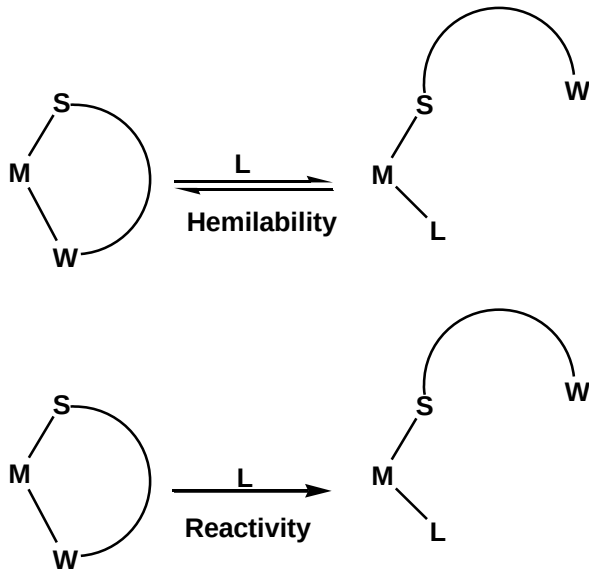

Figure I.4. Different between hemilability and reactivity.

I.3. Types of hemilability

The hemilabile behavior has been classified according to the circumstances that lead to breaking of the **W→M** interaction in a mononuclear, dinuclear or cluster complex. Although several examples of dinuclear [14] and metal clusters complexes [15,16] have been published, herein we will discuss those related to mononuclear complexes.

I.3.1. Type (I) hemilability

This type corresponds to the spontaneous opening of the **S−W** chelate (Figure I.5). These situations are typically encountered with metal centers capable to change easily their coordination numbers: 3↔2 (d^{10}, ML_3/ML_2 complexes); 4↔3 (d^8, ML_4/ML_3 complexes); 5↔4 (d^8, ML_5/ML_4 complexes) and 6↔5 (d^6, ML_6/ML_5 complexes).

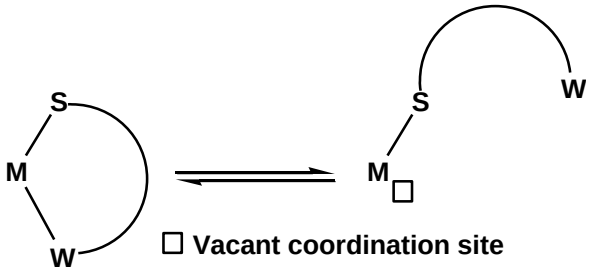

Figure I.5. Type (I) hemilability.

Examples of the reversible change in coordination number from 5 to 4 and 6 to 5 are shown in equations (1) and (2) respectively. In both case, the reversible dissociation of the weakly bonding group gives rise to a transient species coordinatively unsaturated.[17-19]

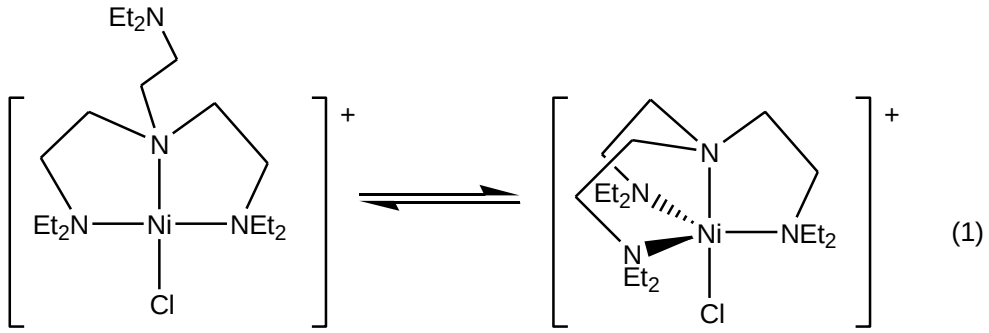

(1)

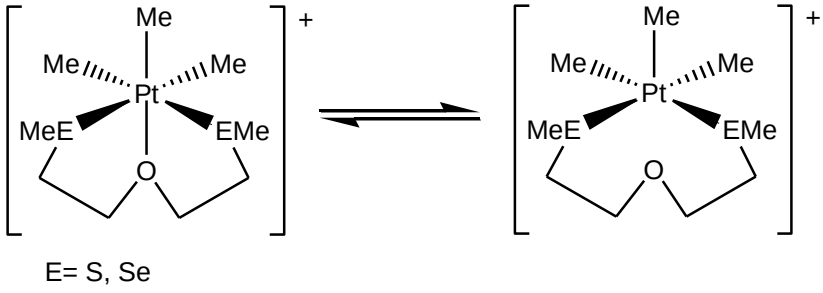

(2)

This hemilabile behavior also involves the intermolecular exchange between weakly bonding groups of ligands and coordinating counterions. The bicycloaminophosphorane ligand in the iron complex exhibits the intramolecular exchange of the bound amino group with a chloride counterion [20] to give rise equilibrium between a cationic and neutral iron complex (Eq. 3). Interestingly, complexes of bicycloaminophosphorane ligands have been found to be active toward styrene hydroformylation [21] and catalytic isomerization of 1-hexene.[22] Similarly, the hemilabile behavior of the phosphino-oxazoline ligand in palladium complex involves an intramolecular exchange between the oxazoline group and chloride

counter ion.[23] This behavior was clearly established by the presence in the IR spectrum in CH_2Cl_2 of the vibration bands assigned to coordinated and uncoordinated oxazoline moieties (Eq. 4).

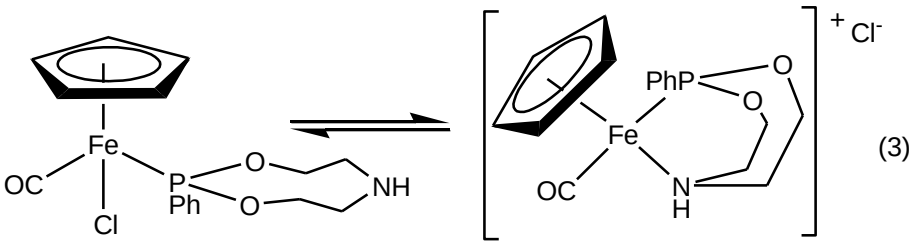

(3)

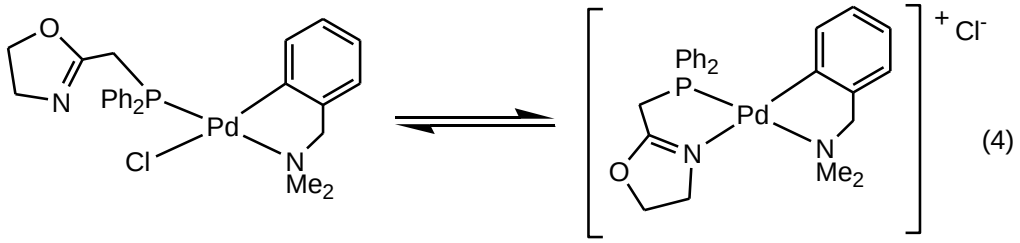

(4)

I.3.2. Type (II) hemilability

This hemilabile behavior is related to the intramolecular competition between two or more labile donor groups within the same ligand or not. It is possible to observe three situations (Figure I.6): Type IIa associated to intramolecular competition between two chemically identical labile donor groups within the same ligand. Type IIb corresponds to intramolecular competition between two chemically different labile donor groups within the same ligand and Type IIc involves two independent but chemically identical ligands in mutual intermolecular exchange owing to the lability the their **W** functions.

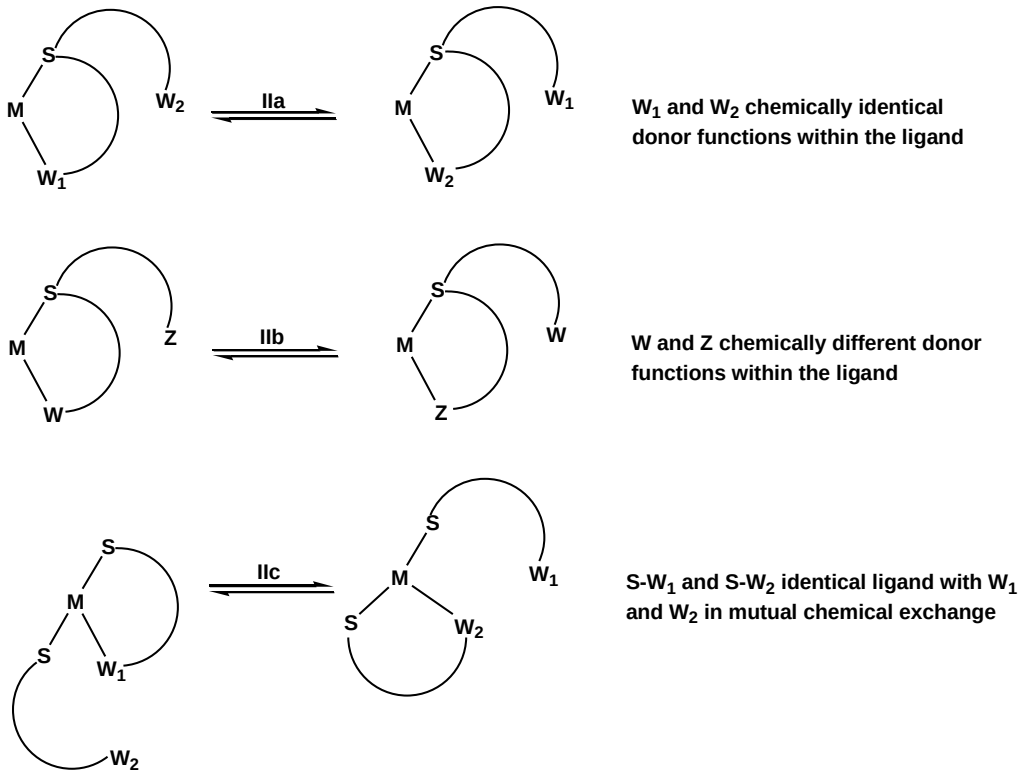

Figure I.6. Type (IIa-c) hemilability.

An example of this type of fluxional process is provided by the carbonyl groups exchange of the diacetylpyridine ligand on the tricarbonyl rhenium complex *fac*-[ReCl(CO)$_3$(DAP)] (Eq. 5). This dynamic behavior has been termed as a "tick-tock".[24] The same way, the fluxional behavior of the hemilabile bidentate ligand bis[*o*-(methylthio)phenyl]phosphine involves a tick-tock process in which the weakly bonding thioether groups exchange between bound and unbound state while strongly bonding phosphorus serves as an anchor (Eq. 6).[25]

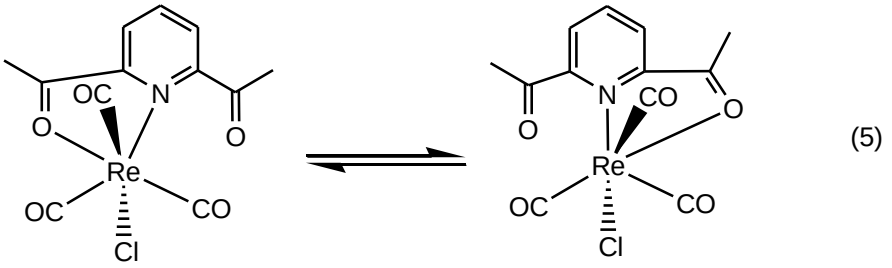

(5)

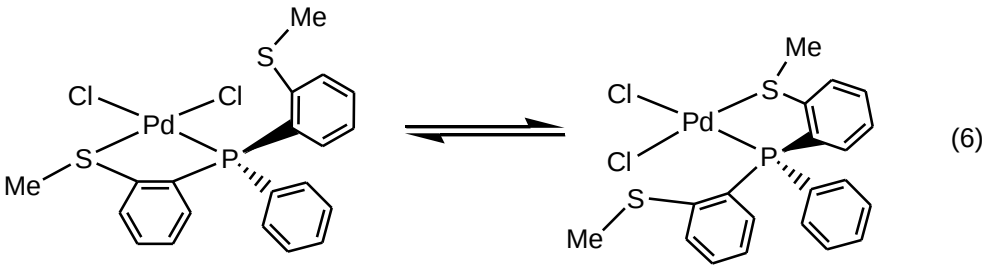

(6)

The reactions IIb in the figure I.6 have been less frequently studied or observed. Two examples are given in the equations (7) and (8), where the fluxional process involves an intramolecular exchange between two chemically different labile donor groups.[26-28] The hemilabile behavior of the phosphine-enolate ligand is manifested in the equilibrium between both isomers, which equilibrates slowly on the NMR time scale at -10 °C in CD_2Cl_2 (Eq. 8).[28]

Phosphine-amino [29] and phosphine-alcohol [30] ligands exhibit hemilabile characteristic on some transition metals through a fluxional ligand exchange process, which involves two independent but chemically identical ligands. The ligand $Ph_2PCH_2C(CH_3)_2OH$ in the platinum(II) complex show an exchange reaction involving a bound and a free alcohol moiety (Eq. 9).[30] This exchange reaction was detected by NMR spectroscopy, and was found to be fast on the NMR time scale in $CDCl_3$ at room temperature, but slow at -40°C.

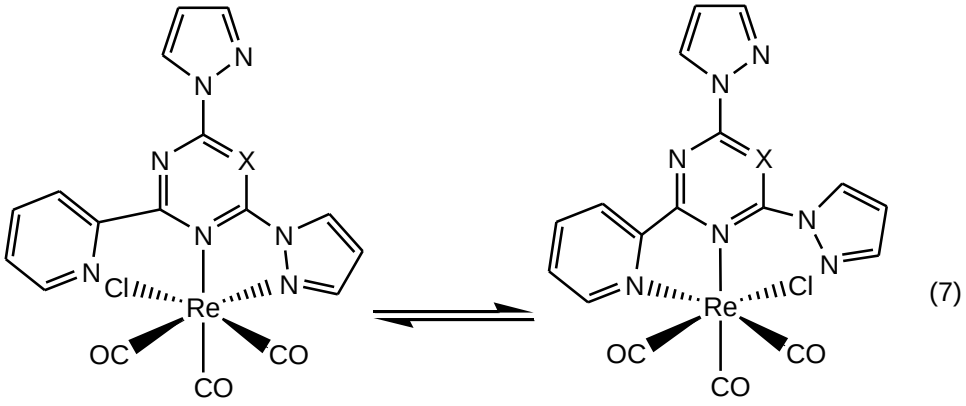

(7)

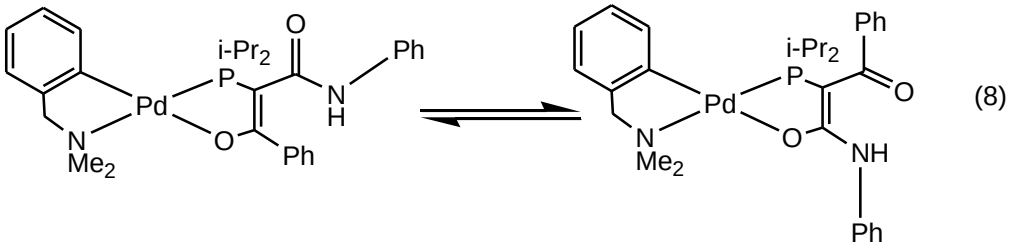

(8)

The ligand $^{i}Pr_2PCH_2(CH_2)_2NMe_2$ in the rhodium complex undergoes a fluxional ligand exchange reaction of bound and unbound amino group at room temperature in CD_2Cl_2 (Eq. 10).[29]

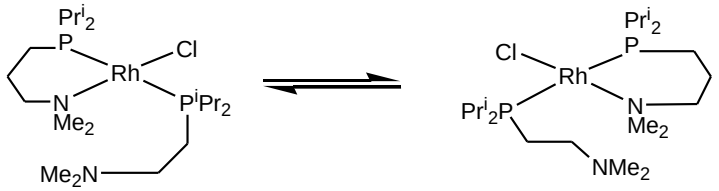

(9)

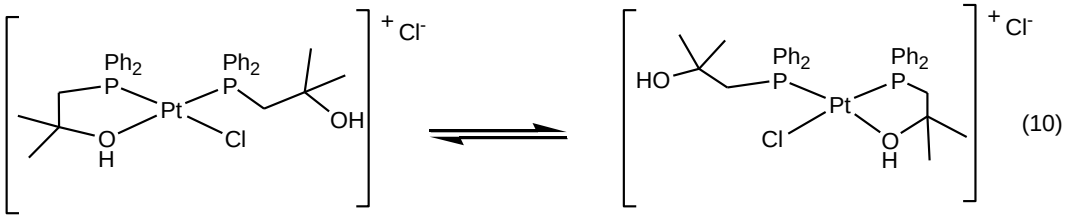

(10)

A recent example involving two P, N, O tridentate ligands in a cationic copper complex is show in equation (11).[31]

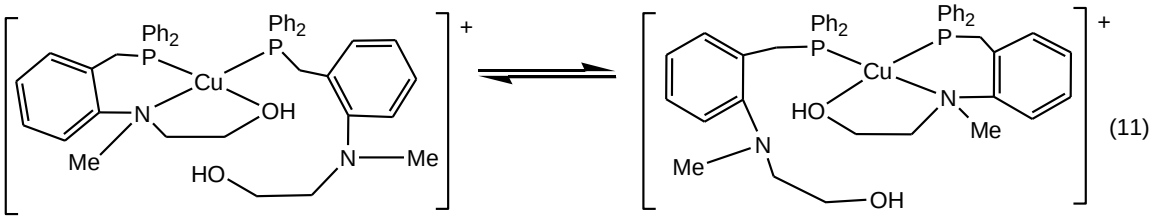

I.3.3. Type (III) hemilability

In these examples, an external reagent (**L**), which can be electrons in the case of redox reactions, is involved in the breaking of the ligand-metal bond (Figure I.7).

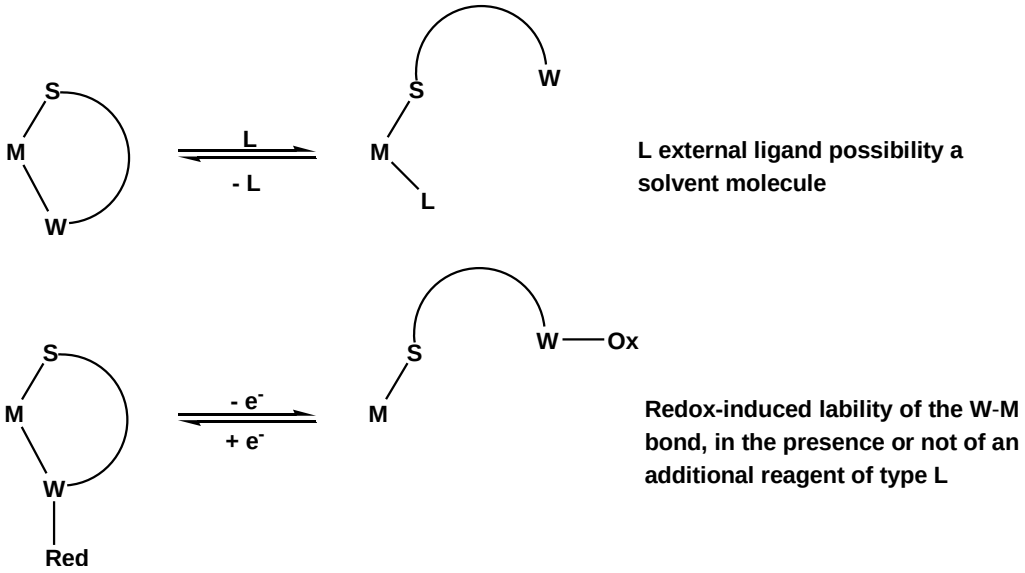

Figure I.7. Type (III) hemilability.

This category displays a range of possibilities depending on the nature of the reagent (**L)**. Systems where the reagent (**L**) is a small molecule, such as CO, which depending on its partial pressure can reversibly coordinate to the metal,[12,32,33] are illustrated in equations (12)-(13).

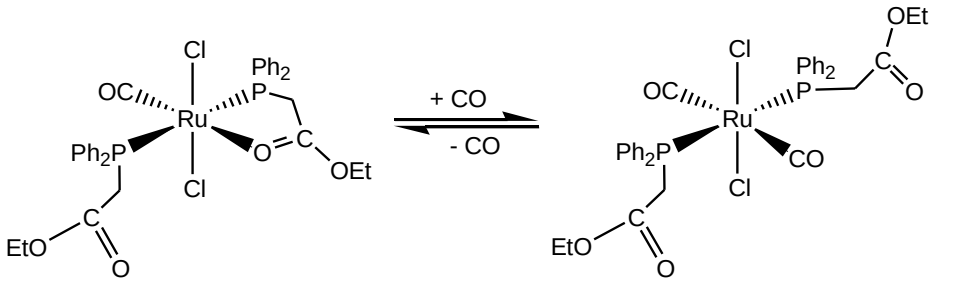

(12)

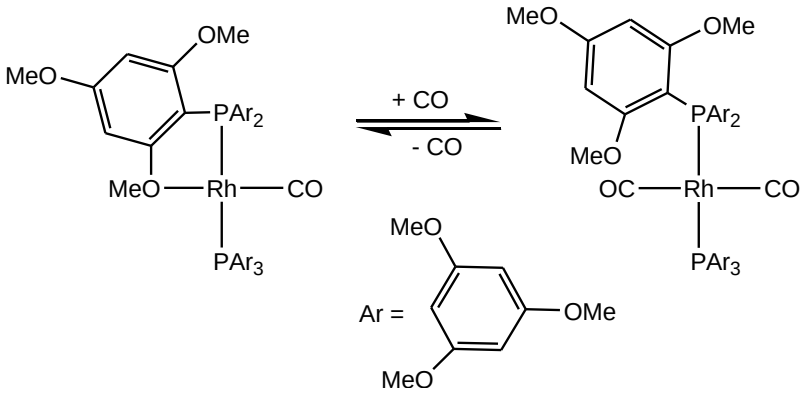

(13)

The rhodium complex in the equation (14) was used as a catalyst in methanol carbonylation.[33]

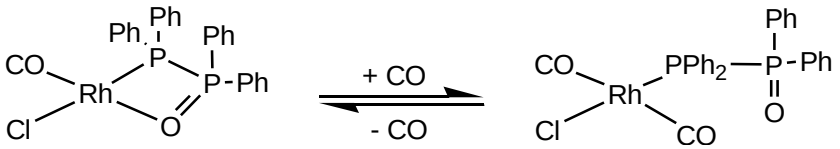

(14)

Similar hemilabile behavior has been observed with cyclopendienyl-amine [34] and cyclopendienyl-thiophene [35,36] ligands, where the amino and thiophene moieties are the weakly bonding groups to the metal center (Equations 15-18).

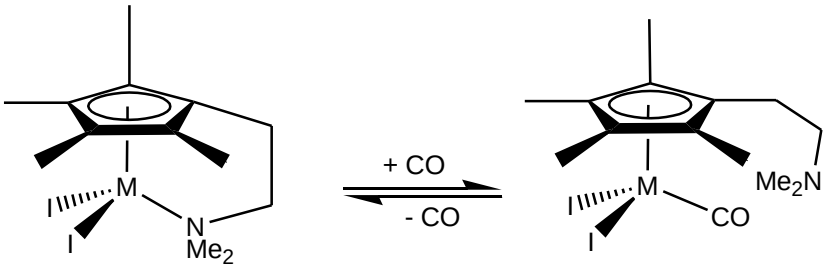

M = Co, Rh, Ir

(15)

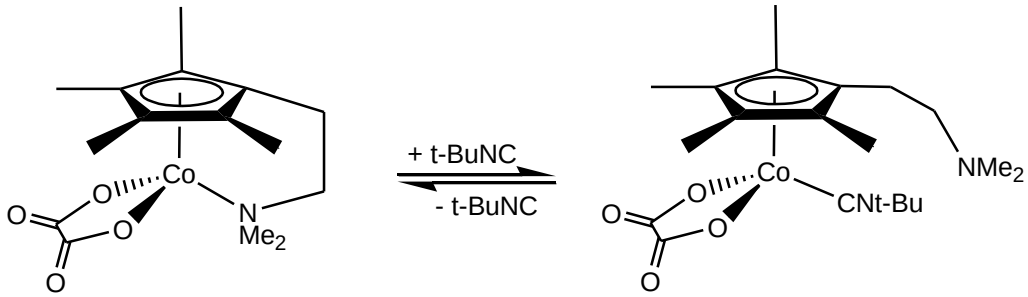

(16)

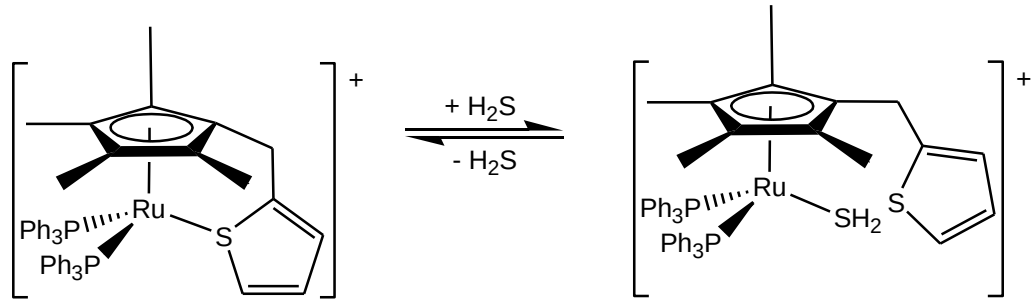

(17)

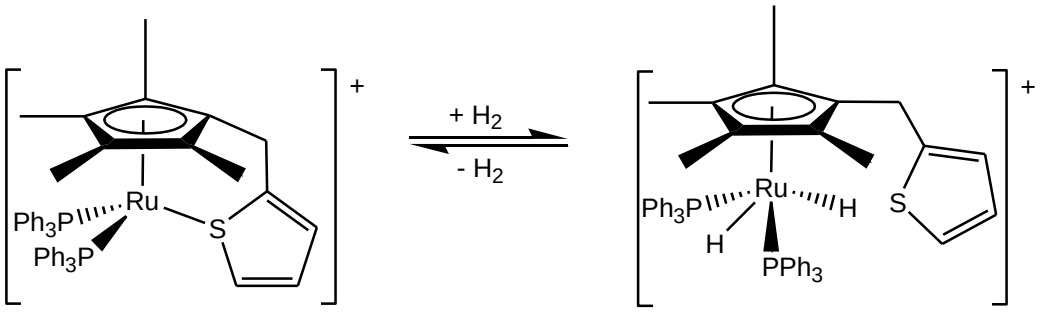

(18)

A solvent molecule may also displace the kinetically more labile **W→M** bond, as shown with the Cu (I) complexes in equation (19).[37] In the absence of a donor solvent, only hemilabile behavior of type (IIc) is observed.

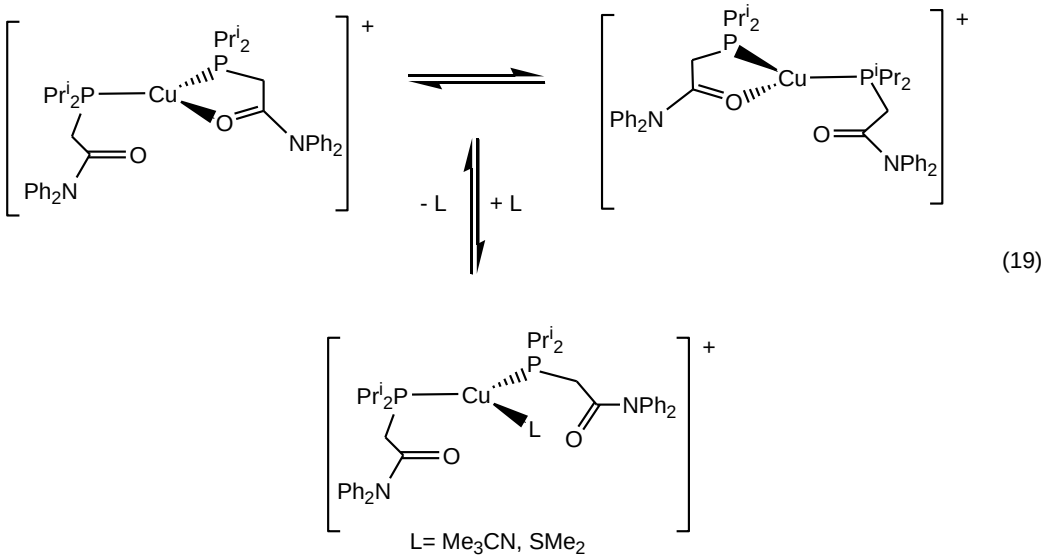

Redox-switchable hemilabile ligands comprise a special class of ligands. Like all hemilabile ligands are comprised of inert moieties (**S**) and labile moieties (**W**). The labile group is placed in direct electronic communication with a redox-active group, as is illustrated in Figure I.7. This communication allows the weakening of the Metal-W upon oxidation of a redox-active group through a combination of inductive and electronic effects. On occasions, oxidation of a redox-active group may lead to labilization of the (**W**) group favoring the coordination of an external reagent or a solvent molecule and under appropriate conditions this is a reversible process.

An example of the hemilabile behavior on redox switchable ligands is showed in equation (20). Electrochemical oxidation of the ferrocenyl groups adjacent to the ether moieties weakens the Rh-ether bonds in the rhodium complex, which induces a dimerization reaction to form a 36-electron η^6-arene-bridged, piano-stool dimer. This process can be reversed completely by electrochemically reducing the ferrocenium moieties.[38]

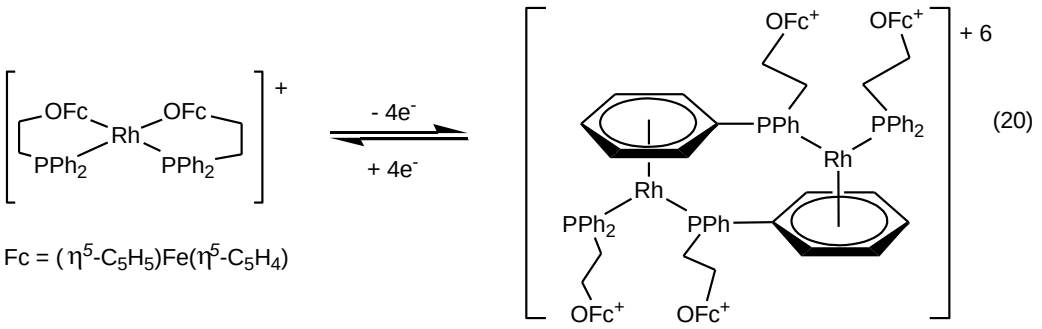

Potential applications of redox-switchable hemilabile ligands include the development of new catalysts, where the reactivity may be adjusted by the redox active centers, the preparation of electro-active films for metal complexation, and the synthesis of novel materials for molecule separation technologies.[9,39-40]

I.4. Coordination chemistry of allylphosphine ligands

Researchers have taken advantage of the weakly ligating ability of alkenes to prepare hemilabile phosphine-alkene ligands. There are many examples of phosphines with alkenes groups as substituent, where the hemilabile properties have been investigated by reaction of their complexes with small molecules.[9] Owing the hemilabile character potential of the diallylphosphine ligands, we have focused our interest on diallylphosphine ligands. These ligands contain a strongly bonding phosphine group (inert group) and two weakly coordinating alkene moieties (labile group). The bifunctional character may allow to these ligands reversibly create or occupy a vacant coordination sites on metal center, as typically observed in fluxional processes, or the reversible bonding of a small molecule. This feature has been shown to enhance both activity and selectivity in catalytic reactions. [1-7]

In this section, we present an overview about the coordination chemistry of the allylphosphine ligands. Herein, highlights of the synthesis, characterization, dynamic behavior, reactivity and applications of the allylphosphine ligands are provided.

The diallylphosphine ligands have been shown to be polydentate ligands to stabilize unsaturated coordinatively metal species. Ocando-Mavarez and coworkers [41] achieved to obtain a six-coordinate iridium complex (**2**) by reaction of four equivalents of diallylphosphine with one equivalent of dimer complex $[Ir(\mu\text{-}Cl)_2(COE)_4]$. It is derivative incorporating a five-membered metallocycle by C-H activation of one allyl moiety of the phosphine ligand (Scheme I.1).

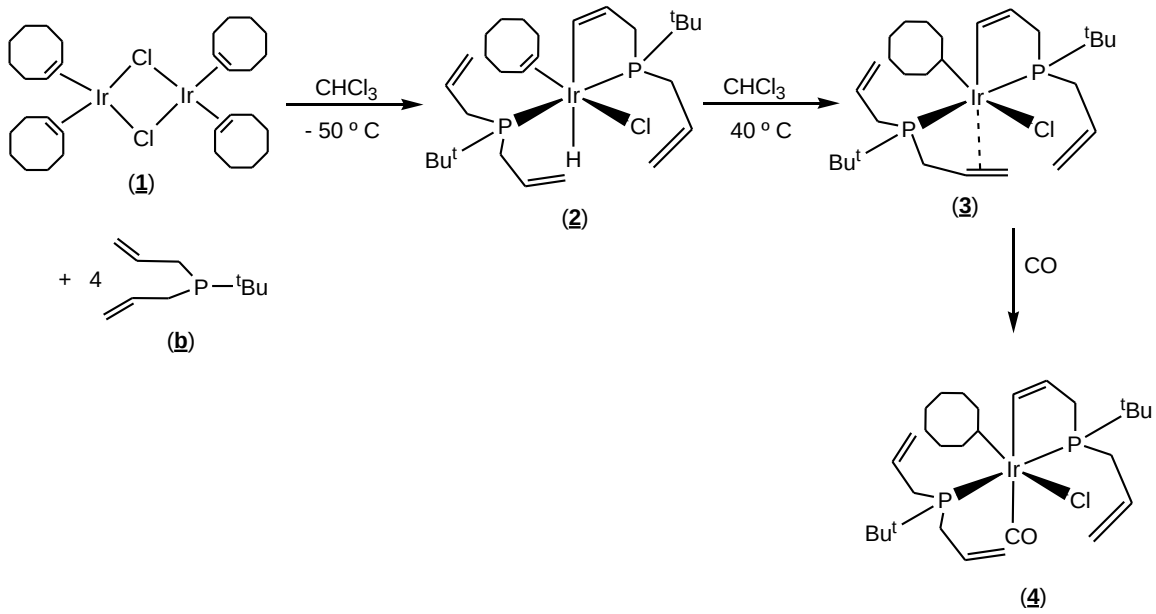

Scheme I.1. Synthesis and reactivity of the iridium complex (**3**).

This result can be compared with the reported reaction of di-t-butylallylphosphine with the same iridium dimer in which the two cyclooctene ligands were displaced and the sixth coordination site is occupied by another coordinating agent from the reaction medium (Scheme I.2).[42-43] When the reaction is carried out without another coordinating agent a five-coordinated metalated species is formed. It is certainly due to the steric hindrance of the two t-butyl groups.

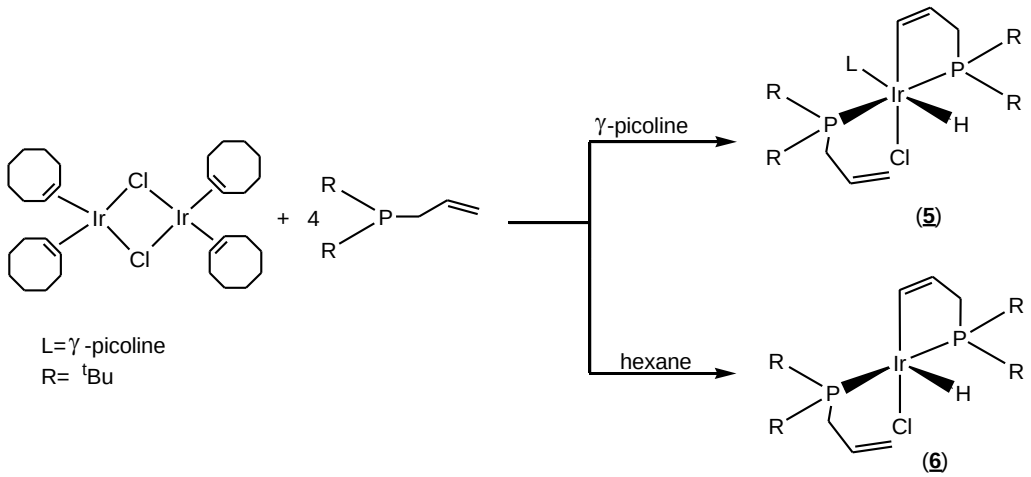

Scheme I.2. Reaction of di-t-butylallylphosphine with $[Ir(.\mu\text{-}Cl)_2(COE)_4]$.

At 40°C, a hydride migrates to the double bound of the cyclooctene to form the unsaturated complex (**3**) (Scheme I.1). The unsaturated at the iridium center is fulfilled by interactions with the allyl moieties, meaning that the diallylphosphine is acting as a bidentate

ligand. It is confirmed by the presence of three types of allyl fragments in the $^{13}C\{^1H\}$ NMR spectrum.

The lability of the diallylphosphine ligand on the complex (**3**) has been demonstrated by bubbling CO into a solution of this complex in $CHCl_3$ at room temperature, resulting in the formation of the complex (**4**) (Scheme I.1). The $^{13}C\{^1H\}$ NMR spectrum shows more significant changes, the appearance of only two types of allyl group clearly demonstrates that there is not interaction with the metal center, the unsaturation is now being filled by the CO ligand.

Monoallylphosphine ligands have shown to be bidentate ligands to form cationic ruthenium complexes. Nelson and coworkers [44] reported the synthesis and reactivity of the ruthenium(II) complex $[Ru(\eta^5\text{-}C_5Me_5)\{\kappa^1(P)Ph_2PCH_2CH{=}CH_2\}\{\kappa^3(P,C,C)Ph_2PCH_2CH{=}CH_2\}][PF_6]$ (**7**), containing a bidentate allylphosphine ligand (Scheme I.3). $^{31}P\{^1H\}$ NMR spectrum of (**7**) at room temperature shows two broad resonances for the inequivalent phosphines at 44 and -72 ppm. The breadth of these resonances and the absence of P-P coupling are the evidence of a dynamic behavior in solution (Figure I.8).

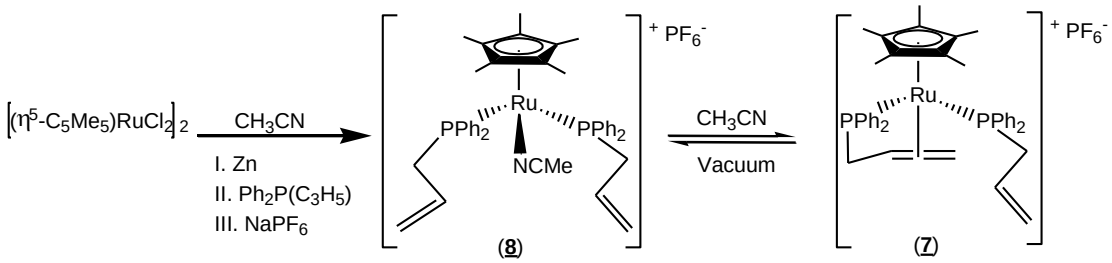

Scheme I.3. Synthesis of $[Ru(\eta^5\text{-}C_5Me_5)\{\kappa^1(P)Ph_2PCH_2CH{=}CH_2\}\{\kappa^3(P,C,C)Ph_2PCH_2CH{=}CH_2\}][PF_6]$ (**7**) .

The fluxional behavior in (**7**) is explained by the isomerization of the metal-coordinated alkene from the presumably preferred parallel position with respect to the η^5-C_5Me_5 ring to a perpendicular position. The dynamic behavior in (**7**) was probed by variable temperature $^{31}P\{^1H\}$ NMR spectroscopy in chloroform from -60 to 50°C as shown in Figure I.8.

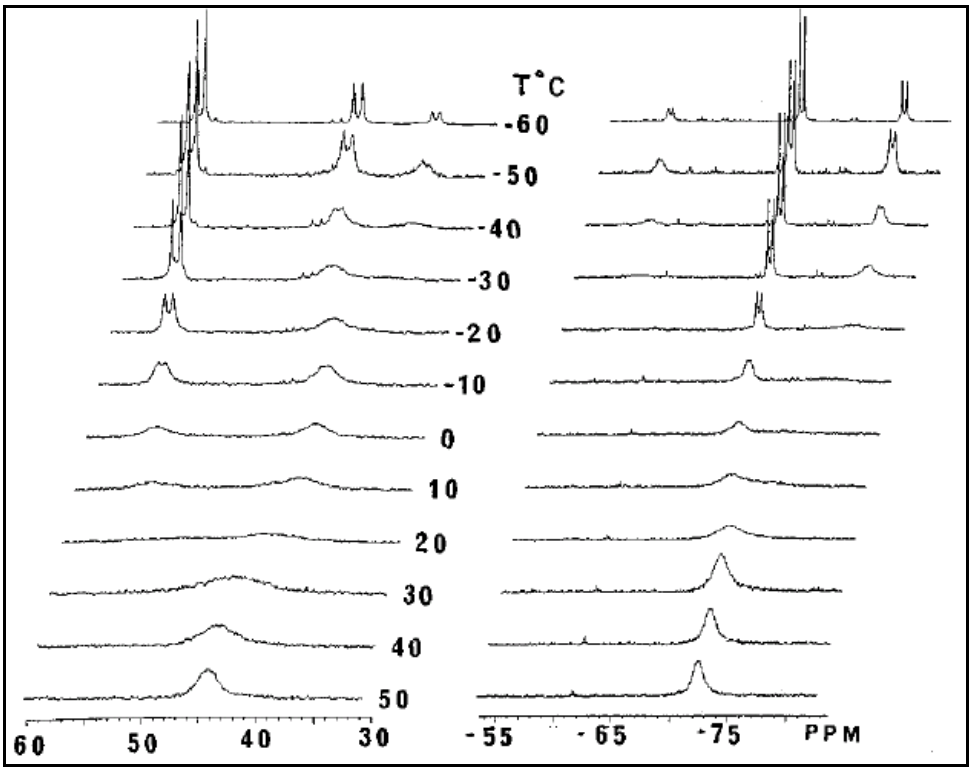

Figure I.8. Variable temperature $^{31}P\{^{1}H\}$ NMR spectra of (**7**) in $CDCl_3$ from -60 to 50°C.

At -60°C, three compounds are present as represented by three sets of doublets at 49.17 y -69.66 ppm ($^{2}J_{PP}$= 42.9 Hz); 42.75 y -77.39 ppm ($^{2}J_{PP}$= 43.9 Hz); 39.57 and -59.88 ppm ($^{2}J_{PP}$= 35.7 Hz), with an integrated intensity ratio of 4.4:2.9:1 respectively. The two major sets of doublets represent the two diastereomeric conformations of the coordinated alkene, since the two faces of the alkenes are diastereotopic when the allyldiphenylphosphine is bound in a bidentate manner. The minor resonances may represent a dimer form of compound (**7**).

The lability of κ^3-allyldiphenylphosphine on the complex (**7**) was studied by reactions with carbon monoxide, sodium thiocyanate and phenylacetylene (Scheme I.4). In these reactions the displacement of the coordinated alkene moiety and the formation of the symmetrical complexes (**9**, **10** and **11**) are confirmed. These results indicate that complex (**7**) reacts reversibly with acetonitrile and irreversible with CO, thiocyanate and phenylacetylene.

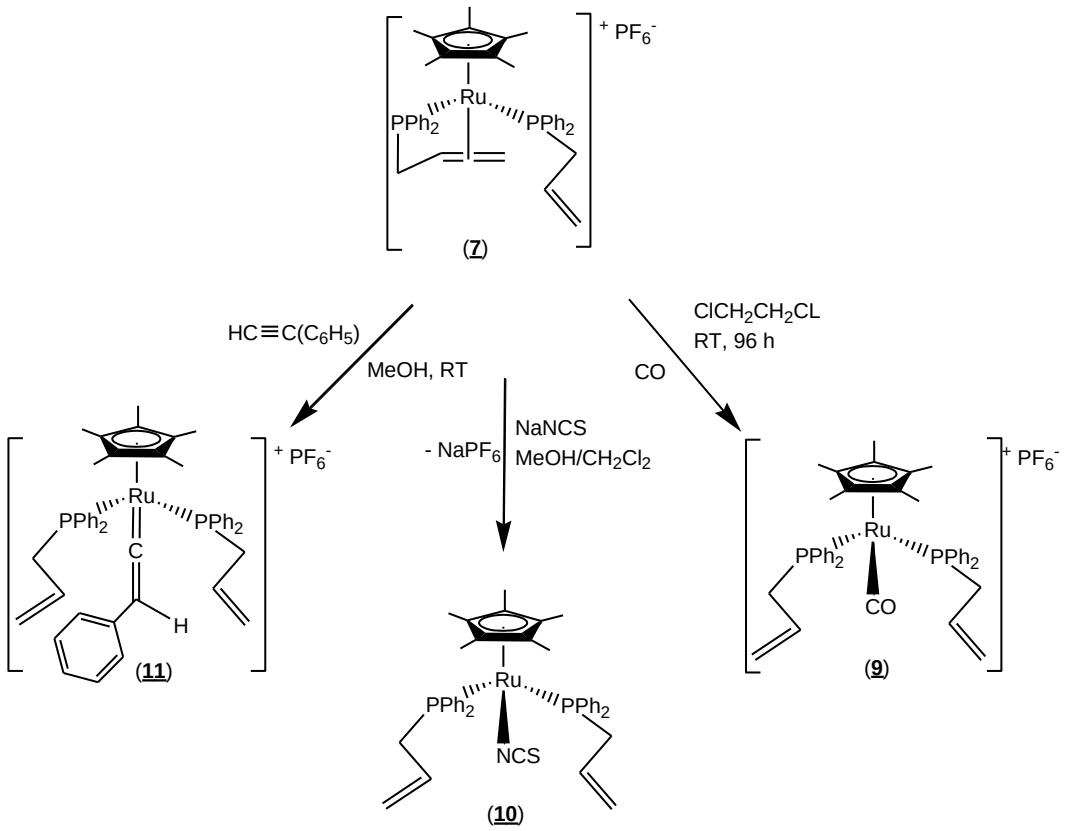

Scheme I.4. Reactivity of complex (**7**) with carbon monoxide, sodium thiocyanate and phenylacetylene.

Similar cationic ruthenium complexes with an κ^3-allyldiphenylphosphine ligand have been reported. Gimeno and coworkers [45] carried out the diastereoselective synthesis and reactivity of the cationic complexes $[Ru(\eta^5\text{-}C_9H_7)\{\kappa^3(P,C,C)Ph_2PCH_2CR{=}CH_2\}(PPh_3)]$ $[PF_6]$ (R= H (**13a**), Me (**13b**) (Scheme I.5).

The NMR data confirmed the coordination mode of the allylphosphine as κ^3-(*P,C,C*). The ^1H and $^{13}C\{^1H\}$ NMR spectra show $CR{=}CH_2$ (R= H, Me) resonances which appear at higher field than those observed in complexes (**12a-c**). $^{31}P\{^1H\}$ NMR spectra also reveal the effect of the olefin coordination, showing the expected resonances for an AB system with the signals for the allylphosphine shifted toward higher field at [δ 55.2 (PPh_3), -69.9 (κ^3-alilfosfina) (**13a**); δ 51.4 (PPh_3), - 63.9 (κ^3-alilfosfina) (**13b**)] with respect to those of the corresponding κ^1(P) precursors.

Since the two faces of the alkenes are diastereotopic, the formation of only one isomer for each complexes (**13a** and **13b**) indicates that the generation of the chelate ring $[Ru\{\kappa^3(P,C,C)Ph_2PCH_2CR{=}CH_2\}]$ (R= H, Me) proceeds in a highly diastereoselective manner. The relatively large difference of geminal CH_2 chemical shifts in ^1H NMR spectra

points to a parallel orientation of the olefin with respect to the indenyl ring. It is interesting to note that the $^{31}P\{^{1}H\}$ NMR spectra within a wide range of temperature (-90 to 50°C) do not reveal a dynamic behavior between the two diastereomers.

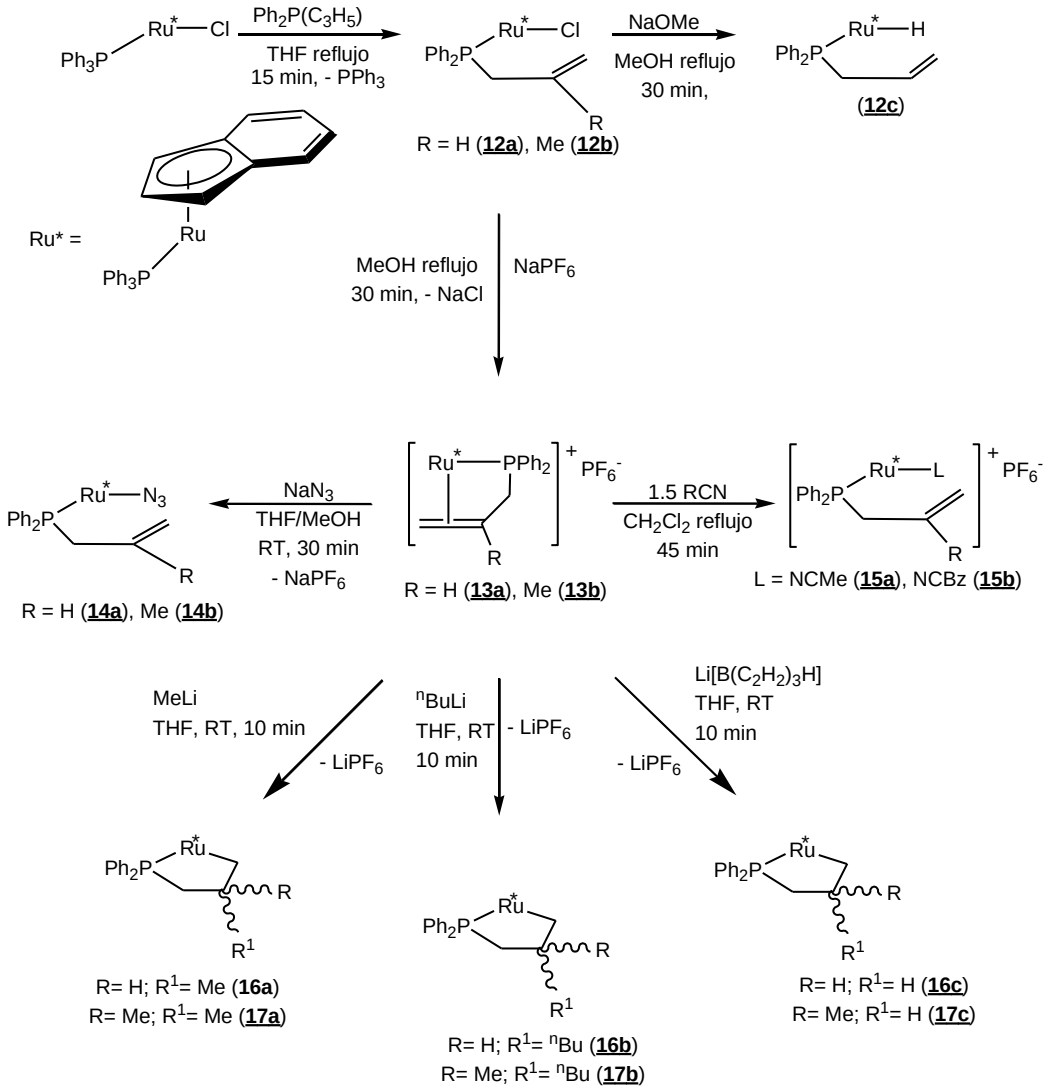

Scheme I.5. Synthesis and reactivity of the complexes

$[Ru(\eta^5C_9H_7)\{\kappa^3(P,C,C)Ph_2PCH_2CR{=}CH_2\}(PPh_3)][PF_6]$ (R= H (**13a**), Me (**13b**).

The structure of complex (**13a**) determined by X-ray crystallography exhibits pseudoctahedral three-legged piano-stool geometry with the η^5-indenyl ligand displaying the usual allylene coordination mode (Figure I.9). It is interesting to note that the indenyl ligand is oriented over the olefin ligand and the benzo ring is slightly displaced toward P(1). In addition, the [Ru(1)-C(23)= 2.228(5), Ru(1)-C(24)= 2.243(5) and C(23)-C(24)= 1.391(8)] bond distances reflect the coordination of the olefin to the metal center.

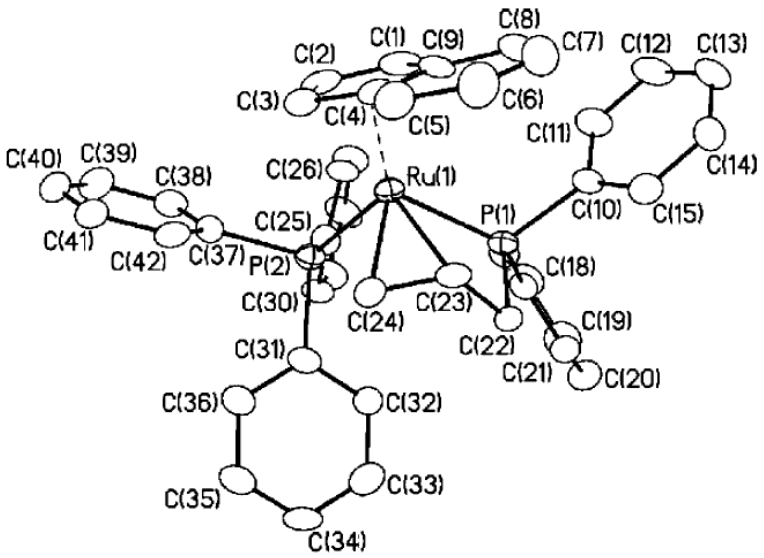

Figure I.9. Molecular structure for complex (**13a**).

The propensity of the coordinated π-olefínic system to undergo nucleophilic addition, due to its electrophilic character, or to behave as a labile group in substitution reactions have been explored by reactions of the complexes (**13a** and **13b**) toward typical neutral and ionic two-electron species such as nitriles, hydrides, azide or alkyl carbanions (Scheme I.5).

Substitution of the coordinated π-olefin group is achieved readily by reactions of complex (**13a**) with nitriles RCN (R= Me, Bz) to form the complexes (**15a** and **15b**). Similarly, the addition of NaN_3 to a solution of (**13a** and **13b**) results in the formation of the neutral complexes (**14a** and **14b**). The $^{31}P\{^1H\}$ NMR spectra for these complexes show the two doublets resonances for the AB system at [δ 49.0 y 44.1 (d, J_{PP}= 36.6 Hz) (**15a**); δ 49.4 y 42.6 (d, J_{PP}= 36.6 Hz) (**15b**); δ 46.5 y 50.8 (d, J_{PP}= 41.5 Hz) (**14a**); δ 46.7 y 51.3 (d, J_{PP}= 41.1 Hz) (**14b**)], values which are in agreement with those found for complexes (**12a** and **12b**), in which the allylphosphine acts as a monodentate ligand.

The addition of lithium carbanions R'Li (R'= H, ^{n}Bu) to solutions of complexes (**13a** and **13b**) results in the regioselective addition at the C_β atom of the coordinated allylic group affording the ruthenaphosphacyclopentane complexes (**16a**, **17a**) and (**16b**, **17b**). Similarly, the complexes (**13a** and **13b**) react with $[LiB(C_2H_3)_3H]$ to give, regioselectively, the analogues addition complexes (**16c** and **17c**).

Recently, allyl nickel complexes bearing allylphosphine ligands have been shown to be active catalyst precursors for the oligomerization of styrene and 4-methylstyrene, as well as, for the regioselective hydrosilylation reactions of these olefins with $PhSiH_3$. Valerga and coworkers [46] carried out the synthesis of the cationic allyl and 2-methylallyl nickel complexes $[Ni(\eta^3\text{-}CH_2\text{-}C(R^1)CH_2)(\kappa^1\text{-}R^2{}_2PCH_2CH{=}CH_2)_2][BAr'_4]$ (**18a-b**) and (**19a-b**) bearing the allylphosphine ligands $R_2PCH_2CH{=}CH_2$ [R= Ph (**18**), ^{i}Pr (**19**)] (Scheme I.6). The catalytic activity of these complexes was evaluated in the reactions of oligomerization and hydrosilylation reactions of styrene and 4-methylstyrene.

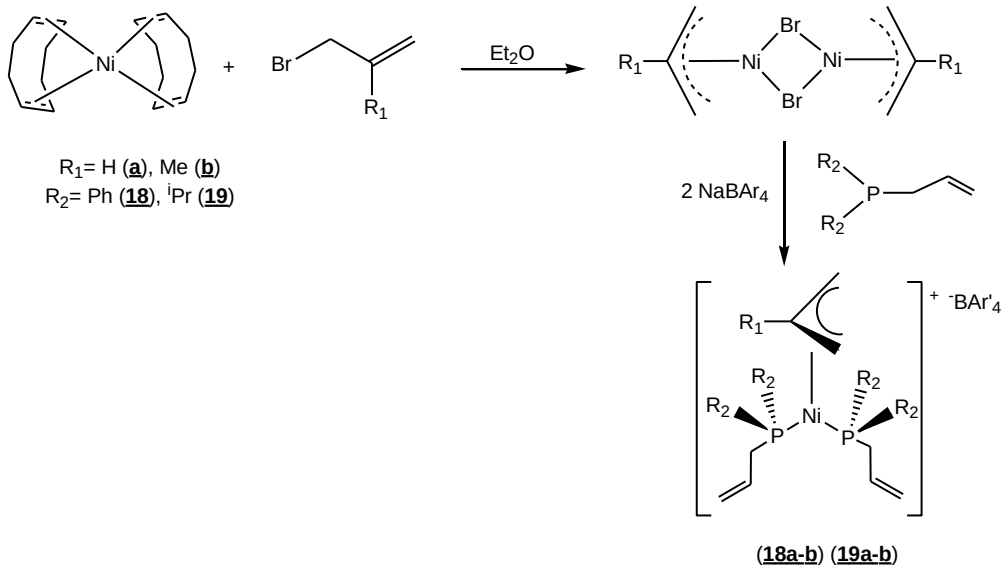

(**18a-b**) (**19a-b**)

Scheme I.6. Synthesis of the complexes $[Ni(\eta^3\text{-}CH_2\text{-}C(R^1)CH_2)(\kappa^1\text{-}R^2{}_2PCH_2CH{=}CH_2)_2][BAr'_4]$ (**18a-b**) and (**19a-b**)**.**

The cationic allyl and methylallyl complexes (**18a-b**) and (**19a-b**) were shown to be active catalysts for the oligomerization of styrene or 4-metylstyrene in the absence of a co-catalyst such as MAO. The best results were obtained using as solvent 1,2-dichloroethane at 40°C, with a monomer/catalyst molar ratio equal to 200 under nitrogen atmosphere. The catalytic activity was found to be in the range from moderate to high. The methylallyl complexes were significantly more active than their counterpart bearing allyl. On the other hand, the complexes containing $Ph_2PCH_2CH{=}CH_2$ (**18a-b**) were in general more active than those with $^iPr_2PCH_2CH{=}CH_2$ (**19a-b**), but the differences are not as remarkable as those attributable to the presence of one methyl on the allyl group. The oligostyrene resulting from the catalytic reactions are highly isotactic with weight distributions (M_n) in the range from 700 to 1900 Dalton with polydispersity indexes (M_w/M_n) between 1.22-1.64. Both the M_n and the P_m values were similar to those observed for the oligostyrenes resulting from the reactions

catalyzed by the system [[Ni(η^3-CH_2-C(CH_3)CH_2)(COD)]$^+$ / PR_3 (PR_3= PPh_3, P(OPh_3), P(*o*-Tol)$_3$, PMe_3, P^nBu_3, PCy_3).[47]

Likewise, the cationic complexes act as catalyst precursors for the regioselective hydrosilylation reactions of styrene or 4-methylstyrene with $PhSiH_3$. These reactions were carried out using a 1% mol catalyst load in 1,2-dichloroethane at 40 °C. Under these conditions, the isolated hydrosilylation products were either $C_6H_5CH(CH_3)SiH_2C_6H_5$ or $CH_3C_6H_5CH(CH_3)SiH_2C_6H_5$, with yields, after 5 h, in the range 50-79%. These results were similar in terms of activity and regioselectively than those reported by Zargarian and co-workers using substituted indenyl nickel complexes as catalyst precursors, although in this case a co-catalyst (MAO o $NaBPh_4$) is not needed. Furthermore, the catalytic activity of the complexes for the hydrosilylation of styrene is higher than that observed in the case of cationic bis(phosphine) complex [Ni(metilindenilo)(Ph_3P)][BPh_4].[48]

The triallylphosphine-substituted has been used as bidentate ligand on metal clusters. Nordlander and coworkers [49] have reported the synthesis of a stable ruthenium cluster [$Ru_3(CO)_{10}$\{κ^3(P,C,C)-CH_2=$CHCH_2P(CH_2CH$=$CH_2)_2$\}] (**20**), in which the ligand triallylphosphine is coordinated via the phosphorus atom as well as one π-coordinated allyl moiety (Scheme I.7).

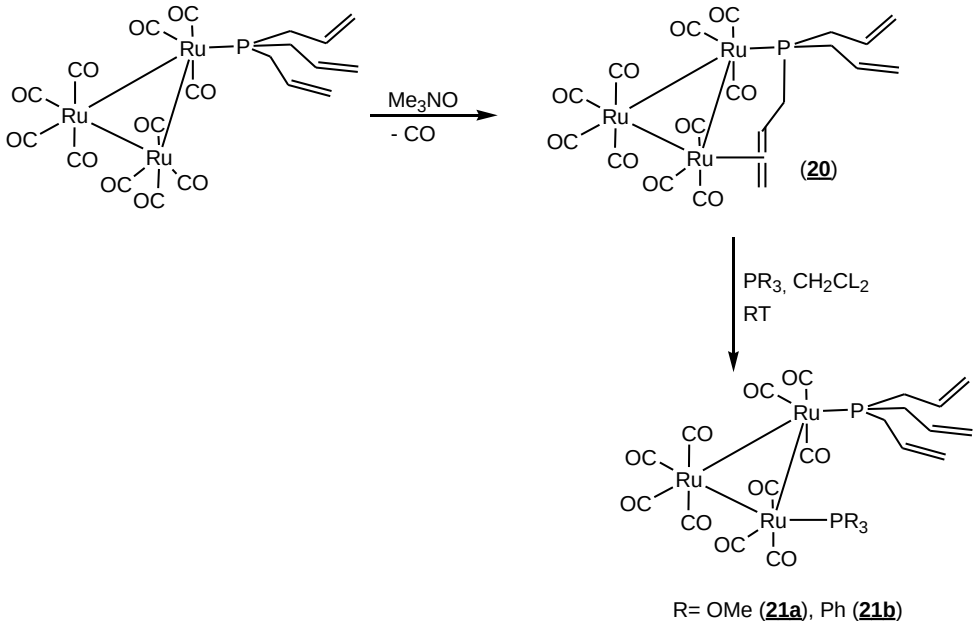

Scheme I.7. Synthesis and reactivity of complex [$Ru_3(CO)_{10}$\{κ^3(P,C,C)-CH_2=$CHCH_2P(CH_2CH$=$CH_2)_2$\}] (**20**).

The reaction of (**20**) with nucleophiles, such as $P(OMe_3)$ or PPh_3, under mild conditions led to the displacement of the π-coordinated alkene and the formation of clusters $[Ru_3(CO)_{10}\{\kappa^1(P)\text{-}P(CH_2CH{=}CH_2)_3\}(PR_3)]$ (R= OMe (**21a**); Ph (**21b**)).

Chapter II

Diallylphosphine as polydentate ligands to stabilize cationic rhodium species

II.1. Introduction

The design of hybrid ligands for the synthesis of catalytic precursors, which would lead to catalytic processes faster, more efficient, selective and friendly environment, has been subject of study for many researchers.[1-7] These ligands are expected to exert more control of the coordination sphere of the metal with the possible consequence of providing new catalytic properties in the resulting complexes.

Hybrid ligands which contain different chemical functionalities, such as hard and soft donors, have found increasing use in organometallic chemistry.[10,13] The hemilabile character of the hybrid ligands has been shown to enhance both activity and selectivity in catalytic reactions.[1-7] Functionalized phosphine containing weakly coordinating carbons moieties and, in particular, the olefins are of special interest,[9, 41, 44,50-57] due to the well-known lability of the metal-olefin bond, which enables the facile generation of a free coordination site at the metal centre, as well as, the stabilization of unsaturated coordinatively metal species.

We have focused our interest on the diallylphosphine ligands. These ligands contain a strongly bonding phosphine group (hard donor) and two weakly coordinating alkene moieties (soft donor). The bifunctional character may allow to the diallylphosphines act as polydentate ligands to stabilize cationic rhodium species. In this chapter, we present the results on the study of the reactivity of different diallylphosphines toward chloro-bridged cyclooctadiene rhodium dimer and its capacity to act as polydentate ligands to obtain cationic rhodium complexes.

II.2. Results and discussions

II. 2.1. Reactions of the diallylphosphines with $[Rh_2(\mu\text{-}Cl)_2(COD)_2]$

Addition of two equivalent of each diallylphosphine (**a**, **b** and **c**) to a solution of one equivalent of dimer complex $[Rh_2(\mu\text{-}Cl)_2(COD)_2]$ led to formation of the neutral complexes $[RhCl(COD)\{\kappa^1(P)RP(CH_2CH{=}CH_2)_2\}]$ [R= $^{i}Pr_2N$ (**22a**), ^{t}Bu (**22b**) and Ph (**22c**)] (Scheme II.1). They were isolated as air-sensitive yellow solid in 98% yield. Elemental analysis and NMR spectroscopic data (^1H, $^{13}C\{^1H\}$, and $^{31}P\{^1H\}$) of (**22a-c**) are in accord with the proposed formulation.

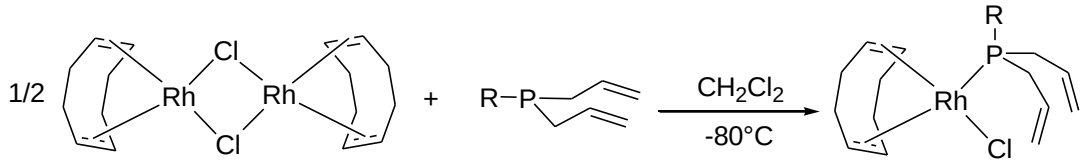

R= $^{i}Pr_2N$ (**a**), ^{t}Bu (**b**), Ph (**c**) (**22a-c**)

Scheme II.1. General reaction for the synthesis of the neutral complexes $[RhCl(COD)\{\kappa^1(P)RP(CH_2CH{=}CH_2)_2\}]$ (**22a-c**).

$^{31}P\{^1H\}$ NMR spectra show one doublet resonance at [δ 66.15 (J_{PRh} = 158.3 Hz) for (**22a**), δ 24.71 (J_{PRh} = 146.8 Hz) for (**22b**) and δ 14.15 (J_{PRh} = 148.4 Hz) for (**22c**)], values which are shifted toward downfield with respect to those of the corresponding free ligands. In addition, coupling constants are similar to observed for analogous rhodium (I) complexes, such as $[RhCl(COD)(PPh_3)]$ [58] ($J_{Rh\text{-}P}$= 149.4 Hz), $[RhCl(COD)(PBz_3)]$ [59] ($J_{Rh\text{-}P}$= 150.5 Hz). These spectroscopic evidences indicate the monodentate coordination mode of the diallylphosphine ligands.

The ^1H and $^{13}C\{^1H\}$ NMR spectra confirm the $\kappa^1(P)$ coordination mode of the diallylphosphine ligands, as indicated the presence the signals corresponding to uncoordinated allyl groups, which are similar to those observed for free ligands. The most significant features are presented in the table II.1.

Table II.1. ^{1}H and $^{13}C\{^{1}H\}$ NMR data of the allylic moieties in the complexes (**22a-c**)

Complexes	δ ^{1}H NMR [a]	δ $^{13}C\{^{1}H\}$ NMR [a]
22a	5.11 (brs, 2H, $=CH_2$), 5.14 (brs, 2H, $=CH_2$), 6.08 (m, 2H, CH=)	118.24 (d, $^{3}J_{CP}$= 10.8 Hz, 2C, $=CH_2$), 131.84 (s, 2C, CH=)
22b	5.03-5.10 (m, 4H, $=CH_2$), 5.87-6.02 (m, 2H, CH=)	118.41 (d, $^{3}J_{CP}$= 9.6 Hz, 2C, $=CH_2$), 132.16 (d, $^{2}J_{CP}$= 4.7 Hz, 2C, CH=)
22c	5.09-5.16 (m, 4H, $=CH_2$), 5.79-5.95 (m, 2H, CH=)	118.78 (d, $^{3}J_{CP}$= 10.3 Hz, 2C, $=CH_2$), 131.09 (d, $^{2}J_{CP}$= 4.7 Hz, 2C, CH=)

[a] Spectra recorded in $CDCl_3$ at 25°C.

II.2.2. Chloride abstraction reaction from complexes (22a-c)

We carried out chloride abstraction reactions from (**22a**), (**22b**) and (**22c**) to prepare cationic rhodium derivative. The intention is that the double bonds of the allyl substituents might fill the vacant position left by chloride ligand. Treatment of a solution of either the chloride complexes (**22a-c**) with one equivalent of $AgBF_4$, led to formation of the cationic complexes $[Rh(COD)\{\kappa^3(P,C,C)RP(CH_2CH{=}CH_2)_2\}][BF_4]$ (**23a-c**) (Scheme II.2). The synthesis and characterization of each of the cationic complexes are described below.

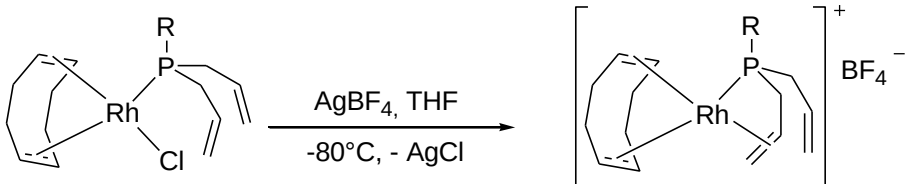

(**22a-c**) (**23a-c**)

R= $^{i}Pr_2N$ (**a**), ^{t}Bu (**b**), Ph (**c**)

Scheme II.2. General reaction for the synthesis of the complexes $[Rh(COD)\{\kappa^3(P,C,C)RP(CH_2CH{=}CH_2)_2\}][BF_4]$ (**23a-c**).

II. 2.2.1. Synthesis and characterization of complex [Rh(COD){κ^3(P,C,C)^{i}Pr$_2$NP(CH$_2$CH=CH$_2$)$_2$}][BF$_4$] (23a)

Complex [Rh(COD){κ^3(P,C,C)^{i}Pr$_2$NP(CH$_2$CH=CH$_2$)$_2$}][BF$_4$] (**23a**) was obtained by reaction of (**22a**) with one equivalent of AgBF$_4$. Complex (**23a**) was isolated as air-sensitive orange solid in 80% yield. ^{31}P{^{1}H} NMR spectrum at RT of (**23a**) shows a doublet resonance [δ -23.79 (d, J_{PRh} = 104.4 Hz)] shifted toward higher field with respect to observed for respective complexes (**22a**), which indicates the chelating coordination mode of the diallyldiisopropylaminephosphine ligand.[60]

^{13}C{^{1}H} and ^{1}H NMR spectra at RT of (**23a**) reveal the chelating coordination mode of the diallyldiisopropylaminephosphine ligand. Spectroscopic analyses show the expected resonances for CH=CH$_2$ moieties, which appear to higher field than those observed in complex (**22a**) (Figure II.1). The breadth of the signals corresponding to carbons of alkenes fragments [δ 100.2 (=CH$_2$), 107.5 (CH=)] suggest a dynamic behavior in solution, which may be ascribable to an intramolecular exchange between the two weakly bonding alkenes groups to the metal center.

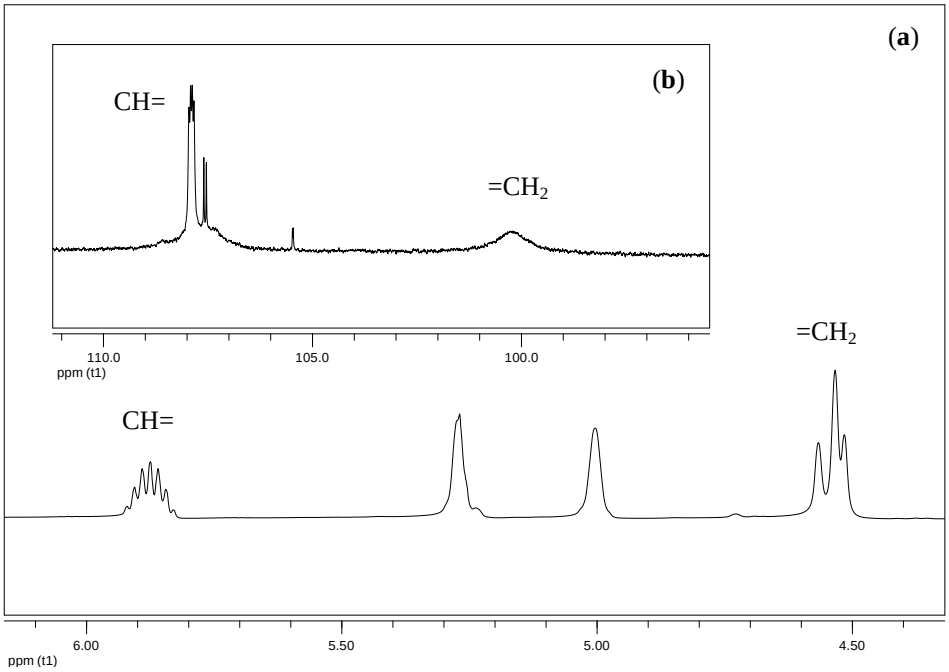

Figure II.1. ^{1}H (**a**) and ^{13}C{^{1}H} (**b**) NMR spectra at RT of (**23a**) in CD$_2$Cl$_2$.

The dynamic behaviour in solution for (**23a**) was detected by NMR spectroscopy to

variable temperature, and was found to be fast on the NMR time scale in CD_2Cl_2 at room temperature, but slow at -90°C. In particular, ^1H NMR spectrum in CD_2Cl_2 at -90°C of (**23a**) shows clearly two sets of resonances [δ 3.67 and 3.77 (=CH_2), 5.98 (CH=)] and [δ 5.20 (=CH_2), 5.64 (CH=)] corresponding to protons of coordinated and uncoordinated alkenes moieties. Moreover, $^{13}C\{^1H\}$ NMR spectrum in CD_2Cl_2 at -90°C of (**23a**) shows the signals corresponding to carbons of the coordinated [δ 77.02 (=CH_2), 83.19 (CH=)] and uncoordinated [δ 120.73 (=CH_2), 127.77 (CH=)] alkene moieties (Figure II.2).

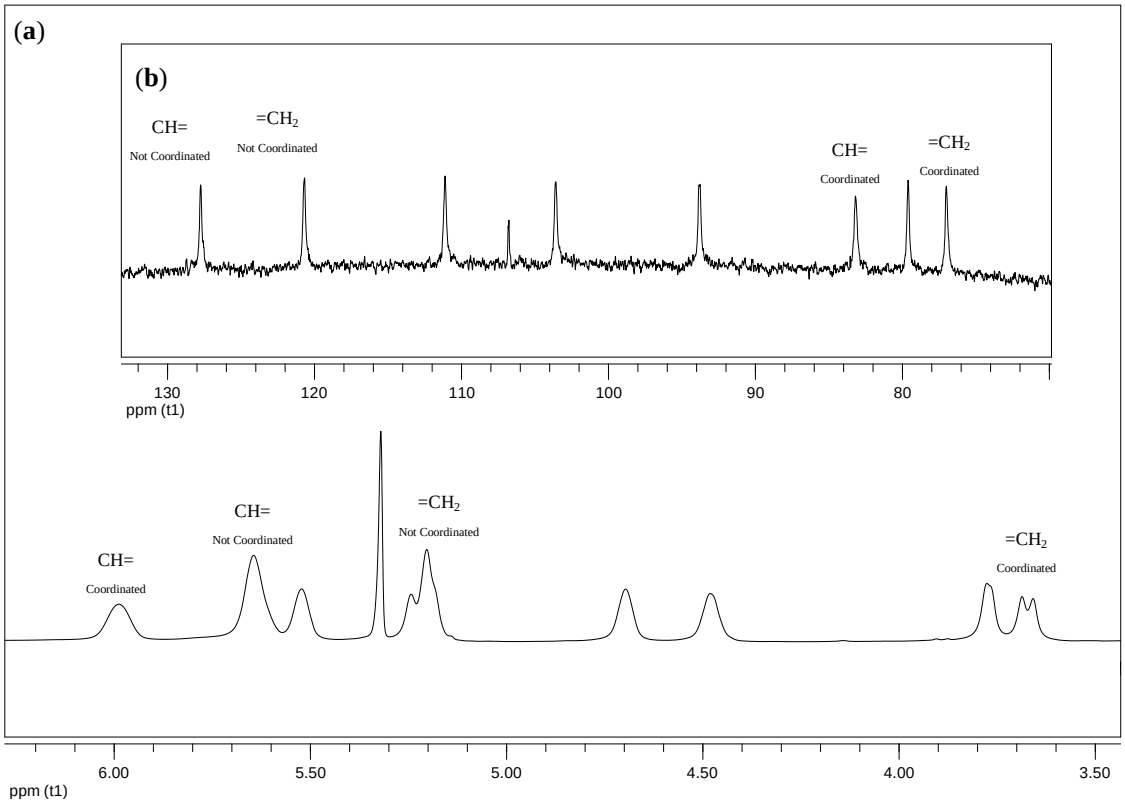

Figure II.2. ^1H (**a**) and $^{13}C\{^1H\}$ (**b**) NMR spectra at -90 °C of (**23a**) in CD_2Cl_2.

The dynamic behavior of complex (**23a**) in solution is an evidence of the hemilabile character of diallyldiisopropylaminephosphine ligand, which involves an intramolecular competition between the two allylic functions while the phosphorus donor serves as an anchor (Scheme II.3). This exchange reaction provides a mixture of the two enantiomers $\boldsymbol{R_P}$-(**23a**) and $\boldsymbol{S_P}$-(**23a'**), because the phosphorus atom can be considered a chiral center, when an alkene moiety is coordinated to metal center while the other remains free.

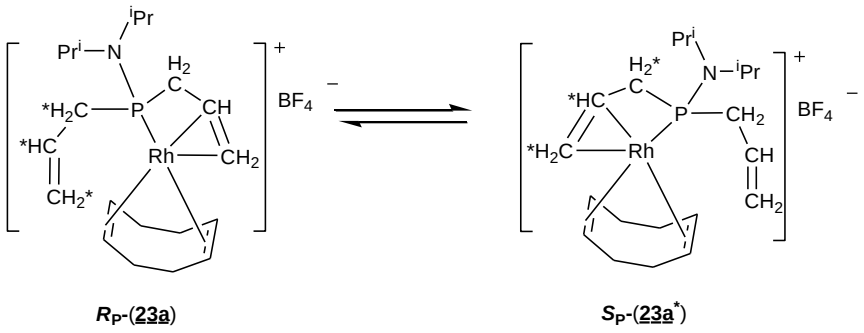

***R*P-(23a)** **S*P-(23a*)**

Scheme II.3. Enantiomeric mixture of complexes ***R*P-(23a)** and ***S*P-(23a')**.

Molecular structure of complexes (23a)

X-ray diffraction analysis of complex (**23a**) shows the presence of an enantiomeric mixture ***R*P-(23a)** and ***S*P-(23a')** in the cell unit. An ORTEP diagram of cations ***R*P-(23a)** and ***S*P-(23a')** is shown in the figure II.3. Selected bond distances and angles are listed in Table II.2.

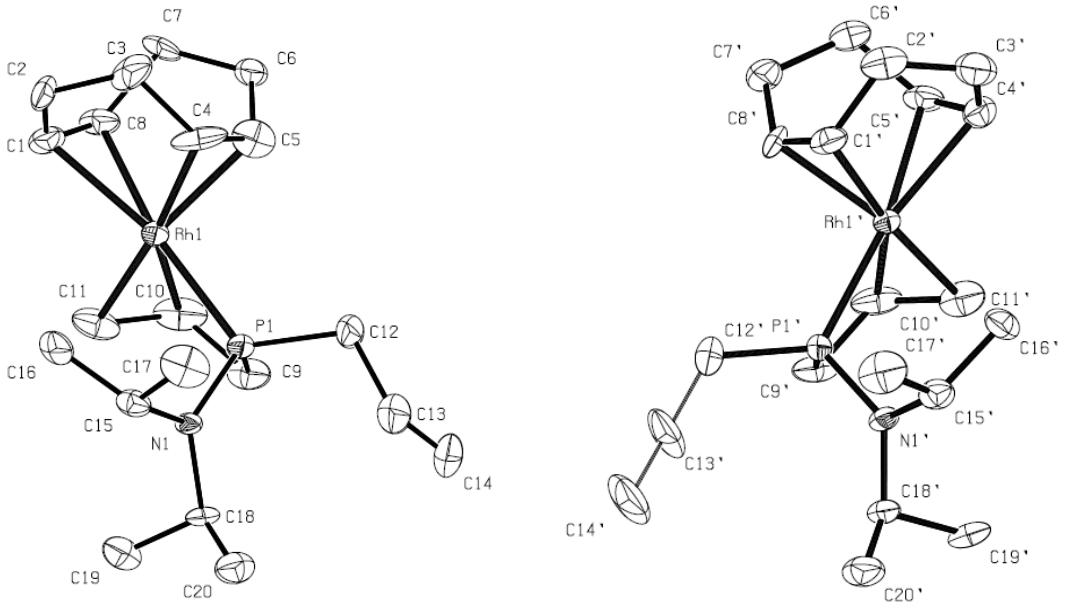

Figure II.3. Molecular structure of ***R*P-(23a)** (left) and ***S*P-(23a')** (right). Thermal ellipsoids represent 30% probability. H atoms and counter-ions BF_4 have been omitted for clarity.

Molecular structures of ***R*P-(23a)** and ***S*P-(23a')** exhibit slightly distorted square plane coordination geometry around rhodium, in which the diallyldiisopropylaminephosphine ligand displays a chelating coordination mode by coordination of an allyl group while other one remains free. (Figure II.3). The Rh(1)−P(1) and Rh(1')−P(1') bond distances, 2.2685(17)

and 2.2663(17) Å, are very similar to the Rh−P bond distance of 2.284 Å in the rhodium complex [{η^5-$C_5(CO_2Et)Me_3$-2-[$CH_2CH_2CH_2P(C_6H_5)_2$]}$RhCl_2$], in which (phosphino-propyl) cyclopentadienyl act as a chelating ligand, but are shorter than the average distance of 2.357 Å in the complex [(η^5-C_5Me_5)Rh{κ^1(P)-$CH_2CHCH_2P(C_6H_5)_2$}$_2$Cl][PF_6].[61]

Table II.2. Selected bond lengths (Å) and bond angles (deg) of complex (**23a**)

Complex	Bond distance		Bond angle	
R_P-(23a)	P(1)−Rh(1)	2.2685(17)	N(1)−P(1)−C(9)	108.7(3)
	Rh(1)−C(10)	2.259(6)	N(1)−P(1)−C(12)	112.3(3)
	Rh(1)−C(11)	2.237(6)	C(12)−P(1)−C(9)	108.0(4)
	C(10)−C(11)	1.381(11)	Rh(1)−P(1)−C(9)	91.45(2)
	C(13)−C(14)	1.192(13)	P(1)−C(9)−C(10)	97.77(4)
			C(11)−C(10)−C(9)	121.0(6)
			C(10)−Rh(1)−P(1)	68.2(2)
			C(11)−Rh(1)−P(1)	83.4(2)
S_P-(23a')	P(1')−Rh(1')	2.2663(17)	N(1')−P(1')−C(9')	107.9(3)
	Rh(1')−C(10')	2.269(7)	N(1')−P(1')−C(12')	111.7(3)
	Rh(1')−C(11')	2.259(6)	C(12')−P(1')−C(9')	107.8(4)
	C(10')−C(11')	1.344(12)	Rh(1')−P(1')−C(9')	90.7(2)
	C(13')−C(14')	1.37(2)	P(1')−C(9')−C(10')	99.5(5)
			C(11')−C(10')−C(9')	122.2(6)
			C(10')−Rh(1')−P(1')	68.35(19)
			C(11')−Rh(1')−P(1')	83.59(19)

The Rh(1)−C(10), Rh(1)−C(11) and Rh(1')−C(10'), Rh(1')−C(11') bond lengths reflect the coordination of alkene moiety to the metal center while other one remains free. As expected, the metal-coordinated alkenes bond distances, C(10)−C(11) and C(10')−C(11'), are longer that those of the uncoordinated alkenes, C(13)−C(14) and C(13')−C(14'), bond distances. In addition, the C(10)−C(11) and C(10')−C(11') bond distances are similar to the metal-coordinated alkene bond distance in the complex [Ru(η^5-C_9H_7){κ^3(P,C,C)$Ph_2PCH_2CR{=}CH_2$}(PPh_3)][PF_6] (R= H (**13a**)).[45]

II.2.2.2. Synthesis and characterization of complex [Rh(COD){κ^3(P,C,C)^{t}BuP($CH_2CH=CH_2$)$_2$}][BF_4] (**23b**)

Complex [Rh(COD){κ^3(P,C,C)^{t}BuP($CH_2CH=CH_2$)$_2$}][BF_4] (**23b**) was obtained by reaction of (**22b**) with one equivalent of $AgBF_4$. Complex (**23b**) was isolated as air-sensitive orange solid in 86% yield. $^{31}P\{^1H\}$ NMR spectrum of (**23a**) shows a doublet resonance [δ -68.22 (d, J_{PRh} = 110.1 Hz)] shifted toward higher field with respect to observed for the complex (**22b**), which indicates the chelating coordination mode of diallyl-tert-butylphosphine ligand [60]. Similar chemical shift toward highfield have been shown for complex [Ru(η^5-C_9H_7){κ^3(P,C,C)$Ph_2PCH_2CR=CH_2$}(PPh_3)][PF_6] (R= H (**13a**), Me (**13b**) [45] and [Ru(η^5-C_5Me_5){κ^1(P)$Ph_2PCH_2CH=CH_2$} {κ^3(P,C,C)$Ph_2PCH_2CH=CH_2$}][PF_6] (**7**).[44]

^1H and $^{13}C\{^1H\}$ NMR spectra of (**23b**) at RT reveal the coordination of both allyl groups to metal center. ^1H NMR spectrum shows two sets doublet-doublet at [δ 4.84 (dd, $^3J_{HH}$= 9.5 Hz, $^4J_{PH}$= 3.5 Hz), 5.06 (dd, $^3J_{HH}$= 16.5 Hz, $^4J_{PH}$= 2.9 Hz)] corresponding to olefinic protons $=CH_2$, as well as, a signal at [δ 5.79-5.89 (m)] for olefinic protons CH= (Figure II.4a). $^{13}C\{^1H\}$ spectrum shows the resonances of olefinic carbons $CH=CH_2$ at [δ 107.23 (brs, $=CH_2$), 107.94 (d, $^3J_{CP}$= 7.6 Hz, $=CH_2$), 113.07 (d, $^2J_{CP}$= 7.4 Hz, 2C, CH=)], which appear shifted toward higher field with respect than those observed in the complex (**22b**) (Figure II.4b).

In order to verify the presence of a dynamic equilibrium in solution, it was performed a NMR spectroscopic analysis to variable temperature in CD_2Cl_2. However, in contrast to analogue complex (**23a**), the characteristic signals of protons and carbons $CH=CH_2$ remain unchanged within a wide range of temperature (-90 to 35°C).

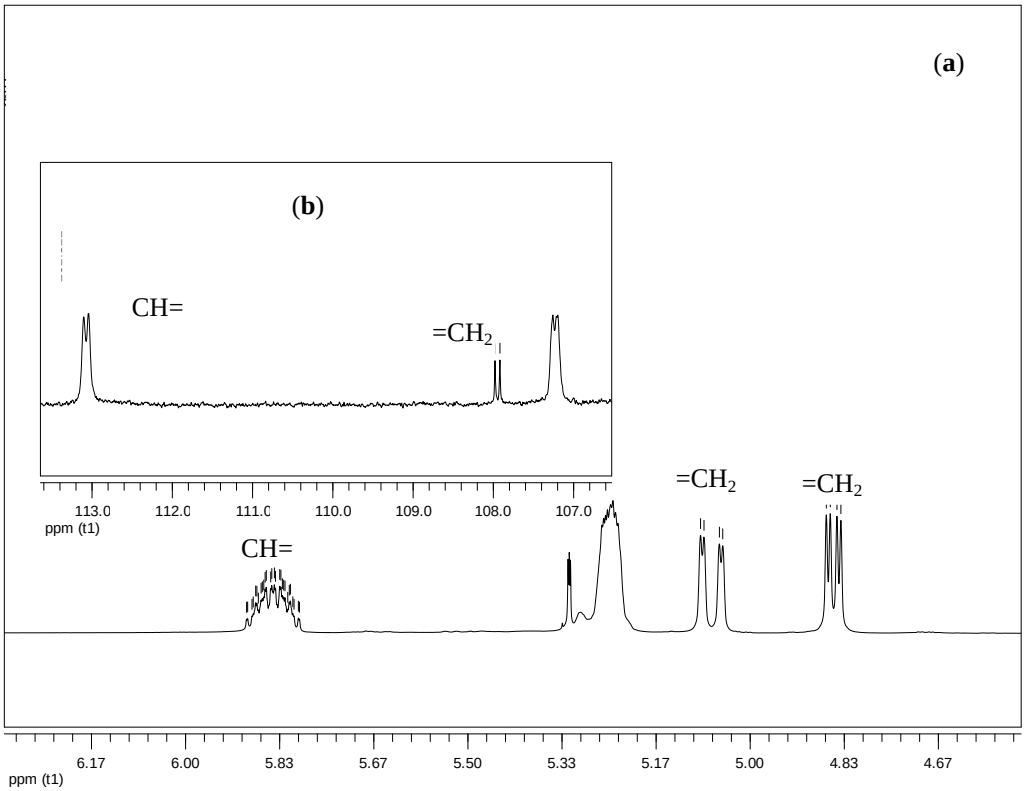

Figure II.4. ^{1}H (**a**) and $^{13}C\{^{1}H\}$ (**b**) spectra at RT of complex (**23b**) in CD_2Cl_2.

*Molecular structure of complex (**23b**)*

An X-ray crystallography analysis confirmed the molecular structure of complex (**23b**). The analysis reveals a slightly distorted square plane coordination geometry around the rhodium, in which the diallyl-tert-butylphosphine ligand displays a chelating coordination mode by coordination of an allyl group while other one remains free. An ORTEP diagram of complex (**23b**) is shown in the figure II.5 and selected bond distances and angles are listed in Table II.3.

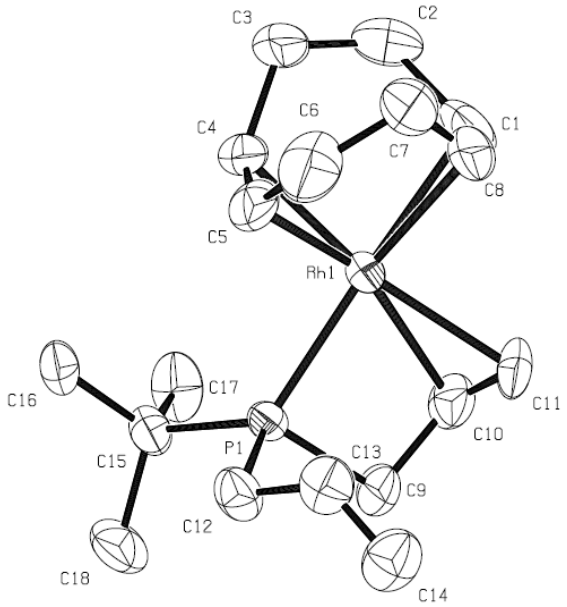

Figure II.5. Molecular structure of complex (**23b**). Thermal ellipsoids represent 30% probability. H atoms and counter-ion BF_4 have been omitted for clarity.

The Rh(1)−P(1) bond distance in (**23b**), 2.2887(4) Å, is not significantly different from the Rh−P bond distance for diallyldiisopropylaminephosphine ligand in complex (**23a**). The C(10)−C(11) is similar to the metal-coordinated alkenes bond distances in complex (**23a**).

Table II.3. Selected bond lengths (Å) and bond angles (deg) of complex (**23b**)

Bond distance		**Bond angle**	
Rh(1)−P(1)	2.2874(4)	C(15)−P(1)−C(9)	109.3(4)
Rh(1)−C(10)	2.339(8)	C(15)−P(1)−C(12)	107.4(3)
Rh(1)−C(11)	2.287(8)	C(12)−P(1)−C(9)	105.5(5)
C(11)−C(10)	1.344(13)	Rh(1)−P(1)−C(9)	92.2(3)
C(13)−C(14)	1.306(12)	P(1)−C(9)−C(10)	99.3(5)
		C(11)−C(10)−C(9)	123.0(9)
		C(10)−Rh(1)−P(1)	66.7(2)
		C(11)−Rh(1)−P(1)	89.8(3)

As expected, the metal-coordinated alkenes bond distances, C(10)−C(11), is longer than that of the uncoordinated alkenes, C(13)−C(14), bond distances. In addition, the

C(10)−C(11) bond distance is similar to the metal-coordinated alkene bond distance in the complex [Ru(η^5-C_9H_7){κ^3(P,C,C)$Ph_2PCH_2CR=CH_2$}(PPh_3)][PF_6] (R= H (**13a**)).[45]

II.2.2.3. Synthesis and characterization of complex [Rh(COD){κ^3(P,C,C)PhP($CH_2CH=CH_2)_2$}][BF_4] (23c)

Complex [Rh(COD){κ^3(P,C,C)PhP($CH_2CH=CH_2)_2$}][BF_4] (**23c**) was obtained by reaction of (**22c**) with one equivalent of $AgBF_4$. Complex (**23c**) was isolated as air-sensitive orange solid in 88% yield. $^{31}P\{^1H\}$ NMR spectrum of (**23a**) shows a doublet resonance [δ 2.88 (d, J_{PRh} = 143.6 Hz)] shifted toward higher field with respect to observed for the complex (**22c**). Although, coupling constant is not significantly different to observed for complex (**22c**), the chemical shift to high field suggests the chelating coordination mode of diallylphenylphosphine ligand.[60]

Similar to analogue complex (**23b**), ^1H and $^{13}C\{^1H\}$ NMR spectra of (**23c**) at RT suggest the coordination of both allyl groups to metal center. ^1H NMR spectrum shows the characteristic resonances of olefinic protons CH=CH_2 at [δ 5.02 (d, $^3J_{HH}$= 17.2 Hz, =CH_2), 5.17 (d, $^3J_{HH}$= 9.8 Hz, =CH_2), 5.44 (m, CH=), 5.82 (m, CH=)] (Figure II.6a). $^{13}C\{^1H\}$ spectrum shows a doublet resonance at 107.52 ppm (d, $^3J_{CP}$= 7.6 Hz) corresponding to olefinic carbons =CH_2, as well as, a broad signal at 120.72 ppm (brs) for olefinic carbons CH=, as expected these signals appear shifted toward higher field with respect than those observed in the complex (**22b**) (Figure II.6b).

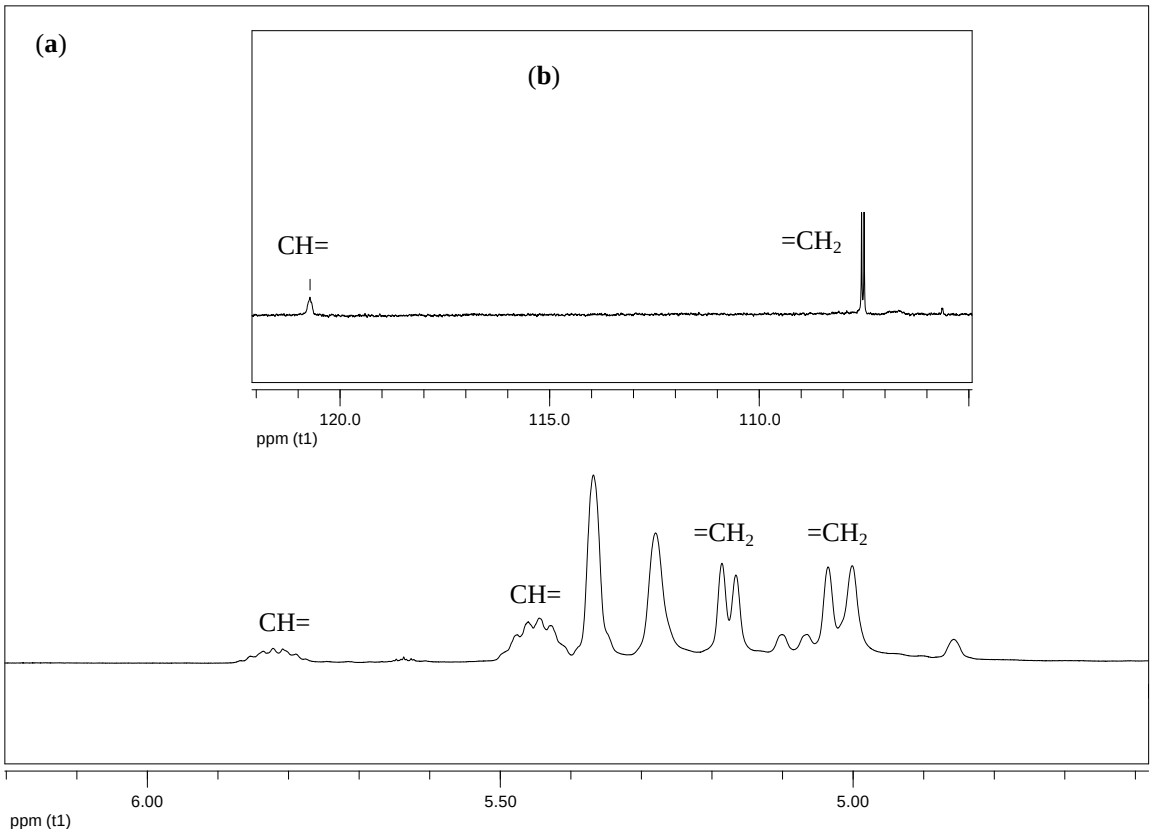

Figure II.6. ^{1}H (**a**) and $^{13}C\{^{1}H\}$ (**b**) spectra at RT of complex (**23c**) in $CDCl_3$.

In this case, it was also carried out a NMR spectroscopic analysis to variable temperature in CD_2Cl_2. However, the characteristic signals of olefinic protons and carbons $CH=CH_2$ remain unchanged within a wide range of temperature (-90 to 35°C), which contrasts to observed for complex (**23a**). This observation suggest that for (**23b**) and (**23c**) the equilibrium of exchange between both coordinated allyl moieties remains too fast and cannot be observed at -90°C.

II.3. Experimental part

II.3.1. General Considerations

All manipulations were performed under an inert atmosphere of argon by using standard Schlenk techniques. Dry, oxygen-free solvents were employed. All reagents were obtained from commercial suppliers. Diallylphosphines (**a**), (**b**) and (**c**) were synthesized as previously reported methods.[62,63] The C, H and N elemental analyses were carried out on a *Fisons Instrument* EA1108 CHNS-O microanalyzer.

^{1}H, $^{13}C\{^{1}H\}$ and $^{31}P\{^{1}H\}$ NMR spectra were recorded on Bruker, Avance 500 or Avance 300 spectrometers. ^{1}H, $^{13}C\{^{1}H\}$ NMR chemical shifts are reported in ppm relative to Me_4Si as external standard. $^{31}P\{^{1}H\}$ NMR chemical shifts are expressed in ppm relative to 85% H_3PO_4.

II.3.2. Synthesis of [RhCl(COD){κ^1(P)^{i}Pr$_2$NP(CH$_2$CH=CH$_2$)$_2$}] (22a)

To a solution of $[Rh_2(\mu\text{-}Cl)_2(COD)_2]$ (100 mg, 0.203 mmol) in CH_2Cl_2 (20 mL) was added dropwise a solution of diallyldiisopropylaminephosphine (**a**) (90.7 mg, 0.426 mmol) in 10 mL of CH_2Cl_2. The solution was stirred for 1 h at -80°C. The solution was evaporated to dryness to give a yellow solid, which was washed with hexane (5 mL) and vacuum-dried. Yield: 192 mg, 98%. $^{31}P\{^{1}H\}$ NMR (121.49 MHz, $CDCl_3$, 25°C): δ 66.15 (d, J_{PRh} = 158.3 Hz). ^{1}H NMR (300.13 MHz, $CDCl_3$, 25°C): δ 1.31 (d, $^{3}J_{HH}$= 6.9 Hz, 12H, CH_{3NiPr}), 1.95 (d, $^{2}J_{PH}$ = 8.9 Hz, 4H, PCH_2), 2.29 (m, 4H, CH_{2COD}), 2.49 (m, 2H, CH_{2COD}), 2.86 (m, 2H, CH_{2COD}), 3.63 (brs, 2H, $CH{=}CH_{COD}$), 4.04 (m, 2H, CH_{NiPr}), 5.11 (brs, 2H, $=CH_2$), 5.14 (brs, 2H, $=CH_2$), 5.33 (brs, 2H, $CH{=}CH_{COD}$), 6.08 (m, 2H, CH=). $^{13}C\{^{1}H\}$ NMR (75.47 MHz, $CDCl_3$, 25°C): δ 28.42 (s, 4C, CH_{3NiPr}), 32.52 (s, 2C, CH_{2COD}), 32.81 (s, 2C, CH_{2COD}), 33.27 (d, J_{CP} = 2.4 Hz, 2C, PCH_2), 51.90 (d, $^{2}J_{CP}$ = 7.4 Hz, 2C, CH_{NiPr}), 67.32 (d, J_{CRh} = 14.2 Hz, 2C, $CH{=}CH_{COD}$), 103.46 (dd, $^{2}J_{CP}$ = 6.8 Hz, J_{CRh} = 12.9 Hz, 2C, $CH{=}CH_{COD}$), 118.24 (d, $^{3}J_{CP}$= 10.8 Hz, 2C, $=CH_2$), 131.84 (s, 2C, CH=). Anal. Calcd for $C_{20}H_{36}ClNPRh$: C, 52.25; H, 7.83; N, 3.04. Found: C, 51.93; H, 8.03; N, 3.07.

II.3.3. Synthesis of [RhCl(COD){κ^1(P)^{t}BuP($CH_2CH{=}CH_2$)$_2$}] (22b)

To a solution of [$Rh_2(\mu\text{-}Cl)_2(COD)_2$] (100 mg, 0.203 mmol) in CH_2Cl_2 (20 mL) was added dropwise a solution of diallyl-tert-butylphosphine (**b**) (72.5 mg, 0.426 mmol) in 10 mL of CH_2Cl_2. The solution was stirred for 1 h at -80°C. The solution was evaporated to dryness to give a yellow solid, which was washed with hexane (5 mL) and vacuum-dried. Yield: 172 mg, 97%. $^{31}P\{^1H\}$ NMR (121.49 MHz, $CDCl_3$, 25°C): δ 24.71 (d, J_{PRh} = 146.8 Hz). ^1H NMR (300.13MHz, $CDCl_3$, 25°C): δ 1.25 (d, $^2J_{PH}$= 13.4 Hz, 9H, $CH_3{}^t_{Bu}$), 1.88 (brs, 4H, CH_{2COD}), 2.15-2.36 (m, 6H, CH_{2COD}, PCH_2), 2.64-2.73 (m, 2H, PCH_2), 3.66 (brs, 2H, $CH{=}CH_{COD}$), 5.03-5.10 (m, 4H, $=CH_2$), 5.22 (brs, 2H, $CH{=}CH_{COD}$), 5.87-6.02 (m, 2H, CH=). $^{13}C\{^1H\}$ NMR (75.47 MHz, $CDCl_3$, 25°C): δ 25.42 (d, J_{CP} = 18.2 Hz, 2C, PCH_2), 28.33 (s, 2C, CH_{2COD}), 29.27 (d, $^2J_{CP}$ = 3.9 Hz, 3C, $CH_3{}^t_{Bu}$), 33.24 (s, 2C, CH_{2COD}), 34.02 (d, J_{CP} = 17.9 Hz, PC^t_{Bu}), 68.00 (d, J_{CRh} = 13.8 Hz, 2C, $CH{=}CH_{COD}$), 103.36 (dd, $^2J_{CP}$ = 7.2 Hz, J_{CRh} = 11.9 Hz, 2C, $CH{=}CH_{COD}$), 118.41 (d, $^3J_{CP}$= 9.6 Hz, 2C, $=CH_2$), 132.16 (d, $^2J_{CP}$= 4.7 Hz, 2C, CH=). Anal. Calcd for $C_{18}H_{31}ClPRh$: C, 51.88; H, 7.44. Found: C, 51.72; H, 7.17.

II.3.4. Synthesis of [RhCl(COD){κ^1(P)PhP($CH_2CH{=}CH_2$)$_2$}] (22c)

To a solution of [$Rh_2(\mu\text{-}Cl)_2(COD)_2$] (100 mg, 0.203 mmol) in CH_2Cl_2 (20 mL) was added dropwise a solution of diallylphenylphosphine (**c**) (81.0 mg, 0.426 mmol) in 10 mL of CH_2Cl_2. The solution was stirred for 1 h at -80°C. The solution was evaporated to dryness to give a yellow solid, which was washed with hexane (5 mL) and vacuum-dried. Yield: 182 mg, 98%. $^{31}P\{^1H\}$ NMR (121.49 MHz, $CDCl_3$, 25°C): δ = 14.15 (d, J_{PRh} = 148.4 Hz). ^1H NMR (300.13 MHz, $CDCl_3$, 25°C): δ = 1.85-1.99 (m, 4H, CH_{2COD}), 2.29 (brs, 4H, PCH_2), 2.78-3.01 (m, 4H, CH_{2COD}), 3.23 (brs, 2H, $CH{=}CH_{COD}$), 5.09-5.16 (m, 4H, $=CH_2$), 5.36 (brs, 2H, $CH{=}CH_{COD}$), 5.79-5.95 (m, 2H, CH=), 7.33-7.35 (m, 3H, CH_{Ar}), 7.50-7.57 (m, 2H, CH_{Ar}). $^{13}C\{^1H\}$ NMR (75.47 MHz, $CDCl_3$, 25°C): δ = 28.46 (s, 2C, CH_{2COD}), 29.98 (d, J_{CP} = 23.7 Hz, 2C, PCH_2), 32.89 (s, 2C, CH_{2COD}), 69.42 (d, J_{CRh} = 13.8 Hz, 2C, $CH{=}CH_{COD}$), 104.54 (dd, $^2J_{CP}$ = 6.8 Hz, J_{CRh} = 11.9 Hz, 2C, $CH{=}CH_{COD}$), 118.78 (d, $^3J_{CP}$= 10.3 Hz, 2C, $=CH_2$), 128.17 (d, $^3J_{CP}$= 8.8 Hz, 2C, CH_{Ar}), 129.70 (s, CH_{Ar}), 130.71 (brs, C_{ipso}), 131.09 (d, $^2J_{CP}$= 4.7 Hz, 2C, CH=), 131.36 (d, $^2J_{CP}$= 8.7 Hz, 2C, CH_{Ar}). Anal. Calcd for $C_{20}H_{27}ClPRh$: C, 54.99; H, 6.18. Found: C, 52.76; H, 6.17.

II.3.5. Synthesis of [Rh(COD){κ^3(P,C,C)^{i}Pr$_2$NP(CH$_2$CH=CH$_2$)$_2$}][BF$_4$] (<u>23a</u>)

A solution of [RhCl(COD){κ^1(P)^{i}Pr$_2$NP(CH$_2$CH=CH$_2$)$_2$}] (100 mg, 0.22 mmol) in THF (20 mL) was treated with $AgBF_4$ (42.4 mg, 0.22 mmol), and the mixture was stirred for 1 h at -80°C. The solution was evaporated to dryness. The resulting solid was extracted with dichloromethane (2 x 20 mL) and vacuum-dried to give the complex as orange solid which was washed with diethyl ether (20 mL) and vaccuum-dried. Suitable orange crystals were obtained by slow diffusion of diethyl ether in a solution of complex (**<u>23a</u>**) in CH_2Cl_2. Yeild: 90 mg, 80%. $^{31}P\{^1H\}$ NMR (202.41 MHz, CD_2Cl_2, 25°C): δ - 23.79 (d, J_{PRh} = 104.4 Hz). ^1H NMR (500.03 MHz, CD_2Cl_2, 25°C): δ 1.17 (d, $^3J_{HH}$= 6.6 Hz, 12H, CH_{3N^iPr}), 2.24-2.44 (m, 8H, CH_{2COD}), 2.93 (t, 4H, J_{PH}= 7.1 Hz, PCH_2), 3.34 (d, $^3J_{HH}$= 5.9 Hz, 2H,CH_{N^iPr}), 4.53 (dd, $^3J_{HH}$= 16.3 Hz, $^3J_{HH}$= 9.0 Hz, 4H, =CH_2), 5.00 (brs, 1H, CH= $_{COD}$), 5.28 (brs, 1H, CH= $_{COD}$), 5.87 (brs, 2H, CH=). $^{13}C\{^1H\}$ (125.74 MHz, CD_2Cl_2, 25°C): δ 24.93 (s, CH_{3NiPr}), 29.05 (s, 2C, CH_{2COD}), 31.97 (s, CH_{2COD}), 32.00 (s, CH_{2COD}), 34.51 (d, J_{CP} = 27.5 Hz, PCH_2), 47.30 (s, CH_{NiPr}), 89.15 (d, J_{CRh} = 7.6 Hz, CH=CH_{COD}), 100.18 (brs, =CH_2), 107.56 (d, $^2J_{CP}$ = 7.6 Hz, CH=), 107.88 (dd, $^2J_{CP}$ = 5.0 Hz, J_{CRh} = 9.9 Hz, 2C, CH=CH_{COD}). Anal. Calcd for $C_{20}H_{36}NBF_4PRh$: C, 46.99; H, 7.04; N, 2.74. Found: C, 44.91; H, 7.06; N, 2.86. $^{31}P\{^1H\}$ NMR (202.41 MHz, CD_2Cl_2, -90°C): δ - 22.79 (d, J_{PRh} = 100.7 Hz). ^1H NMR (500.03 MHz, CD_2Cl_2, -90°C): δ 0.99 (brs, 9H, CH_{3NiPr}), 1.41 (brs, 3H, CH_{3NiPr}), 2.07-2.63 (m, 10H, $PCH_{2\ not\ coordinated}$, CH_{2COD}), 3.20 (brs, 4H, $PCH_{2\ coordinated}$, CH_{NiPr}), 3.67 (d, $^3J_{HH}$= 13.9 Hz, 1H, $=CH_{2\ coordinated}$), 3.77 (brs, 1H, $=CH_{2\ coordinated}$), 4.48 (brs, 1H, CH= $_{COD}$), 4.69 (brs, 1H, CH= $_{COD}$), 5.20 (brs, 2H, $=CH_{2\ not\ coordinated}$), 5.52 (brs, 1H, CH= $_{COD}$), 5.64 (brs, 2H, CH= $_{COD}$, CH= $_{not\ coordinated}$), 5.98 (brs, 1H, CH= $_{coordinated}$) . $^{13}C\{^1H\}$ NMR (125.74 MHz, CD_2Cl_2, -90°C): δ 20.80 (brs, CH_{3NiPr}), 21.49 (brs, CH_{3NiPr}), 25.84 (brs, CH_{3NiPr}), 27.11 (s, CH_{2COD}), 28.73 (s, CH_{2COD}), 30.05 (s, CH_{2COD}), 31.07 (brs, CH_{3NiPr}), 31.97 (s, CH_{2COD}), 32.35 (d, J_{CP} = 36.3 Hz, $PCH_{2\ not\ coordinated}$), 34.63 (s, CH_{2COD}), 35.50 (d, J_{CP} = 20.3 Hz, $PCH_{2\ coordinated}$), 41.74 (brs, CH_{NiPr}), 50.23 (brs, CH_{NiPr}), 76.99 (s, $=CH_{2\ coordinated}$), 79.59 (s, CH= $_{COD}$), 83.18 (s, CH= $_{coordinated}$), 93.75 (s, CH= $_{COD}$), 103.56 (s, CH= $_{COD}$), 111.10 (s, CH= $_{COD}$), 120.66 (s, $=CH_{2\ not\ coordinated}$), 127.73 (s, CH= $_{not\ coordinated}$).

II.3.6. Synthesis of [Rh(COD){κ^3(P,C,C)^{t}BuP($CH_2CH{=}CH_2$)$_2$}][BF_4] (<u>23b</u>)

A solution of [RhCl(COD){κ^1(P)^{t}BuP($CH_2CH{=}CH_2$)$_2$}] (100 mg, 0.24 mmol) in THF (20 mL) was treated with $AgBF_4$ (46.7 mg, 0.24 mmol), and the mixture was stirred for 1 h at -80°C. The solution was evaporated to dryness. The resulting solid was extracted with dichloromethane (2 x 20 mL) and vacuum-dried to give the complex as orange solid which was washed with diethyl ether (20 mL) and vaccuum-dried. Suitable orange crystals were obtained by slow diffusion of diethyl ether in a solution of complex (<u>**23b**</u>) in CH_2Cl_2. Yeild: 88 mg, 86%. $^{31}P\{^1H\}$ NMR (202.41 MHz, CD_2Cl_2, 25°C): δ - 68.22 (d, J_{PRh} = 110.1 Hz). ^1H NMR (500.03 MHz, CD_2Cl_2, 25°C): δ 1.21 (d, $^2J_{PH}$= 16.1 Hz, 9H, $CH_3{}^t{}_{Bu}$), 2.27-2.59 (m, 8H, CH_{2COD}), 2.96-3.07 (m, 4H, PCH_2), 4.84 (dd, $^3J_{HH}$= 9.5 Hz, $^4J_{PH}$= 3.5 Hz, 2H, $=CH_2$), 5.06 (dd, $^3J_{HH}$= 16.5 Hz, $^4J_{PH}$= 2.9 Hz, 2H, $=CH_2$), 5.25 (brs, 2H, $CH{=}CH_{COD}$), 5.79-5.89 (m, 2H, CH=). $^{13}C\{^1H\}$ NMR (125.74 MHz, CD_2Cl_2, 25°C): δ 25.99 (d, J_{CP} = 20.5 Hz, 2C, PCH_2), 26.91 (d, $^2J_{CP}$ = 3.8 Hz, 3C, $CH_3{}^t{}_{Bu}$), 29.23 (s, 2C, CH_{2COD}), 31.69 (d, J_{CP} = 17.0 Hz, $PC^t{}_{Bu}$), 32.03 (s, CH_{2COD}), 32.05 (s, CH_{2COD}), 90.99 (d, J_{CRh} = 10.3 Hz, 2C, $CH{=}CH_{COD}$), 105.86 (dd, $^2J_{CP}$ = 6.0 Hz, J_{CRh} = 8.5 Hz, 2C, $CH{=}CH_{COD}$), 107.23 (brs, $=CH_2$), 107.94 (d, $^3J_{CP}$= 7.6 Hz, $=CH_2$), 113.07 (d, $^2J_{CP}$= 7.4 Hz, 2C, CH=). Anal. Calcd for $C_{18}H_{31}BF_4PRh$: C, 46.18; H, 6.62. Found: C, 45.20; H, 6.56.

II.3.7. Synthesis of [Rh(COD){κ^3(P,C,C)PhP($CH_2CH{=}CH_2$)$_2$}][BF_4] (<u>23c</u>)

A solution of [RhCl(COD){κ^1(P)PhP($CH_2CH{=}CH_2$)$_2$}] (100 mg, 0.23 mmol) in THF (20 mL) was treated with $AgBF_4$ (44.6 mg, 0.23 mmol), and the mixture was stirred for 1 h at -80 °C. The solution was evaporated to dryness. The resulting solid was extracted with dichloromethane (2 x 20 mL) and vacuum-dried to give the complex as orange solid which was washed with diethyl ether (20 mL) and vaccuum-dried. Yeild: 94 mg, 88%. $^{31}P\{^1H\}$ NMR (202.40 MHz, $CDCl_3$, 25°C): δ = 2.88 (d, J_{PRh} = 143.6 Hz). ^1H NMR (500.00 MHz, CD_2Cl_2, 25°C): δ = 2.06-2.15 (m, 3H, 3/2 PCH_2), 243-265 (m, 8H, CH_{2COD}), 3.08 (m, 1H, ½ PCH_2), 5.02 (d, $^3J_{HH}$= 17.2 Hz, 2H, $=CH_2$), 5.17 (d, $^3J_{HH}$= 9.8 Hz, 2H, $=CH_2$), 5.28 (brs, 2H, $CH{=}CH_{COD}$), 5.37 (brs, 2H, $CH{=}CH_{COD}$) 5.44 (m, 1H, CH=), 5.82 (m, 1H, CH=), 7.26 (brs, 2H, CH_{Ar}), 7.49 (m, 3H, CH_{Ar}). $^{13}C\{^1H\}$ NMR (125.73 MHz, $CDCl_3$, 25°C): δ = 26.92 (m, PCH_2), 28.19 (brs, PCH_2), 29.72 (s, 3C, CH_{2COD}), 30.67 (s, CH_{2COD}), 97.69 (brs, 2C, $CH{=}CH_{COD}$), 106.63 (brs, 2C, $CH{=}CH_{COD}$), 107.52 ppm, (d, $^3J_{CP}$= 7.6 Hz, 2C, $=CH_2$), 120.72

(brs, 2C, CH=), 129.32 (s, CH_{Ar}), 131.66 (m, 2C, CH_{Ar}), 131.22 (s, C_{ipso}), 131.69 (m, 2C, CH_{Ar}). Anal. Calcd for $C_{20}H_{27}BF_4PRh$: C, 49.21; H, 5.53. Found: C, 49.24; H, 5.32.

II.3.8. Crystallographic data

The data of the structures (**23a**) and (**23b**) were collected on a *Rigaku AFC-7S* diffractometer at temperature of 298 and 150K with graphite-monochromated MoKα radiation (wavelength = 0.71073 Å). The structure was solved by direct methods, using SHELXS97.

23a: $C_{20}H_{36}BF_4NPRh$, M= 511.19, Orthorhombic, space group $Pca2_1$, a= 16.644(6) Å, b= 11.351(5) Å, c= 23.436(7) Å, V= 4428(3) $Å^3$, Z= 8, crystal size 0.49 x 0.32 x 0.25 mm^3, 27780 reflections collected (7962 independent, R_{int}= 0.045), 524 parameters, $R1$ [I>2σ(I)]= 0.045, $wR2$ [all data]= 0.121, largest diff. peak and hole: 1.94 and -0.59 e.$Å^{-3}$.

23b: $C_{18}H_{31}BF_4PRh$, M= 468.12, Triclinic, space group $P\bar{1}$, a= 7.823(3) Å, b= 9.890(5) Å, c= 14.034(6) Å, α= 105.467(9), β=91.059(13)°, γ= 94.402(15)°, V=1042.5(8) $Å^3$, Z= 2, crystal size 0.46 x 0.23 x 0.22 mm^3, 11518 reflections collected (3899 independent, R_{int}=0.033), 263 parameters, $R1$ [I>2σ(I)]= 0.0703, $wR2$ [all data]= 0.2002, largest diff. peak and hole: 066 and -0.79 e.$Å^{-3}$.

II.4. Conclusions

Diallylphosphine ligands (**a-c**) react with dimer complex $[Rh_2(\mu\text{-}Cl)_2(COD)_2]$ (2:1 ratio molar) to give the neutral complexes $[RhCl(COD)\{\kappa^1(P)RP(CH_2CH{=}CH_2)_2\}]$ [R= $^{i}Pr_2N$ (**22a**), ^{t}Bu (**22b**) and Ph (**22c**)].

Chloride abstraction reactions from (**22a**), (**22b**) and (**22c**) led to formation of the cationic complexes $[Rh(COD)\{\kappa^3(P,C,C)RP(CH_2CH{=}CH_2)_2\}][BF_4]$ (**23a-c**), where the diallylphosphines act as chelating ligands by π-coordination of one allyl moiety to fill the vacant position left by chloride ligand.

Diallyldiisopropylaminephosphine (**a**) ligand in the complex (**23a**) exhibits a hemilabile behavior in solution, which involves the intramolecular exchange of the weakly bonding alkenes groups on the metal center. This behavior in solution provides a mixture equilibrium of the two enantiomers $\boldsymbol{R_P}$-(**23a**) and $\boldsymbol{S_P}$-(**23a'**). Molecular structure of $\boldsymbol{R_P}$-(**23a**) and $\boldsymbol{S_P}$-(**23a'**) was confirmed by X-ray diffraction analysis.

Molecular structures of complexes (**23a**) and (**23b**) showed the coordination of one of allyl groups on the rhodium demonstrating the bidentate character of the diallylphosphine ligands.

Diallylphosphines (**a-c**) showed to be versatile ligands to act as monodentate or polydentate ligands to stabilize cationic metal species.

Charpter III

Hemilabile properties of the diallylphosphine ligands

III.1 Introduction

An important feature that may arise from hemilability in the metal complex is the facility to undergo ligand interchange reactions that involve equilibria between weakly bonding groups of hemilabile ligand and external molecules, such as a monodentate ligand, a small molecule, or an organic substrate (Figure III.1). These interchange processes are detected by variable temperature NMR spectroscopic.[9,10]

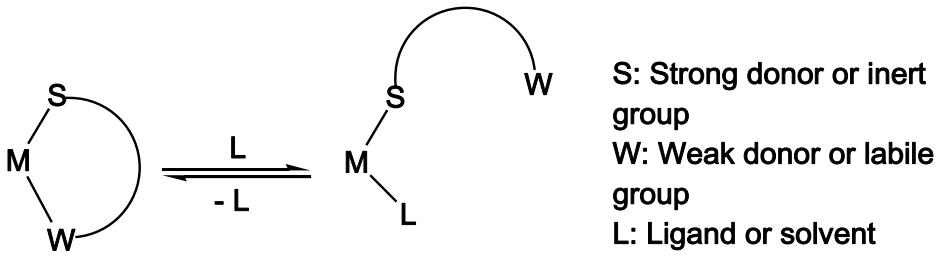

Figure III.1. Hemilability of hibrid ligands.

The bifunctional character of diallylphosphines may enable to these ligands the facile displacement of weakly coordinated alkene by a small molecule, remaining available for recoordination to the metal center to restore the original complex.[9] In this sense and in order to evaluate the hemilabile properties of diallylphosphine ligands (**a-c**), were carried out the reaction of complexes (**23a-c**) in presence of acetonitrile.

III.2. Results and discussions

III.2.1. Reaction of complexes [Rh(COD){κ^3(P,C,C)RP($CH_2CH=CH_2)_2$}][BF_4] (23a-c) with acetonitrile

Addition of excess acetonitrile to a CD_2Cl_2 solution of complexes (**23a-c**) produced the displacement of the allylic double bond from the rhodium center, leading to the formation of the acetonitrile substituted cationic rhodium complexes [Rh(COD){κ^1(P)RP($CH_2CH=CH_2)_2$}(CH_3CN)][BF_4] [R= $^iPr_2N$ (**24a**), ^{t}Bu (**24b**) and Ph (**24c**)], as orange oil (Scheme III.1).

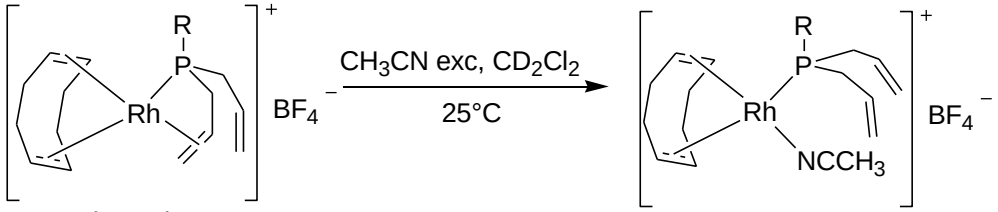

(**23a-c**) (**24a-c**)

R= $^iPr_2N$ (**a**), ^{t}Bu (**b**), Ph (**c**)

Scheme III.1. General reaction of [Rh(COD){κ^3(P,C,C)RP($CH_2CH=CH_2)_2$}][BF_4] (**23a-c**) with excess of acetonitrile.

Complexes (**24a-c**) show in the $^{31}P\{^1H\}$ NMR spectra doublet resonances shifted toward downfield with respect to observed for respective complexes (**23a-c**) and similar to those observed for complexes (**22a-c**), [δ 56.40 (d, J_{PRh} = 150.4 Hz) for (**24a**), δ 27.26 (d, J_{PRh} = 142.4 Hz) for (**24b**) and δ = 13.25 (d, J_{PRh} = 144.9 Hz) for (**24c**)], which is in agreement with a non metallacycle compound.[60] In the ^1H and $^{13}C\{^1H\}$ NMR spectra can also be observed the reappearance of the signals corresponding to the uncoordinated doublet bonds of the allyl groups (Table III.1).

An attempt for isolating the complexes (**24a-c**), as solids, revealed the existence of an equilibrium between the cationic rhodium species (**23**) and (**24**) respectively (Scheme III.2). Interestingly, the $^{31}P\{^1H\}$ NMR spectra at -80°C showed that after four days under high vacuum (10^{-3} mmHg) acetonitrile ligand was almost fully displaced in the case of (**24a**), whereas for (**24b**) and (**24c**) were observed a mixture corresponding to allyl coordinated (**23**) and acetonitrile coordinated (**24**) in a ratio of 7.8:2.2 and 6:4 respectively (Figure III.2).

Table III.1. ^{1}H and $^{13}C\{^{1}H\}$ NMR data of complexes (**24a-c**)

Complexes	δ ^{1}H NMR [a]	δ $^{13}C\{^{1}H\}$ NMR [a]
24a	2.20 (s, CH_{3CN}) 5.30 (m, $=CH_2$) 6.05 (m, CH=)	3.26 (s, CH_{3CN}) 118.20 (brs, 2C, $=CH_2$) 123.26 (brs, NC) 127.56 (s, 2C, CH=)
24b	2.23 (s, CH_{3CN}) 5.25 (m, $=CH_2$) 5.95 (m, CH=)	3.42 (s, CH_{3CN}) 116.93 (brs, 2C, $=CH_2$) 125.73 (brs, 2C, CH=) 127.97 (brs, NC)
24c	2.27 (s, CH_{3CN}) 5.24 (m, $=CH_2$) 5.72 (m, CH=)	3.09 (s, CH_{3CN}) 120.60 (d, $^{3}J_{CP}$= 9.97 Hz, 2C, $=CH_2$) 126.78 (brs, NC) 130.87 (brs, 2C, CH=)

[a] Spectra recorded in CD_2Cl_2 at 25°C.

These results indicate that allylic double bond can be reversibly displaced from rhodium center in the presence of acetonitrile. This observation reveals the hemilabile properties of the diallylphosphine ligands. Moreover, the results indicate that the displacement of acetonitrile ligand under vacuum is easier in the complex (**24a**) that for complexes (**24b**) and (**24c**).

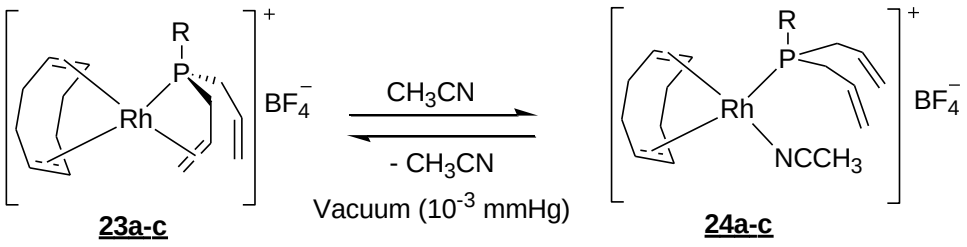

23a-c **24a-c**

R= $^{i}Pr_2N$ (**a**), ^{t}Bu (**b**), Ph (**c**)

Scheme III.2. Reversible displacement of the coordinated allyl bonds by acetonitrile.

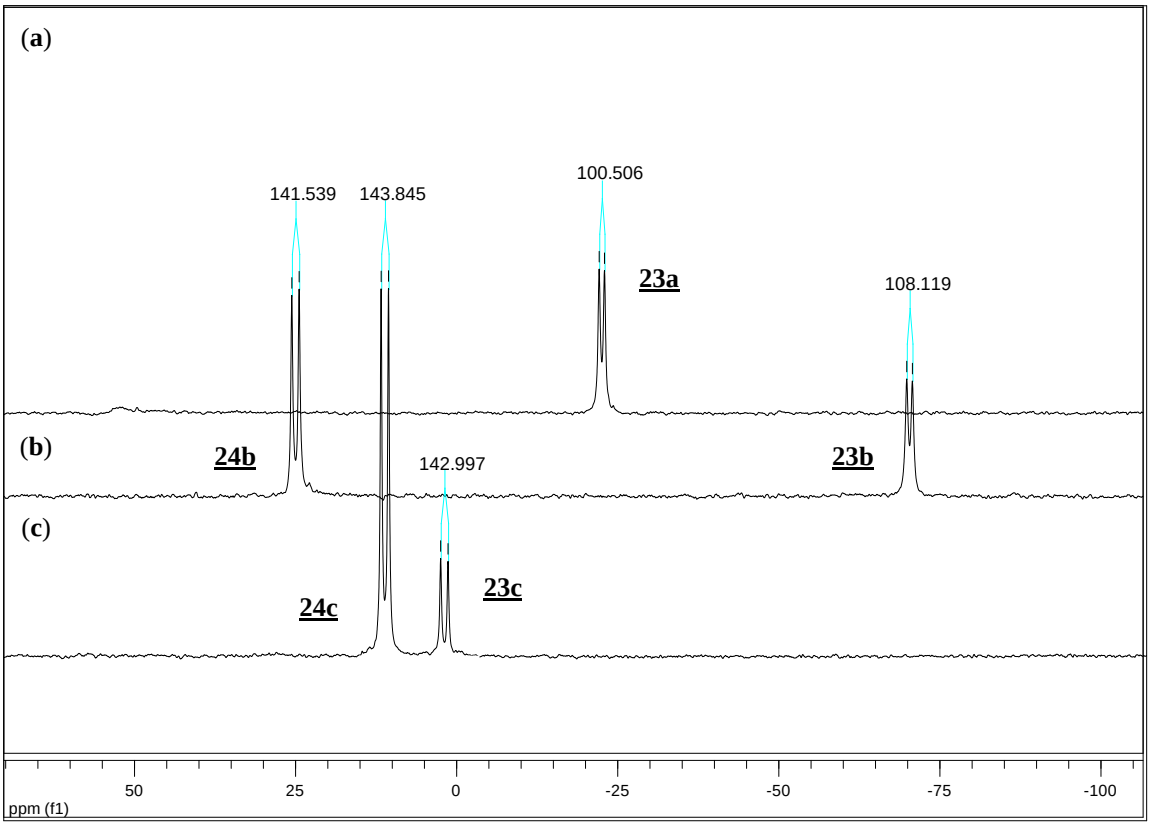

Figure III.2. $^{31}P\{^{1}H\}$ NMR spectra at -80°C after of four days under high vacuum for complexes (**a**) (**24a**), (**b**) (**24b**) and (**c**) (**24c**).

In order to gain more understanding of these experimental results, DFT calculations were performed on the reaction of complexes (**23a-c**) with acetonitrile (Figure III.3). The theoretical calculations predict a single-step mechanism for the ligand exchange reaction, which proceeds exothermically through the formation of a five-coordinate cationic rhodium species in the TS (Figure III.3).

In the table III.2 are shown the calculated energy values for (**23a-c**), (**24a-c**) and the obtained transition state geometries, as well as, selected distances bond corresponding to the structures (**23a-c**) and (**24a-c**). Meanwhile, in table III.3 4 are shown the calculated Bader charges (q) of some atoms and the value of the electronic density at the bond critical point (BCP) for some interactions (ρ).

As expected, the atomic charge values indicate that the rhodium atom is electron deficient in both (**23a-c**) and (**24a-c**) set of molecules (Table III.3), which can explain the observed interaction of the nitrile with the metal center when the first one is introduced on the system, even if is located relatively far away (d_{RhN} ~ 5-6 Å) from the metal center, inducing a

slight elongation of bond distance between the rhodium and both the carbon atoms of the coordinated double bond, if it is compared with experimental values obtained by X-ray diffraction.

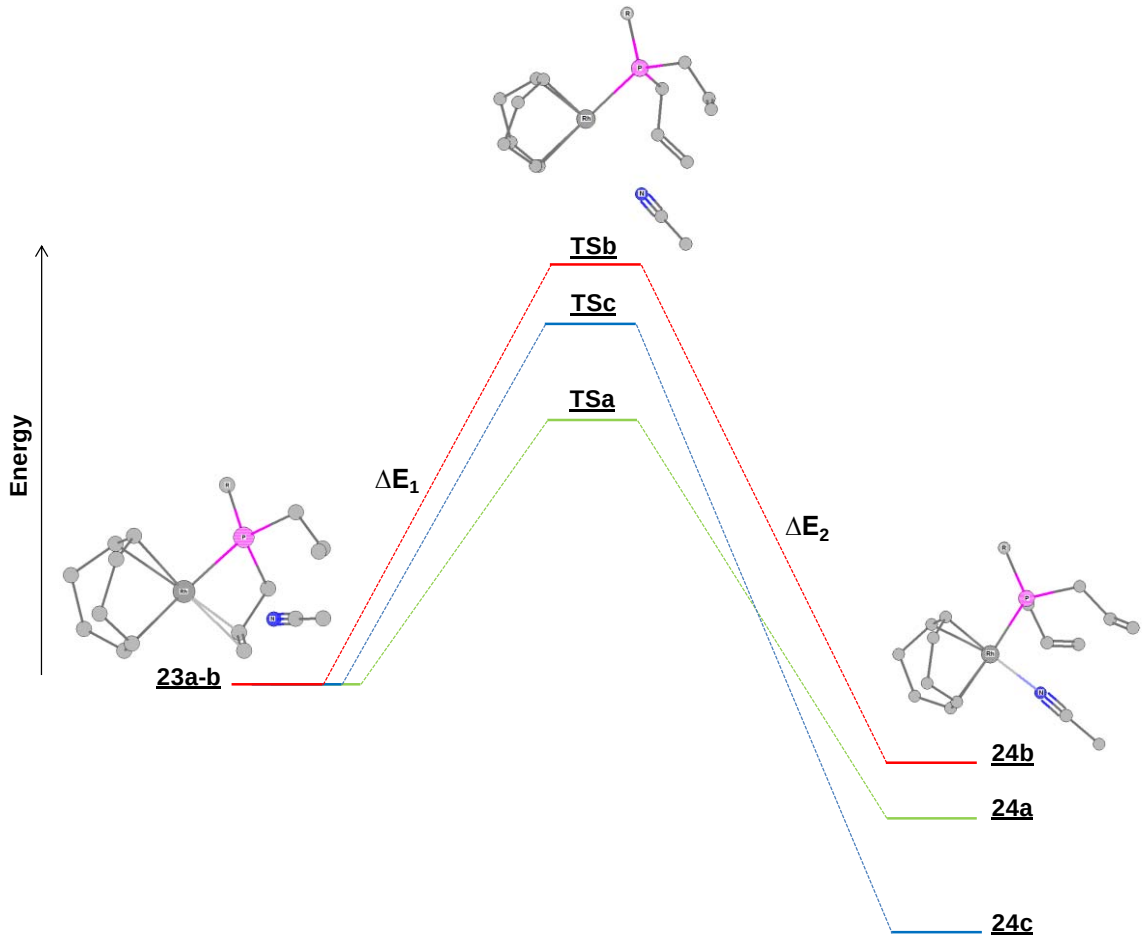

Figure III.3. Energy diagram for reaction of complexes (**23a-c**) with acetonitrile calculated at DFT level.

Table III.2. Calculated energies (in kcal/mol) for complexes (**23a-c**), (**24a-c**) and (**TSa-c**) and selected distance bonds (Å) for los complexes (**23a-c**) and (**24a-c**)

	23				**24**				**TS**		
	E	d_{Rh-N}	d_{Rh-C} [a]	d_{Rh-P}	E	d_{Rh-N}	d_{Rh-C} [a]	d_{Rh-P}	E_{TS}	ΔE_1	ΔE_2
a, $^{i}Pr_2N$	0.0	5.597	2.340	2.381	- 5.30	2.129	4.797	2.460	9.45	9.45	14.75
b, ^{t}Bu	0.0	4.807	2.374	2.406	- 3.22	2.126	4.927	2.543	15.20	15.20	18.42
c, Ph	0.0	5.790	2.306	2.380	- 9.62	2.127	4.913	2.441	13.05	13.05	22.67

[a] $Rh-CH_{2allyl}$ distance bonds.

The energy barrier values, ΔE_1 and ΔE_2 in figure III.3, indicate that theoretical calculations are in agreement with the experimental observations. In this sense, complexes (**24a-c**) are more stable than the corresponding (**23a-c**) and ΔE_1 barriers are enough lower to explain the equilibrium displacement to (**24a-c**) at room temperature, moreover, the energy values calculated for inverse reactions (**24** → **23**) indicate that the displacement of acetonitrile ligand is easier in the complexes (**24a**) that in the complexes (**24b**) and (**24c**) respectively (order of ΔE_2 = (**24a**) < (**24b**) < (**24c**)), which agrees with the order observed experimentally.

The calculated values of the whole charge on both phosphine and acetonitrile ligands in complexes (**24a-c**) are similar (Table III.3), showing that covalent character of bonds Rh−P and Rh−N do not significantly changes when we go from (**24a**) to (**24b**) and from (**24b**) to (**24c**). Nevertheless, the low values of ρ at the Rh−N BCP, suggests that the Rh-N bonds are polarized, showing a marked ionic character. Indeed, the values of ρ at the Rh−N BCP, are in the same order to calculated values of ρ for some inorganic salts.[64,65] In this way, a comparison of charge on the rhodium atom and nitrogen atom of acetonitrile ligand, in complexes (**24a-c**), shows that $\Delta q_{Rh\text{-}N}$ increases in the order (**24a**) < (**24b**) < (**24c**), this trend indicates that the electrostatic interaction between the acetonitrile ligand and the rhodium atom increases in the same order, which might explain why it is easier experimentally to displacement under high vacuum the acetonitrile ligand for complex (**24a**) that for complexes (**24b**) and (**24c**) respectively.

Table III.3. Atomic charge (q) and electron density (ρ) at the BCP (in a.u.)

	24							**23**
	q_{Rh} [a]	q_N [b]	$\Delta q_{Rh\text{-}N}$ [c]	q_{TP} [d]	q_{TCN} [d]	$\rho_{Rh\text{-}N}$ [e]	$\rho_{Rh\text{-}P}$ [e]	q_{Rh} [a]
a, $^{i}Pr_2N$	0.51	- 1.35	- 0.84	0.89	0.17	0.075	0.087	1.33
b, ^{t}Bu	0.96	- 1.20	- 0.27	0.88	0.17	0.074	0.081	0.87
c, Ph	1.43	- 1.23	+ 0.23	0.89	0.19	0.075	0.086	1.14

[a] Rh atomic charge. [b] N atomic charge of nitrile. [c] Difference between q_{Rh} and q_N. [d] Overall charge for the phosphine and acetonitrile ligands (q_{TP}) and (q_{TCN}). [e] Electron density at the Rh-N and Rh-P bond critical points.

We can then conclude that, since the covalent component of the interaction between the acetonitrile ligand and rhodium atoms are almost equivalents, is the electrostatic component of the interaction, which is responsible of the experimentally observed behaviour.

III.3. Experimental part

III.3.1. General Considerations

All manipulations were performed under an inert atmosphere of argon by using standard Schlenk techniques. Dry, oxygen-free solvents were employed. All reagents were obtained from commercial suppliers.

^{1}H, $^{13}C\{^{1}H\}$, $^{31}P\{^{1}H\}$ NMR spectra were recorded on Bruker, Avance 500 or Avance 300 spectrometers. ^{1}H, $^{13}C\{^{1}H\}$ NMR chemical shifts are reported in ppm relative to Me_4Si as external standard. $^{31}P\{^{1}H\}$ NMR chemical shifts are expressed in ppm relative to 85% H_3PO_4.

III.3.2. Reaction of [Rh(COD){κ^3(P,C,C)^{i}PrNP($CH_2CH=CH_2)_2$}][BF_4] (<u>23a</u>) with acetonitrile

To a solution of [Rh(COD){κ^3(P,C,C)^{i}PrNP($CH_2CH=CH_2)_2$}][BF_4] (60 mg, 0.117 mmol) in CD_2Cl_2 (50 µL) was added a solution of CH_3CN (12.5 µL , 0.234 mmol). The solution was stirred for 15 min at RT, and then was evaporated to dryness to give an orange oil. $^{31}P\{^{1}H\}$ NMR (121.49 MHz, CD_2Cl_2, 25°C): δ 56.40 (d, J_{PRh} = 150.4 Hz). ^{1}H NMR (300.13 MHz, CD_2Cl_2, 25°C): δ 1.33 (d, $^{3}J_{HH}$= 6.8 Hz, 12H, CH_{3NiPr}), 2.08 (m, 4H, CH_{2COD}), 2.20 (s, 5H, CH_{3CN}), 2.38-2.75 (m, 8H, CH_{2COD}, PCH_2), 3.76 (m, 2H, CH_{NiPr}), 4.10 (brs, 2H, $CH=CH_{COD}$), 5.20-5.32 (m, 6H, $=CH_2$, $CH=CH_{COD}$), 6.05 (m, 2H, CH=). $^{13}C\{^{1}H\}$ NMR (75.47 MHz, $CDCl_3$, 25°C): δ 3.26 (s, CH_{3CN}), 25.37 (s, 2C, CH_{3NiPr}), 25.40 (s, 2C, CH_{3NiPr}), 28.92 (brs, 2C, PCH_2), 32.86 (s, CH_{2COD}), 32.89 (s, CH_{2COD}), 33.22 (s, CH_{2COD}), 33.54 (s, CH_{2COD}), 50.61 (d, $^{2}J_{CP}$ = 4.4 Hz, 2C, CH_{NiPr}), 78.55 (d, J_{CRh} = 13.6 Hz, 2C, $CH=CH_{COD}$), 104.53 (dd, $^{2}J_{CP}$ = 6.4 Hz, J_{CRh} = 10.6 Hz, 2C, $CH=CH_{COD}$), 118.20 (brs, 2C, $=CH_2$), 123.26 (brs, NC), 127.56 (s, 2C, CH=).

III.3.3. Reaction of [Rh(COD){κ^3(P,C,C)^{t}BuP($CH_2CH=CH_2)_2$}][BF_4] (<u>23b</u>) with acetonitrile

To a solution of [Rh(COD){κ^3(P,C,C)^{t}BuP($CH_2CH=CH_2)_2$}][BF_4] (60 mg, 0.128 mmol) in CD_2Cl_2 (50 µL) was added a solution of CH_3CN (13.6 µL , 0.256 mmol). The

solution was stirred for 15 min at RT, and then was evaporated to dryness to give an orange oil. $^{31}P\{^{1}H\}$ NMR (121.49 MHz, CD_2Cl_2, 25°C): δ 27.26 (d, J_{PRh} = 142.4 Hz). ^{1}H NMR (300.13MHz, CD_2Cl_2, 25°C): δ 1.35 (d, $^{2}J_{PH}$= 14.7 Hz, 9H, $CH_3{}^{t}_{Bu}$), 2.17 (brs, 4H, CH_{2COD}), 2.23 (s, 5H, CH_{3CN}), 2.43 (brs, 4H, CH_{2COD}), 2.53 (m, 4H, PCH_2), 4.27 (brs, 2H, $CH{=}CH_{COD}$), 5.28-5.32 (m, 6H, $CH{=}CH_{COD}$, $=CH_2$), 5.95 (m, 2H, CH=). $^{13}C\{^{1}H\}$ NMR (75.47 MHz, $CDCl_3$, 25°C): δ 3.42 (s, CH_{3CN}), 25.38 (d, J_{CP} = 19.6 Hz, 2C, PCH_2), 28.17 (d, $^{2}J_{CP}$ = 2.9 Hz, 3C, $CH_3{}^{t}_{Bu}$), 28.64 (s, 2C, CH_{2COD}), 32.37 (s, 2C, CH_{2COD}), 33.92 (d, J_{CP} = 19.01 Hz, PC^{t}_{Bu}), 80.64 (d, J_{CRh} = 10.3 Hz, 2C, $CH{=}CH_{COD}$), 104.19 (t, $^{2}J_{CP}$ = 8.0 Hz, 2C, $CH{=}CH_{COD}$), 116.93 (brs, 2C, $=CH_2$), 125.73 (brs, 2C, CH=), 127.97 (brs, NC).

III.3.4. Reaction of $[Rh(COD)\{\kappa^3(P,C,C)PhP(CH_2CH{=}CH_2)_2\}][BF_4]$ (<u>23c</u>) with acetonitrile

To a solution of $[Rh(COD)\{\kappa^3(P,C,C)PhP(CH_2CH{=}CH_2)_2\}][BF_4]$ (62 mg, 0.127 mmol) in CD_2Cl_2 (50 µL) was added a solution of CH_3CN (13.5 µL , 0.254 mmol). The solution was stirred for 15 min at RT, and then was evaporated to dryness to give an orange oil. $^{31}P\{^{1}H\}$ NMR (121.49 MHz, CD_2Cl_2, 25°C): δ 13.25 (d, J_{PRh} = 144.9 Hz). ^{1}H NMR (300.13 MHz, $CDCl_3$, 25°C): δ 2.05 (m, 4H, CH_{2COD}), 2.27 (s, 8H, CH_{3CN}, PCH_2), 2.78 (m, 4H, CH_{2COD},), 3.76 (m, 2H, CH_{NiPr}), 3.84 (brs, 2H, $CH{=}CH_{COD}$), 5.19-5.24 (m, 6H, $=CH_2$, $CH{=}CH_{COD}$), 5.72 (m, 2H, CH=), 7.43-7.47 (m, 3H, CH_{Ar}), 7.51-7.56 (m, 2H, CH_{Ar}). $^{13}C\{^{1}H\}$ NMR (75.47 MHz, $CDCl_3$, 25°C): δ 3.09 (s, CH_{3CN}), 27.81, 28.07 (2xs, 2C, PCH_2), 28.64 (s, CH_{2COD}), 32.34 (s, CH_{2COD}), 78.22 (brs, 2C, $CH{=}CH_{COD}$), 104.77 (brs, 2C, $CH{=}CH_{COD}$), 120.60 (d, $^{3}J_{CP}$= 9.97 Hz, 2C, $=CH_2$), 126.78 (brs, NC), 128.82 (brs, CH_{Ar}), 128.91 (s, CH_{Ar}), 129.03 (s, CH_{Ar}), 129.33 (brs, C_{ipso}), 130.87 (brs, 2C, CH=), 131.54 (d, $^{2}J_{CP}$= 9.6 Hz, 2C, CH_{Ar}).

III.3.5. Theoretical data

All structures were optimized using DMol^3.[66-68] This DFT Based program allows us determining the relative stability of all studied species based on their electronic structure. The calculations were performed using Kohn-Sham Hamiltonian with the Perdew-Wang 1991 gradient correction [69] and the double-zeta plus (DNP) numerical basic set.[66-68] The utilization of the numerical basics sets combined with DFT permits the program to obtain a high

accuracy by keeping a relative low computational cost, compared with ab-initio methods. DMol^3 calculates variational self-consistent solutions to the density functional theory (DFT) equations. The solutions to these equations provide the molecular electron densities, which can be integrated among the atomic volume (defined by the interatomic surfaces and/or the Van der Walls envelope) in order to obtain the Bader charge on each atom of the system.[64,65] TS were determined with the same code. DMol^3 uses the nudged elastic band (NEB) [70,71] method for minimum energy path calculations. The NEB method introduces a fictitious spring force that connects neighbouring points on the path to ensure continuity of the path and projection of the force so that the system converges to the minimum energy path (MEP). The NEB method has been widely used in solid-state physics and has recently been applied to molecules as well. The advantage of the NEB algorithm is that it provides a fast qualitative examination of the MEP.[66] Frecuency calculations of all transition states (TS) showed one negative frequency.

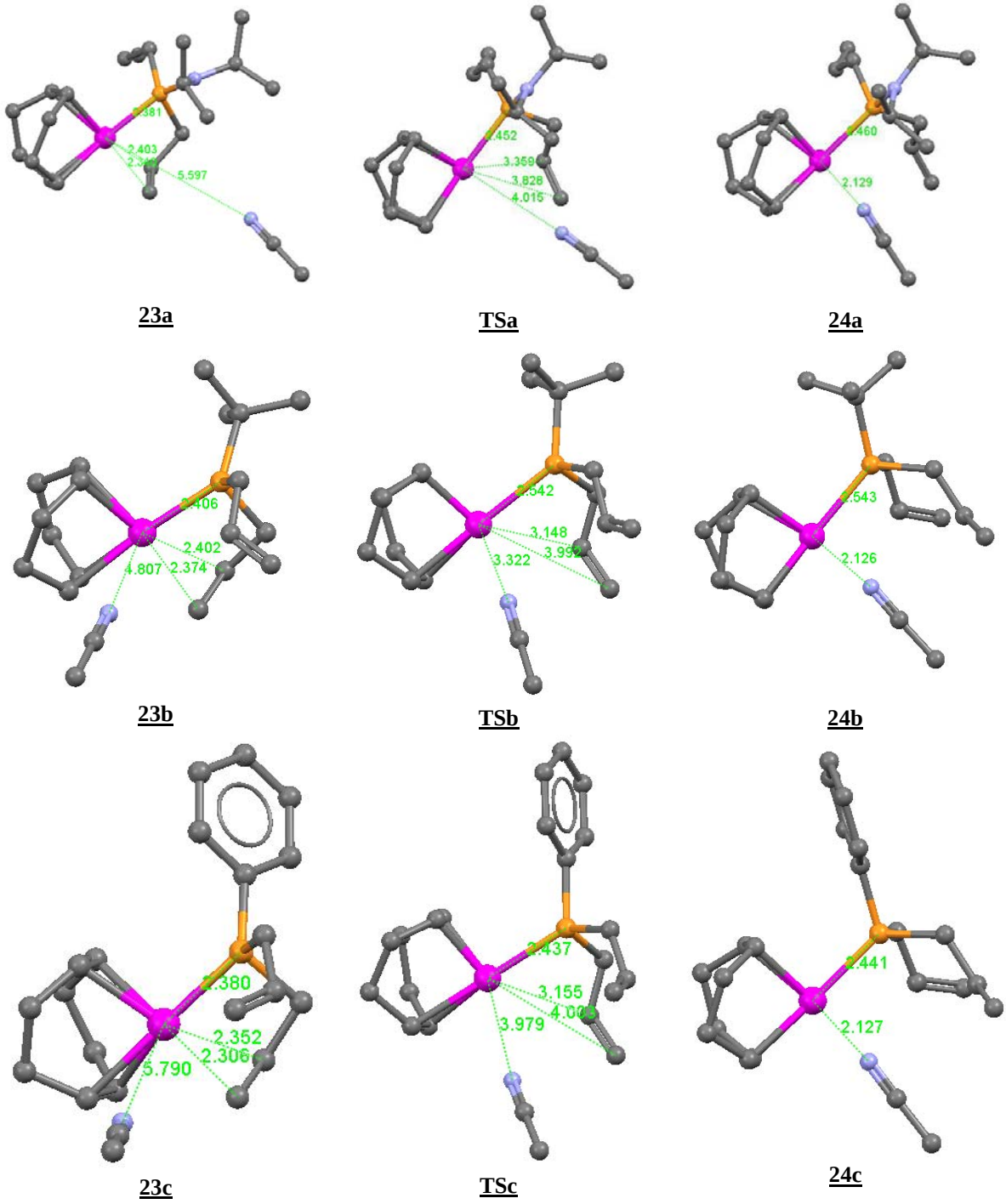

Figure III.4. Geometrical parameters for the optimized structures.

III.4. Conclusions

The hemilabile character of the diallylphosphine ligands has been demonstrated by the ligand displacement reaction with acetonitrile which can be removed under vacuum returning to original complexes.

The experimental results reveal that the displacement of acetonitrile ligand is easier in the complex (**24a**) that in the complexes (**24b**) and (**24c**). This trend has been explained on the basis of DFT calculations indicating that the electrostatic interaction between the acetonitrile ligand and the rhodium center is responsible of the experimentally observed behavior.

Charpter IV

Synthesis and reactivity of intramolecularly phosphine-stabilized germylenes

IV.1. Introduction

The chemistry of the heavier homologue of carbenes: germylenes (R_2Ge:) has received considerable attention due to their many differences and similarities to carbenes. [72-74] It has been established that the ground state of germylenes is singlet with an electron pair in σ-orbital and a vacant p-orbital and thus behave as electrophiles and nucleophiles, because both the electron pair and vacant orbital can take part in the reactions (Figure IV.1).[72]

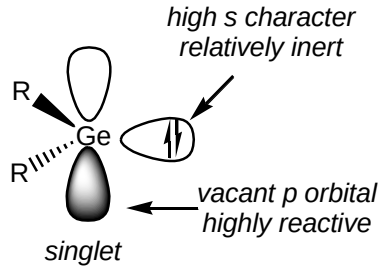

Figure IV.1. Singlet ground state of germylene.

Generally these compounds are highly reactive and tend to oligomerise or polymerize. However, germylenes can be stabilized kinetically by sterically demanding ligands and/or thermodynamically by inter- and intramolecular coordination with Lewis base ligands.[75]

1. Use of ligands that are σ- or π-donors to the germanium center.

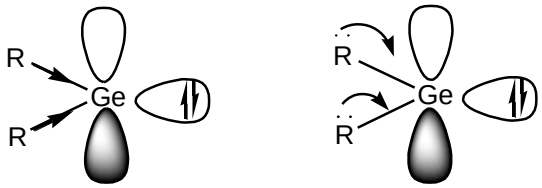

2. Use of bulky groups bonded to the germanium center.

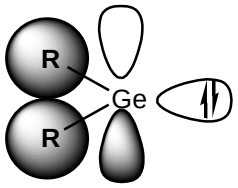

3. Coordination of a donor (Lewis base) B on the germanium center.

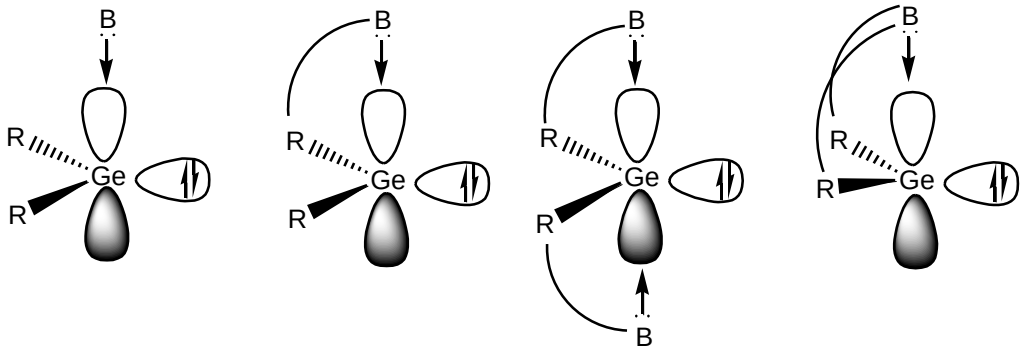

Particularly, different nitrogen and/or phosphorus containing ligands have been used to stabilize divalent germanium compounds. A large number of homoleptic divalent germanium species have been isolated using these concepts but fewer examples of heteroleptic derivates have been reported.[76-85] β-diketiminato (**25** and **26**) [79,82,81] and aminophosphinide [83] (**27** and **28**) ligands have been used to stabilize divalent germanium species. The stability of germylenes (**25**-**28**) is ascribed an effective overlap of the heteroatom lone pairs with the vacant p_π orbital, as well as, to coordination of amino groups; both effects compensate the electron deficiency on the germanium(II) center.

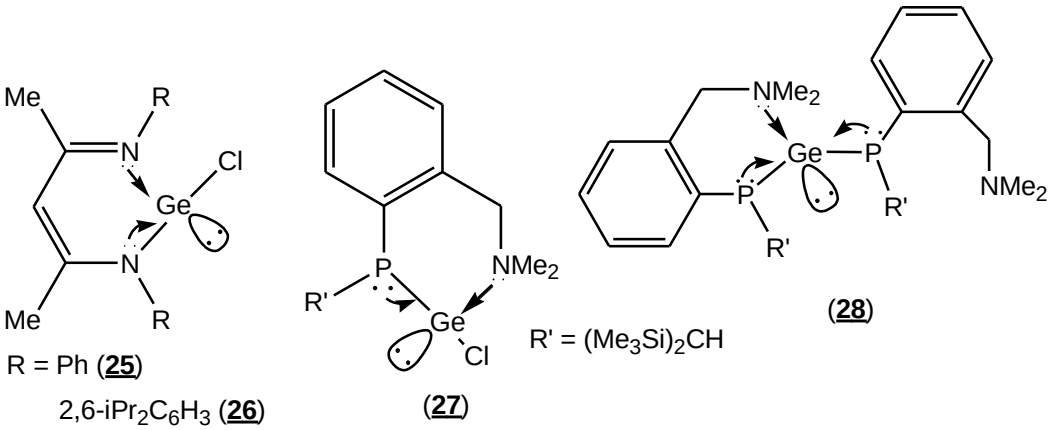

The reactivity of β-diketiminato coordinated germylenes was studied,[81,82] a summary is given in Scheme IV.1.

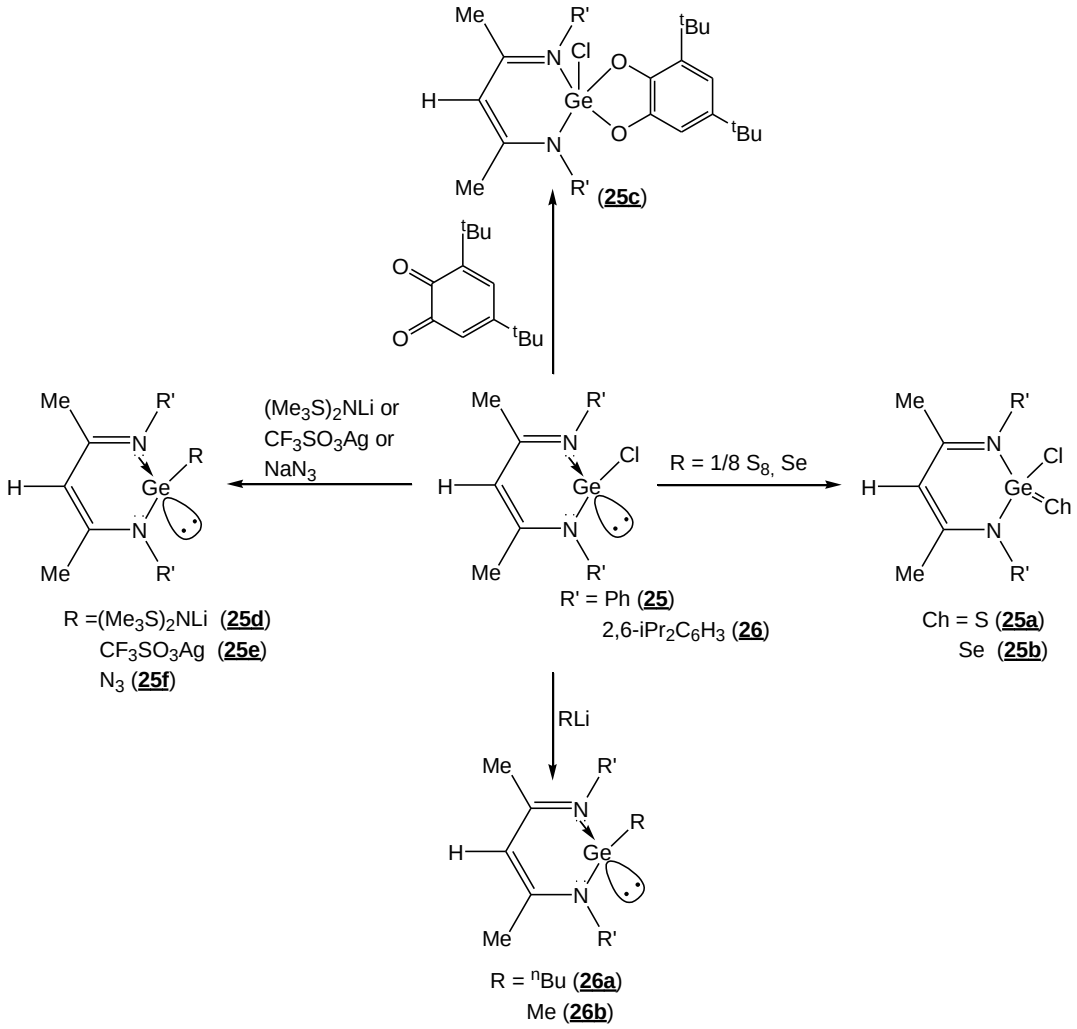

Scheme IV.1. Reactivity of stabilized germylene (**25**) and (**26**).

Chalcogen derivatives (**25a** and **25b**) have been prepared by oxidation of germylene (**25**) with elemental chalcogens, such as, sulfur and selenium. Heterocyclization reactions have been observed for germylene (**25**) with 3,5-di-tertbutyl-1,2-benzo-quinone to give (**25c**), and for free germylenes with 1,2-quinones.[73,86]

Furthermore, the chloro group in germylenes (**25** and **26**) can be substituted by nucleophilic substitution reactions. Interestingly, the N→Ge bond distance in (**26**) (1.988 Å) is shorter than those observed in germylenes (**26a** and **26b**) (2.025 and 2.038 Å). These structure features suggest that the imine group in germylene (**26**) transfers greater electron density to germanium center than in the germylenes (**26a** and **26b**), because the presence of chloro atom (an electronegative group) increases the electron deficiency on the germanium center.

Contrary to free or kinetically stabilized germylene compounds, the *β*-diketiminato-stabilized germylenes are unreactive toward dienes and conjugated carbonyl compounds. Meanwhile, a similar stabilized germylene (**29**) has shown to be reactive toward terminal alkynes to form the cycloadduct (**30**) (Scheme IV.2).[87]

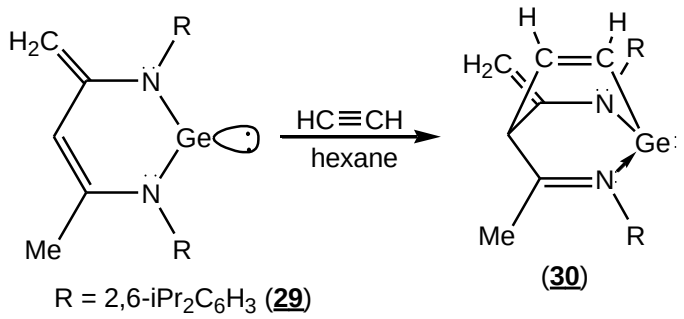

Scheme IV.2. Reaction of stabilized germylene (**29**) with acetylene.

In the other hand, base-stabilized germylenes, formed by coordination of Lewis base to the vacant orbital, may also represented as zwitterionic species: a germa-ylide. With this resonance canonical form the germanium center should have a nucleophilic character rather than an electrophilic character (Scheme IV.3). Although the chemistry of base-stabilized germylenes (base: amine or imine) has fairly been studied, the germa-ylide character has rarely been reflected in the reaction products.[87]

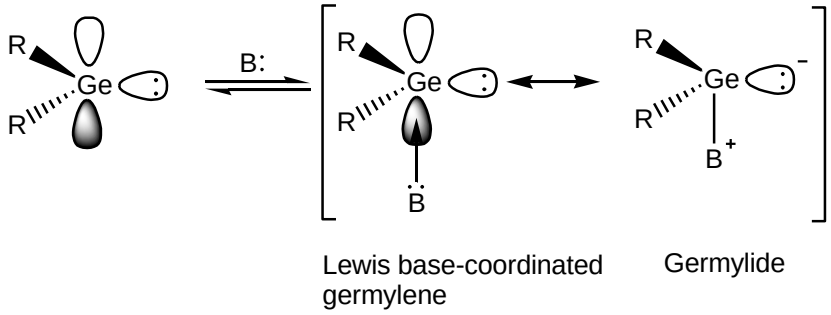

Scheme IV.3. Structure resonance of Lewis base-stabilized germanium (II) compounds.

It is worthy to note that, the chemistry of germanium(II) compounds stabilized by complexation with a phosphine, as phosphonium germa-ylide, has not been developed early as fully. Indeed, only an example of phosphonium germa-ylide (**31**), or phosphine-stabilized germylene (**31'**), has been reported by Du Mont.[88,89] Nevertheless, the most typical and useful reaction of phosphonium ylides, the Wittig reaction, has never been demonstrated from phosphonium germa-ylide.

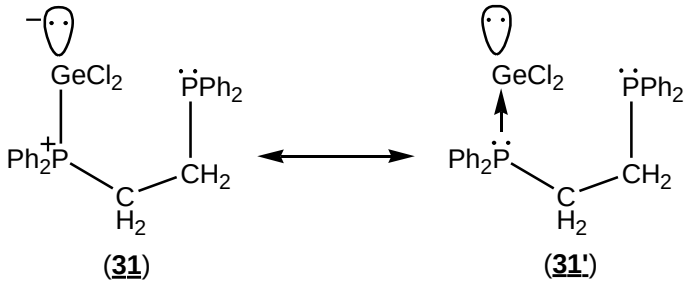

In contrast, the corresponding phosphine-stabilized silylenes, the phosphonium sila-ylides have been involved in a sila-Wittig type reaction with aldehydes. Recently, Baceiredo and Kato [90-92] reported the synthesis of phosphonium sila-ylide (**33**) and evaluated its reactivity toward carbonyl derivatives, substituted acetylene derivatives and dienes (Scheme IV.4).

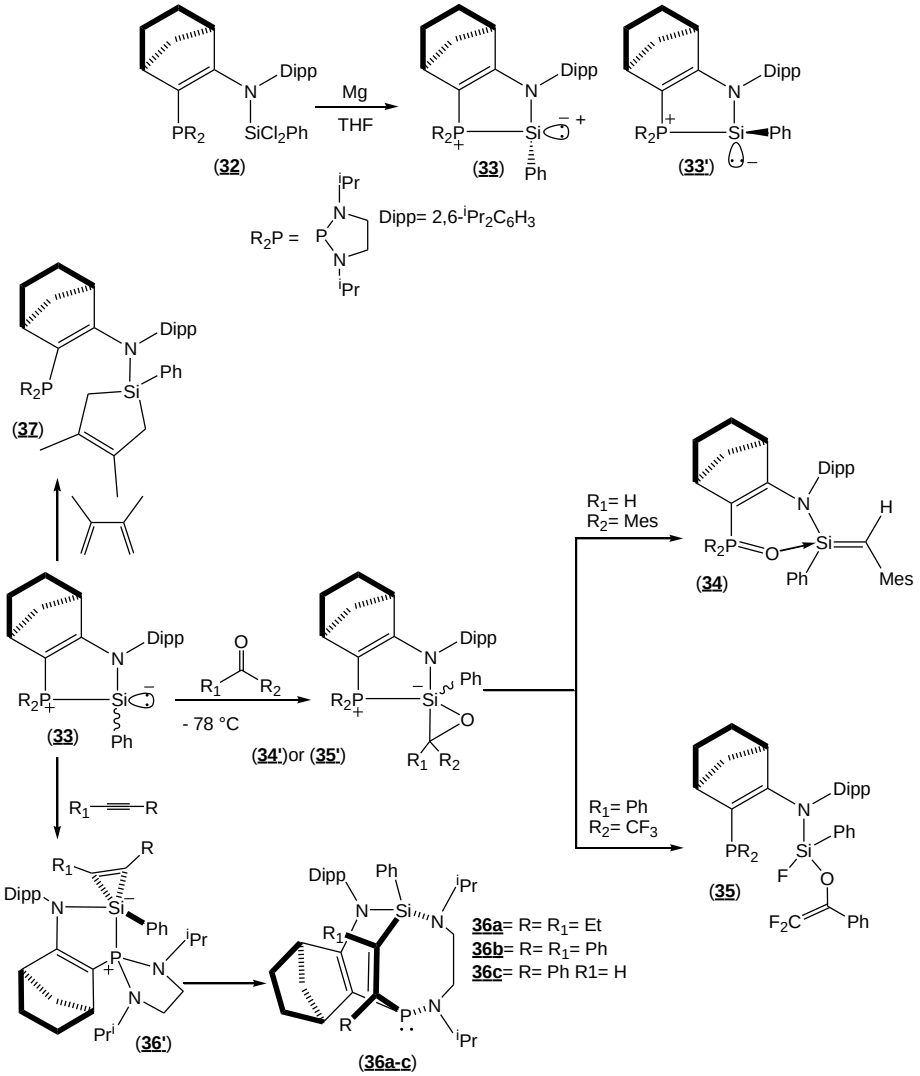

Scheme IV.4. Synthesis and reactivity of phosphonium sila-ylide (**33**).

A mechanistic study has demonstrated that phosphonium sila-ylide (**33**) reacts with unsaturated derivatives via a [2+1] cycloaddition process, affording labile pentacoordinate silicon intermediates, which demonstrates its behavior as a nucleophilic silylenoid. In addition, sila-ylide (**33**) reacts with classical silylene trapping agents such as 2,3-dimethylbutadiene.

Since divalent germanium species stabilized by phosphine ligands present a large synthetic potential, due their ylide-like properties, we have focused our interest on the synthesis and reactivity of germanium(II) species stabilized by a phosphine ligand. Theoretical calculations indicate that phosphine-germylene adducts present low stability.[93] The binding energies for $H_3P{-}EH_2$ adducts (E = C, Si, Ge, Sn) calculated by Schöller and Schneider,[94] (given in Table IV.1) indicate that the bond strength decreases ion the order CH_2> SiH_2 > GeH_2 > SnH_2. It is interesting to note the lower binding energies for $H_3P{-}EH_2$ adduct formation of silylene, germylene and stannylene in comparison with that for $H_3P{-}CH_2$ adduct.

Table IV.1. Binding energies (kcal/mol) for adducts formation $H_3P{-}EH_2$

$H_3P{=}CH_2$	$H_3P{=}SiH_2$	$H_3P{=}GeH_2$	$H_3P{=}SnH_2$
37.4 [a]	20.9 [a]	16.3 [a]	12.5 [a]

[a] Calculations level: MP2/CEP-31g(2d,1p) + zero point vibrational energy (ZPE) correction.[94,95]

Theoretical data reveal that phosphine-stabilized germylene may be difficult to obtain experimentally, due to their low stability. For overcome this problem, we have chosen the 2-phosphino imine (**d**) as ligand (Scheme IV.5). It presents steric and electronic properties which can provide a suitable kinetically and thermodynamically stabilizing system for the synthesis of phosphine-stabilized germylenes.

In this chapter, we present the synthesis of several intramolecularly phosphine-stabilized germylenes with different substituents on the germanium center. In order to gain knowledge about the chemistry of phosphine-stabilized germylenes, we have studied the reactivity of these germanium(II) compounds toward different organic reagents.

IV.2. Results and discussions

IV.2.1. Synthesis and characterization of germylene (38)

The reaction of 2-phosphine imine (**d**) with one equiv of n-butyllithium followed by addition of one equiv of [$GeCl_2(C_4H_8O_2)$] led to the formation of phosphine-stabilized chlorogermylene (**38**) (Scheme IV.5). The product was isolated as air-sensitive pale-yellow solid in 65% yield.

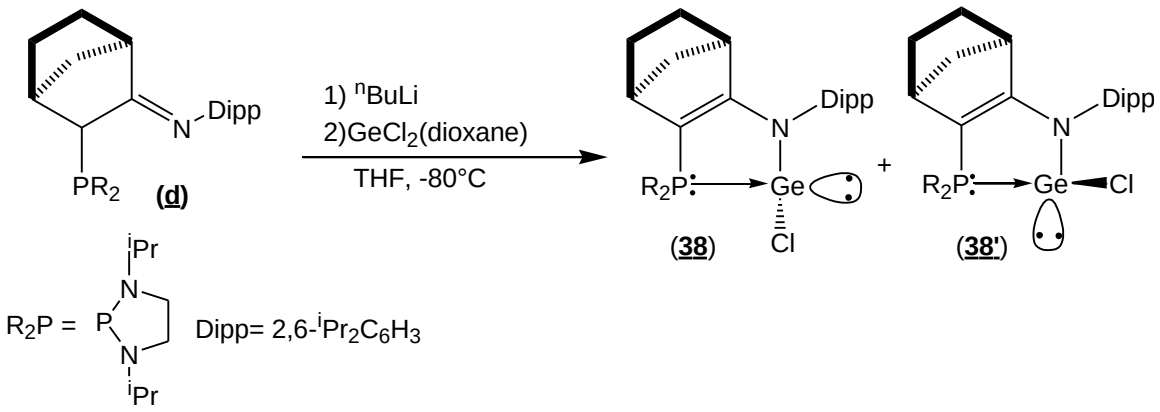

Scheme IV.5. Synthesis of germylene (**38**).

Germylene (**38**) was obtained as a mixture of two diastereomers (**38**/**38'**= 50:50), as indicated by the presence of two signals, in the same ratio, in the $^{31}P\{^{1}H\}$ NMR spectrum [δ 72.02 (**38**) and 62.23 ppm (**38'**)] (Figure IV.2). These chemical shifts are at relatively high field compared with that of the 2-phosphine imine (**d**) (δ 102 ppm) and are same chemical shift range than that observed for structurally similar phosphonium sila-ylide (**33**) (δ 70.4 and 68.0 ppm).[90]

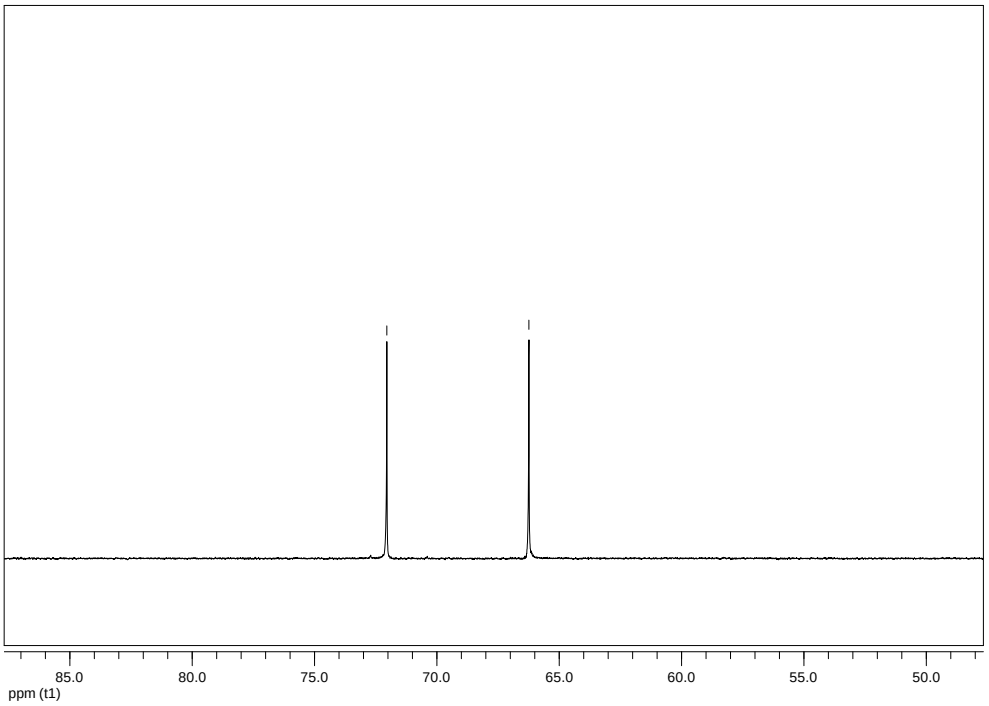

Figure IV.2. $^{31}P\{^{1}H\}$ NMR spectrum of germylenes (**38**).

Molecular structure of germylene (38)

Germylene (**38**) was isolated as yellow crystals from a saturated pentane solution at -30°C, and its structure was unambiguously established by single-crystal X-ray diffraction analysis. An ORTEP diagram of enantiomer (**38**) is shown in Figure IV.3. Selected bond lengths and angles are listed in Table IV.2.

The X-ray diffraction analysis of complex (**38**) shows the presence of a racemic mixture of the two enantiomers (**38**) and (**38'**) in the cell unit. The values of the sum of the bond angles about germanium [ΣGe_{α}= 275.5° (**38**) and 276.1° (**38'**)] is in agreement with a strongly pyramidalized center.

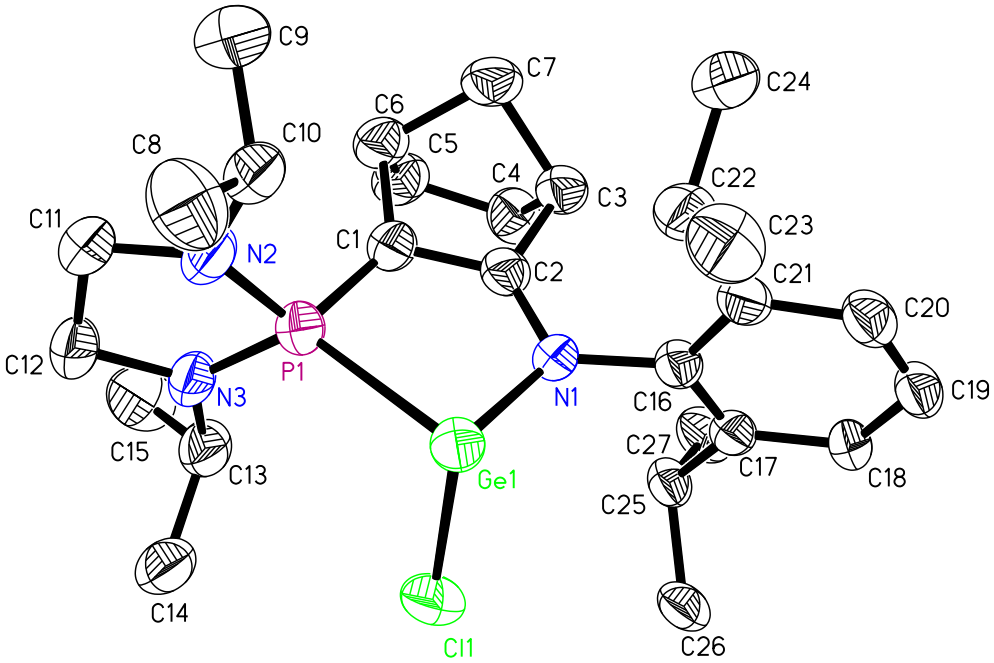

Figure VI.3. Molecular structure of germylenes (**38**). Thermal ellipsoids represent 50% probability and H atoms have been omitted for clarity.

The P−Ge bond distances (2.454(6) and 2.443'(10) Å) are quite long for a Ge=P double bond (2.138 Å),[96] and rather comparable to that for the P−Ge single bond (2.402-2.411 Å),[97] observed in the diphosphagermylene $[R(C_6H_4\text{-}2\text{-}CH_2NMe_2)P]_2Ge$ (**28**), and it is slightly shorter than that for P−Ge bond [2.514 Å] in compound (**31**).[88] The Ge−Cl bond distances (2.264 and 2.264' Å) are comparable with those (2.332 and 2.236 Å) observed in compound (**31**).

These structural features suggest a polarized P−Ge bond, and the ylidic character of the P−Ge bond. Moreover, the relatively short C(2)−N(1) (1.338(8) and 1.344'(12) Å) and P(1)−C(1) (1.720(6) and 1,714'(12) Å) bonds and the elongated C(1)−C(2) bond (1.384(9) and 1.386'(13) Å) reveal the delocalization of the enamine π electrons toward a positively charged phosphorus atom.

Table IV.2. Selected bond lengths (Å) and bond angles (deg) of germylenes (**38**)

Germylene	Bond distance		Bond angle	
38	Ge(1)−P(1)	2.454(6)	N(1)−Ge(1)−P(1)	83.9(3)
	Cl(1)−Ge(1)	2.264(3)	Cl(1)−Ge(1)−P(1)	96.0(3)
	Ge(1)−N(1)	1.985(9)	N(1)−Ge(1)−Cl(1)	95.6(7)
	C(2)−N(1)	1.338(8)	C(2)−N(1)−Ge(1)	116.3(7)
	C(1)−C(2)	1.384(9)	N(1)−C(2)−C(1)	126.5(8)
	P(1)−C(1)	1.720(6)	C(2)−C(1)−P(1)	116.6(7)
			C(1)−P(1)−Ge(1)	95.4(4)
38'	Ge(1')−P(1')	2.443(10)	N(1')−Ge(1')−P(1')	84.1(6)
	Cl(1')−Ge(1')	2.264(6)	Cl(1')−Ge(1')−P(1')	96.1(4)
	Ge(1')−N(1')	1.993(13)	N(1')−Ge(1')−Cl(1')	95.9(12)
	C(2')−N(1')	1.344(12)	C(2')−N(1')−Ge(1')	115.3(11)
	C(1')−C(2')	1.386(13)	N(1')−C(2')−C(1')	125.0(12)
	P(1')−C(1')	1.714(12)	C(2')−C(1')−P(1')	117.8(11)
			C(1')−P(1')−Ge(1')	93.8(7)

IV.2.2. Reactivity of phosphine-stabilized germylene

Phosphine-stabilized germylene compounds have a high synthetic potential, because they may exhibit a germa-ylide-like reactivity. With these properties in mind, we studied the reactivity of phosphine-stabilized germylenes on base to reactions with different organic reagent. We can distinguish four different reaction centers, as shown in Scheme IV.6.

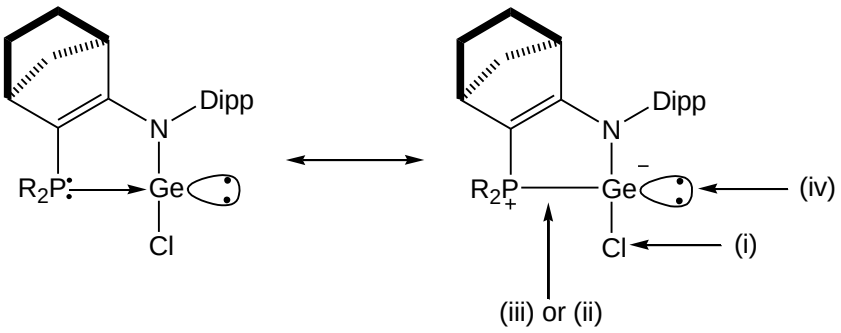

Scheme IV.6. Reactive centers present on the phosphine-stabilized germylene: (i) nucleophilic substitution of chloro group; (ii) lability of P-Ge bond; (iii) reaction on P-Ge ylidic bond and (iv) nucleophilic character.

IV.2.2.1. Nucleophilic substitution reactions

We carried out nucleophilic substitution reactions on germylene (**38**) to prepare phosphine-stabilized germylene compounds substituted with alkyl and aryl groups. The reaction of (**38**) with one equiv of phenyllithium in THF at -80°C led to formation of the substituted phenyl-germylene (**39**) (Scheme IV.7). The product was isolated as an air-sensitive pale-yellow solid in 45% yield.

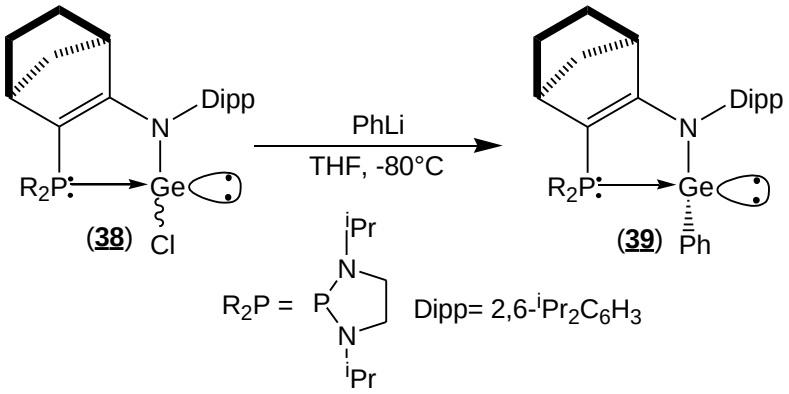

Scheme IV.7. Synthesis of germylene (**39**).

The $^{31}P\{^{1}H\}$ NMR spectrum of (**39**) shows one singlet resonance at 80.5 ppm (Figure IV.4a); this chemical shift is similar to that observed for phosphonium sila-ylide (**33**).[90] The introduction the phenyl group was confirmed by a doublet at 152.05 ppm ($^{2}J_{PC}$ = 6.8 Hz), in the $^{13}C\{1H\}$ NMR spectrum, corresponding to the C*ipso* carbon atom.

*Molecular structure of germylene (**39**)*

Germylene (**39**) was isolated as yellow crystals from a saturated pentane solution at -30°C, and its structure was unambiguously established by an X-ray diffraction analysis. Selected bond lengths and angles are listed in Table IV.3.

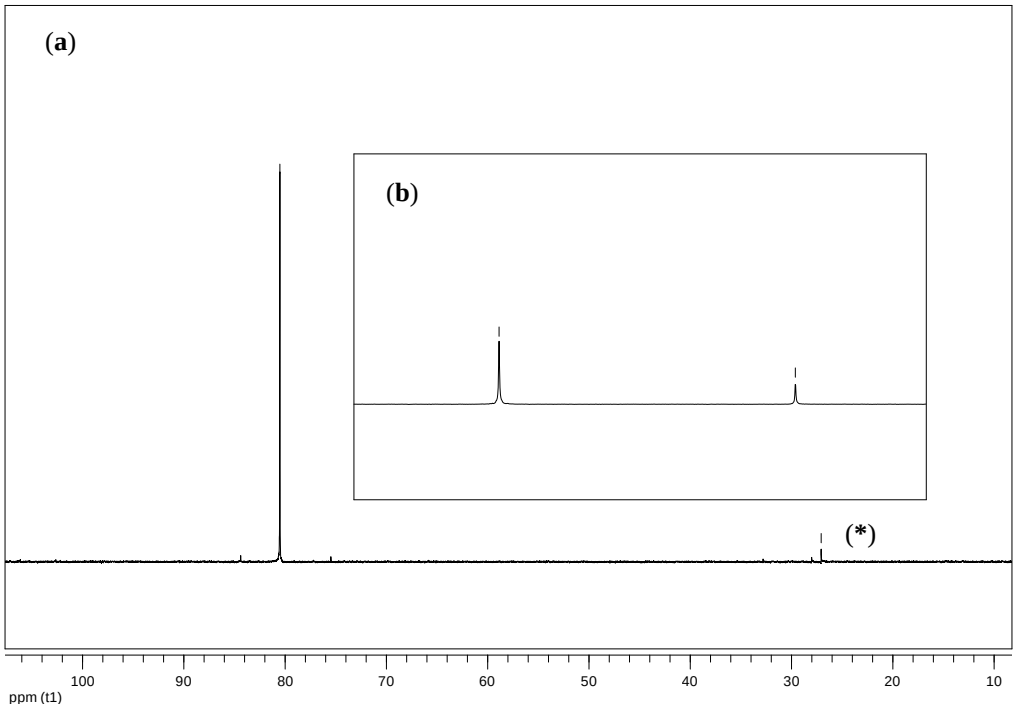

Figure IV.4. $^{31}P\{^{1}H\}$ NMR spectra of germylene (**39**): (**a**) at 25°C; (**b**) after heated at 50°C for 15 min; (*) hydrolysis product.

Asymmetric unit is constituted by diastereomer (**39**), in which the phenyl group on the germanium is situated on the side with less hindrance due to the asymmetric bicyclic fragment (Figure IV.5). The value of the sum of the bond angles about germanium (ΣGe_{α}= 288.6°) is in agreement with a strongly pyramidalized center.

Table IV.3. Selected bond lengths (Å) and bond angles (deg) of germylene (**39**)

Bond distance		**Bond angle**	
Ge(1)−P(1)	2.434(6)	N(1)−Ge(1)−P(1)	84.69(3)
Ge(1)−C(28)	2.003(3)	C(28)−Ge(1)−P(1)	104.43(3)
Ge(1)−N(1)	1.993(18)	N(1)−Ge(1)−C(28)	99.55(7)
C(2)−N(1)	1.343(3)	C(2)−N(1)−Ge(1)	114.01(14)
C(1)−C(2)	1.387(3)	N(1)−C(2)−C(1)	124.7(2)
P(1)−C(1)	1.724(2)	C(2)−C(1)−P(1)	118.06(17)
		C(1)−P(1)−Ge(1)	92.32(8)

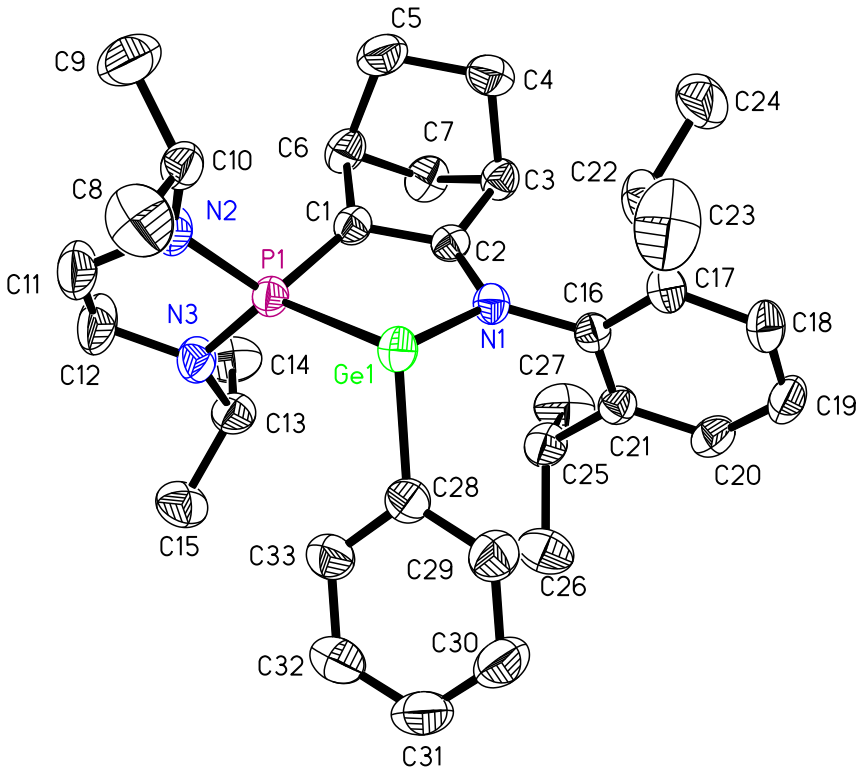

Figure VI.5. Molecular structure of germylene (**39**). Thermal ellipsoids represent 50% probability and H atoms have been omitted for clarity.

The P−Ge bond distance (2.434(6) Å) is quite long for a Ge=P double bond (2.138 Å),[96] rather comparable to that for the P−Ge single bond (2.402-2.411 Å),[97] observed in the diphosphagermylene $[R(C_6H_4\text{-}2\text{-}CH_2NMe_2)P]_2Ge$ (**28**), and it is slightly shorter than that for P−Ge bond [2.514 Å] in compound (**31**).[88]

These structural features suggest a polarized P−Ge bond, and an ylidic character of the P−Ge bond. Moreover, the relatively short C(2)−N(1) (1.343(3) Å) and P(1)−C(1) (1.724(2) Å) bonds and the elongated C(1)−C(2) bond (1.387(3) Å) reveal the delocalization of the enamine π electrons toward the positively charged phosphorus atom.

An isomerization reaction was observed by rising of temperature at 50°C, as indicated by apparition of second signal at 75 ppm in the $^{31}P\{^1H\}$ (Figure IV.4b). It is reasonable to think that the isomerization of diastereomer (**39**) would involve the P−Ge bond dissociation and a rotation around of the Ge−N bond to result in the formation of germylene (**39'**) (Scheme IV.8). The formation of diastereomer (**39'**) reveals the lability of coordination bonding P−Ge in the phosphine-stabilized germylenes.

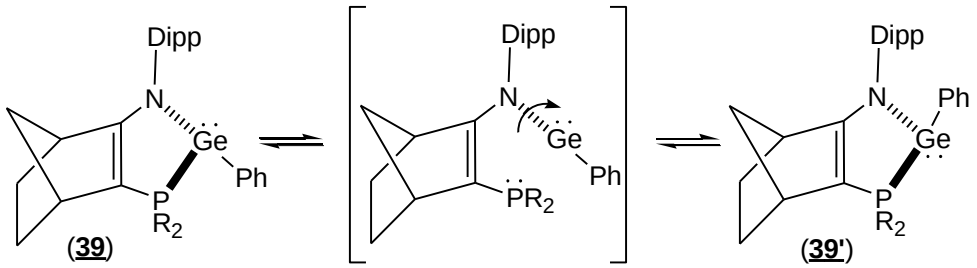

Scheme IV.8. Possible mechanism for the isomerization of (**39**).

The substitution reaction can be also performed methylmagnesium bromide in THF at -80°C, leading to the formation of substituted methyl-germylene (**40**) (Scheme IV.9). The product was isolated as air-sensitive pale-yellow solid in 30% yield.

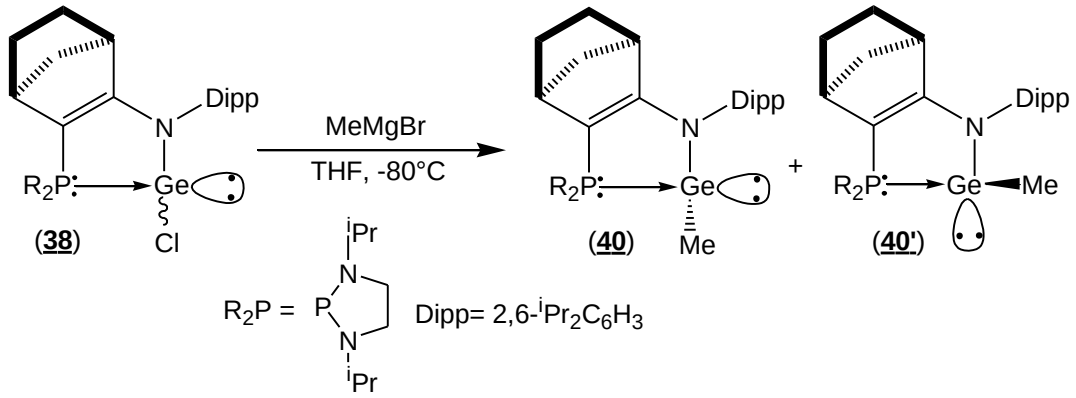

Scheme IV.9. Synthesis of germylenes (**40**).

Germylene (**40**) was obtained as a mixture of two diastereomers (**40**/**40'**= 60:40), as indicated by the presence of two signals in the $^{31}P\{^{1}H\}$ NMR spectrum [δ 85.62 (**40**) and 80.96 ppm (**40'**)] (Figure IV.6).

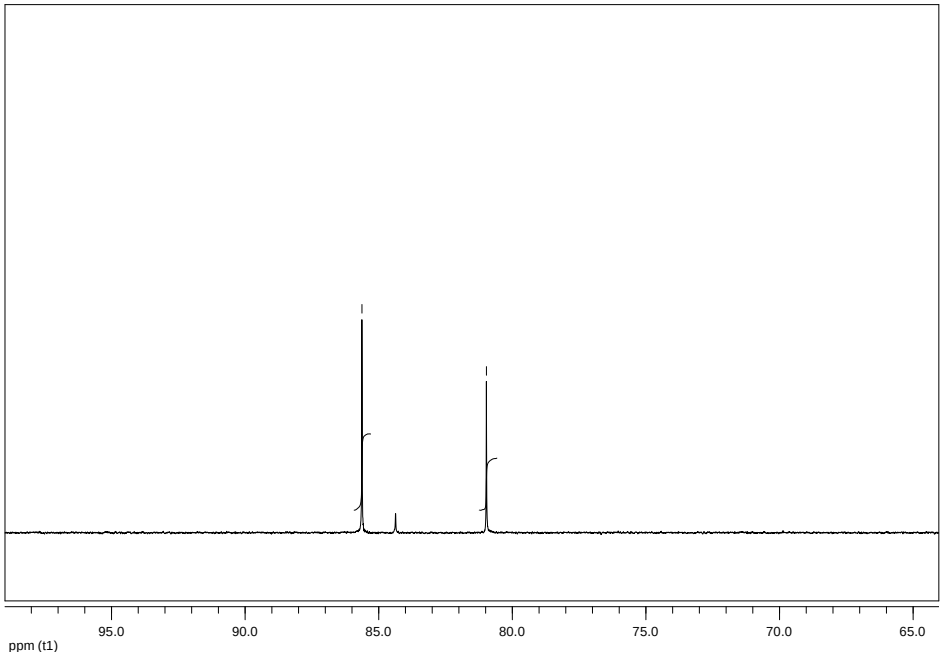

Figure IV.6. $^{31}P\{^{1}H\}$ NMR spectrum of germylenes (**40**).

The chemical shift of (**40**) in the $^{31}P\{^{1}H\}$ NMR spectrum is similar to those observed for the germylenes (**38**) and (**39**). The $^{13}C\{^{1}H\}$ NMR spectrum shows two doublets signals at [2.96 ppm ($^{2}J_{PC}$ = 4.6 Hz) (**40**); 4.28 ppm ($^{2}J_{PC}$ = 2.7 Hz) (**40'**)], corresponding to methyl substituent on the germanium center.

Moreover, the addition of one equiv of n-butyllithium to a solution of (**38**) in THF at -80°C, led to the formation of n-butyl-substituted germylene (**41**) (Scheme IV.10). The product was isolated as air-sensitive pale-yellow solid in 35% yield.

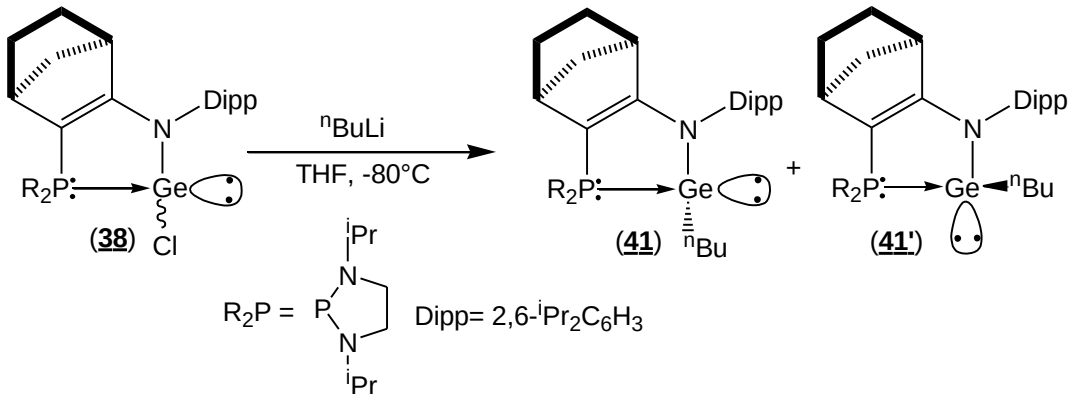

Scheme IV.10. Synthesis of germylenes (**41**).

Here again germylene (**41**) was obtained as a mixture of two diastereomers (**41**/**41'**= 84:16), as indicated by two signals in the $^{31}P\{^{1}H\}$ NMR [δ 85.72 (**41**) and 80.95 (**41'**)] (Figure IV.7). These chemical shifts are similar to those observed for germylenes (**39**-**40**).

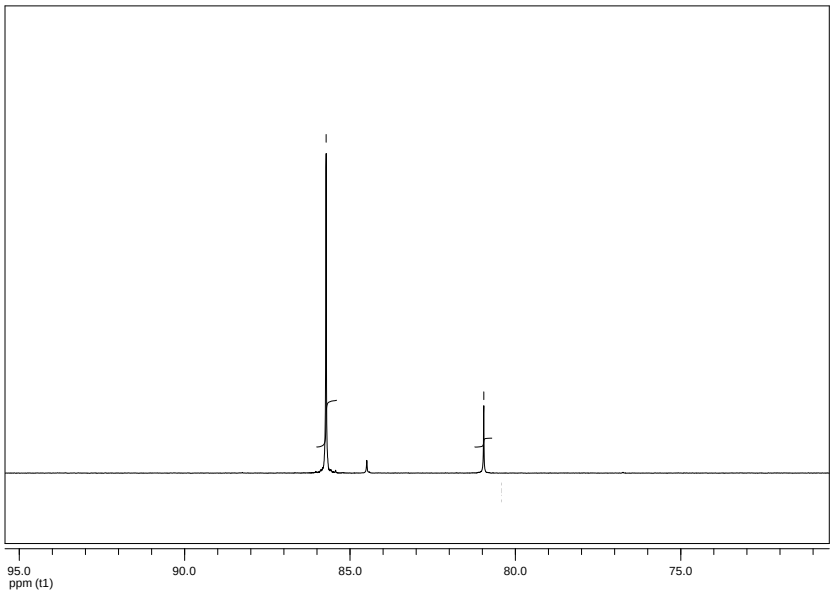

Figure IV.7. $^{31}P\{^{1}H\}$ NMR spectrum of germylenes (**41**).

Germylenes (**38**-**41**) are stable at room temperature under inert atmosphere. They are soluble in organic solvents such as: tetrahydrofuran, benzene, toluene, pentane and ethyl ether.

IV.2.2.2. Hydrolysis reaction

Although germylenes (**38**-**41**) are stable in solution, as well as, in the solid state at room temperature under inert atmosphere, they were found to be highly reactive. Indeed, the addition of an excess of H_2O at RT to a solution of germylene (**40**) in C_6D_6 gives a mixture of 1,3-Diisopropyl-2-oxo-1,3,2-diazaphospholidine (**43a**) and the imine (**43b**) (Scheme IV.11). The formation of (**43a**) and (**43b**) was confirmed by $^{31}P\{^{1}H\}$, ^{1}H and $^{13}C\{^{1}H\}$ NMR spectroscopy.

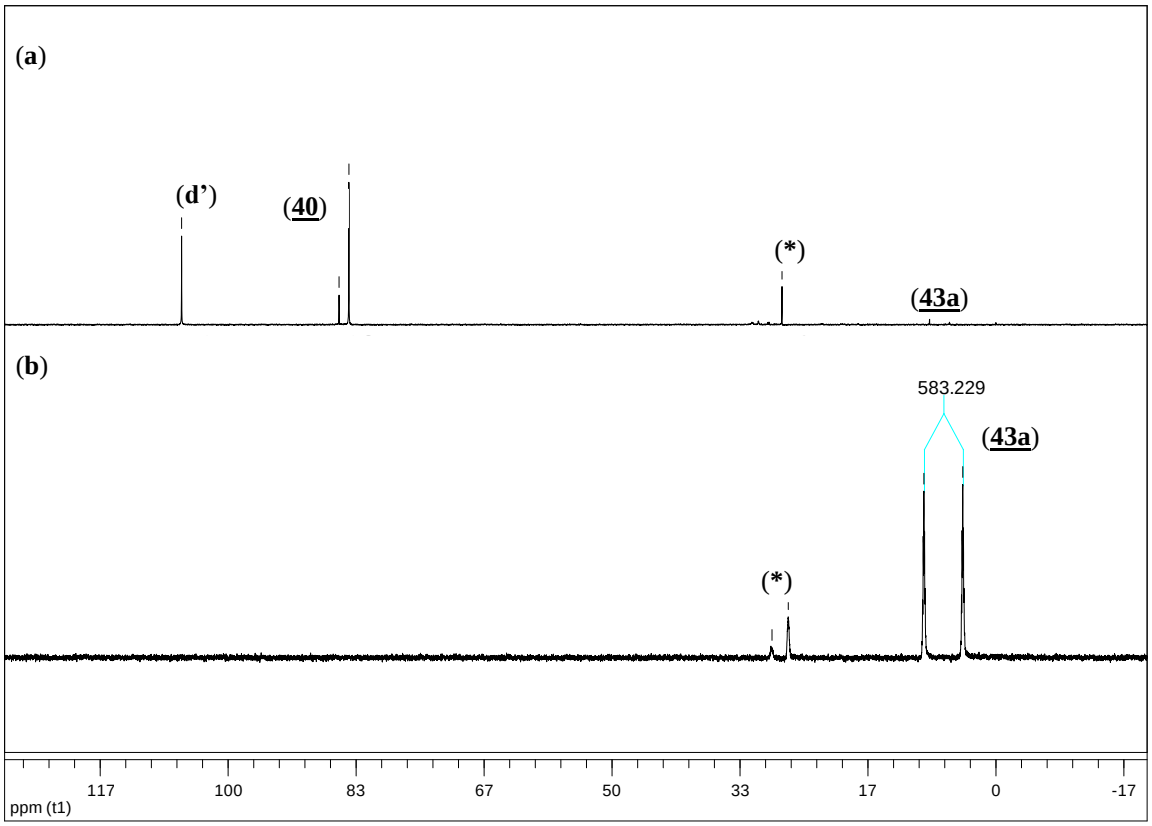

Figure IV.8. (**a**): $^{31}P\{^{1}H\}$ NMR spectrum after 1 hour reaction; (**b**): $^{31}P\{^{1}H\}$ NMR spectrum after 12 hour reaction; phosphine oxide (*****).

After 1 h, the $^{31}P\{^{1}H\}$ NMR spectrum showed the appearance of a signal at 106 ppm (Figure IV.8a), which possibly corresponds to phosphino-enamine tautomer (**d'**), due the similitude of this chemical shift with that observed for 2-phosphino imine (**d**) (102 ppm) (Scheme IV.11). This signal at 106 ppm disappears after 12 h, and it appears a doublet at 8.57 ppm (J_{PH} = 583.2 Hz) in the ^{31}P NMR spectrum of the mixture (Figure IV.8b), which corresponds to phosphine oxide (**43a**). Furthermore, ^{1}H NMR spectrum showed a doublet resonance at 7.44 ppm, with the same large J_{PH} coupling constant, confirms the presence of P-H fragment. Similar chemical shifts have been reported for diazaphospholidines [$^{31}P\{^{1}H\}$: 11.4 ppm and ^{1}H: 7.38 (J_{PH} = 597.2 Hz)].[98]

Moreover, the $^{13}C\{^{1}H\}$ NMR spectrum of the mixture shows the characteristics signal corresponding to carbons of imine of (**43b**) at 180.07 ppm.

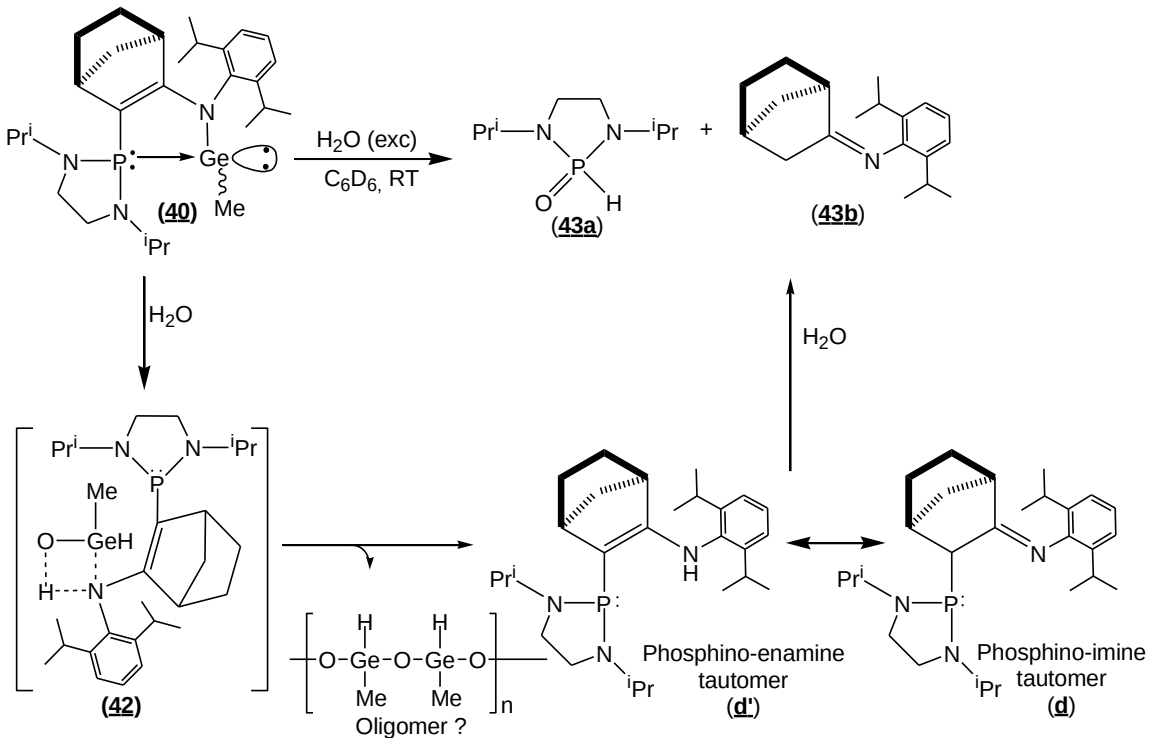

Scheme IV.11. Reaction mechanism proposed for the hydrolysis of germylene (**40**).

These spectroscopic data suggest that (**43a**) and (**43b**) are formed from the hydrolysis of phosphino-imine (**d**), which results from tautomerization of phosphine-enamine (**d'**) (Scheme IV.11). Although we could not detect the possible intermediate (**42**), it is reasonable to think that phosphine-enamine (**d'**) is formed from (**42**) by 1,3-migration of hydrogen from oxygen to the nitrogen atom, followed by the rapid oligomerization of the germanium fragment (Scheme IV.11). The formation of intermediate (**42**), which could have arisen from germanium center insertion into H-OH bond, reveals the germylene character of (**40**).[99,100]

In order to verify the reaction mechanism proposed, we carried out the reaction de 2-phosphino imine (**d**) with H_2O. Hydrolysis of (**d**) led to the formation of diazaphospholidine (**43a**), as indicated by the presence of a doublet at 8.28 ppm (J_{PH} = 571.5 Hz), in the ^{31}P NMR spectrum.

IV.2.2.3. Wittig reaction

In order to evaluate ylide-like properties, we carried out the reaction of germylenes (**39** and **40**) with carbonyl derivatives. Surprisingly, the reaction of germylene (**40**) with mesitylaldehyde did not lead to the formation of the expected corresponding germene (**44b**),

which would be formed in the case of a germa-Wittig reaction (Scheme IV.12), but only hydrolysis reaction was observed. A similar result was observed with germylene (**39**) (Scheme IV.12), and all attempts to avoid the hydrolysis process were unsuccessful.

In an attempt to reduce the presence of water traces and therefore to avoid the formation of hydrolysis product, we chose a solid ketone, as the benzophenone, to carry out the reaction with germylenes (**39** and **40**). However, germylenes (**39** and **40**) showed to be unreactive toward benzophenone, even under heating at 60°C for 10 days (Scheme IV.12).

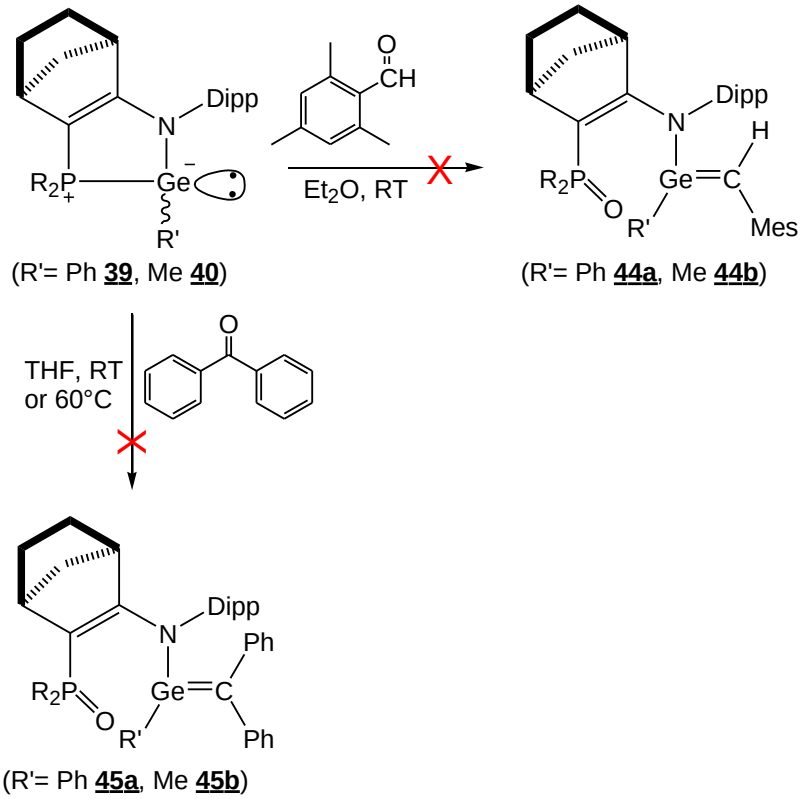

(R'= Ph **39**, Me **40**)

(R'= Ph **44a**, Me **44b**)

(R'= Ph **45a**, Me **45b**)

Scheme IV.12. Reaction attempts of germylenes (**39** and **40**) with carbonyl derivatives.

These results indicate that germanium (II) center into the phosphine-stabilized germylenes (**38**-**41**) presents a low ylide character, which reveals that phosphine-stabilized germylenes (**39**-**41**) do not exhibit a phosphonium ylide-like reactivity.

IV.2.2.4. Cycloaddition reactions

Germylene (**40**) reacts toward classical free germylene trapping agents such as 2,3-dimethylbutadiene. The [1+4] cycloadduct (**46**) was obtained by reaction of (**40**) with two equiv of 2,3-dimethyl-1,3-butadiene (Scheme IV.13).

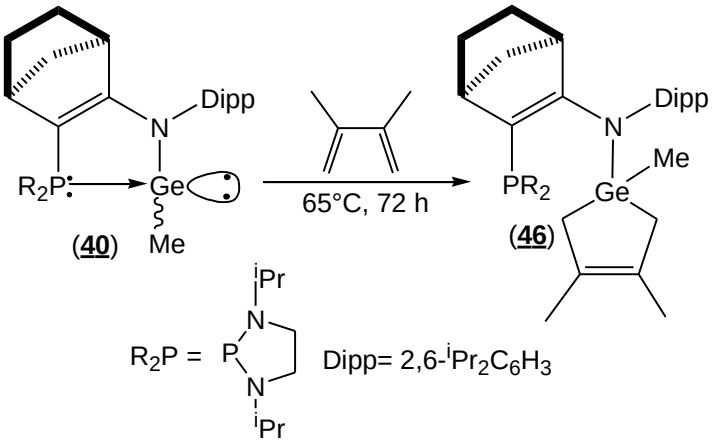

Scheme IV.13. Reaction of germylene (**40**) with 2,3-dimethyl-1,3-butadiene.

$^{31}P\{^{1}H\}$, ^{1}H and $^{13}C\{^{1}H\}$ NMR spectra confirmed the formation of (**46**). The $^{31}P\{^{1}H\}$ NMR spectrum shows one singlet signal at 84.47 ppm, very similar to that observed for the silicon homologue, cycloadduct (**37**) (81.3 ppm).[91] Furthermore, $^{13}C\{^{1}H\}$ NMR spectrum shows the signals corresponding to carbons of germacyclopentene: one singlet at 130.03 ppm, characteristic for vinyl carbon (C=C), as well as, the characteristic signals for the methyl (19.19 ppm) and methylene (28.57 ppm) carbons.

In order to have more insight into chemistry of phosphine-stabilized germylenes, we have studied the reactivity of germylenes (**39**-**41**) toward unsaturated organic compounds, such as alkenes and alkynes. To this end, we have carried out the reaction of germylene (**39**) with 1-cyclohexene and diphenylacetylene. Nevertheless, germylene (**39**) showed to be unreactive toward the 1-cyclohexene and diphenylacetylene, even under heating at 60°C for 7 days (Scheme IV.14).

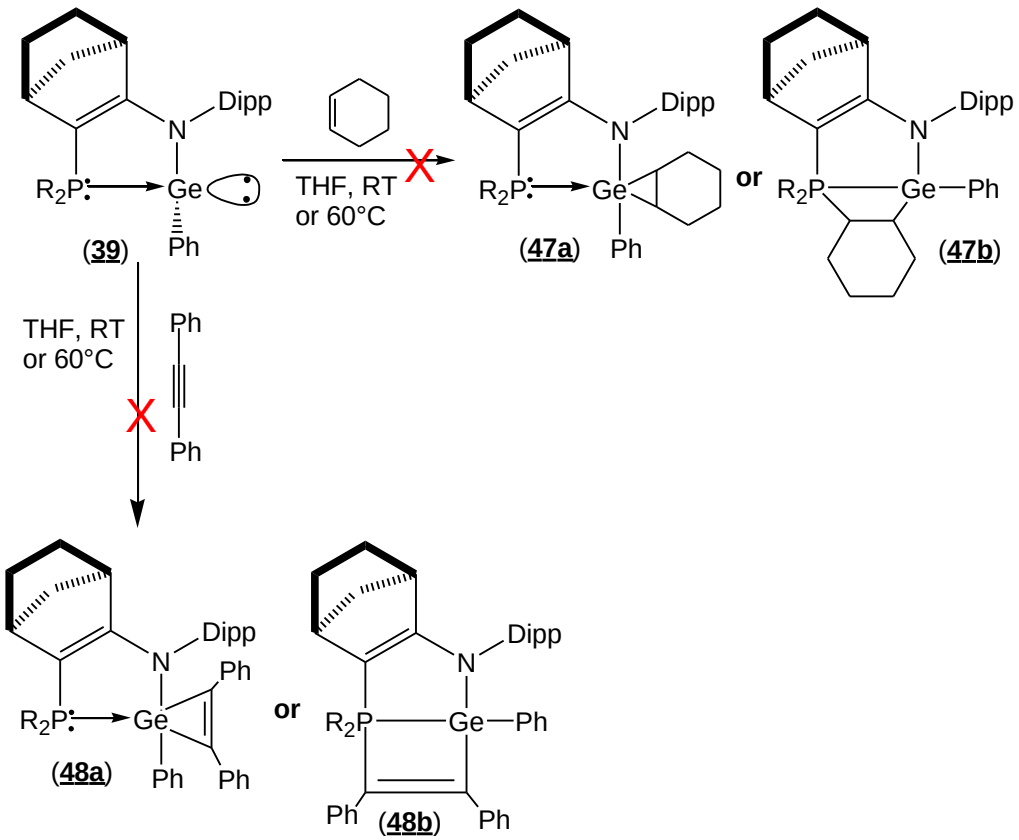

Scheme IV.14. Reaction attempts of germylene (**39**) with 1-cyclohexene and diphenylacetylene.

IV.2.2.5. Complexation reaction with Lewis acid

Phosphine-stabilized germylenes (**38**-**41**) have a heteroleptic germanium (II) center with a lone pair. This feature confers them the ability to act as Lewis base to form stable complexes with Lewis acid, therefore, they can be considered isovalent analogues of phosphines. Recently, Baines and coworkers demonstrated that a transient diorganogermylene stabilized by *N*-heterocyclic carbene acts as a strong Lewis base toward BH_3 to afford a carbene-germylene-borane complex.[101-103]

In order to evaluate the potential of phosphine-stabilized germylenes (**38**-**41**) to act as Lewis bases, we carried out the reaction of germylene (**39**) with one equiv of BH_3·THF (Scheme IV.15).

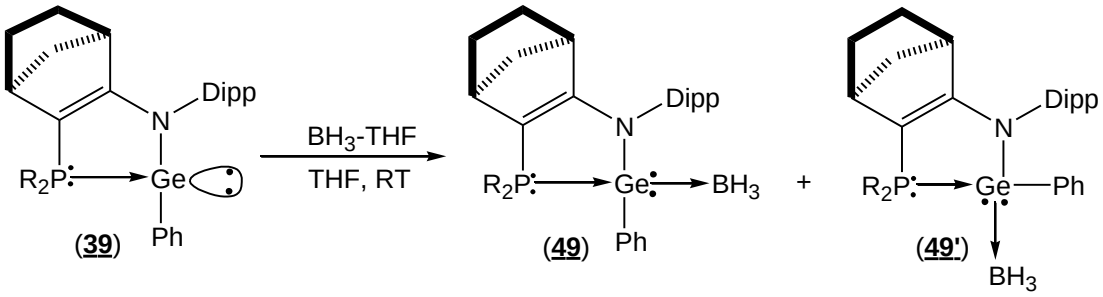

Scheme IV.15. Reaction of germylene (**39**) with BH_3·THF.

The expected germylene-borane complex was obtained as a mixture of two diastereomers (**49**/**49'**= 50:50), as indicated by the presence of two signals, in nearly same ratio, in the NMR spectra [$^{31}P\{^1H\}$ NMR, 60.55 and 57.10 ppm; $^{11}B\{^1H\}$ NMR -35.88 and -40.61 ppm] (Figure IV.9).

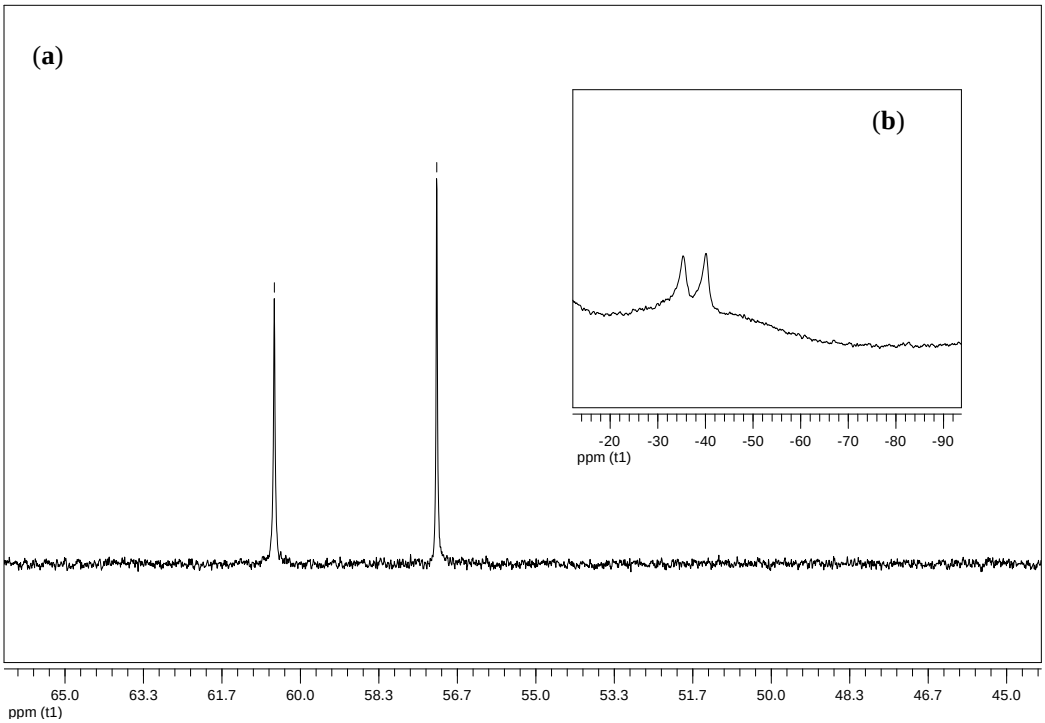

Figure IV.9. NMR spectra of germylene complexes (**49**); (**a**): $^{31}P\{^1H\}$ NMR spectrum at 25°C ; (**b**): $^{11}B\{^1H\}$ NMR spectrum at 25°C.

This result indicates that phosphine-stabilized germylenes (**38**-**41**) can be capable of behaving as σ-donor/π-acceptor ligands resembling phosphines (PR_3). Therefore, the use of phosphine-stabilized germylene as ligands in transition metal complexes represents an interesting area of research. In this sense, we have studied the reactivity of phosphonium-

stabilized germylenes toward transition metal complexes; these results will be presented in the chapter (V).

IV.3. Experimental part

IV.3.1. General Considerations

All manipulations were performed under an inert atmosphere of argon by using standard Schlenk techniques. Dry, oxygen-free solvents were employed. All reagents were obtained from commercial suppliers. 2-phosphino enamine (**d**) was synthesized as previously reported methods.[104] The C, H and N elemental analyses were carried out on a *Fison Instrument* EA1108 CHNS-O microanalyzer.

^{1}H, $^{13}C\{^{1}H\}$, $^{31}P\{^{1}H\}$ and $^{11}B\{^{1}H\}$ NMR spectra were recorded on Bruker, Avance 500 or Avance 300 spectrometers. ^{1}H, $^{13}C\{^{1}H\}$ NMR chemical shifts are reported in ppm relative to Me_4Si as external standard. $^{31}P\{^{1}H\}$ NMR chemical shifts are expressed in ppm relative to 85% H_3PO_4. $^{11}B\{^{1}H\}$ NMR chemical shifts are reported in ppm relative to decaborane as external standard.

IV.3.2. Synthesis of germylene (38)

To a solution of (**d**) (11.5 g, 0.026 mol) in THF (100 mL) was added dropwise a solution of n-butyllithium (17.15 mL, 0.027 mol) in hexane (1.6 M) and stirred for 1 h at -80°C. The crude was to warm at room temperature and stirred for 1 h. Then it was cooled at -80°C and added dropwise solution of dichlorogermylene dioxane complex (6.03 g, 0.026 mol) in THF (25 mL). The resulting solution was warmed to RT and the solvent removed under vacuum. Germylenes (**38**) were extracted with pentane and yellow crystals were obtained from a saturated pentane solution at -30°C (9.26 g, 65%). **Isomer 38** (50%): ^{1}H NMR (300.18 MHz, C_6D_6, 25°C): δ = 0.93 (d, J_{HH} = 6.5 Hz, 3H, CH_{3PNiPr}), 0.98 (d, J_{HH} = 6.6 Hz, 3H, CH_{3PNiPr}), 1.01 (d, J_{HH} = 6.8 Hz, 3H, CH_{3PNiPr}), 1.18 (overlapped with the methyl signal, 1H, ½ $CH_{2bridge}$), 1.19 (d, J_{HH} = 7.3 Hz, 3H, CH_{3iPr}), 1.26 (overlapped with the methyl signal, 1H, ½ $CH_{2CbridgeheadCN}$), 1.27 (d, J_{HH} = 7.1 Hz, 3H, CH_{3iPr}), 1.28 (d, J_{HH} = 6.9 Hz, 3H, CH_{3PNiPr}), 1.33 (d, J_{HH} = 6.8 Hz, 3H, CH_{3iPr}), 1.52 (overlapped with the methyl signal, 1H, ½ $CH_{2CbridgeheadCP}$), 1.53 (d, J_{HH} = 6.5 Hz, 3H, CH_{3iPr}), 1.60-1.76 (m, 3H, ½ $CH_{2bridge}$, ½ $CH_{2CbridgeheadCP}$, ½ $CH_{2CbridgeheadCN}$), 2.32 (m, 1H, $PCCH_{bridgehead}$), 2.42-2.70 (m, 4H, 2 $PNCH_2$), 2.73 (brs, 1H, $NCCH_{bridgehead}$), 3.14 (sept, $^{3}J_{HH}$ = 6.9 Hz, 1H, CH_{iPr}), 3.26 (m, 1H,

PNCH$_{iPr}$), 3.50 (m, 1H, PNCH$_{iPr}$), 4.00 (sept, $^{3}J_{HH}$ = 6.7 Hz, 1H, CH$_{iPr}$), 7.07-7.22 (m, 3H, H$_{Ar}$). $^{13}C\{^{1}H\}$ NMR (75.47 MHz, C_6D_6, 25°C): δ = 20.34 (d, $^{3}J_{PC}$ = 2.1 Hz, CH$_{3PNiPr}$), 20.66 (s, CH$_{3PNiPr}$), 21.14 (d, $^{3}J_{PC}$ = 5.4 Hz, CH$_{3PNiPr}$), 22.20 (d, $^{3}J_{PC}$ = 4.3 Hz, CH$_{3PNiPr}$), 23.96 (s, CH$_{3iPr}$), 24.59 (s, CH$_{3iPr}$), 25.50 (s, *C*H$_{2CbridgeheadCN}$), 25.86 (s, CH$_{3iPr}$), 26.17 (s, CH$_{3iPr}$), 27.80 (s, CH$_{iPr}$), 28.77 (s, CH$_{iPr}$), 29.57 (d, $^{3}J_{PC}$ = 0.8 Hz, *C*H$_{2CbridgeheadCP}$), 38.66 (s, PNCH$_2$), 39.32 (d, $^{2}J_{PC}$ = 1.9 Hz, PNCH$_2$), 40.48 (d, $^{3}J_{PC}$ = 8.0 Hz, NC*C*H$_{bridgehead}$), 43.42 (d, $^{2}J_{PC}$ = 14.2 Hz, PC*C*H$_{bridgehead}$), 44.45 (d, $^{2}J_{PC}$ = 9.7 Hz, PNCH$_{iPr}$), 44.96 (d, $^{2}J_{PC}$ = 1.75 Hz, PNCH$_{iPr}$), 48.82 (d, $^{3}J_{PC}$ = 3.1 Hz, CH$_{2bridge}$), 91.83 (d, J_{PC} = 21.6 Hz, P*C*=CN), 123.75, 124.49, 126.63 (3 x s, 3C, CH$_{Ar}$), 140.29 (d, $^{3}J_{PC}$ = 5.7 Hz, NC$_{ipso}$), 146.33, 147.65 (2 x s, 2C, NC$_{orto}$), 191.08 (d, $^{2}J_{PC}$ = 42.4 Hz, PC=*C*N). $^{31}P\{^{1}H\}$ NMR (121.49 MHz, C_6D_6, 25°C): δ = 72.02 (s). **Isomer <u>38'</u>** (50%): ^{1}H NMR (300.18 MHz, C_6D_6, 25°C): δ = 0.91 (d, $^{3}J_{HH}$ = 6.4 Hz, 3H, CH$_{3PNiPr}$), 0.99 (d, $^{3}J_{HH}$ = 6.6 Hz, 3H, CH$_{3PNiPr}$), 1.04 (d, $^{3}J_{HH}$ = 6.7 Hz, 3H, CH$_{3PNiPr}$), 1.20 (overlapped with the methyl signal, 1H, ½ CH$_{2bridge}$), 1.22 (d, $^{3}J_{HH}$ = 7.8 Hz, 3H, CH$_{3iPr}$), 1.24 (d, $^{3}J_{HH}$ = 7.5 Hz, 3H, CH$_{3iPr}$), 1.26 (overlapped with the methyl signal, 1H, ½ CH$_{2CbridgeheadCN}$), 1.30 (d, $^{3}J_{HH}$ = 6.5 Hz, 3H, CH$_{3PNiPr}$) 1.31 (d, $^{3}J_{HH}$ = 7.2 Hz, 3H, CH$_{3iPr}$), 1.35 (overlapped with the methyl signal, 1H, ½ CH$_{2CbridgeheadCP}$), 1.51 (d, $^{3}J_{HH}$ = 6.5 Hz, 3H, CH$_{3iPr}$), 1.52 (overlapped with the methyl signal, 1H, ½ CH$_{2CbridgeheadCP}$), 1.60-1.76 (m, 2H, ½ CH$_{2bridge}$, ½ CH$_{2CbridgeheadCN}$), 2.42-2.70 (m, 5H, 2 PNCH$_2$, PCCH$_{bridgehead}$), 2.88 (m, 1H, NCCH$_{bridgehead}$), 3.27 (m, 1H, CH$_{iPr}$), 3.71 (sept, $^{3}J_{HH}$ = 6.7 Hz, 1H, CH$_{iPr}$), 4.07 (m, 1H, PNCH$_{iPr}$), 4.20 (m, 1H, PNCH$_{iPr}$), 7.07-7.22 (m, 3H, H$_{Ar}$). $^{13}C\{^{1}H\}$ NMR (75.47 MHz, C_6D_6, 25°C): δ = 20.44 (d, $^{3}J_{PC}$ = 0.72 Hz, CH$_{3PNiPr}$), 2101 (d, $^{3}J_{PC}$ = 2.3 Hz, CH$_{3PNiPr}$), 21.27 (d, $^{3}J_{PC}$ = 5.6 Hz, CH$_{3PNiPr}$), 21.98 (d, $^{3}J_{PC}$ = 6.9 Hz, CH$_{3PNiPr}$), 24.25 (s, CH$_{3iPr}$), 24.40 (s, CH$_{3iPr}$), 25.39 (s, CH$_{3iPr}$), 25.49 (s, *C*H$_{2CbridgeheadCN}$), 26.07 (s, J_{PC} = 2.0 Hz, CH$_{3iPr}$), 27.94 (s, CH$_{iPr}$), 28.72 (s, CH$_{iPr}$), 29.64 (d, J_{PC} = 1.2 Hz, *C*H$_{2CbridgeheadCP}$), 38.66 (s, PNCH$_2$), 39.39 (d, $^{2}J_{PC}$ = 2.8 Hz, PNCH$_2$), 40.86 (d, $^{3}J_{PC}$ = 8.5 Hz, NC*C*H$_{bridgehead}$), 44.16 (d, $^{2}J_{PC}$ = 13.4 Hz, PC*C*H$_{bridgehead}$), 44.84 (d, $^{2}J_{PC}$ = 3.4 Hz, PNCH$_{iPr}$), 45.20 (d, $^{2}J_{PC}$ = 9.0 Hz, PNCH$_{iPr}$), 46.79 (d, $^{3}J_{PC}$ = 4.7 Hz, CH$_{2bridge}$), 89.73 (d, J_{PC} = 25.2 Hz, P*C*=CN), 123.34, 124.33, 126.60 (3 x s, 3C, CH$_{Ar}$), 139.53 (d, $^{3}J_{PC}$ = 4.1 Hz, NC$_{ipso}$), 145.51, 147.65 (2 x s, 2C, NC$_{orto}$), 190.47 (d,$^{2}J_{PC}$ = 41.1 Hz, PC=*C*N). $^{31}P\{^{1}H\}$ NMR (121.49 MHz, C_6D_6, 25°C): δ = 66.23 (s). Anal calcd. For $C_{27}H_{43}N_3PGeCl$: C 59.12, H 7.84, N 7.66; found: C 60.88, H 8.04, N 7.98.

IV.3.3. Synthesis of germylene (39)

To a solution of (**38**) (1.5 g, 2.73 mmol) in THF (20 mL) was added dropwise a solution of phenyl lithium (1.58 mL 2.86 mmol) in dibutyl ether (1.8 M) and stirred for 1 h at -80°C. The crude was to warm at room temperature and stirred for 1 h. Then, all the volatiles were removed under vacuum and the residue was extracted twice in pentane. The concentrated pentane solution at -30°C gave the analytically pure (**39**) as yellow crystals (0.72 g, 45%). ^{1}H NMR (300.18 MHz, C_6D_6, 25°C): δ = 0.56 (d, $^{3}J_{HH}$ = 6.7 Hz, 3H, CH_{3PNiPr}), 0.90 (d, $^{3}J_{HH}$ = 6.2 Hz, 3H, CH_{3PNiPr}), 0.91 (overlapped with the methyl signal, 1H, ½ $CH_{2bridge}$), 0.92 (d, $^{3}J_{HH}$ = 6.6 Hz, 3H, CH_{3PNiPr}), 0.93 (d, $^{3}J_{HH}$ = 6.1 Hz, 3H, CH_{3PNiPr}), 1.04 (d, $^{3}J_{HH}$ = 6.5 Hz, 3H, CH_{3iPr}), 1.09 (d, $^{3}J_{HH}$ = 6.8 Hz, 3H, CH_{3iPr}), 0.91 (brs, 1H, ½ $CH_{2bridge}$), 1.17 (d, $^{3}J_{HH}$ = 6.9 Hz, 3H, CH_{3iPr}), 1.32-1.41 (m, 2H, ½ $CH_{2CbridgeheadCP}$, ½ $CH_{2CbridgeheadCN}$), 1.46 (d, $^{3}J_{HH}$ = 6.7 Hz, 3H, CH_{3iPr}), 1.55 (m, 1H, ½ $CH_{2CbridgeheadCP}$), 1.69 (m, 1H, ½ $CH_{2CbridgeheadCP}$), 2.48-2.69 (m, 5H, 2 $PNCH_2$, $PCCH_{bridgehead}$), 2.88 (m, 2H, $PNCH_{iPr}$) 2.88 (m, 1H, $NCCH_{bridgehead}$), 3.00 (sep, $^{3}J_{HH}$ = 6.8 Hz, 1H, CH_{iPr}), 3.41 (m, 1H, $PNCH_{iPr}$), 3.78 (sept, $^{3}J_{HH}$ = 6.8 Hz, 1H, CH_{iPr}), 3.95 (m, 1H, PNCH, CH_{iPr}), 6.96-7.36 (m, 3H, H_{Ar}). $^{13}C\{^{1}H\}$ NMR (75.47 MHz, C_6D_6, 25°C): δ = 19.90 (d, $^{3}J_{PC}$ = 0.5 Hz, CH_{3PNiPr}), 20.38 (d, $^{3}J_{PC}$ = 0.93 Hz, CH_{3PNiPr}), 20.73 (d, $^{3}J_{PC}$ = 4.5 Hz, CH_{3PNiPr}), 21.27 (d, $^{3}J_{PC}$ = 7.7 Hz, CH_{3PNiPr}), 23.43 (s, CH_{3iPr}), 24.43 (s, CH_{3iPr}), 24.83 (s, CH_{3iPr}), 25.55 (d, $^{4}J_{PC}$ = 1.6 Hz, *C*$H_{2CbridgeheadCN}$), 26.04 (d, J_{PC} = 2.5 Hz, CH_{3iPr}), 27.80 (s, CH_{iPr}), 28.48 (s, CH_{iPr}), 30.25 (d, $^{3}J_{PC}$ = 2.3 Hz, *C*$H_{2CbridgeheadCP}$), 38.91 (d, $^{2}J_{PC}$ = 3.0 Hz, $PNCH_2$), 38.95 (d, $^{2}J_{PC}$ = 2.8 Hz, $PNCH_2$), 41.09 (d, $^{3}J_{PC}$ = 7.9 Hz, NC*C*$H_{bridgehead}$), 43.90 (d, $^{2}J_{PC}$ = 5.8 Hz, $PNCH_{iPr}$), 44.06 (d, $^{2}J_{PC}$ = 11.1 Hz, PC*C*$H_{bridgehead}$), 44.28 (d, $^{2}J_{PC}$ = 12.5 Hz, $PNCH_{iPr}$), 46.28 (d, $^{3}J_{PC}$ = 4.0 Hz, $CH_{2bridge}$), 93.38 (d, J_{PC} = 31.3 Hz, P*C*=CN), 123.54, 124.04, 126.02 (2 x s, 3C, CH_{Ar}), 126.31 (d, $^{3}J_{PC}$ = 1.68 Hz, 2C, $GeCH_{orto}$), 137.19, 134.60, 134.76 (3 x s, 3C, CH_{Ar}), 140.81 (d, $^{3}J_{PC}$ = 1.4 Hz, NC_{ipso}), 145.75, 147.09 (2 x s, 2C, NC_{orto}), 152.05 (d, $^{2}J_{PC}$ = 6.8 Hz, GeC_{ipso}), 183.76 (d, $^{2}J_{PC}$ = 37.2 Hz, PC=*C*N). $^{31}P\{^{1}H\}$ NMR (121.49 MHz, C_6D_6, 25°C): δ = 80.51 (s). Anal calcd. For $C_{33}H_{48}N_3PGe$: C 67.16, H 8.14, N 7.66; found: C, 68.81; H, 8.50; N, 7.22.

IV.3.4. Synthesis of germylene (40)

To a solution of (**38**) (1.0 g, 1.82 mmol) in THF (20 mL) was added dropwise a solution of methyl magnesium bromide (0.64 mL 1.92 mmol) in dibutyl ether (3.0 M) and

stirred for 1 h at -80°C. The crude was to warm at room temperature and stirred for 1 h. Then, all the volatiles were removed under vacuum and the residue was extracted twice in pentane. The concentrated pentane solution at -30°C gave the pure (**40**) as yellow powder (0.28 g, 30%). **Isomer 40** (60%): ^{1}H NMR (300.18 MHz, C_6D_6, 25°C): δ = 0.61 (d, $^{3}J_{HP}$ = 18.2 Hz, 3H, $GeCH_3$), 0.91 (d, $^{3}J_{HH}$ = 6.7 Hz, 3H, CH_{3PNiPr}), 0.95 (d, $^{3}J_{HH}$ = 6.6 Hz, 3H, CH_{3PNiPr}), 1.02 (d, $^{3}J_{HH}$ = 6.8 Hz, 3H, CH_{3PNiPr}), 1.05 (d, $^{3}J_{HH}$ = 6.6 Hz, 3H, CH_{3PNiPr}), 1.13 (d, $^{3}J_{HH}$ = 6.0 Hz, 3H, CH_{3iPr}), 1.15 (d, $^{3}J_{HH}$ = 6.9 Hz, 3H, CH_{3iPr}), 1.16 (overlapped with the methyl signal, 1H, ½ $CH_{2bridge}$), 1.17 (d, $^{3}J_{HH}$ = 6.8 Hz, 3H, CH_{3PNiPr}), 1.36 (m, 2H, $CH_{2CbridgeheadCN}$), 1.43 (d, $^{3}J_{HH}$ = 6.7 Hz, 3H, CH_{3iPr}), 1.57 (m, 1H, ½ $CH_{2bridge}$), 1.69 (m, 2H, $CH_{2CbridgeheadCP}$), 2.44-2.67 (m, 5H, 2 $PNCH_2$, $PCCH_{bridgehead}$), 2.88 (brs, 1H, $NCCH_{bridgehead}$), 3.20 (sept, $^{3}J_{HH}$ = 6.8 Hz, 1H, CH_{iPr}), 3.53-3.64 (m, 2H, CH_{iPr}, $PNCH_{iPr}$), 3.77 (m, 1H, $PNCH_{iPr}$), 7.06-7.09 (m, 3H, H_{Ar}). $^{13}C\{^{1}H\}$ NMR (75.47 MHz, C_6D_6, 25°C): δ = 2.96 (d, $^{2}J_{PC}$ = 4.6 Hz, $GeCH_3$), 20.23 (d, $^{3}J_{PC}$ = 1.6 Hz, CH_{3PNiPr}), 20.42 (d, $^{3}J_{PC}$ = 1.7 Hz, CH_{3PNiPr}), 20.82 (d, $^{3}J_{PC}$ = 4.3 Hz, CH_{3PNiPr}), 21.73 (d, $^{3}J_{PC}$ = 0.9 Hz, CH_{3PNiPr}), 24.40 (s, CH_{3iPr}), 24.61 (s, CH_{3iPr}), 24.71 (s, CH_{3iPr}), 25.57 (d, $^{4}J_{PC}$ = 1.6 Hz, *C*$H_{2CbridgeheadCN}$), 26.30 (d, J_{PC} = 2.6 Hz, CH_{3iPr}), 27.61 (s, CH_{iPr}), 28.27 (s, CH_{iPr}), 30.25 (s, *C*$H_{2CbridgeheadCP}$), 39.12 (d, $^{2}J_{PC}$ = 1.1 Hz, $PNCH_2$), 39.40 (s, $PNCH_2$), 40.87 (d, $^{3}J_{PC}$ = 8.0 Hz, NC*C*$H_{bridgehead}$), 43.93 (d, $^{2}J_{PC}$ = 12.0 Hz, PC*C*$H_{bridgehead}$), 44.96 (d, $^{2}J_{PC}$ = 7.8 Hz, $PNCH_{iPr}$), 44.67 (d, $^{2}J_{PC}$ = 12.1 Hz, $PNCH_{iPr}$), 46.88 (d, $^{3}J_{PC}$ = 4.2 Hz, $CH_{2bridge}$), 90.99 (d, J_{PC} = 28.2 Hz, P*C*=CN), 123.42, 123.46, 124.12 (3 x s, 3C, CH_{Ar}), 140.76 (d, $^{3}J_{PC}$ = 2.5 Hz, NC_{ipso}), 146.59, 147.26 (2 x s, 2C, NC_{orto}), 185.00 (d, $^{2}J_{PC}$ = 39.4 Hz, PC=*C*N). $^{31}P\{^{1}H\}$ NMR (121.49 MHz, C_6D_6, 25°C): δ = 85.62 (s). **Isomer 40'** (40%): ^{1}H NMR (300.18 MHz, C_6D_6, 25°C): δ = 0.81 (d, $^{3}J_{HP}$ = 18.4 Hz, 3H, $GeCH_3$), 0.87 (d, $^{3}J_{HH}$ = 6.5 Hz, 3H, CH_{3PNiPr}), 0.92 (d, $^{3}J_{HH}$ = 6.6 Hz, 3H, CH_{3PNiPr}), 1.01 (d, $^{3}J_{HH}$ = 6.5 Hz, 3H, CH_{3PNiPr}), 1.11 (d, $^{3}J_{HH}$ = 5.8 Hz, 3H, CH_{3iPr}), 1.12 (d, $^{3}J_{HH}$ = 6.9 Hz, 3H, CH_{3PNiPr}), 1.17 (overlapped with the methyl signal, 1H, ½ $CH_{2bridge}$), 1.19 (d, $^{3}J_{HH}$ = 6.7 Hz, 3H, CH_{3iPr}), 1.20 (d, $^{3}J_{HH}$ = 6.8 Hz, 3H, CH_{3PNiPr}), 1.36 (m, 2H, ½ $CH_{2CbridgeheadCN}$, ½ $CH_{2CbridgeheadCP}$), 1.42 (d, $^{3}J_{HH}$ = 6.8 Hz, 3H, CH_{3iPr}), 1.43 (overlapped with the methyl signal, 2H, ½ $CH_{2CbridgeheadCN}$, ½ $CH_{2CbridgeheadCP}$), 1.69 (m, 1H, ½ $CH_{2bridge}$), 2.33 (brs, 1H, $PCCH_{bridgehead}$), 2.44-2.67 (m, 4H, 2 $PNCH_2$), 2.78 (brs, 1H, $NCCH_{bridgehead}$), 3.21 (sept, $^{3}J_{HH}$ = 6.8 Hz, 1H, CH_{iPr}), 3.38 (m, 1H, $PNCH_{iPr}$), 3.46 (sept, $^{3}J_{HH}$ = 6.8 Hz, 1H, CH_{iPr}), 3.94 (m, 1H, $PNCH_{iPr}$), 7.06-7.09 (m, 3H, H_{Ar}). $^{13}C\{^{1}H\}$ NMR (75.47 MHz, C_6D_6, 25°C): δ = 4.28 (d, $^{2}J_{PC}$ = 2.7 Hz, $GeCH_3$), 19.86 (d, $^{3}J_{PC}$ = 1.5 Hz, CH_{3PNiPr}), 21.19 (d, $^{3}J_{PC}$ = 1.7 Hz, CH_{3PNiPr}), 21.25 (d, $^{3}J_{PC}$ = 1.1 Hz, CH_{3PNiPr}), 21.80 (d, $^{3}J_{PC}$ = 4.1 Hz, CH_{3PNiPr}), 24.23 (s, CH_{3iPr}), 24.95 (s, CH_{3iPr}), 25.01 (s, CH_{3iPr}), 25.98 (s, CH_{3iPr}), 26.26 (d, $^{4}J_{PC}$ = 1.4 Hz, *C*$H_{2CbridgeheadCN}$), 27.43 (s, CH_{iPr}), 28.27 (s, CH_{iPr}), 30.25 (s,

C$H_{2Cbridgehead CP}$), 38.89 (s, $PNCH_2$), 39.10 (d, $^2J_{PC}$ = 1.9 Hz, $PNCH_2$), 40.68 (d, $^3J_{PC}$ = 7.2 Hz, NC*C*$H_{bridgehead}$), 43.35 (d, $^2J_{PC}$ = 13.5 Hz, PC*C*$H_{bridgehead}$), 43.93 (d, $^2J_{PC}$ = 7.4 Hz, $PNCH_{iPr}$), 44.42 (d, $^2J_{PC}$ = 11.1 Hz, $PNCH_{iPr}$), 48.65 (d, $^3J_{PC}$ = 2.7 Hz, $CH_{2bridge}$), 91.49 (d, J_{PC} = 23.5 Hz, P*C*=CN), 123.83, 125.93, 126.01 (3 x s, 3C, CH_{Ar}), 141.57 (d, $^3J_{PC}$ = 4.7 Hz, NC_{ipso}), 146.01, 146.34 (2 x s, 2C, NC_{orto}), 187.37 (d, $^2J_{PC}$ = 41.2 Hz, PC=*C*N). $^{31}P\{^1H\}$ NMR (121.49 MHz, C_6D_6, 25°C): δ = 80.96 (s).

IV.3.5. Synthesis of germylene (41)

To a solution of (**38**) (1.0 g, 1.82 mmol) in THF (20 mL) was added dropwise a solution of n-butyl lithium (1.20 mL 1.92 mmol) in hexane (1.6 M) and stirred for 1 h at -80°C. The crude was to warm at room temperature and stirred for 1 h. Then, all the volatiles were removed under vacuum and the residue was extracted twice in pentane. The concentrated pentane solution at -30°C gave the pure (**41**) as yellow powder (0.36 g, 35 %). **Isomer 41** (84%): ^1H NMR (300.18 MHz, C_6D_6, 25°C): δ = 0.86 (t, $^3J_{HH}$ = 6.9 Hz, 3H, $CH_3{}^n{}_{Bu}$), 0.98 (d, $^3J_{HH}$ = 6.7 Hz, 3H, CH_{3PNiPr}), 1.06 (d, $^3J_{HH}$ = 6.6 Hz, 3H, CH_{3PNiPr}), 1.13 (d, $^3J_{HH}$ = 6.6 Hz, 3H, CH_{3PNiPr}), 1.15 (d, $^3J_{HH}$ = 6.7 Hz, 3H, CH_{3PNiPr}), 1.21 (d, $^3J_{HH}$ = 6.8 Hz, 3H, CH_{3iPr}), 1.24 (overlapped with the methyl signal, 2H, $GeCH_2CH_2{}^n{}_{Bu}$), 1.25 (overlapped with the methyl signal, 1H, ½ $CH_{2bridge}$), 1.26 (d, $^3J_{HH}$ = 6.9 Hz, 3H, CH_{3iPr}), 1.33 (d, $^3J_{HH}$ = 6.8 Hz, 3H, CH_{3iPr}), 1.38-1.45 (m, 3H, ½ $CH_{2CbridgeheadCN}$, $CH_2CH_3{}^n{}_{Bu}$), 1.51 (d, $^3J_{HH}$ = 6.7 Hz, 3H, CH_{3iPr}), 1.52 (overlapped with the methyl signal, 2H, ½ $CH_{2CbridgeheadCN}$, ½ $GeCH_2{}^n{}_{Bu}$), 1.54-1.64 (m, 3H, ½ $CH_{2bridge}$, ½ $CH_{2CbridgeheadCP}$, ½ $GeCH_2{}^n{}_{Bu}$), 1.77 (m, 1H, ½ $CH_{2CbridgeheadCP}$), 2.54-2.65 (m, 3H, $PNCH_2$, $PCCH_{bridgehead}$), 2.69-2.80 (m, 2H, $PNCH_2$), 2.96 (brs, 1H, $NCCH_{bridgehead}$), 3.29 (sept, $^3J_{HH}$ = 6.6 Hz, 1H, CH_{iPr}), 3.56-3.65 (m, 1H, $PNCH_{iPr}$), 3.76 (sept, $^3J_{HH}$ = 6.9 Hz, 1H, CH_{iPr}), 3.91-4.00 (m, 1H, $PNCH_{iPr}$), 7.13-7.17 (m, 3H, H_{Ar}). $^{13}C\{^1H\}$ NMR (75.47 MHz, C_6D_6, 25°C): δ = 13.98 (s, $CH_3{}^n{}_{Bu}$), 19.14 (d, $^2J_{PC}$ = 4.1 Hz, $GeCH_2{}^n{}_{Bu}$), 20.10 (d, $^3J_{PC}$ = 1.5 Hz, CH_{3PNiPr}), 20.43 (d, $^3J_{PC}$ = 1.5 Hz, CH_{3PNiPr}), 20.70 (d, $^3J_{PC}$ = 4.2 Hz, CH_{3PNiPr}), 21.70 (d, $^3J_{PC}$ = 7.1 Hz, CH_{3PNiPr}), 24.30 (s, CH_{3iPr}), 24.40 (s, CH_{3iPr}), 24.87 (s, CH_{3iPr}), 25.58 (d, $^3J_{HP}$ = 1.3 Hz, 3H, $GeCH_2CH_2{}^n{}_{Bu}$), 26.19 (d, J_{PC} = 2.7 Hz, CH_{3iPr}), 26.41 (s, *C*$H_{2CbridgeheadCN}$), 27.59 (s, CH_{iPr}), 28.20 (s, CH_{iPr}), 30.08 (d, $^4J_{HP}$ = 10.2 Hz, 3H, *C*$H_2CH_3{}^n{}_{Bu}$), 30.33 (d, $^3J_{PC}$ = 1.8 Hz,*C*$H_{2CbridgeheadCP}$), 39.05 (d, $^2J_{PC}$ = 2.5 Hz, $PNCH_2$), 39.21 (d, $^2J_{PC}$ = 1.5 Hz, $PNCH_2$), 40.92 (d, $^3J_{PC}$ = 7.8 Hz, NC*C*$H_{bridgehead}$), 43.81 (d, $^2J_{PC}$ = 10.7 Hz, PC*C*$H_{bridgehead}$), 43.84 (d, $^2J_{PC}$ = 7.2 Hz, $PNCH_{iPr}$), 44.63 (d, $^2J_{PC}$ = 12.8 Hz, $PNCH_{iPr}$), 48.73

(d, $^{3}J_{PC}$ = 3.8 Hz, $CH_{2bridge}$), 90.15 (d, J_{PC} = 29.4 Hz, P*C*=CN), 123.36, 124.12, 125.86 (3 x s, 3C, CH_{Ar}), 141.07 (d, $^{3}J_{PC}$ = 2.1 Hz, NC_{ipso}), 146.16, 146.53 (2 x s, 2C, NC_{orto}), 183.85 (d, $^{2}J_{PC}$ = 38.6 Hz, PC=*C*N). $^{31}P\{^{1}H\}$ NMR (121.49 MHz, C_6D_6, 25°C): δ = 85.72 (s). **Isomer <u>41'</u>** (16%): ^{1}H NMR (300.18 MHz, C_6D_6, 25°C): δ = 0.87 (t, $^{3}J_{HH}$ = 7.3 Hz, 3H, $CH_3{}^{n}{}_{Bu}$), 0.98 (d, $^{3}J_{HH}$ = 6.7 Hz, 3H, CH_{3PNiPr}), 1.06 (d, $^{3}J_{HH}$ = 6.6 Hz, 3H, CH_{3PNiPr}), 1.13 (d, $^{3}J_{HH}$ = 6.6 Hz, 3H, CH_{3PNiPr}), 1.15 (d, $^{3}J_{HH}$ = 6.7 Hz, 3H, CH_{3PNiPr}), 1.22 (d, $^{3}J_{HH}$ = 6.7 Hz, 3H, CH_{3iPr}), 1.24 (overlapped with the methyl signal, 2H, $GeCH_2CH_2{}^{n}{}_{Bu}$), 1.25 (overlapped with the methyl signal, 1H, ½ $CH_{2bridge}$), 1.26 (d, $^{3}J_{HH}$ = 6.9 Hz, 3H, CH_{3iPr}), 1.33 (d, $^{3}J_{HH}$ = 6.8 Hz, 3H, CH_{3iPr}), 1.38-1.45 (m, 3H, ½ $CH_{2CbridgeheadCN}$, $CH_2CH_3{}^{n}{}_{Bu}$), 1.51 (d, $^{3}J_{HH}$ = 6.7 Hz, 3H, CH_{3iPr}), 1.52 (overlapped with the methyl signal, 2H, ½ $CH_{2CbridgeheadCN}$, ½ $GeCH_2{}^{n}{}_{Bu}$), 1.54-1.64 (m, 2H, ½ $CH_{2CbridgeheadCP}$, ½ $GeCH_2{}^{n}{}_{Bu}$), 1.76-185 (m, 2H, ½ $CH_{2CbridgeheadCP}$, ½ $CH_{2bridge}$), 2.44 (brs, 1H, $PCCH_{bridgehead}$), 2.54-2.65 (m, 2H, $PNCH_2$), 2.69-2.80 (m, 2H, $PNCH_2$), 2.88 (brs, 1H, $NCCH_{bridgehead}$), 3.29 (sept, $^{3}J_{HH}$ = 6.6 Hz, 1H, CH_{iPr}), 3.56-3.65 (m, 1H, $PNCH_{iPr}$), 3.76 (sept, $^{3}J_{HH}$ = 6.9 Hz, 1H, CH_{iPr}), 3.91-4.00 (m, 1H, $PNCH_{iPr}$), 7.13-7.17 (m, 3H, H_{Ar}). $^{13}C\{^{1}H\}$ NMR (75.47 MHz, C_6D_6, 25°C): δ = 13.94 (s, $CH_3{}^{n}{}_{Bu}$), 19.30 (d, $^{2}J_{PC}$ = 2.1 Hz, $GeCH_2{}^{n}{}_{Bu}$), 19.82 (d, $^{3}J_{PC}$ = 1.4 Hz, CH_{3PNiPr}), 20.10 (d, $^{3}J_{PC}$ = 1.5 Hz, CH_{3PNiPr}), 21.21 (d, $^{3}J_{PC}$ = 6.4 Hz, CH_{3PNiPr}), 21.47 (d, $^{3}J_{PC}$ = 3.1 Hz, CH_{3PNiPr}), 24.49 (s, CH_{3iPr}), 24.69 (s, CH_{3iPr}), 24.67 (s, CH_{3iPr}), 25.58 (d, $^{3}J_{HP}$ = 1.3 Hz, 3H, $GeCH_2CH_2{}^{n}{}_{Bu}$), 26.19 (d, J_{PC} = 2.7 Hz, CH_{3iPr}), 26.82 (s, $CH_{2CbridgeheadCN}$), 27.37 (s, CH_{iPr}), 28.26 (s, CH_{iPr}), 30.11 (d, $^{3}J_{PC}$ = 0.9 Hz,$CH_{2CbridgeheadCP}$), 30.62 (d, $^{4}J_{HP}$ = 9.8 Hz, 3H, $CH_2CH_3{}^{n}{}_{Bu}$), 39.05 (d, $^{2}J_{PC}$ = 2.5 Hz, $PNCH_2$), 39.21 (d, $^{2}J_{PC}$ = 1.5 Hz, $PNCH_2$), 40.92 (d, $^{3}J_{PC}$ = 7.8 Hz, $NCCH_{bridgehead}$), 43.42 (d, $^{2}J_{PC}$ = 13.5 Hz, $PCCH_{bridgehead}$), 43.98 (d, $^{2}J_{PC}$ = 6.4 Hz, $PNCH_{iPr}$), 44.72 (d, $^{2}J_{PC}$ = 11.3 Hz, $PNCH_{iPr}$), 48.95 (d, $^{3}J_{PC}$ = 3.0 Hz, $CH_{2bridge}$), 92.09 (d, J_{PC} = 30.2 Hz, P*C*=CN), 123.44, 123.97, 126.06 (3 x s, 3C, CH_{Ar}), 141.65 (d, $^{3}J_{PC}$ = 5.2 Hz, NC_{ipso}), 145.96, 147.32 (2 x s, 2C, NC_{orto}), 186.83 (d, $^{2}J_{PC}$ = 40.2 Hz, PC=*C*N). $^{31}P\{^{1}H\}$ NMR (121.49 MHz, C_6D_6, 25°C): δ = 80.95 (s). Anal calcd. For $C_{31}H_{52}N_3PGe$: C 65.31, H 9.12, N 7.37; found: C, 66.65; H, 9.34; N, 7.60.

IV.3.6. Reaction of (<u>40</u>) with H_2O

To a C_6D_6 solution (0.5 mL) of (**<u>40</u>**) (50.0 mg, 0.095 mmol) was added at RT H_2O (3.4 µL, 0.19 mmol). After stirring for 1 night at RT, all the volatiles were removed under vacuum to obtain the products as yellow oil. The products were analyzed without any further

purification. **43a**: ^{1}H NMR (300.18 MHz, C_6D_6, 25°C) δ = 0.98 (d, $^{3}J_{HH}$ = 6.6 Hz, 6H, CH_{3PNiPr}), 1.07 (d, $^{3}J_{HH}$ = 6.6 Hz, 6H, CH_{3PNiPr}), 2.43-2.50 (m, 2H, $PNCH_2$), 2.69-2.78 (m, 2H, $PNCH_2$), 3.3 (sept, $^{3}J_{HH}$ = 3.6 Hz, 2H, $PNCH_{iPr}$), 7.45 (d, J_{PH} = 586.1 Hz, P-H). $^{13}C\{^{1}H\}$ NMR (75.47 MHz, C_6D_6, 25°C): δ = 21.11 (d, $^{3}J_{PC}$ = 3.6 Hz, CH_{3PNiPr}), 21.24 (d, $^{3}J_{PC}$ = 3.5 Hz, CH_{3PNiPr}), 40.61 (d, $^{2}J_{PC}$ = 9.3 Hz, $PNCH_{iPr}$), 45.67 (d, $^{2}J_{PC}$ = 5.9 Hz, $PNCH_2$). $^{31}P\{^{1}H\}$ NMR (121.49 MHz, C_6D_6, 25°C): δ = 8.57 (d, J_{PH} = 583.2 Hz, P-H). **43b**: ^{1}H NMR (300.18 MHz, C_6D_6, 25°C) δ = 1.18 (d, $^{3}J_{HH}$ = 1.4 Hz, 3H, CH_{3iPr}), 1.19 (d, $^{3}J_{HH}$ = 1.1 Hz, 3H, CH_{3iPr}), 1.20 (d, $^{3}J_{HH}$ = 1.6 Hz, 3H, CH_{3iPr}), 1.22 (d, $^{3}J_{HH}$ = 0.8 Hz, 3H, CH_{3iPr}), 125-139 (m, 4H, CH_{2nor}), 1.44-159 (m, 4H, CH_{2nor}), 2.03 (brs, 1H, CH_{nor}), 2.94 (brs, 1H, CH_{nor}), 3.03 (m, 2H, CH_{iPr}), 7.13-7.18 (m, 3H, H_{Ar}).$^{13}C\{^{1}H\}$ NMR (75.47 MHz, C_6D_6, 25°C): δ = 22.68 (s, CH_{3iPr}), 22.91 (s, CH_{3iPr}), 23.42 (s, CH_{3iPr}), 23.60 (s, CH_{3iPr}), 26.49, 27.51 (2xs, 2C, *C*H_{2nor}), 27.73, 28.05 (2xs, 2C, CH_{iPr}), 35.87 (s, CH_{nor}), 38.11, 38.79 (2xs, 2C, *C*H_{2nor}), 47.05 (s, CH_{nor}), 123.07, 123.11, 123.43 (3xs, 3C, CH_{Ar}), 135.89, 136.26 (2xs, 2C, NC_{orto}), 147.06 (s, NC_{ipso}), 180.07 (s, CH_2=*C*N).

IV.3.7. Synthesis of cycloadduct (46)

To a solution of (**40**) (50 mg, 0.095 mmol) in C_6D_6 (0.5 mL) 2,3-dimethyl-1,3-butadiene (21.4 μL, 0.189 mmol) was added at RT. After heating for 72 h at 65ºC, all the volatiles were removed under vacuum and the cyclic adduct (**46**) was obtained as yellow oil and was analyzed without any further purification.^{1}H NMR (300.18 MHz, C_6D_6, 25°C): the most representative signals δ = 0.48 (brs, 3H, $GeCH_3$), 1.47 (brs, 3H, CH_3vinyl), 1.47 (brs, 1H, ½CH_2vinyl), 1.66 (brs, 3H, CH_3vinyl), 1.70 (brs, 3H, 3/2CH_2vinyl). $^{13}C\{^{1}H\}$ NMR (75.47 MHz, C_6D_6, 25°C): δ = 1.06 (s, $GeCH_3$), 19.19 (s, 2C, CH_3vinyl), 22.02 (d, $^{3}J_{PC}$ = 15.2 Hz, 2C, CH_{3PNiPr}), 22.18 (d, $^{3}J_{PC}$ = 10.6 Hz, CH_{3PNiPr}), 22.77 (d, $^{3}J_{PC}$ = 11.8 Hz, CH_{3PNiPr}), 23.15 (s, CH_{3iPr}), 23.28 (s, CH_{3iPr}), 23.38 (s, CH_{3iPr}), 23.52 (s, CH_{3iPr}), 25.90 (s, *C*$H_{2CbridgeheadCN}$), 27.62 (s, CH_{iPr}), 27.73 (s, CH_{iPr}), 28.57 (s, 3C, *C*$H_{2CbridgeheadCP}$, CH_2vinyl), 43.73 (d, $^{2}J_{PC}$ = 1.6 Hz, PC*C*$H_{bridgehead}$), 44.30 (d, $^{3}J_{PC}$ = 3.7 Hz, $CH_{2bridge}$), 44.84 (d, $^{2}J_{PC}$ = 22.6 Hz, $PNCH_{iPr}$), 49.42 (d, $^{2}J_{PC}$ = 8.7 Hz, $PNCH_2$), 49.71 (d, $^{2}J_{PC}$ = 15.0 Hz, $PNCH_{iPr}$), 50.09 (d, $^{2}J_{PC}$ = 6.7 Hz, $PNCH_2$), 51.41 (d, $^{3}J_{PC}$ = 22.1 Hz, NC*C*$H_{bridgehead}$), 106.62 (d, J_{PC} = 33.0 Hz, P*C*=CN), 123.11, 123.29, 126.30 (3 x s, 3C, CH_{Ar}), 129.97, 130.02 (brs, 2C, C=C), 137.15 (s, 2C, NC_{orto}), 147.24 (brs, NC_{ipso}), 158.97 (d, $^{2}J_{PC}$ = 5.5 Hz, PC=*C*N). $^{31}P\{^{1}H\}$ NMR (121.49 MHz, C_6D_6, 25°C): δ = 84.47 (s).

IV.3.8. Synthesis of germylene-borane complex (49)

To a solution of (**39**) (100 mg, 0.169 mmol) in THF (20 mL) was added dropwise a solution of BH_3 (93 µL 0.186 mmol) in THF (2 M) and stirred for 1 h at -80°C. The crude was to warm at room temperature and stirred for 1 h. Then, all the volatiles were removed under vacuum and the residue was extracted twice in pentane. The concentrated pentane solution at -30 °C gave (**49**) as white powder (30.6 mg, 30 %). **Isomer 49** (50%): $^{31}P\{^{1}H\}$ NMR (121.49 MHz, C_6D_6, 25°C): δ = 60.53 (s). $^{11}B\{^{1}H\}$ NMR (96.29 MHz, C_6D_6, 25°C): δ = -35.88 (brs). **Isomer 49'** (50%): $^{31}P\{^{1}H\}$ NMR (121.49 MHz, C_6D_6, 25 °C): δ = 57.10 (s). $^{11}B\{^{1}H\}$ NMR (96.29 MHz, C_6D_6, 25°C): δ = -40.61 (brs).

IV.3.9. Crystallographic data

The data of the structures for the compounds (**38**) and (**39**) were collected on a Bruker-AXSAPEX II diffractometer at a temperature of 193K with graphite-monochromated MoKα radiation (wavelength = 0.71073 Å) by using phi- and omega-scans. We solved the structure by direct methods, using SHELXS-97.

38: $C_{27}H_{43}ClGeN_3P$, M= 548.65, Monoclinic, space group $P2_1/c$, a=10.3296(5) Å, b= 18.4260(9) Å, c= 15.6319(7) Å, V= 2941(2) Å^3, Z= 4, crystal size 0.25 x 0.10 x 0.08 mm^3, 29957 reflections collected (5537 independent, R_{int}= 0.1458), 596 parameters, 1224 restraints, $R1$ [I>2σ(I)]= 0.0617, $wR2$ [all data]= 0.1999, largest diff. peak and hole: 0.446 and -0.397 e.Å^{-3}.

39: $C_{33}H_{48}GeN_3P$, M= 590.30, Monoclinic, space group $P2_1/c$, a= 18.7398(3) Å, b= 16.2976(2) Å, c= 10.7861(2) Å, β= 101.6100(10)°, V= 3226.82(9) Å^3, Z= 4, crystal size 0.25 x 0.15 x 0.10 mm^3, 56460 reflections collected (6542 independent, R_{int}= 0.0908), 351 parameters, $R1$ [I>2σ(I)]= 0.0363, $wR2$ [all data]= 0.0908, largest diff. peak and hole: 0.543 and -0.238 e.Å^{-3}.

IV.4. Conclusions

The synthesis of heteroleptic divalent germanium species (**38**-**41**), intramolecularly base-stabilized by coordination of a phosphine ligand, has been described. These compounds showed to be stable at room temperature under inert atmosphere, and soluble in organic solvents such as: tetrahydrofuran, benzene, toluene, pentane and ethyl ether.

The Chloro substituent on the germanium center of (**38**) can be replaced by alkyl and phenyl groups. This fact suggests that one can easily modulate the electron density, and therefore the nucleophilic character, on the germanium(II) center.

Stabilized-phosphine germylenes (**38**-**41**) were obtained as a mixture of two diastereomers owing to the chiral norbonadiene fragment and to the pyramidalized chiral germanium(II) center.

Hydrolysis of germylene (**40**) led to the fragmentation of the molecule to form 1,3-diisopropyl-2-oxo-1,3,2-diazaphospholidine (**43a**) and the imine (**43b**). 2-phosphine enamine (**d'**) was detected as a reaction intermediate, and its hydrolysis leads to formation of (**43a**) and (**43b**).

Phosphine-stabilized germylenes (**39** and **40**) showed to be inert toward unsaturated compounds, such as: alkyne, alkene and carbonyl derivatives. The absence of reactivity with carbonyl derivatives suggests that phosphine-stabilized germylenes (**38**-**41**) do not exhibit a phosphonium ylide-like reactivity.

Germylene (**40**) showed to be reactive toward 2,3-dimethylbutadiene to form [1+4] cycloadduct (**46**). This reactivity is typical of free kinetically stabilized germylenes.

Germylene (**39**) reacts with $BH_3 \cdot THF$, as a Lewis bases, to form the corresponding germylene-borane complex (**49**). This indicates that phosphine-stabilized germylenes (**39**-**41**) can be capable of behaving as σ-donor/π-acceptor ligands resembling phosphines (PR_3).

Chapter V

Phosphine-stabilized germylenes as ligands for transition metal complexes

V.1. Introduction

Since pioneering work of T. J. Marks,[105] divalent germanium compounds have attracted growing interest not only as possible synthetic tools in organic chemistry but also for their potential use as ligands for transition metals.[106-110] Over the last year, many efforts have been devoted to study the coordination chemistry and ligating properties of germylene compounds.[81,101,103,111-119] However, there has been little research in comparison to the more studied transition metal carbene chemistry.[120]

The ability of these compounds to coordinate to transition metals is based on the presence of a singlet lone pair capable of interacting with metals in a dative bonding sense, as well as an empty π-acidic p orbital localized on the germanium (II) center capable to accept electron density from metal center, as a M→Ge π-back bonding (Figure V.1).

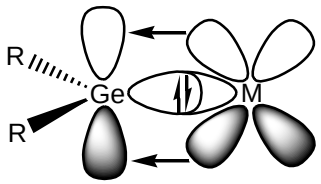

Figure V.I. Bonding in germylene-metal complexes.

The majority of characterized complexes involve three- four- or five-coordinate Ge atoms. These complexes can roughly be classified in three types, shown in figure V.II. In these arrangements, X and Y are σ-bonded substituents, and B stands for a neutral Lewis base molecule. GeXY (I) and GeXY←B (II) are neutral entities and coordinated to a transition metal through a lone pair of electrons. Type III complexes contain germanium atoms with more than one neutral donor molecule B.

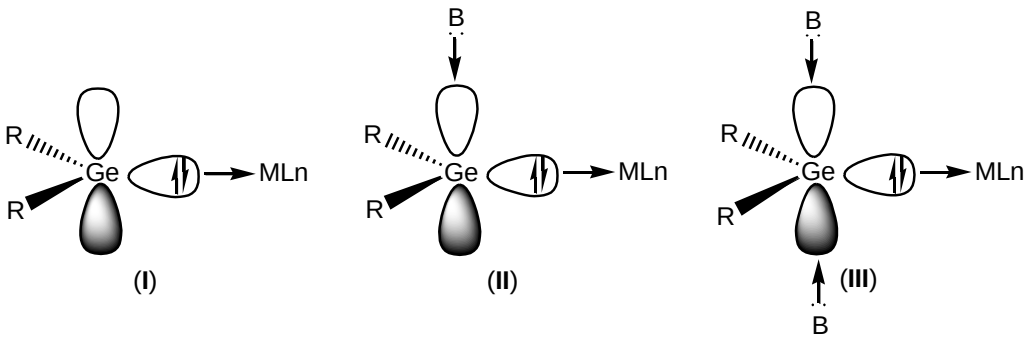

Figure V.II. Types of germylene-metal complexes.

Recently, inter- and intramolecularly base-stabilized germylenes have shown useful applications as ligands in coordination chemistry. A number of metal complexes bearing by *N*-heterocyclic-stabilized germylenes ligands.[115,118,119] and *N*-heterocyclic carbenes [101,103] are known. However, coordination chemistry of phosphine-stabilized germylenes has not yet been studied.

We have demonstrated that germylene (**39**) can react as a Lewis base with BH_3 leading to the formation of phosphine-germylene-borane complex (**49**). This result prompted us to study the ligating properties of the phosphine-stabilized germylenes. In this sense, we have studied the reactivity of germylenes toward the dimer complex $[Rh_2(\mu\text{-}Cl)_2(COD)_2]$**.**

V.2. Results and discussions

V.2.1. Reaction of germylene (38) with dimer complex $[Rh_2(\mu\text{-}Cl)_2(COD)_2]$

Addition at room temperature of a THF solution of germylene (**38**) to $[Rh_2(\mu\text{-}Cl)_2(COD)_2]$ in THF led to the formation of an orange solution, which corresponds to a mixture of three complexes, as indicated by the presence of three doublets in the $^{31}P\{^1H\}$ NMR spectrum [δ = 61.91 (d, J_{PRh} = 153.8 Hz, 37%, **51**), 51.78 (d, J_{PRh} = 28.4 Hz, 37%, **50**), 49.34 (d, J_{PRh} = 24.2 Hz, 26%, **50'**)] (Figure V.3a). After 2 h at RT, the solution changes to red and the $^{31}P\{^1H\}$ NMR spectrum only showed the signal corresponding to complex (**51**) (Figure V.3b).

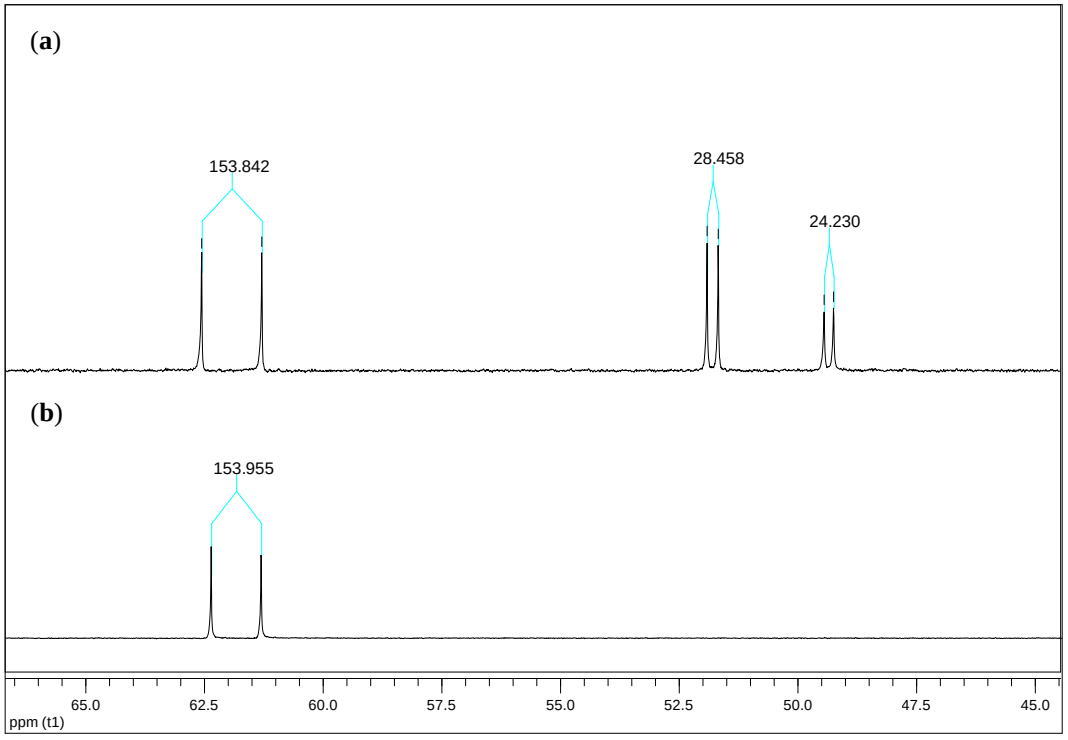

Figure V.3. $^{31}P\{^1H\}$ NMR spectra at RT of reaction of (**38**) with $[Rh_2(\mu\text{-}Cl)_2(COD)_2]$ (**a**): 1 h of reaction, and (**b**): 2 h of reaction.

The chemical shifts for intermediate complexes (**50** and **50'**) are similar to that of germanium-borane complexes (**49**), suggesting the coordination of germylene moiety to rhodium center. Furthermore, chemical shift and coupling constant observed for complex (**51**) reveal the coordination of phosphine moiety to rhodium center, which means the loss of

coordination bonding P→Ge. It is reasonable to think that the complex (**51**) arises from the intermediate complexes (**50**), by migration of chloride ligand from rhodium to germanium atom, which leads to the oxidation of germanium atom from Ge(II) to Ge(IV) (Scheme V.1).

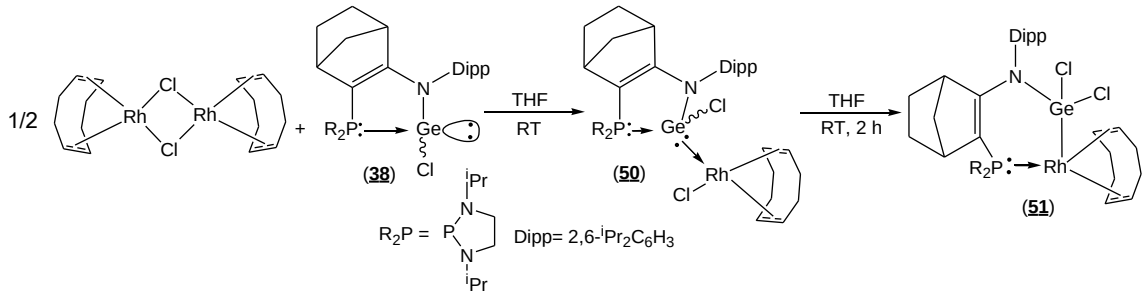

Scheme V.1. Reaction of (**38**) with $[Rh_2(\mu\text{-}Cl)_2(COD)_2]$.

Complex (**51**) was isolated as red crystals from a concentrated THF solution at -30°C and its structure was confirmed by an X-ray diffraction analysis. In addition, complex (**51**) was fully characterized by ^{1}H, $^{13}C\{^{1}H\}$, $^{31}P\{^{1}H\}$ NMR spectroscopy. The formation of complex (**51**) indicates that germylene (**38**) can be regarded as a chelate ligand, which contains two different chemical functions: a phosphine and a dichlorogermyl fragment.

Molecular structure of complex (51)

Structure of (**51**) was unambiguously established by a single-crystal X-ray diffraction analysis. Selected bond lengths and angles are listed in Table V.1. Molecular structure of (**51**) clearly exhibits the six-membered metallacycle formed by chelating coordination of germylene (**38**) ligand. Likewise, complex (**51**) shows slightly distorted square planar coordination geometry (Figure V.4). This distortion may result from steric bulk of the phosphino-dichlorogermyl ligand.

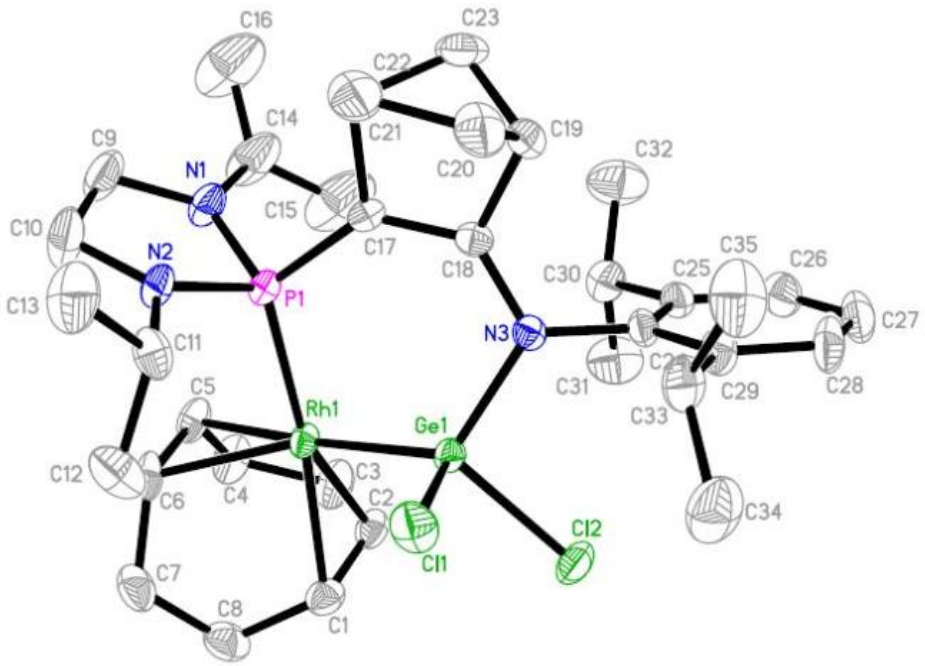

Figure V.4. Molecular structure of complex (**51**). Thermal ellipsoids represent 30% probability and H atoms have been omitted for clarity.

The Rh−P bond length [Rh(1)−P(1) = 2.2865(12) Å] compares well with the Rh−P bonds of Rh (I) cyclooctadiene phosphine complexes having a square planar coordination geometry, such as cationic complex (**23b**) (2.287(4) Å). In addition, molecular structure of (**51**) shows a strongly distorted tetrahedral geometry around the germanium atom, as shown by the Cl(2)−Ge(1)−Cl(1) bond angle [98.32(6)°], which is considerably more acute than N(3)−Ge(1)−Rh(1) angle [119.93(10)°]. A similar distortion was previously observed in several trichlorogermyl tungsten complexes.[121-123] The Ge−Cl bond lengths [Ge(1)−Cl(1) = 2.2316(12) Å and Ge(1)−Cl(2) = 2.2114(13) Å] are in the range observed for various halogermanium (IV) complexes (η^5-C_5R_5)$M(CO)_3GeCl_3$ (R= H, Me; M = Mo, W) (2.203-2.244 Å) [121-123] but are larger than that of $GeCl_4$ (2.113(3) Å).[124] Furthermore, the Ge(1)−Rh(1) bond length (2.3575(6) Å) is shorter than the Ge−Rh distance, 2.5061(4) Å, in the complex $Rh(CO)_4$-($GePh_3$).[125] These structure features suggest the presence of a rhodium-dichlorogermyl π-back bonding.

Table V.1. Selected bond lengths (Å) and bond angles (deg) of complex (**51**)

Bond distances		Bond angles	
Rh(1)−P(1)	2.2865(12)	Cl(2)−Ge(1)−Cl(1)	98.32(6)
Rh(1)−Ge(1)	2.3575(6)	N(3)−Ge(1)−Rh(1)	119.93(10)
Ge(1)−Cl(1)	2.2316(12)	N(3)−Ge(1)−Cl(2)	100.65(11)
Ge(1)−Cl(2)	2.2114(13)	N(3)−Ge(1)−Cl(1)	101.56(10)
Ge(1)−N(3)	1.882(3)	Cl(2)−Ge(1)−Rh(1)	119.65(4)
N(3)−C(18)	1.372(5)	Cl(1)−Ge(1)−Rh(1)	113.19(4)
C(17)−C(18)	1.395(6)	P(1)−Rh(1)−Ge(1)	87.46(3)
P(1)−C(17)	1.764(4)	C(17)−P(1)−Rh(1)	118.57 (3)
P(1)−N(1)	1.693(4)	C(18)−C(17)−P(1)	132.3(3)
P(1)−N(2)	1.687(3)	N(3)−C(18)−C(17)	131.1(4)
N(3)−C(24)	1.450(5)	C(18)−N(3)−Ge(1)	117.4(3)

V.2.2. Reaction of germylene (39) with dimer complex $[Rh_2(\mu\text{-}Cl)_2(COD)_2]$

The addition at room temperature of a solution germylene (**39**) in THF to $[Rh_2(\mu\text{-}Cl)_2(COD)_2]$ led to an orange solution corresponding to the new complex (**52**), which remains unchanged over 2 h reaction. Suitable yellow crystals of (**52**) were obtained from a THF-Et_2O solution at -30°C.

The $^{31}P\{^1H\}$ NMR spectrum at RT of obtained product shows a broad signal at 60.27 ppm (Figure V.5). This chemical shift is similar to that observed for germanium-borane complex (**49**), which suggests the coordination of germylene (**39**) to rhodium through σ-bonding coordination Ge(II)−Rh forming complex (**52**).

Moreover, the breadth of this resonances and the absence of P-Rh coupling suggests the presence of a dynamic behavior, however, $^{31}P\ \{^1H\}$ NMR spectrum remains unchanged within a wide range of temperature (-80 to 35°C).

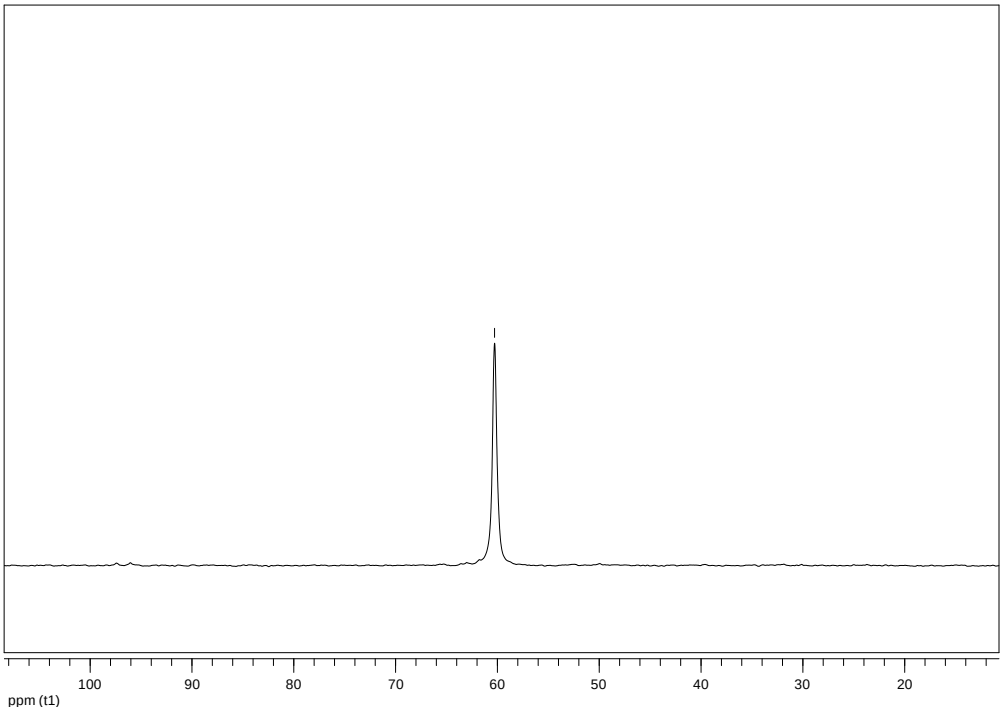

Figure V.5. $^{31}P\{^{1}H\}$ NMR spectrum at RT of reaction of (**39**) with $[Rh_2(\mu\text{-}Cl)_2(COD)_2]$.

The structure of complex (**52**) was established by an X-ray diffraction analysis, and by ^{1}H, $^{13}C\{^{1}H\}$, $^{31}P\{^{1}H\}$ NMR spectroscopies (Scheme V.2).

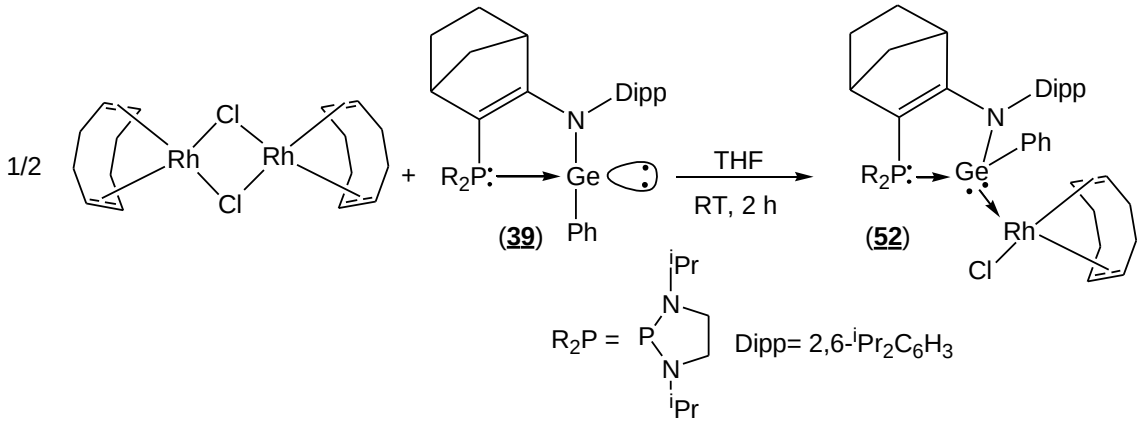

Scheme V.2. Reaction of (**39**) with $[Rh_2(\mu\text{-}Cl)_2(COD)_2]$.

The formation of complex (**52**) reveals that germylene (**39**) can behave as a σ-donor ligand, furthermore, it demonstrates that the ligating properties of phosphine-stabilized germylene can be modified by replacing the germanium substituent.

*Molecular structure of complex (**52**)*

The molecular structure of (**52**) is shown in Figure V.6, and selected bond lengths and angles are listed in Table V.2. Complex (**52**) shows a square planar coordination geometry, in which germylene ligand (**39**) is coordinated to metal center through of lone pair on the germanium atom.

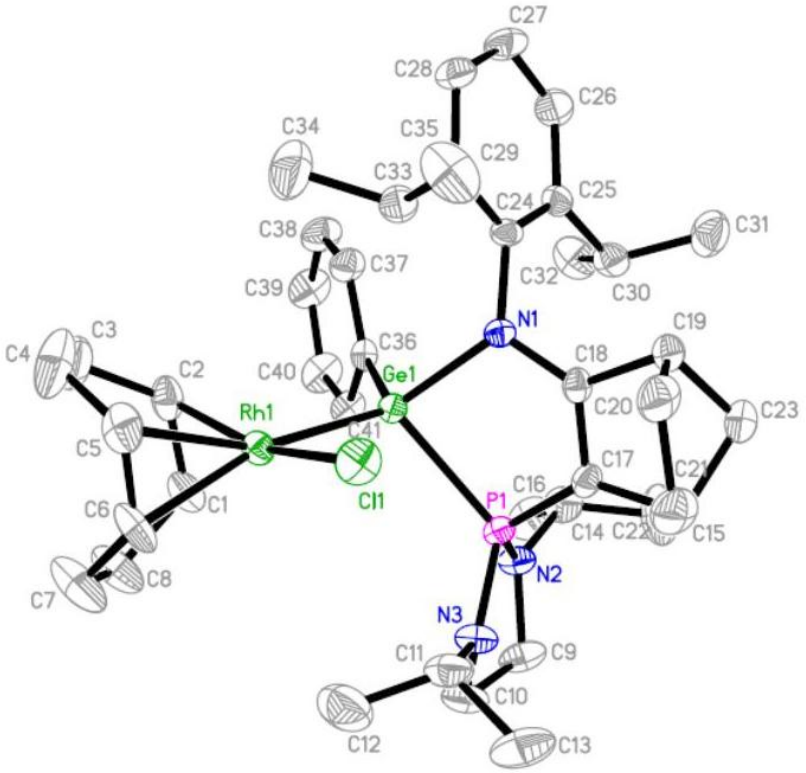

Figure V.6. Molecular structure of complex (**52**). Thermal ellipsoids represent 30% probability and H atoms have been omitted for clarity.

Molecular structure of (**52**) shows a strongly distorted tetrahedral geometry around the germanium atom, as shown by the N(1)−Ge(1)−P(1) bond angle [86.67(14)°], which is considerably more acute than C(36)−Ge(1)−Rh(1) angle [117.80(17)°]. The N(1)−Ge(1)−P(1) angle is wider than that observed in the free ligand [N(1)−Ge(1)−P(1), 84.69(3)], probably due to the change of coordination number of the germanium atom [tricoordinate for (**39**) and tetracoordinate for (**52**)].

The Ge(1)−P(1) and Ge(1)−C(36) bond lengths [2.3946(17) and 1.971(6) Å] in the complex (**52**) are slightly shorter than those in the germylene (**39**) [Ge(1)−P(1) = 2.434(6) and

Ge(1)−C(28) = 2.003(3) Å] . These differences may be ascribable to the diminished densities around the germanium atom in (**52**) compared to free ligand (**39**).

Table V.2. Selected bond lengths (Å) and bond angles (deg) of complex (**52**)

Bond distances		**Bond angles**	
Ge(1)−N(1)	1.957(5)	Cl(1)−Rh(1)−Ge(1)	93.07(6)
Ge(1)−C(36)	1.971(6)	C(36)−Ge(1)−Rh(1)	117.80(17)
Ge(1)−P(1)	2.3946(17)	N(1)−Ge(1)−C(36)	102.5(2)
P(1)−C(17)	1.734(7)	C(36)−Ge(1)−P(1)	109.09(18)
C(17)−C(18)	1.381(9)	N(1)−Ge(1)−P(1)	86.67(14)
P(1)−N(3)	1.653(5)	C(18)−N(1)−Ge(1)	113.0(4)
P(1)−N(2)	1.666(6)	N(1)−C(18)−C(17)	129.1(3)
N(1)−C(24)	1.448(7)	C(18)−C(17)−P(1)	117.0(4)
Ge(1)−Rh(1)	24501(9)	C(11)−P(1)−Ge(1)	92.5(2)

In addition, the Ge−Rh bond length in complex (**52**) [2.4501(9) Å] is longer than that observed for complex (**51**) [2.3575(6) Å], but slightly shorter than that reported for complex $Rh(CO)_4$-($GePh_3$) [125] [2.5061(4) Å]. Likewise, Ge−Rh bond distance in complex (**52**) is shorter than the Ge−M bond distances observed in the pentacarbonyltungsten complexes with base-stabilized germylene ligands (2.571 Å) [(115) (126)] and even for various halogermanium (IV) complexes (η^5-C_5R_5)$M(CO)_3GeCl_3$ (R= H, Me; M = Mo, W).[121-123] Based on the obtained results, germylene (**39**) can be regarded a σ-donor ligand, however, it is difficult to evaluate or quantify its π-acceptor properties toward transition metal complexes.

V.3. Experimental part

V.3.1. General Considerations

All manipulations were performed under an inert atmosphere of argon by using standard Schlenk techniques. Dry, oxygen-free solvents were employed. All reagents were obtained from commercial suppliers.

^{1}H, $^{13}C\{^{1}H\}$, $^{31}P\{^{1}H\}$ NMR spectra were recorded on Bruker, Avance 500 or Avance 300 spectrometers. ^{1}H, $^{13}C\{^{1}H\}$ NMR chemical shifts are reported in ppm relative to Me_4Si as external standard. $^{31}P\{^{1}H\}$ NMR chemical shifts are expressed in ppm relative to 85% H_3PO_4.

V.3.2. Synthesis of complex (51)

To a solution of $[Rh_2(\mu\text{-}Cl)_2(COD)_2]$ (30.0 mg, 0.062 mmol) in THF (7 µL) was added (**38**) at RT (66 mg, 0.121 mmol). After stirring for 2 h at RT, all the volatiles were removed under vacuum. Suitable red crystals were obtained from a saturated THF solution at -30°C. ^{1}H NMR (300.18 MHz, C_6D_6, 25°C): δ = 0.71 (d, J_{HH} = 8.2 Hz, 1H, ½ $CH_{2bridge}$), 1.15 (d, J_{HH} = 6.5 Hz, 3H, CH_{3PNiPr}), 1.18 (d, J_{HH} = 6.7 Hz, 3H, CH_{3PNiPr}), 1.17 (overlapped with the methyl signal, 1H, ½ $CH_{2bridge}$), 1.27 (d, J_{HH} = 6.9 Hz, 3H, CH_{3iPr}), 1.29 (d, J_{HH} = 6.9 Hz, 3H, CH_{3iPr}), 1.33 (d, J_{HH} = 6.4 Hz, 3H, CH_{3PNiPr}), 1.45 (d, J_{HH} = 6.8 Hz, 3H, CH_{3iPr}), 1.48 (d, J_{HH} = 6.4 Hz, 3H, CH_{3PNiPr}), 1.55 (m, 3H, $CH_{2CbridgeheadCP}$, ½ $CH_{2CbridgeheadCN}$), 1.69 (d, J_{HH} = 6.6 Hz, 3H, CH_{3iPr}), 1.68 (overlapped with the methyl signal, 1H, ½ $CH_{2CbridgeheadCN}$), 1.76-2.11 (m, 8H, $4CH_{2COD}$), 2.53 (m, 1H, $PCCH_{bridgehead}$), 2.58-2.66 (m, 2H, $PNCH_2$), 2.77-2.85 (m, 3H, $NCCH_{bridgehead}$, $PNCH_2$), 3.26 (m, 1H, $PNCH_{iPr}$), 3.70 (sept, J_{HH} = 6.8 Hz, 1H, CH_{iPr}), 4.13 (sep, J_{HH} = 6.7 Hz, 1H, CH_{iPr}), 4.30 (m, 2H, $PNCH_{iPr}$), 4.80, 4.91 (2xbrs, 2H, $CH{=}CH_{COD}$), 5.45, 5.79 (2xbrs, 2H, $CH{=}CH_{COD}$), 7.17-7.28 (m, 3H, H_{Ar}). $^{13}C\{^{1}H\}$ NMR (75.47 MHz, C_6D_6, 25°C): δ = 21.65 (d, $^{3}J_{PC}$ = 5.4 Hz, CH_{3PNiPr}), 22.00 (d, $^{3}J_{PC}$ = 5.5 Hz, CH_{3PNiPr}), 22.40 (d, $^{3}J_{PC}$ = 2.5 Hz, CH_{3PNiPr}), 22.91 (d, $^{3}J_{PC}$ = 6.0 Hz, CH_{3PNiPr}), 24.63 (s, 2C, CH_{3iPr}), 24.85 (s, CH_{3iPr}), 25.84 (s, CH_{3iPr}), 26.11 (d, $^{4}J_{PC}$ = 1.2 Hz, $CH_{2CbridgeheadCN}$), 28.05 (s, CH_{iPr}), 28.25 (s, CH_{iPr}), 28.27 (s, $CH_{2CbridgeheadCP}$), 29.12 (d, $^{2}J_{RhC}$ = 2.1 Hz, CH_{2COD}), 29.66 (d, $^{2}J_{RhC}$ = 1.8 Hz, CH_{2COD}), 30.57 (d, $^{2}J_{RhC}$ = 3.2 Hz, CH_{2COD}), 30.89 (d, $^{2}J_{RhC}$ = 1.4 Hz, CH_{2COD}), 39.95 (d, $^{2}J_{PC}$ = 1.7 Hz, $PNCH_2$), 42.72 (d, $^{3}J_{PC}$ = 3.6 Hz, $CH_{2bridge}$), 44.95 (d, $^{2}J_{PC}$ = 13.4 Hz, $PNCH_{iPr}$),

45.76 (d, $^{3}J_{PC}$ = 1.7 Hz, NC*C*H$_{bridgehead}$), 45.90 (d, $^{2}J_{PC}$ = 1.2 Hz, PNCH$_2$), 47.20 (d, $^{2}J_{PC}$ = 6.3 Hz, PNCH$_{iPr}$), 48.21 (d, $^{2}J_{PC}$ = 8.2 Hz, PC*C*H$_{bridgehead}$), 94.73 (d, J_{RhC} = 8.2 Hz, HC=*C*H$_{COD}$), 96.21 (t, J_{RhC} = 2.7 Hz, HC=*C*H$_{COD}$), 96.36 (d, J_{RhC} = 5.9 Hz, H*C*=CH$_{COD}$), 100.29 (dd, J_{RhC} = 6.2 Hz,$^{2}J_{PC}$ = 10.2Hz, H*C*=CH$_{COD}$), 105.19 (dd, J_{PC} = 40.3 Hz, $^{2}J_{RhC}$ = 7.3 Hz, P*C*=CN), 123.33, 124.22, 126.86 (3 x s, 3C, CH$_{Ar}$), 140.29 (s, NC$_{ipso}$), 147.21, 148.77 (2 x s, 2C, NC$_{orto}$), 174.65 (d, $^{2}J_{PC}$ = 17.8 Hz, PC=*C*N). $^{31}P\{^{1}H\}$ NMR (121.49 MHz, C_6D_6, 25°C): δ = 61.75 (d, J_{PRh} = 153.9 Hz).

V.3.3. Synthesis of complex (52)

To a solution of [Rh$_2$(μ-Cl)$_2$(COD)$_2$] (30.0 mg, 0.062 mmol) in THF (7 μL) was added (**39**) at RT (71 mg, 0.121 mmol). After stirring for 2 h at RT, the product precipitates as a yellow solid. Suitable yellow crystals were obtained from a THF-Et$_2$O solution at -30°C. ^{1}H NMR (300.18 MHz, $CDCl_3$, 25°C): δ = 0.94 (d, $^{3}J_{HH}$ = 6.8 Hz, 3H, CH$_{3iPr}$), 1.03 (d, $^{3}J_{HH}$ = 6.5 Hz, 6H, CH$_{3PNiPr}$), 1.14 (d, $^{3}J_{HH}$ = 6.7 Hz, 3H, CH$_{3iPr}$), 1.15 (overlapped with the methyl signal, 1H, ½ CH$_{2CbridgeheadCP}$), 1.18 (d, $^{3}J_{HH}$ = 6.6 Hz, 3H, CH$_{3PNiPr}$), 1.44 (m, 4H, CH$_{2bridge}$, ½ CH$_{2CbridgeheadCP}$, ½ CH$_{2CbridgeheadCN}$), 1.69 (d, $^{3}J_{HH}$ = 6.8 Hz, 12H, CH$_{3PNiPr}$, 2CH$_{3iPr}$), 1.70 (overlapped with the methyl signal, 1H, ½ CH$_{2CbridgeheadCN}$), 1.98 (m, 4H, PNCH$_2$), 2.28 (m, 4H, PNCH$_2$), 2.62 (brs, 1H, PCCH$_{bridgehead}$), 2.70 (m, 1H, CH$_{iPr}$), 2.93 (brs, 1H, NCCH$_{bridgehead}$), 2.98-3.09 (m, 4H, 2 PNCH$_2$), 3.17-3.23 (m, 2H, PNCH$_{iPr}$), 3.29 (m, 1H, CH$_{iPr}$), 4.96, 5.07 (2xbrs, 4H, CH=CH$_{COD}$), 6.96 (m, 6H, H$_{Ar}$), 7.22 (m, 3H, H$_{Ar}$). $^{13}C\{^{1}H\}$ NMR (75.47 MHz, $CDCl_3$, 25°C): δ = 20.29 (s, CH$_{3PNiPr}$), 21.08 (d, $^{3}J_{PC}$ = 2.5 Hz, CH$_{3PNiPr}$), 21.44 (d, $^{3}J_{PC}$ = 8.6 Hz, CH$_{3PNiPr}$), 21.82 (d, $^{3}J_{PC}$ = 1.7 Hz, CH$_{3PNiPr}$), 22.47 (s, CH$_{3iPr}$), 25.23 (s, CH$_{3iPr}$), 25.51 (s, CH$_{3iPr}$), 25.66 (s, CH$_{3iPr}$), 26.84 (s, CH$_{2COD}$), 27.41 (s, CH$_{2COD}$), 27.53 (s, CH$_{iPr}$), 27.82 (s, CH$_{iPr}$), 29.01 (s, CH$_{2COD}$), 29.42 (s, CH$_{2COD}$), 32.32 (s, *C*H$_{2CbridgeheadCN}$), 34.81 (s, *C*H$_{2CbridgeheadCP}$), 39.03 (brs, 2C, PNCH$_2$), 40.87 (d, $^{3}J_{PC}$ = 4.6 Hz, NC*C*H$_{bridgehead}$), 43.96 (d, $^{2}J_{PC}$ = 6.3 Hz, PNCH$_{iPr}$), 44.06 (d, $^{2}J_{PC}$ = 9.6 Hz, PNCH$_{iPr}$), 45.25 (d, $^{2}J_{PC}$ = 9.1 Hz, PC*C*H$_{bridgehead}$),46.43 (brs, CH$_{2bridge}$), 63.25 (m, HC=*C*H$_{COD}$), 65.12 (m, HC=*C*H$_{COD}$), 91.50 (d, J_{PC} = 51.4 Hz, P*C*=CN), 98.88 (m, H*C*=CH$_{COD}$), 99.63 (m, H*C*=CH$_{COD}$), 123.46, 124.46, 127.58, 126.88, 134.76 (5 x s, 6C, CH$_{Ar}$), 134.28 (d, $^{3}J_{PC}$ = 6.4 Hz, 2C, GeCH$_{orto}$), 139.67 (s, NC$_{ipso}$), 140.17 (brs, GeC$_{ipso}$), 147.36, 147.88 (2 x s, 2C, NC$_{orto}$),190.75 (d, $^{2}J_{PC}$ = 32.4 Hz, PC=*C*N). $^{31}P\{^{1}H\}$ NMR (121.49 MHz, $CDCl_3$, 25°C): δ = 60.27 (brs).

V.3.4. Crystallographic data

The data of the structure (**51**) and (**52**) were collected on a *Rigaku AFC-7S* diffractometer at a temperature of 293K with graphite-monochromated MoKα radiation (wavelength = 0.71073 Å). The structure was solved by direct methods, using SHELXS97.

51: $C_{35}H_{54}Cl_2GeN_3PRh$, *M*= 794.18, Orthorhombic, space group *Fdd2*, *a*= 32.830(8) Å, *b*= 39.870(7) Å, *c*= 11.240(3) Å, *V*= 14712(6) $Å^3$, *Z*= 16, crystal size 0.42 x 0.26 x 0.20 mm^3, 42901 reflections collected (7482 independent, R_{int}= 0.037), 596 parameters, 1 restraints 390 parameters, *R*1 [I>2σ(I)]= 0.031, *wR*2 [all data]= 0.080, largest diff. peak and hole: 0.60 and -0.42 e.$Å^{-3}$.

52: $C_{33}H_{50}ClGeN_3O_3PRh$, *M*= 778.68, Monoclinic, space group *C2/c*, *a*= 40.324(10) Å, *b*= 10.852(2) Å, *c*=20.025(5) Å, β= 105.206(6)º, *V*= 8456(4) $Å^3$, *Z*= 8, 47358 reflections collected (7927 independent, R_{int}= 0.058), 441 parameters, *R*1 [I>2σ(I)]=0.065, *wR*2 [all data]= 0.179, largest diff. peak and hole: 1.60 and -0.87e.$Å^{-3}$.

V.4. Conclusions

Rhodium complex (**51**) has been synthesized by reaction of dimer complex $[Rh_2(\mu\text{-}Cl)_2(COD)_2]$ with two equiv of germylene (**38**). The formation of complex (**51**) arises from the intermediate complexes (**50**), by migration of chloride ligand from rhodium to germanium atom, which leads to the oxidation of germanium atom from Ge(II) to Ge(IV).

Molecular structure of (**51**) clearly exhibits the six-membered metallacycle formed by chelating coordination of germylene (**38**) ligand. This ligand can be regarded a polydentate ligand, which contains two different chemical functions (such as phosphine and dichlorogermyl) coordinated to rhodium center.

Rhodium (I) complex (**52**) has been synthesized by reaction of dimer complex $[Rh_2(\mu\text{-}Cl)_2(COD)_2]$ with two equiv of germylene (**39**). Complex (**52**) is formed by σ-bonding coordination of germylene (**39**), through lone pair on the germanium atom.

The phosphine-stabilized germylene can be regarded as two-electron σ-donor ligands, such as the homologues carbenes and silylenes. Interestingly, the coordination mode of these divalent germanium species can be modified by replacing the germanium substituent.

Phosphine-stabilized germylenes emerge as useful ligands with high potential in organometallic chemistry.

Chapter VI

Synthesis of phosphine-stabilized germynes: Analogue of alkynes

VI. Introduction

The chemistry of compounds with triple bonds between heavier main elements has attracted growing interest in the last years.[127,128] Indeed, the stable homonuclear alkyne analogues of all the heavier group 14 elements R−E≡E−R (**I:** E = Si−Pb) have been isolated and characterized.[129-134] The structure of these triply bonded compounds has shown a *trans*-bent rather than linear geometry in which the bending angle increases from silicon to lead.[127] This trend indicates increasing lone pair character and decreasing E−E bond order (canonical structure **II**, in figure VI.1) upon descending the group.

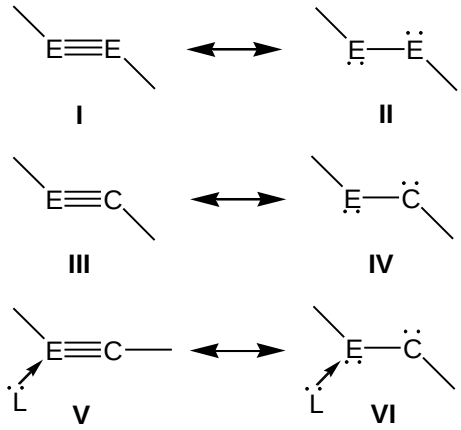

Figure VI.1. Canonical structures of homonuclear and heteronuclear alkyne analogues of heavier group 14 elements (E = Si−Pb).

Similar geometrical and electronic trends have been theoretically predicted for heteronuclear alkyne analogues, in which one of the carbon atoms is replaced by a heavier group 14 element R−E≡C−R (**III**, **IV:** E = Si−Pb).[128,135,136] In spite of increased interest, the chemistry of stable heteronuclear alkyne analogues remains still elusive and there are only a few reports concerning the synthesis of transient species.[137-142]

The first isolable compound with a triple bond between carbon and silicon has recently been synthesized and characterized by Kato and Baceiredo.[137] Silyne (**55**), stabilized by coordination of a phosphine ligand, was prepared by photolysis of the diazomethylsilylene (**54**) (Scheme VI.1). Interestingly, silyne (**55**) shows a very short silicon−carbon bond and a linear geometry around the carbon center, which can be regarded as silyne-base adduct with a partial Si−C triple bond (type **V**).

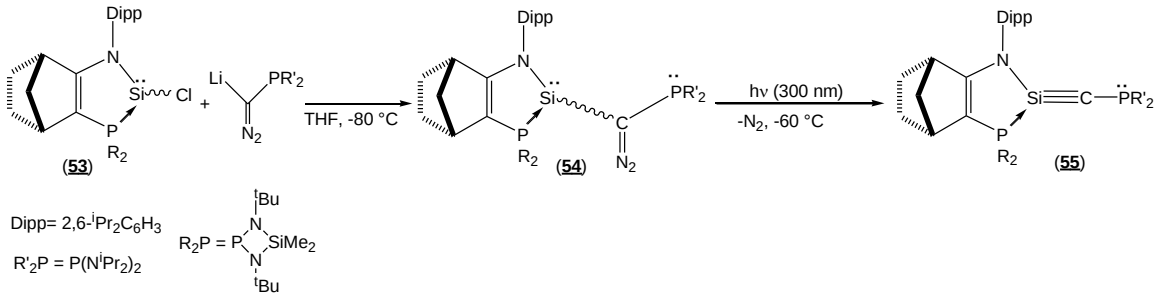

Scheme VI.1. Synthesis of silyne (**55**).

In contrast, compounds with an RC≡GeR triple bond (known as germynes) are still rare or unknown. In fact, only two transient germynes have been described in the literature.[139-140] These compounds have been characterized by trapping reactions (Scheme VI.2).

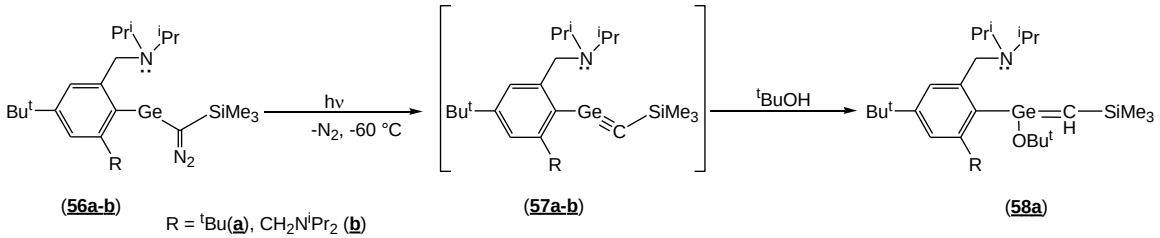

Scheme VI.2. Synthesis of transient germynes (**56a-b**).

Several computational studies predict a *trans*-bent geometry (**B**) for these triply bonded compounds (RGe≡CR) and a linear structure (**A**) that is not a minimum on the potential-energy surface.[143-147] One major obstacle for the synthesis of such triply bonded compounds RGe≡CR is the energetically favored isomerization of (**B**) into germavinylidene (**C**). Theoretical calculations, on the parent molecule HGe≡CH, indicated that the *trans*-bent germyne (**B**) requires 7 kcal/mol to isomerize to the germavinylidene isomer :Ge=CH_2 (**C**), which is 43 kcal/mol more stable than linear germyne (**A**).[143]

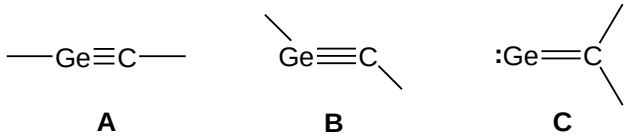

Moreover, the effect of substituents on carbon−germanium triple bonds has been systematically studied by performing density functional (DFT) calculations.[147] These theoretical studies indicate that the smaller substituents (F, H, OH, CH_3, SiH_3) neither kinetically or thermodynamically stabilize the triply bonded RC≡GeR species. However,

triply bonded derivatives can be stabilized by bulky substituents in which steric hindrance acts to prevent isomerization, dimerization or oligomerization.

In view that the synthesis of stable triply bonded compounds containing carbon and germanium (RC≡GeR) remains a major challenge, we have focused our interest on preparing stable germynes stabilized by coordination of phosphine ligand. In this sense, we decided to adopt a similar synthetic strategy used for silyne (**55**).

VI.2. Results and discussions

VI.2.1. Synthesis and characterization of phosphino(germyl)diazomethane (61a-b)

The precursors phosphino(germyl)diazomethanes (**61a-b**) were prepared by reaction of the phosphine-stabilized germylenes (**38a-b**) with the lithiated phosphinediazomethane (**60**).[148-149] Diazomethane derivatives (**61a-b**) were obtained as a mixture of two diastereomers [64:36 for (**61a**) and 80:20 for (**61b**)], and were isolated as orange crystals [81% (**61a**) and 65% (**61b**)] from a saturated pentane solution at -30°C (Scheme VI.3).

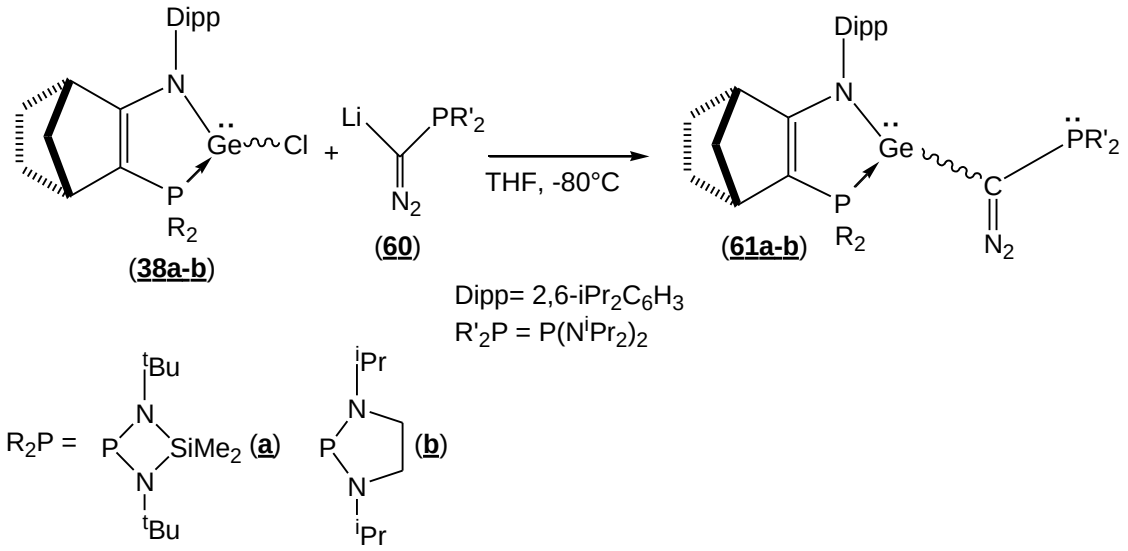

Scheme IV.3. Synthesis of phosphino(germyl)diazomethanes (**61a-b**).

The $^{31}P\{^{1}H\}$NMR spectra of (**61a-b**) show two sets of signals [AX-systems: for (**61a**): 64.1 ppm, 70.0 ppm ($^{3}J_{PP}$= 91.1 Hz) and 64.0 ppm, 80.9 ppm ($^{3}J_{PP}$= 54.6 Hz); for (**61b**): 60.6 ppm, 73.9 ppm ($^{3}J_{PP}$= 10.3 Hz) and 63.9 ppm, 73.6 ppm ($^{3}J_{PP}$= 51.3 Hz)], which is in agreement with the presence of two diastereomers (Figure VI.2). In addition, an intense IR-absorption band at [for (**61a**): 1995 cm^{-1}; for (**61b**): 1980 cm^{-1} and 2040 cm^{-1}] confirmed the presence of a diazo-function.

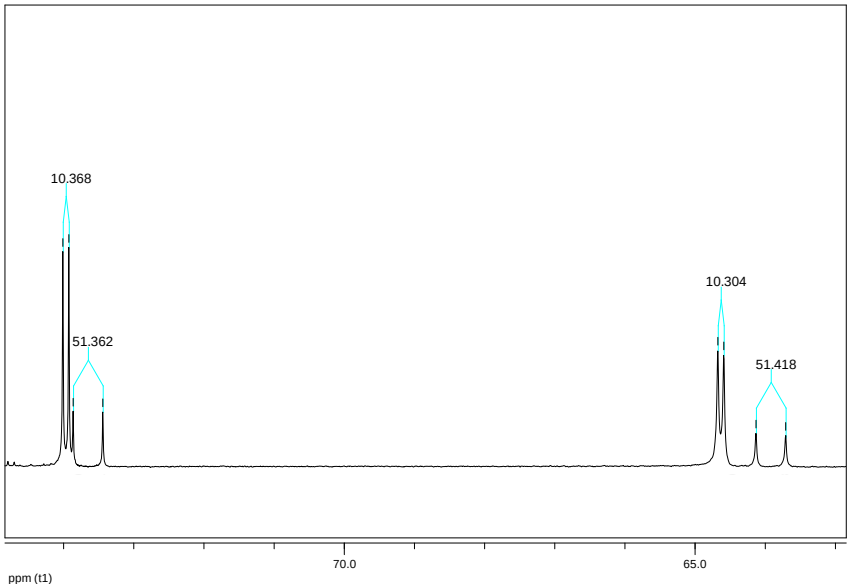

Figure VI.2. ^{31}P {^{1}H} NMR spectra at RT of phosphino(germyl)diazomethane (**61b**).

*Molecular structure of phosphino(germyl)diazomethane (**61b**)*

Molecular structures of (**61a-b**) were unambiguously confirmed by an X-ray analysis. An ORTEP diagram of (**61b**) is shown in the figure VI.3 and selected bond lengths and angles are listed in Table VI.1. Meanwhile, molecular structure of (**61a**) is shown in the experimental part.

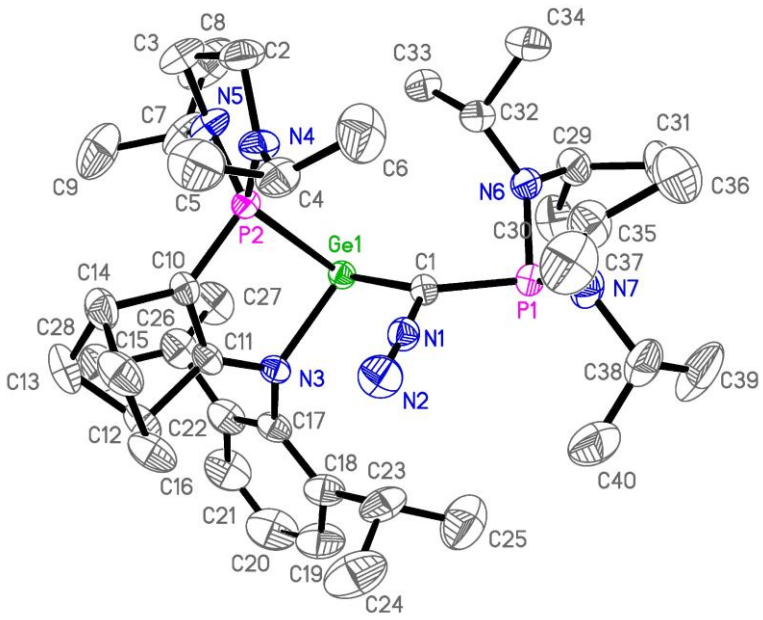

Figure VI.3. Molecular structure (**61b**). Thermal ellipsoids represent 50% probability and H atoms have been omitted for clarity.

Table VI.1. Selected bond lengths (Å) and bond angles (deg) of (**61b**)

Bond distances		**Bond angle**	
C(1)−Ge(1)	2.0311(16)	C(1)−Ge(1)−P(2)	92.24(5)
C(1)−P(1)	1.8297(16)	N(3)−Ge(1)−C(1)	98.61(6)
C(1)−N(1)	1.284(2)	N(3)−Ge(1)−P(2)	84.50(4)
N(1)−N(2)	1.145(2)	N(6)−P(1)−N(7)	110.72(14)
Ge(1)−P(2)	2.4551(5)	N(6)−P(1)−C(1)	98.21(7)
Ge(1)−N(3)	1.9971(12)	N(7)−P(1)−C(1)	104.10(8)
P(2)−C(10)	1.7282(16)	N(4)−C(1)−P(2)	122.63(12)
C(10)−C(11)	1.384(2)	P(1)−C(1)−Ge(1)	118.65(8)
C(11)−N(3)	1.351(2)	N(1)−C(1)−Ge(1)	117.13(11)
		N(1)−C(1)−P(1)	119.70(12)
$\sum P_{\alpha 1} = 313.03°$		$\sum Ge_{\alpha} = 275.35°$	

The molecular structure reveals the substitution of chloro atom on germylene (**38**) by the phosphinodiazomethane fragment to form phosphino(germyl)diazomethane (**61b**). The value of the sum of the bond angles about germanium (ΣGe_{α}= 275.35°) is in agreement with a strongly pyramidalized center, which is consistent with the observation of two diastereomers.

The Ge(1)−C(1) bond length (2.0311(16) Å) is close to standard value for a σ-bond germanium-carbon (1.90−2.05 Å),[150] this bond distance is similar to those observed on the diazomethylgermylenes (**56a-b**).[139-140] The P(1)−C(1)−Ge(1) angle bond (118.65°) reveals the sp^2 hybridization of carbon atom C(1) and a slight repulsive steric interaction between the germylene moiety and the N^iPr_2 groups on the phosphine fragment.

The Ge(1)−P(2) bond length (2.4551(5) Å) is similar to those observed for the germylene (**38** and **39**). Meanwhile, the C(1)−P(1) and C(1)−N(1) bond lengths in diazomethane (**61b**) are in same range that the C−P and C=N bond distances observed in the diazomethane derivatives (**55**) [137] and (**56**).[139-140]

VI.2.2. Photolysis of phosphino(germyl)diazomethane (61a-b)

Photolysis of diazomethane derivatives (**61a-b**) (λ = 300 nm) at -60°C in THF afforded a dark red solution of (**62a-b**) (Scheme VI.4). Monitoring the reaction by $^{31}P\{^{1}H\}$ NMR spectroscopy at -80°C shows the complete disappearance of the starting diazomethane derivatives (**61a-b**) after 48 h of irradiation, and the appearance of a new set of signals corresponding to (**62a-b**) [AX system: for (**62a**): $P_{(1)}$ = -20.3 ppm and $P_{(2)}$ = 82.1 ppm ($^{3}J_{PP}$ = 102.6 Hz); for (**62b**): $P_{(1)}$ = -14.9 ppm and $P_{(2)}$ = 77.4 ppm ($^{3}J_{PP}$ = 102.0 Hz)] (Figure VI.4a).

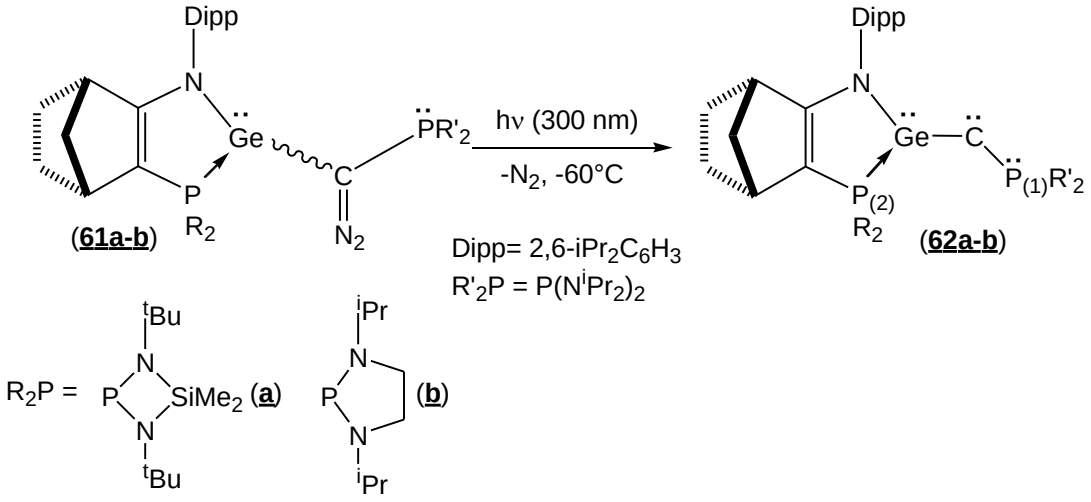

Scheme VI.4. Photolysis of phosphino(germyl)diazomethanes (**61a-b**).

Interestingly, the chemical shifts of $P_{(2)}$ remain almost unchanged compared to the values of the starting diazo derivatives (**61a-b**), while the $P_{(1)}$ signals appear at higher field than that for silicon analogue (**55**) [AX system: $P_{(1)}$ = 3.1 ppm and $P_{(2)}$ = 46.2 ppm ($^{3}J_{PP}$ = 47.3 Hz)], in the typical region for phosphinocarbenes.[151] In addition, the $^{13}C\{^{1}H\}$ NMR signal of the central carbon atom [for (**62a**): 162.4 ppm, $^{1}J_{CP}$ = 43.4 Hz, $^{3}J_{CP}$ = 11.3 Hz; for (**62b**): 161.1 ppm, $^{1}J_{CP}$ = 11.0 Hz, $^{3}J_{CP}$ = 10.7 Hz] is in the region expected for a phosphinocarbene with a relatively small phosphorus-carbon coupling constant (Figure VI.4b).[151]

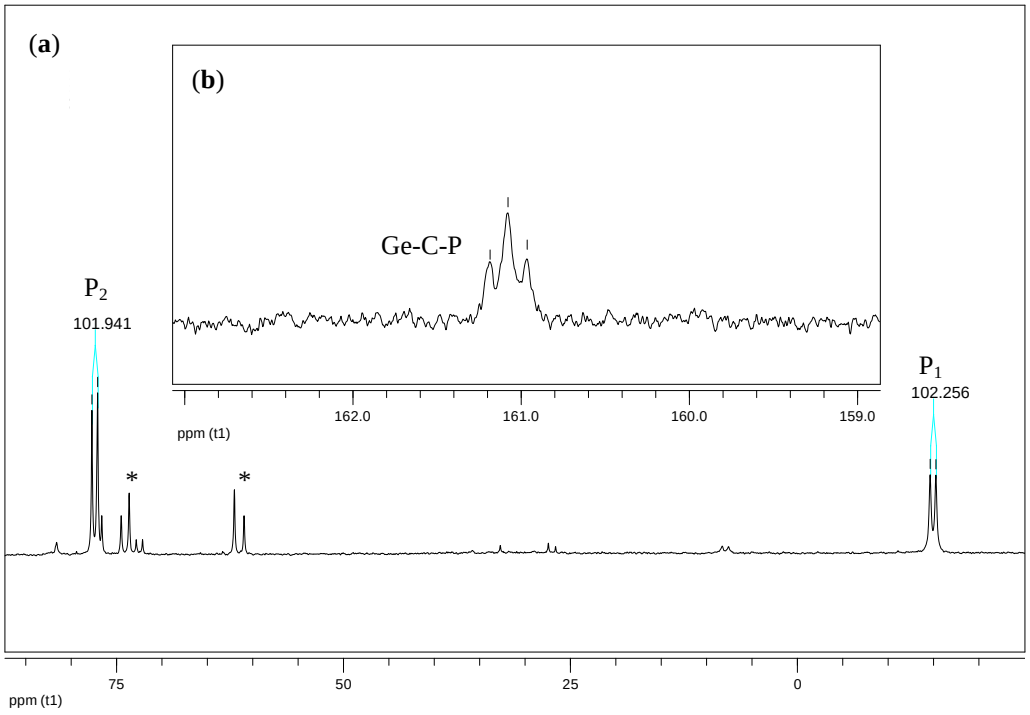

Figure VI.4. (**a**) $^{31}P\{^{1}H\}$ and (**b**) $^{13}C\{^{1}H\}$ NMR spectra at -90°C of (**62b**); (*) starting diazomethane derivative (**61b**).

Molecular structure of (62a)

Derivative (**62a**) was successfully isolated as orange crystals from a diethyl ether solution at -60°C. The molecular structure of (**62a**) determined by X-ray crystallography (Figure VI.5) reveals a twisted *trans*-bent arrangement with a dihedral angle N(1)−Ge(1)−C(1)−P(1) of 159.9°. The P(2)−Ge(1) bond length (2.4895(12) Å) is longer than those in the precursors (**61**) (2.443(4) and 2.4551(5) Å for **61a** and **61b** respectively).

The Ge(1)−C(1) bond length (1.887(5) Å) is quite longer than the calculated value for a Ge≡C triple bond (1.73 Å) in the parent compound HGe≡CH.[143-144] This bond distance is in the range between a single (1.98 Å) [150] and a double-bond (1.80 Å) [127] germanium−carbon, however, it is comparable with the theoretically predicted values (1.862−1.887 Å) for germynes with electron-withdrawing and π-donating substituents such as –F and –OH.[145,147] Moreover, germanium center remains strongly pyramidalized (ΣGe_{α}= 298.76°) in comparison with precursor (**61a**) (ΣGe_{α}= 298.17°). This structural feature indicates the non-existence of a Ge≡C triple bond in (**61a**).

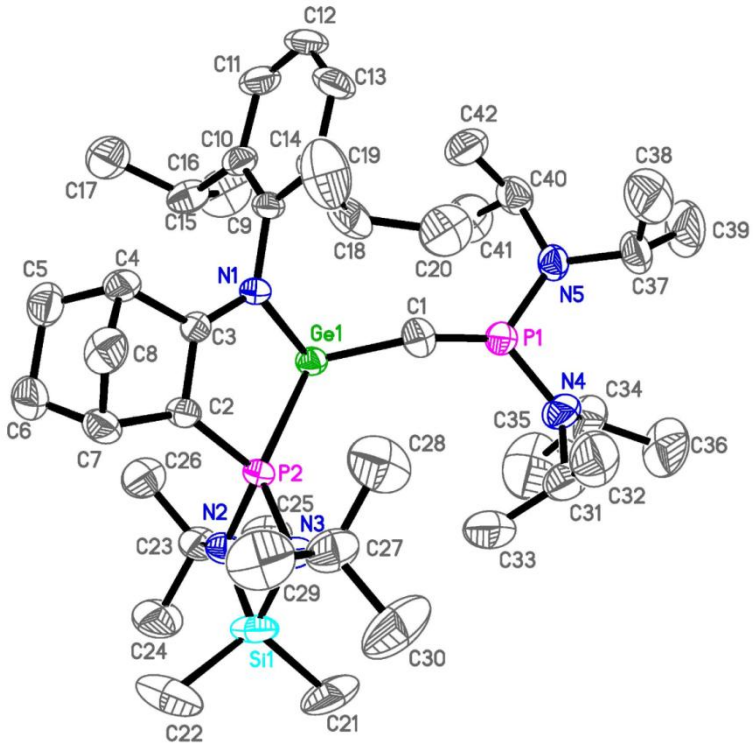

Figure VI.5. Molecular structure of (**62a**). Thermal ellipsoids represent 50% probability and H atoms have been omitted for clarity.

The trigonal planar geometry around P_1 atom ($\sum P_{1\alpha}$ = 359.70°) and the short P(1)−C(1) bond distance (1.549 Å) clearly indicate a strong π-interaction of the phosphino substituent with the germyne fragment. Indeed, the P(1)−C(1) bond distance is in agreement with those observed for phosphinocarbenes [151] or phosphaalkynes.[152] Nevertheless, in spite of the P(1)−C(1) multiple bond character, the trigonal planar phosphino fragment is strongly twisted relative to the P(1)−C(1)−Ge(1) fragment with a torsion angle N(4)−P(1)−C(1)−Ge(1) -73.7°. This value is even larger than that reported for methylenephosphonium salts [($^{i}Pr_2N)_2P=C(TMS)_2$·TfO with an extremely twisted P=C double bond 60°].[153-154]

The structural features of (**62a**) suggest the bis-carbenoid structure (**62**) with a modest contribution of the structure (**62'**), as consequence of the π-interaction of the phosphino substituent with the carbenic center (Figure VI.6). Interestingly, molecular structure of (**62a**) is completely different from that of silicon analogue (**55**), which shows a multiple-bonded structure of type **V** (in figure VI.1).

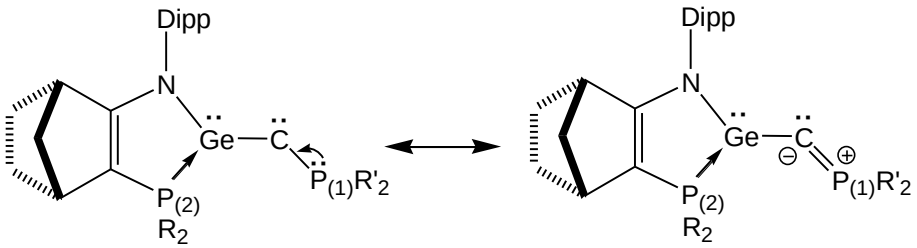

(**62**) (**62'**)

Figure VI.6. Possible structures of germyne (**62a**).

Table VI.2. Selected bond lengths (Å), bond angles and torsion angles (deg) of (**62a**)

Bond distances		**Bond angles**	
C(1)−Ge(1)	1.887(5)	C(1)−Ge(1)−N(1)	102.42(18)
C(1)−P(1)	1.549(5)	C(1)−Ge(1)−P(2)	113.57(14)
Ge(1)−N(1)	2.005(3)	N(1)−Ge(1)−P(2)	84.77(10)
Ge(1)−P(2)	2.4895(12)	C(1)−P(1)−N(5)	126.8(2)
P(1)−N(5)	1.657(4)	C(1)−P(1)−N(4)	130.5(2)
P(1)−N(4)	1.670(4)	N(5)−P(1)−C(1)	106.05(8)
Torsion angles		N(4)−P(1)−N(5)	102.4(2)
N(4)−P(1)−C(1)−Ge(1)	-73.6(6)	Ge(1)−C(1)−P(1)	147.3(3)
N(5)−P(1)−C(1)−Ge(1)	113.9(5)	$\sum Ge_{\alpha}$ = 298.76°	
N(1)−Ge(1)−C(1)−P(1)	159.9(5)	$\sum P_{1\alpha}$ = 359.70°	

VI.2.3. Theoretical calculations on (62a-b)

To gain more insight on (**62a-b**), DFT calculations were performed. Theoretical calculations indicated that the structures featuring Ge≡C triple bond and a linear geometry around the carbon atom (**62-I**, figure VI.7), which are similar to the case for the silicon analogue (**55**), are not energy minima on the respective potential energy surfaces. Instead, for (**62b**) was found a *trans*-bent structure, as a local energy minimum, which presents a Ge=C double bond with a lone pair on the central carbon atom. However, the most stable isomer of (**62b**) is similar to the experimentally obtained structure with a P−C double character (**62a-III**). Isomer (**62b-III**) is more stable than (**62b-II**) by ca. 10 kcal/mol. For (**62a**), only isomer (**62a-III**) was found as a local minimum energy. This difference might result from a distortion of molecules due to steric reasons. Indeed, calculated torsion angle N(2)−P(1)−C(1)−Ge(1)

[84.89° for (**62a**) and 26.28° for (**62b**)] indicates that (**62a**), bearing a more hindered phosphine ligand, is more strongly twisted than (**62b**) (see experimental part).

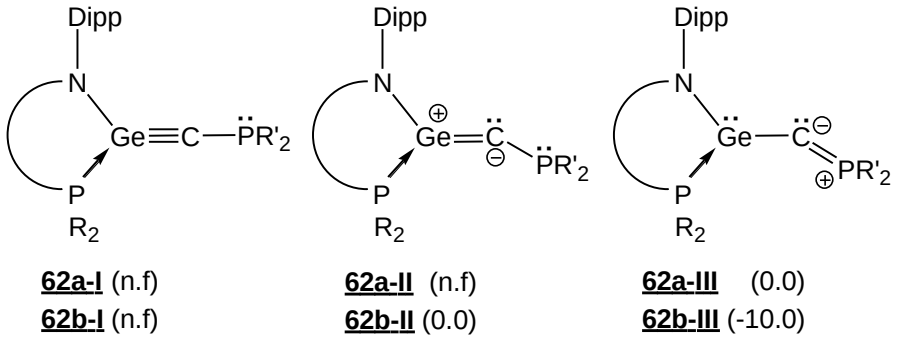

62a-I (n.f) **62a-II** (n.f) **62a-III** (0.0)
62b-I (n.f) **62b-II** (0.0) **62b-III** (-10.0)

Figure VI.7. Isomers of (**62a-b**). Calculated relative energies (kcal/mol) are in parenthesis (BHandH/6-31G* level of theory). Isomers (**62a-I**, **62b-I** and **62a-II**) were not found (n.f).

DFT calculations indicate that in both compounds (**62a-b**) the Ge−C multiple bonding character is not favored because of the partial stabilization of the germyne by the cyclic phosphine, as well as, a strongly π-donation from the exocyclic (bis-diisopropylamino)phosphine moiety, which results in a stabilization of the C=P(N^iPr_2) unit. Indeed, NBO analysis of (**62a-III**) shows the presence of the two lone pairs on the germanium (LP_{Ge}) and carbon atoms (LP_C), as well as, the PC-π-bond (Figure VI.8). Interestingly, in contrast to the LP_{Ge} with an enhanced s character [s(64.37%), p(35.54%), d(0.09%)], the LP_C shows an extremely high p character [s(1.88%), p(98.09%), d(0.04%)], indicating that the central carbon is sp^2-hybridized.

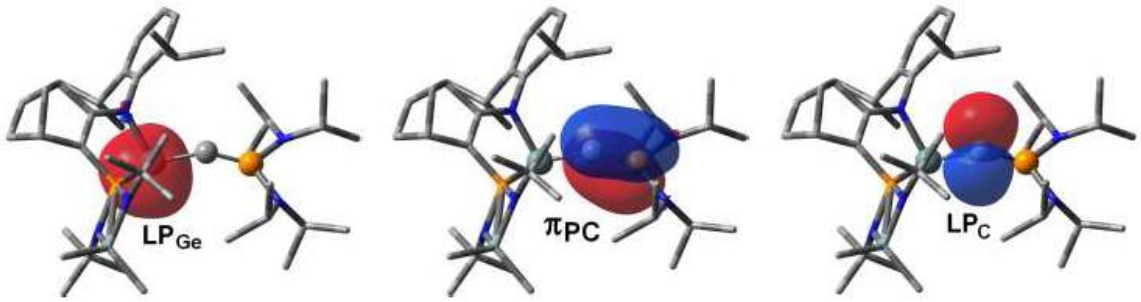

Figure VI.8. Most representative Natural Bond Orbitals for (**62a-III**).

VI.2.4. Isomerization of (62a-b)

Derivatives (**62a-b**) are thermally unstable and they undergo an isomerization reaction above -30°C. The isomerization of (**62b**) led to the formation of cyclic germylene (**63b**) (Scheme VI.5). $^{31}P\{^{1}H\}$ spectrum of (**63b**) shows a AX-system at [30.2 ppm and 77.2 ppm ($^{2}J_{PP}$ = 156.7 Hz)] (Figure VI.9). In addition, $^{13}C\{^{1}H\}$ spectrum shows a signal doublet-doublet at [117.8 ppm, J_{PC} = 59.0 Hz, J_{PC} = 42.3 Hz] for the carbon center $R_2P{=}C{-}PR'_2$.

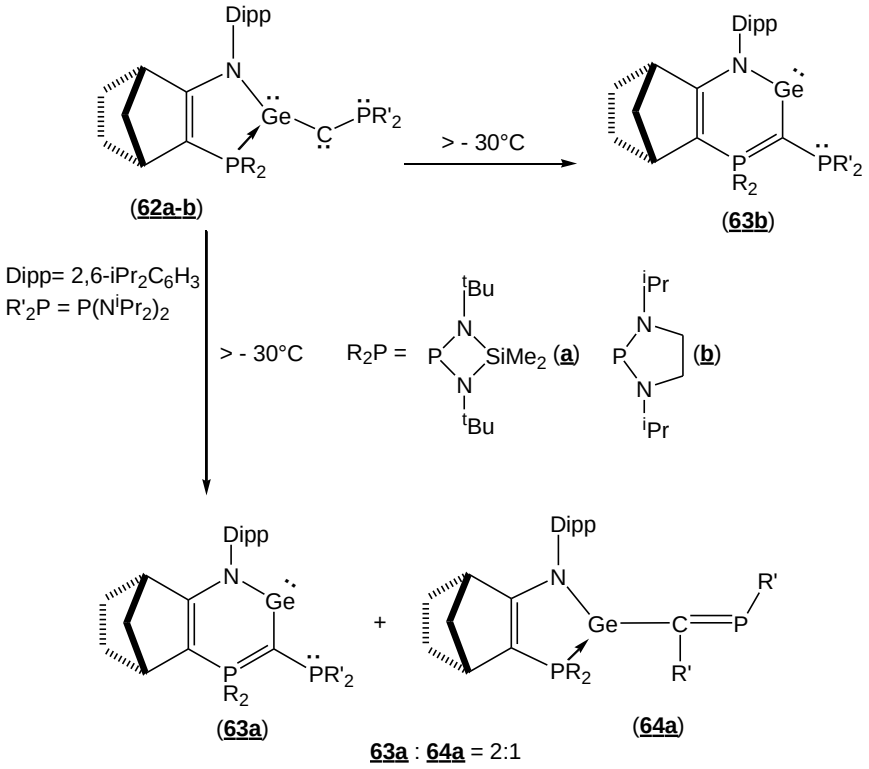

Scheme VI.5. Isomerization reactions of (**62a**) and (**62b**).

Meanwhile, the isomerization of (**62a**) affords a mixture of phosphaalkene (**64a**) and cyclic germylene derivative (**63a**) (Scheme VI.5). The Cyclic germylene (**63a**) was systematically obtained as the major product (**63a** : **64a** = 2 : 1) and its spectroscopic data are very similar to those of (**63b**) (see experimental part).

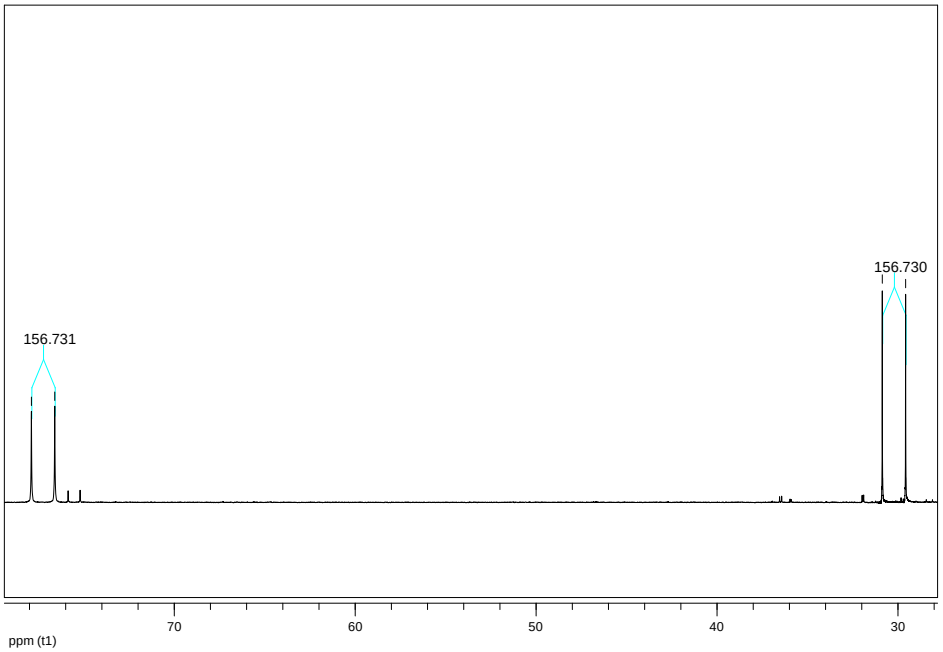

Figure VI.9. ^{31}P {^{1}H} NMR spectra at RT of cyclic germylene (**63b**).

This result contrasts with silyne analogue (**55**), which transforms selectively into a phosphaalkene derivative.[137] The phosphaalkene derivative (**64a**) is formed by 1,2-migration of a diisopropylamino group from phosphorus to the carbon center, which is a typical rearrangement for singlet carbenes.[155]

Moreover, the formation of germylene derivatives (**63a-b**) involves the migration of the phosphine ligand from the germanium to carbon center. In comparison with (**62a**), the presence of a less hindered phosphine ligand on (**62b**) probably facilitates the migration of phosphine moiety to carbon center, which possibly favors the exclusive formation of cyclic germylene (**63b**).

*Molecular structures of (**63a**) and (**63b**)*

The molecular structures of (**63a-b**) were confirmed by X-ray diffraction analysis clearly showing the tricyclic structures which contain a six-membered C_3NPGe ring bearing a two-coordinate Ge (II) center (Figure VI.10).

The most noteworthy structural features of (**63a-b**) are the Ge(1)−C(1) bond distances (1.9023(15) Å and 1.8915(14) Å for **63a** and **63b** respectively) which are slightly shorter than those of the corresponding single bonds,[150] while the Ge(1)−N(1) bond distances (1.9149(13)

Å and 1.9196(12) Å for **63a** and **63b** respectively) are shorter than those in germylene (**38**), but comparable to those Ge−N bonds (1.894 Å) found in an *N*-heterocyclic 6π aromatic germyliumylidene cation [156] and related compound.[157] These structural features suggest that the germylene center is well stabilized by two π-donating groups such as amino and phosphonium ylide.

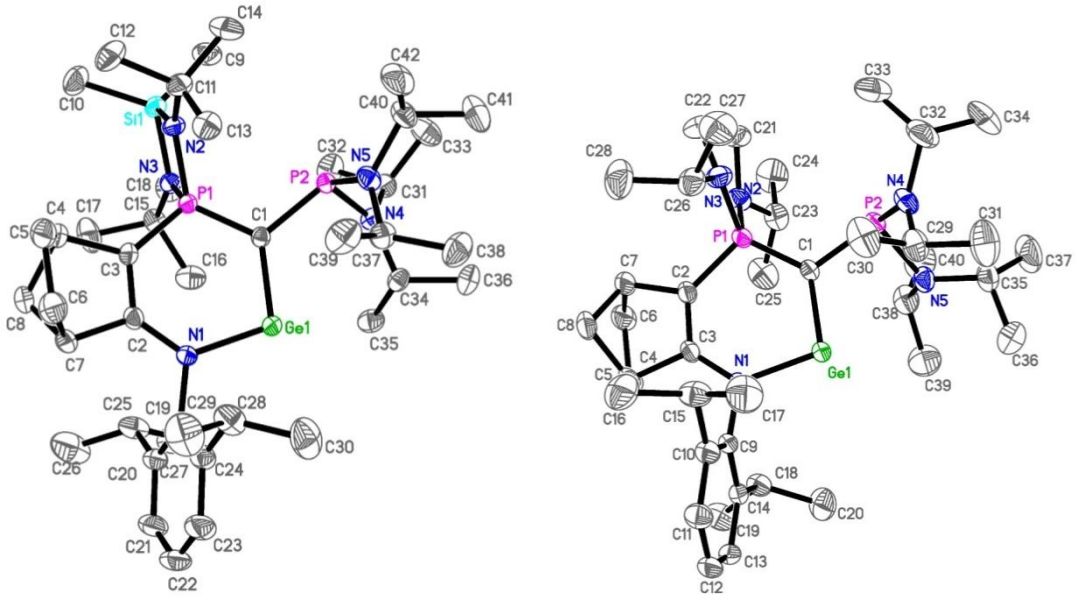

Figure VI.10. Molecular structures of (**63a**) (Left) and (**63b**) (right). Thermal ellipsoids represent 50% probability and H atoms have been omitted for clarity. Selected bond lengths and angles are listed in Table VI.3.

Furthermore, the P(1)−C(1) bond distances (1.7192(15) Å and 1.7175(15) Å for **63a** and **63b** respectively) are in agreement to the calculated values for the P−C ylidic bonds.[158] The P(2)−C(1) bond distances (1.8382(15) Å and 1.8325(14) Å for **63a** and **63b** respectively) are as expected for a P−C single bond, with a P_2 atom strongly pyramidalized ($\sum\theta P_{2\alpha}$ = 318.53° and 307.86° for **63a** and **63b** respectively) In addition, the values of the P(1)−C(1)−Ge(1) angles (122.36° and 125.79° for **63a** and **63b** respectively) are in agreement with an sp^2-hybridized carbon atom.

These crystallographic data confirm the isomerization of compounds (**62a-b**) affording a new stable *N*-heterocyclic germylenes (**63a-b**).[159-160]

Table VI.3. Selected bond lengths (Å) and bond angles (deg) of (**63a**) and (**63b**)

Compounds	Bond distance		Bond angle	
63a	Ge(1)−C(1)	1.9023(15)	C(1)−Ge(1)−N(1)	103.18(3)
	P(1)−C(1)	1.7192(15)	P(1)−C(1)−Ge(1)	122.36(8)
	P(2)−C(1)	1.8382(15)	C(1)−P(1)−C(3)	108.97(7)
	P(1)−C(3)	1.7489(16)	C(2)−C(3)−P(1)	128.25(12)
	C(2)−C(3)	1.376(2)	N(1)−C(2)−C(3)	128.06(14)
	N(1)−C(2)	1.356(2)	C(2)−N(1)−Ge(1)	125.60(10)
	Ge(1)−N(1)	1.9149(13)	P(1)−C(1)−P(2)	113.85(8)
	P(1)−N(2)	1.6957(13)	P(2)−C(1)−Ge(1)	123.17(8)
	P(1)−N(3)	1.7030(13)	N(4)−P(2)−N(5)	108.10(1)
	P(2)−N(4)	1.7127(14)	N(4)−P(2)−C(1)	107.79(7)
	P(2)−N(5)	1.7262(14)	N(5)−P(2)−C(1)	102.64(7)
63b	Ge(1)−C(1)	1.8915(14)	C(1)−Ge(1)−N(1)	101.22(5)
	P(1)−C(1)	1.7175(15)	P(1)−C(1)−Ge(1)	125.79(8)
	P(2)−C(1)	1.8325(14)	C(1)−P(1)−C(2)	108.79(7)
	P(1)−C(2)	1.7403(15)	C(3)−C(2)−P(1)	128.30(12)
	C(2)−C(3)	1.372(2)	N(1)−C(3)−C(2)	128.42(13)
	N(1)−C(3)	1.3596(19)	C(3)−N(1)−Ge(1)	126.45(10)
	Ge(1)−N(1)	1.9196(12)	P(1)−C(1)−P(2)	115.45(8)
	P(1)−N(2)	1.6949(13)	P(2)−C(1)−Ge(1)	118.70(7)
	P(1)−N(3)	1.6888(14)	N(4)−P(2)−N(5)	102.74(7)
	P(2)−N(4)	1.6926(14)	N(4)−P(2)−C(1)	106.79(7)
	P(2)−N(5)	1.7764(14)	N(5)−P(2)−C(1)	98.33(6)

VI.3. Experimental part

VI.3.1. General Considerations

All manipulations were performed under an inert atmosphere of argon by using standard Schlenk techniques. Dry, oxygen-free solvents were employed. All reagents were obtained from commercial suppliers. Stabilized-phosphine germylene (**38b**) was prepared by a similar synthetic strategy to using for (**38a**). The lithiated phosphinodiazomethane (**60**) was synthesized as previously reported methods.[148-149]

^{1}H, $^{13}C\{^{1}H\}$, $^{29}S\{^{1}H\}$ and $^{31}P\{^{1}H\}$ NMR spectra were recorded on Bruker, Avance 300 or Avance 400 spectrometers. ^{1}H, $^{13}C\{^{1}H\}$ and $^{29}S\{^{1}H\}$ NMR chemical shifts are reported in ppm relative to Me_4Si as external standard. $^{31}P\{^{1}H\}$ NMR chemical shifts are expressed in ppm relative to 85% H_3PO_4. Infrared spectra were obtained with a Varian 640-IR FT IR spectrophotometer.

VI.3.2. Synthesis of germylene (38a)

To a THF solution (15 mL) of iminophosphine (2.50 g, 5.0 mmol) was added at -80°C *n*-butyllithium in hexane (3.13 mL, 5.0 mmol). The solution was slowly warmed to RT for 1h. The mixture back at -80°C, a THF solution (5 mL) of dichlorogermylene dioxane complex (1.16 g, 5.0 mmol) was added. The solution was warmed to RT and stirred for 1h. All the volatiles were removed under vacuum and the residue was extracted twice with diethyl ether. Germylene (**38a**) was obtained as pale yellow crystals from a concentrated diethyl ether solution at -30°C (2.3 g, 76%). MP: 209°C. **Major isomer 38a** (64%): ^{1}H NMR (300 MHz, C_6D_6, 25°C): δ = 0.22 (s, 3H, $SiMe_3$), 0.27 (s, 3H, $SiMe_3$), 1.18 (s, 9H, CH_{3tBu}), 1.19 (d, J_{HH} = 9.1 Hz, 1H, CH_2), 1.24 (d, J_{HH} = 6.7 Hz, 3H, CH_{3iPr}), 1.29 (d, $^{3}J_{HH}$ = 6.7 Hz, 3H, CH_{3iPr}), 1.29 (d, J_{HH} = 7.1 Hz, 1H, CH_2), 1.33 (d, J_{HH} = 7.1 Hz, 1H, CH_2), 1.38 (d, $^{3}J_{HH}$ = 6.7 Hz, 3H, CH_{3iPr}), 1.39 (s, 9H, CH_{3tBu}), 1.59 (d, $^{3}J_{HH}$ = 6.0 Hz, 3H, CH_{3iPr}), 1.64 (m, 2H, CH_2), 1.67 (d, J_{HH} = 9.1 Hz, 1H, CH_2), 2.58 (b, 1H, $CH_{bridgehead}$), 3.05 (b, 1H, $CH_{bridgehead}$), 3.47 (sept, $^{3}J_{HH}$ = 6.9 Hz, 1H, CH_{iPr}), 3.68 (sept, J_{HH} = 6.6 Hz, 1H, CH_{iPr}), 7.12 (m, 1H, CH_{Ar}), 7.21 (m, 1H, CH_{Ar}), 7.23 (m, 1H, CH_{Ar}). $^{13}C\{^{1}H\}$ NMR (75 MHz, C_6D_6, 25°C): δ = 3.6 (d, $^{3}J_{PC}$ = 1.3 Hz, $SiMe_3$), 5.5 (d, $^{3}J_{PC}$ = 5.0 Hz, $SiMe_3$), 24.3 (s, CH_{3iPr}), 24.6 (s, CH_{3iPr}), 25.2 (d, J_{PC} = 1.3 Hz,

CH_2), 25.5 (s, CH_{3iPr}), 26.1 (d, J_{PC} = 2.1 Hz, CH_{3iPr}), 27.7 (s, CH_{iPr}), 28.4 (s, CH_{iPr}), 29.0 (d, J_{PC} = 1.5 Hz, CH_2), 32.7 (d, $^3J_{PC}$ = 3.0 Hz, 3C, CH_{3tBu}), 32.8 (d, $^3J_{PC}$ = 4.2 Hz, 3C, CH_{3tBu}), 40.5 (d, J_{PC} = 7.1 Hz, $CH_{bridgehead}$), 43.8 (d, J_{PC} = 14 Hz, $CH_{bridgehead}$), 46.5 (d, J_{PC} = 5.2 Hz, CH_2), 51.0 (d, J_{PC} = 2.9 Hz, C_{tBu}), 51.5 (d, $^2J_{PC}$ = 3.0 Hz, C_{tBu}), 98.9 (d, J_{PC} = 21 Hz, P*C*CN), 123.7 (s, CH_{Ar}), 124.2 (s, CH_{Ar}), 126.7 (s, CH_{Ar}), 139.1 (d, J_{PC} = 3.9 Hz, C_{Ar}), 145.5 (s, C_{Ar}), 147.5 (s, C_{Ar}), 184.6 (d, $^2J_{PC}$ = 42 Hz, PC*C*N). $^{31}P\{1H\}$ NMR (121 MHz, C_6D_6, 25°C): δ = 83.6 (s). $^{29}Si\{^1H\}$ NMR (59 MHz, C_6D_6, 25°C): δ = 11.1 (d, $^2J_{PSi}$ = 4.14 Hz). **Minor isomer <u>38a</u>** (34%): $^{13}C\{^1H\}$ NMR (75 MHz, C_6D_6, 25°C): δ = 3.9 (d, $^3J_{PC}$ = 1.3 Hz, $SiCH_3$), 5.5 (d, $^3J_{PC}$ = 5.0 Hz, $SiCH_3$), 23.9 (s, CH_3), 25.2 (s, CH_3), 25.4 (s, CH_3), 25.6 (d, J_{PC} = 1.3 Hz, CH_2), 26.1 (d, J_{PC} = 2.1 Hz, CH_{3ipr}), 27.6 (s, CH_{iPr}), 28.4 (s, CH_{iPr}), 28.6 (d, J_{PC} = 1.5 Hz, CH_2), 32.4 (d, $^3J_{PC}$ = 4.0 Hz, 3C, CH_{3tBu}), 32.9 (d, $^3J_{PC}$ = 2.9 Hz, 3C, CH_{3tBu}), 40.6 (d, J_{PC} = 7 Hz, $CH_{bridgehead}$), 43.3 (d, J_{PC} = 14 Hz, $CH_{bridgehead}$), 48.7 (d, J_{PC} = 6 Hz, CH_2), 51.5 (d, $^2J_{PC}$ = 3.9 Hz, 2C, C_{tBu}), 98.9 (d, J_{PC} = 21 Hz, P*C*CN), 123.7 (s, CH_{Ar}), 124.4 (s, CH_{Ar}), 126.8 (s, CH_{Ar}), 139.5 (s, C_{Ar}), 145.9 (s, C_{Ar}), 147.8 (s, C_{Ar}), 184.5 (d, $^2J_{PC}$ = 23 Hz, PC*C*N). $^{31}P\{^1H\}$ NMR (121 MHz, C_6D_6, 25°C): δ = 84.4 (s). $^{29}Si\{^1H\}$ NMR (59 MHz, C_6D_6, 25°C): δ = 11.0 (d, $^2J_{PSi}$ = 4.30 Hz).

VI.3.3. Synthesis of phosphino(germyl)diazomethane (<u>61a</u>)

To a THF solution (15 mL) of bis(diisopropylamino)phosphinediazomethane (**<u>60</u>**) (294 mg, 1.08 mmol) was added at -80°C n-butyllithium in hexane solution (0.675 mL, 1.08 mmol). The solution was stirred for 15 min at -80°C and for 45 min at RT. The solution was cooled at -80°C and a THF solution (5 mL) of (**<u>38b</u>**) (655 mg, 1.08 mmol) was added. The solution was slowly warmed to RT and stirred for two days. All the volatiles were removed under vacuum and the residue was extracted twice with pentane. Diazo derivative (**<u>61a</u>**) was obtained as orange crystals from a concentrated pentane solution at -30°C (0,738 g, 81%). IR: ν(N_2) 1995 cm^{-1}. **Major isomer (<u>61a</u>)** (64%): ^1H NMR (300 MHz, C_6D_6, 25°C): δ = 0.36 (s, 3H, $SiCH_3$), 0.39 (s, 3H, $SiCH_3$), 0.98 (d, $^3J_{HH}$ = 6.8 Hz, 6H, CH_{3iPr}), 1.17-1.41 (m, 24H, CH_{3iPr}), 1.22 (d, J_{HH} = 9.2 Hz, 1H, CH_2), 1.35 (m, 2H, CH_2), 1.37 (s, CH_{3tBu}), 1.62 (m, 6H, CH_{3iPr}), 1.70 (b, 2H, CH_2), 1.76 (d, J_{HH} = 6.9 Hz, 1H, CH_2), 2.65 (b, 1H, $CH_{bridgehead}$), 3.18 (b, 1H, $CH_{bridgehead}$), 3.27 (sept, $^3J_{HH}$ = 5.2 Hz, 1H, CH_{iPr}), 3.41 (m, 2H, CH_{iPr}), 3.50 (m, 2H, CH_{iPr}), 3.55 (sept, $^3J_{HH}$ = 7.0 Hz, 1H, CH_{iPr}), 7.13-7.20 (m, 3H,CH_{Ar}). $^{13}C\{^1H\}$ NMR (75 MHz, C_6D_6, 25°C): δ = 3.7 (d, $^3J_{PC}$ = 1.5 Hz, $SiCH_3$), 6.1 (d, $^3J_{PC}$ = 5.1 Hz, $SiCH_3$), 23.8-25.4

(m, 12C, CH_{3iPr}), 25.4 (s, CH_2), 27.6 (s, CH_{iPr}), 28.4 (s, CH_{iPr}), 28.9 (d, J_{PC} = 1.1 Hz, CH_2), 32.8 (d, $^3J_{PC}$ = 5.3 Hz, 3C, CH_{3tBu}), 33.2 (d, $^3J_{PC}$ = 2.6 Hz, 3C, CH_{3tBu}), 40.6 (d, J_{PC} = 5.9 Hz, $CH_{bridgehead}$), 44.1 (d, J_{PC} = 11.2 Hz, $CH_{bridgehead}$), 46.3 (d, J_{PC} = 4.2 Hz, CH_2), 47.3 (d, $^2J_{PC}$ = 12.4 Hz, 2C, CH_{iPr}), 47.8 (d, $^2J_{PC}$ = 12.3 Hz, 2C, CH_{iPr}), 51.0 (d, $^2J_{PC}$ = 3.9 Hz, C_{tBu}), 51.6 (d, $^2J_{PC}$ = 2.0 Hz, C_{tBu}), 98.8 (dd, J_{PC} = 26.1Hz, $^3J_{PC}$ = 4.1 Hz, P*C*CN), 123.9 (s, 2C, CH_{Ar}), 126.1 (s, CH_{Ar}), 139.8 (d, J_{PC} = 1.6 Hz, C_{Ar}), 145.9 (s, C_{Ar}), 146.8 (s, C_{Ar}), 179.2 (d, $^2J_{PC}$ = 35.5 Hz, PC*C*N), GeC(N2)P not observed. $^{31}P\{^1H\}$ NMR (121 MHz, C_6D_6, 25°C): δ = 64.1 (d, $^2J_{PP}$ = 91.1 Hz), 70.0 (d, $^2J_{PP}$ = 91.1 Hz). $^{29}Si\{^1H\}$ NMR (59 MHz, C_6D_6, 25°C): δ = 7.54 (d, $^2J_{PSi}$ = 3.1 Hz). **Minor isomer (<u>61a</u>)** (36%): $^{13}C\{^1H\}$ NMR (75 MHz, C_6D_6, 25°C): δ = 3.9 (d, $^3J_{PC}$ = 1.2 Hz, $SiCH_3$), 6.2 (d, $^3J_{PC}$ = 5.5 Hz, $SiCH_3$), 23.8-25.4 (m,12C, CH_{3iPr}), 26.4 (s, CH_2), 27.2 (s, CH_{iPr}), 28.2 (s, CH_{iPr}), 29.0 (s, CH_2), 32.3 (d, $^3J_{PC}$ = 5.7 Hz, 3C, CH_{3tBu}), 33.0 (d, $^3J_{PC}$ = 2.9 Hz, 3C, CH_{3tBu}), 40.8 (d, J_{PC} = 5.8 Hz, $CH_{bridgehead}$), 43.8 (d, J_{PC} = 12.1 Hz, $CH_{bridgehead}$), 47.5 (d, $^2J_{PC}$ = 12.8 Hz, 2C, CH_{iPr}), 47.7 (d, $^2J_{PC}$ = 12.5 Hz, 2C, CH_{iPr}), 48.7 (d, J_{PC} = 4.6 Hz, CH_2), 51.0 (d, $^2J_{PC}$ = 4.4 Hz, C_{tBu}), 51.5 (d, $^2J_{PC}$ = 1.8 Hz, C_{tBu}), 102.7 (dd, J_{PC} = 23.2 Hz, $^3J_{PC}$ = 2.4 Hz, P*C*CN), 123.7 (s, 2C, CH_{Ar}), 126.2 (s, CH_{Ar}), 140.0 (d, J_{PC} = 5.0 Hz, C_{Ar}), 146.6 (s, C_{Ar}), 147.4 (s, C_{Ar}), 181.1 (d, $^2J_{PC}$ = 33.7 Hz, PC*C*N). $^{31}P\{^1H\}$ NMR (121 MHz, C_6D_6, 25°C): δ = 64.0 (d, $^2J_{PP}$ = 54.6 Hz), 80.9 (d, $^2J_{PP}$ = 54.6 Hz). $^{29}Si\{^1H\}$ NMR (59 MHz, C_6D_6, 25°C): δ = 7.79 (d, $^2J_{PSi}$ = 3.4 Hz).

VI.3.4. Synthesis of phosphino(germyl)diazomethane (<u>61b</u>)

To a solution of bis(diisopropylamino)phosphinediazomethane (**<u>60</u>**) (0.59 g, 2.18 mmol) in THF (40 mL) was added dropwise a solution of n-butyl lithium (1.43 mL, 2.28 mmol) in hexane (1.6 M) at -80°C. The mixture was stirred at -80°C for 45 min, and then a solution of (**<u>38</u>**) (1.20 g, 2.18 mmol) in THF (20 mL) was added dropwise. The resulting solution was slowly (1 h) warmed to room temperature and volatiles were removed in vacuum. Products (**<u>61b</u>**) were extracted with pentane and orange crystals were obtained from a saturated pentane solution at -30°C (0.76 g, 45%). **Major isomer (<u>61b</u>)** (81%): ^1H NMR (300.18 MHz, C_6D_6, 25°C): δ = 1.04 (d, $^3J_{HH}$ = 6.6 Hz, 3H, CH_{3PNiPr}), 1.07 (d, $^3J_{HH}$ = 6.5 Hz, 3H, CH_{3PNiPr}), 1.09 (d, $^3J_{HH}$ = 5.3 Hz, 3H, CH_{3PNiPr}), 1.13 (d, $^3J_{HH}$ = 6.7 Hz, 3H, CH_{3PNiPr}), 1.20 (d, $^3J_{HH}$ = 6.8Hz, 6H, 2 $PNCH_{3iPr}$), 1.22 (overlapped with the methyl signal, 1H, ½ $CH_{2bridge}$), 1.25 (d, $^3J_{HH}$ = 6.9Hz, 6H, 2 $PNCH_{3iPr}$), 1.26 (d, $^3J_{HH}$ = 6.6Hz, 6H, 2 $PNCH_{3iPr}$), 1.27 (d, $^3J_{HH}$ = 7.0 Hz, 6H, 2 $PNCH_{3iPr}$), 1.35 (d, $^3J_{HH}$ = 6.8 Hz, 3H, CH_{3iPr}), 1.41 (d, $^3J_{HH}$ =

6.8 Hz, 3H, CH_{3iPr}), 1.41 (d, $^{3}J_{HH}$ = 6.8 Hz, 3H, CH_{3iPr}), 1.54-1.57 (m, 2H, ½ $CH_{2CbridgeheadCN}$, ½ $CH_{2CbridgeheadCP}$), 1.63 (d, $^{3}J_{HH}$ = 6.7 Hz, 3H, CH_{3iPr}), 1.67-1.79 (m, 3H, ½ $CH_{2CbridgeheadCN}$, ½ $CH_{2CbridgeheadCP}$, ½ $CH_{2bridge}$), 2.40 (brs, 1H, $PCCH_{bridgehead}$), 2.64-2.80 (m, 4H, 2 $PNCH_2$), 2.79 (brs, 1H, $NCCH_{bridgehead}$), 3.28 (sep, $^{3}J_{HH}$ = 6.8 Hz, 1H, CH_{iPr}), 3.32-3.73 (m, 4H, 4 NCH_{ipr}), 3.83-4.04(m, 3H, 2 $PNCH_{iPr}$, CH_{iPr}), 7.06-7.18 (3H, H_{Ar}). $^{13}C\{^{1}H\}$ NMR (75.47 MHz, C_6D_6, 25°C): δ = 19.79 (d, $^{3}J_{PC}$ = 0.74 Hz, CH_{3PNiPr}), 21.21 (d, $^{3}J_{PC}$ = 6.9 Hz, CH_{3PNiPr}), 21.39 (d, $^{3}J_{PC}$ = 2.7 Hz, CH_{3PNiPr}), 21.76 (d, $^{3}J_{PC}$ = 4.0 Hz, CH_{3PNiPr}), 24.36 (d, $^{3}J_{PC}$ = 8.8 Hz, 2C, $PNCH_{3iPr}$), 24.69 (d, $^{3}J_{PC}$ = 6.9 Hz, 2C, $PNCH_{3iPr}$), 24.74 (d, $^{3}J_{PC}$ = 7.8 Hz, 2C, $PNCH_{3iPr}$), 25.02 (d, $^{3}J_{PC}$ = 6.7 Hz, 2C, $PNCH_{3iPr}$), 25.07 (s, CH_{3iPr}), 25.17 (s, CH_{3iPr}), 25.27 (s, CH_{3iPr}), 25.73 (s, CH_{3iPr}), 26.91 (s, CH_{iPr}), 27.37 (d, $^{4}J_{PC}$ = 0.7 Hz, *C*$H_{2CbridgeheadCN}$), 28.40 (s, CH_{iPr}), 30.08 (brs, *C*$H_{2CbridgeheadCP}$), 39.11 (brs, 2C, $PNCH_2$), 41.18 (d, $^{3}J_{PC}$ = 7.5 Hz, NC*CH*$_{bridgehead}$), 43.94 (d, $^{2}J_{PC}$ = 12.3 Hz, PC*C*$H_{bridgehead}$), 43.88 (d, $^{2}J_{PC}$ = 8.7 Hz, $PNCH_{iPr}$), 44.02 (d, $^{2}J_{PC}$ = 12.8 Hz, $PNCH_{iPr}$), 47.21 (d, $^{2}J_{PC}$ = 11.8 Hz, 2C, NCH_{iPr}), 47.28 (d, $^{2}J_{PC}$ = 11.5 Hz, 2C, NCH_{iPr}), 48.62 (d, $^{3}J_{PC}$ = 2.3 Hz, $CH_{2bridge}$), 92.29 (dd, J_{PC} = 18.8 Hz, $^{4}J_{PC}$ = 0.9 Hz, P*C*=CN), 123.61, 123.90, 126.33 (3 x s, 3C, CH_{Ar}), 141.39 (d, $^{3}J_{PC}$ = 5.0 Hz, NC_{ipso}), 146.94, 147.15 (2 x s, 2C, NC_{orto}), 190.99 (d, $^{2}J_{PC}$ = 41.0 Hz, PC=*C*N), Ge-C(N_2)P Not observed. $^{31}P\{^{1}H\}$ NMR (121.49 MHz, C_6D_6, 25°C): δ = 73.96 (d, $^{3}J_{PP}$ = 10.3 Hz), 60.62 (d, $^{3}J_{PP}$ = 10.3 Hz). IR: ν (N_2) 1980 cm^{-1}. **Minor isomer (<u>61b</u>)** (19 %): ^{1}H NMR (300.18 MHz, C_6D_6, 25°C): δ = 1.00 (d, $^{3}J_{HH}$ = 6.7 Hz, 3H, CH_{3PNiPr}), 1.02 (d, $^{3}J_{HH}$ = 7.3 Hz, 3H, CH_{3PNiPr}), 1.12 (d, $^{3}J_{HH}$ = 6.5 Hz, 3H, CH_{3PNiPr}), 1.15 (d, $^{3}J_{HH}$ = 6.5 Hz, 3H, CH_{3PNiPr}), 1.21 (overlapped with the methyl signal, 1H, ½ $CH_{2bridge}$), 1.22 (d, $^{3}J_{HH}$ = 6.0Hz, 6H, 2 $PNCH_{3iPr}$), 1.24 (d, $^{3}J_{HH}$ = 5.6 Hz, 6H, 2 $PNCH_{3iPr}$), 1.26 (d, $^{3}J_{HH}$ = 5.3 Hz, 6H, 2 $PNCH_{3iPr}$), 1.28 (d, $^{3}J_{HH}$ = 4.4 Hz, 6H, 2 $PNCH_{3iPr}$), 1.33 (d, $^{3}J_{HH}$ = 8.3 Hz, 6H, 2 CH_{3iPr}), 1.54 (d, $^{3}J_{HH}$ = 6.8 Hz, 3H, CH_{3iPr}), 1.54-1.57 (overlapped with the methyl signal, 2H, ½ $CH_{2CbridgeheadCN}$, ½ $CH_{2CbridgeheadCP}$), 1.60 (d, $^{3}J_{HH}$ = 6.8 Hz, 3H, CH_{3iPr}), 1.67-1.79 (m, 3H, ½ $CH_{2CbridgeheadCN}$, ½ $CH_{2CbridgeheadCP}$, ½ $CH_{2bridge}$), 2.64-2.80 (m, 5H, 2 $PNCH_2$, $PCCH_{bridgehead}$), 2.95 (brs, 1H, $NCCH_{bridgehead}$), 3.32-3.73 (m, 6H, 4 NCH_{ipr}, 2 CH_{iPr}), 3.83-4.04(m, 2H, 2 $PNCH_{iPr}$,), 7.06-7.18 (3H, H_{Ar}). $^{13}C\{^{1}H\}$ NMR (75.47 MHz, C_6D_6, 25°C): δ = 20.38 (s, CH_{3PNiPr}), 20.59 (d, $^{3}J_{PC}$ = 0.8 Hz, CH_{3PNiPr}), 21.04 (d, $^{3}J_{PC}$ = 4.5 Hz, CH_{3PNiPr}), 22.02 (d, $^{3}J_{PC}$ = 7.3 Hz, CH_{3PNiPr}), 24.46 (d, $^{3}J_{PC}$ = 6.8 Hz, 2C, $PNCH_{3iPr}$), 24.47 (d, $^{3}J_{PC}$ = 8.7 Hz, 2C, $PNCH_{3iPr}$), 24.25 (d, $^{3}J_{PC}$ = 7.4 Hz, 2C, $PNCH_{3iPr}$), 25.26 (d, $^{3}J_{PC}$ = 6.3 Hz, 2C, $PNCH_{3iPr}$), 24.90 (s, CH_{3iPr}), 25.39 (s, CH_{3iPr}), 25.43 (s, CH_{3iPr}), 25.61 (s, CH_{3iPr}), 27.37 (d, $^{4}J_{PC}$ = 0.7 Hz, *C*$H_{2CbridgeheadCN}$), 27.61 (s, CH_{iPr}), 28.67 (s, CH_{iPr}), 29.72 (brs, *C*$H_{2CbridgeheadCP}$), 39.99 (brs, 2C, $PNCH_2$), 41.218 (d, $^{3}J_{PC}$ = 7.0 Hz, NC*CH*$_{bridgehead}$), 44.40 (d, $^{2}J_{PC}$ = 7.7 Hz, $PNCH_{iPr}$), 44.53 (d, $^{2}J_{PC}$ = 12.1 Hz, PC*C*$H_{bridgehead}$),

44.43 (d, $^{2}J_{PC}$ = 11.8 Hz, $PNCH_{iPr}$), 46.30 (d, $^{3}J_{PC}$ = 5.5 Hz, $CH_{2bridge}$), 47.59 (d, $^{2}J_{PC}$ = 11.8 Hz, 4C, NCH_{iPr}), 92.29 (dd, J_{PC} = 18.8 Hz, $^{4}J_{PC}$ = 0.9 Hz, P*C*=CN), 123.83, 123.94, 126.20 (3 x s, 3C, CH_{Ar}), 141.40 (d, $^{3}J_{PC}$ = 3.2 Hz, NC_{ipso}), 145.87, 147.03 (2 x s, 2C, NC_{orto}), 187.659 (d, $^{2}J_{PC}$ = 42.8 Hz, PC=*C*N), Ge-C(N_2)P (Not observed). $^{31}P\{^{1}H\}$ NMR (121.49 MHz, C_6D_6, 25°C): δ = 73.64 (d, $^{3}J_{PP}$ = 51.3 Hz), 63.91 (d, $^{3}J_{PP}$ = 51.3 Hz). IR: $\nu(N_2)$ 2040 cm^{-1}.

VI.3.5. Photolysis of phosphino(germyl)diazomethane (61a)

A diethyl ether (2 mL) solution of (**61a**) (155 mg, 0.184 mmol) was irradiated (λ = 300 nm) at -60°C. After 3 days of irradiation, germyne (**62a**) was obtained as dark red crystals from a cold (-60°C) concentrated ether solution. (80% NMR yield). ^{1}H NMR (300 MHz, THF-d_8, -60 °C): δ = 0.49 (s, 3H, $SiCH_3$), 0.53 (s, 3H, $SiCH_3$), 1.12 (d, $^{3}J_{HH}$ = 6.3 Hz, 3H, CH_{3iPr}), 1.13 (d, $^{3}J_{HH}$ = 6.9 Hz, 12H, CH_{3iPr}), 1.18 (d, $^{3}J_{HH}$ = 6.3 Hz, 3H, CH_{3iPr}), 1.19 (b, 1H, CH_2), 1.25 (d, $^{3}J_{HH}$ = 6.9 Hz, 12H, CH_{3iPr}), 1.26 (d, $^{3}J_{HH}$ = 6.5 Hz, 3H, CH_{3iPr}), 1.27 (b, 1H, CH_2), 1.28 (d, $^{3}J_{HH}$ = 7.0 Hz, 3H, CH_{3iPr}), 1.31 (d, J_{HH} = 6.9 Hz, 1H, CH_2), 1.32 (s, 9H, CH_{3tBu}), 1.42 (s, 9H, CH_{3tBu}), 1.56 (d, J_{HH} = 6.5 Hz, 1H, CH_2), 1.65 (b, 1H, CH_2), 1.76 (b, 1H, CH_2), 2.57 (b, 1H, $CH_{bridgehead}$), 3.20 (b, 1H, $CH_{bridgehead}$), 3.26 (sept, $^{3}J_{HH}$ = 6.5 Hz, 1H, CH_{iPr}), 3.55 (m, 4H, CH_{iPr}), 3.63 (sept, $^{3}J_{HH}$ = 7.0 Hz, 1H, CH_{iPr}), 7.10 (m, 3H, CH_{Ar}). $^{13}C\{1H\}$ NMR (75 MHz, THF-d_8, - 60°C): δ = 3.7 (d, $^{3}J_{PC}$ = 1.6 Hz, $SiCH_3$), 5.6 (d, $^{3}J_{PC}$ = 6.3 Hz, $SiCH_3$), 22.2 (s, 4C, CH_{3iPr}), 22.9 (s, 4C, CH_{3iPr}), 23.8 (s, CH_{3iPr}), 24.4 (s, CH_{3iPr}), 25.1 (s, CH_{3iPr}), 25.6 (s, CH_2), 25.8 (s, CH3*i*Pr), 27.4 (s, CH_{iPr}), 28.1 (s, CH_{iPr}), 29.3 (s, CH_2), 32.3 (d, $^{3}J_{PC}$ = 5.0 Hz, 3C, CH_{3tBu}), 32.7 (s, 3C, CH_{3tBu}), 41.0 (d, J_{PC} = 7.4 Hz, $CH_{bridgehead}$), 43.5 (d, J_{PC} = 9.6 Hz, $CH_{bridgehead}$), 45.5 (s, CH_2), 48.2 (s, 4C, CH_{iPr}), 50.5 (d, $^{2}J_{PC}$ = 4.5 Hz, C_{tBu}), 51.4 (d, $^{2}J_{PC}$ = 3.1 Hz, C_{tBu}), 97.5 (d, J_{PC} = 16.4 Hz, P*C*CN), 122.7 (s, CH_{Ar}), 122.8 (s, CH_{Ar}), 124.4 (s, CH_{Ar}), 142.3 (s, C_{Ar}), 144.7 (s, C_{Ar}), 146.0 (s, C_{Ar}), 162.4 (dd, J_{PC} = 43.0 Hz, $^{3}J_{PC}$ = 11.3 Hz, GeCP), 177.6 (d, $^{2}J_{PC}$ = 35.5 Hz, PC*C*N). $^{31}P\{^{1}H\}$ NMR (121 MHz, THF-d_8, -60°C): δ = - 20.3 (d, $^{3}J_{PP}$ = 102.6 Hz, P_1), 82.1 (d, $^{3}J_{PP}$ = 102. 6 Hz, P_2).

VI.3.6. Photolysis of phosphino(germyl)diazomethane (61b)

A solution of (**61b**) (80 mg, 0.102 mmol) in THF-d_8 (0.5 mL) was irradiated, at -80°C, at λ = 300 nm, for 48 h. The orange solution changes to red and low temperature (-60°C) NMR reveals one major compound (**62b**). $^{13}C\{^{1}H\}$ NMR (100 MHz, THF-d_8, -80°C):

δ = 19.9 (s, CH_{3iPr}), 20.3 (s, CH_{3iPr}), 20.9 (s, CH_{3iPr}), 21.3 (s, CH_{3iPr}), 22.3 (s, 4C, CH_{3iPr}), 23.1 (s, 4C, CH_{3iPr}), 23.8 (s, CH_{3iPr}), 25.0 (s, CH_{3iPr}), 25.2 (s, CH_{3iPr}), 25.3 (b, CH_2), 25.6 (s, CH_{3iPr}), 27.6 (s, CH_{iPr}), 28.0 (s, CH_{iPr}), 30.5 (b, CH_2), 38.5 (b, CH_2), 39.4 (b, CH_2), 40.8 (d, J_{PC} = 8.2 Hz, $CH_{bridgehead}$), 43.7 (d, J_{PC} = 8.8 Hz, $CH_{bridgehead}$), 44.0 (d, J_{PC} = 18.0 Hz, CH_{iPr}), 44.2 (d, $^{2}J_{PC}$ = 16.1 Hz, CH_{iPr}), 45.9 (b, CH_2), 48.2 (s, 4C, CH_{iPr}), 90.9 (d, J_{PC} = 22.9 Hz, P*C*CN), 122.7 (s, CH_{Ar}), 122.8 (s, CH_{Ar}), 124.2 (s, CH_{Ar}), 142.3 (s, C_{Ar}), 144.4 (s, C_{Ar}), 146.6 (s, C_{Ar}), 161.1 (dd, J_{PC} = 11.0 Hz, $^{3}J_{PC}$ = 10.7 Hz, GeCP), 181.1 (d, $^{2}J_{PC}$ = 34.1 Hz, PC*C*N). $^{31}P\{^{1}H\}$ NMR (161 MHz, THF-d_8, - 80°C): δ = - 14.97 (d, $^{3}J_{PP}$ = 102.2 Hz, P_1), 77.4 (d, $^{3}J_{PP}$ = 101.9 Hz, P_2).

VI.3.7. Isomerization of (62a)

A diethyl ether solution of (**62a**) (119 mg, 0.150 mol) was warmed to RT. The germylene (**64a**) was obtained as orange crystals from a cold (-20°C) concentrated solution of Et_2O (70 mg, 60%). **(63a):** ^{1}H NMR (300 MHz, C_6D_6, 25°C): δ = 0.42 (s, 3H, $SiCH_3$), 0.65 (s, 3H, $SiCH_3$), 1.15 (m, 1H, CH_2), 1.23 (d, $^{3}J_{HH}$ = 6.7 Hz, 3H, CH_{3iPr}), 1.29 (d, $^{3}J_{HH}$ = 6.7 Hz, 6H, CH_{3iPr}), 1.32 (d, $^{3}J_{HH}$ = 6.7 Hz, 3H, CH_{3iPr}), 1.34 (s, 9H, CH_{3tBu}), 1.35 (s, 9H, CH_{3tBu}), 1.40 (d, $^{3}J_{HH}$ = 6.7 Hz, 6H, CH_{3iPr}), 1.45 (d, $^{3}J_{HH}$ = 6.8 Hz, 6H, CH_{3iPr}), 1.47 (d, J_{HH} = 6.7 Hz, 6H, CH_{3iPr}), 1.51 (d, $^{3}J_{HH}$ = 6.8 Hz, 6H, CH_{3iPr}), 1.73 (m, 2H, CH_2), 1.88 (m, 1H, CH_2), 2.64 (b, 1H, $CH_{bridgehead}$), 3.22 (sept, $^{3}J_{HH}$ = 6.7 Hz, 1H, CH_{iPr}), 3.36 (b, 1H, $CH_{bridgehead}$), 3.38 (sept, $^{3}J_{HH}$ = 6.7 Hz, 1H, CH_{iPr}), 4.40 (sept, $^{3}J_{HH}$ = 6.8 Hz, 2H, CH_{iPr}), 4.63 (sept, $^{3}J_{HH}$ = 6.7 Hz, 2H, CH_{iPr}), 7.19 (m, 1H, CH_{Ar}), 7.22 (m, 1H, CH_{Ar}), 7.26 (m, 1H,CH_{Ar}). $^{13}C\{^{1}H\}$ NMR (75 MHz, C_6D_6, 25°C): δ = 4.1 (dd, $^{4}J_{PC}$ = 7.3 Hz, $^{3}J_{PC}$ = 2.3 Hz, $SiCH_3$), 4.3 (d, $^{3}J_{PC}$ = 1.8 Hz, $SiCH_3$), 23.2 (s, CH_{3iPr}), 23.4 (s, CH_{3iPr}), 25.1 (s, CH_{3iPr}), 25.2 (s, CH_{3iPr}), 25.4 (s, CH_{3iPr}), 25.5 (s, CH_{3iPr}), 25.6 (s, CH_2), 25.6 (d, $^{3}J_{PC}$ = 4.7 Hz, 2C, CH_{3iPr}), 25.7 (d, $^{3}J_{PC}$ = 1.7 Hz, 2C, CH_{3iPr}), 25.8 (s, 2C, CH_{3iPr}), 27.9 (s, CH_{iPr}), 28.0 (s, CH_{iPr}), 28.3 (s, CH_2), 32.6 (d, $^{3}J_{PC}$ = 5.2 Hz, 3C, CH_{3tBu}), 32.8 (dd, $^{3}J_{PC}$ = 5.3 Hz, J_{PC} = 1.2 Hz, 3C,CH_{3tBu}), 44.4 (dd, J_{PC} = 8.6 Hz, J_{PC} = 4.3 Hz, $CH_{bridgehead}$), 46.3 (d, J_{PC} = 8.0 Hz, $CH_{bridgehead}$), 47.6 (d, J_{PC} = 7.4 Hz, CH_2), 51.1 (d, $^{2}J_{PC}$ = 15.5 Hz, 2C, CH_{iPr}), 51.6 (s, C_{tBu}), 51.9 (s, C_{tBu}), 52.1 (d, $^{2}J_{PC}$ = 16.2 Hz, 2C, CH_{iPr}), 100.1 (dd, J_{PC} = 129.2 Hz, $^{3}J_{PC}$ = 8.8 Hz, P*C*CN), 122.6 (dd, J_{PC} = 48.4 Hz, J_{PC} = 37.8 Hz, PCP), 123.4 (s, CH_{Ar}), 123.9 (s, CH_{Ar}), 126.9 (s, CH_{Ar}), 144.4 (s, C_{Ar}), 145.6 (s, C_{Ar}), 146.4 (s, C_{Ar}), 170.1 (dd, $^{2}J_{PC}$ = 5.6 Hz, $^{4}J_{PC}$ = 1.4 Hz, PC*C*N). $^{31}P\{^{1}H\}$ NMR (121 MHz, C_6D_6, 25°C): δ = 24.3 (d, $^{2}J_{PP}$ = 199 Hz), 93.1 (d, $^{2}J_{PP}$ = 199 Hz). $^{29}Si\{^{1}H\}$ NMR (59 MHz, C_6D_6,

25°C): δ = 1.4 (s). **(64a):** ^{1}H NMR (300 MHz, C_6D_6, 25°C): δ = 0.46 (s, 6H, $SiCH_3$), 0.96 (d, J_{HH} = 7.8 Hz, 6H, CH_{3iPr}), 1.05-1.63 (m, 30H, CH_{3iPr}), 1.25 (d, J_{HH} = 8.1 Hz, 1H, CH_2), 1.52 (s, 9H, CH_{3tBu}), 1.54 (s, 9H, CH_{3tBu}), 1.73 (d, J_{HH} = 7.7 Hz, 1H, CH_2), 1.77 (b, 2H, CH_2), 2.50 (b, 1H, $CH_{bridgehead}$), 3.21 (sept, J_{HH} = 7.5 Hz, 1H, CH_{iPr}), 3.27 (m, 2H, CH_{iPr}), 3.31 (b, 1H, $CH_{bridgehead}$), 3.70 (sept, J_{HH} = 7.5 Hz, 1H, CH_{iPr}), 4.65 (m, 2H, CH_{iPr}), 7.10-7.25 (m, 3H, CH_{Ar}). ^{13}C{^{1}H} NMR (75 MHz, C_6D_6, 25°C): δ = 6.3 (d, J_{PC} = 4.2 Hz, 2C, $SiCH_3$), 22.1 (b, 2C, CH_{3iPr}), 24.0 (b, 2C, CH_{3iPr}), 24.2 (d, J_{PC} = 4.0 Hz, 2C, CH_{3iPr}), 24.3 (d, J_{PC} = 5.7 Hz, 2C, CH_{3iPr}), 24.6 (s, CH_{3iPr}), 25.3 (s, CH_{3iPr}), 26.0 (s, CH_{3iPr}), 26.2 (d, J_{PC} = 1.7 Hz, CH_2), 26.3 (d, J_{PC} = 2.2 Hz, CH_{3iPr}), 28.1 (s, CH_{iPr}), 28.4 (s, CH_{iPr}), 29.2 (m, CH_2), 32.8 (d, J_{PC} = 5.3 Hz, 3C, CH_{3tBu}), 33.6 (m, 3C, CH_{3tBu}), 42.3 (b, $CH_{bridgehead}$), 44.1 (d, J_{PC} = 10.7 Hz, $CH_{bridgehead}$), 46.8 (d, J_{PC} = 3.5 Hz, CH_2), 49.8 (d, $^{2}J_{PC}$ = 4.2 Hz, 2C, CH_{iPr}), 51.7 (s, CH_{3tBu}), 51.9 (s, CH_{3tBu}), 56.6 (b, 2C, CH_{iPr}), 98.9 (dd, J_{PC} = 32.8 Hz, $^{4}J_{PC}$ = 5.7 Hz, P*C*CN), 123.7 (s, CH_{Ar}), 124.3 (s, CH_{Ar}), 125.9 (s, CH_{Ar}), 143.7 (s, C_{Ar}), 145.7 (s, C_{Ar}), 146.6 (s, C_{Ar}), 177.1 (d, $^{2}J_{PC}$ = 31.7 Hz, PC*C*N), 205.0 (dd, $^{2}J_{PC}$ = 136.2 Hz, J_{PC} = 20.7 Hz, GeCP). ^{31}P{^{1}H} NMR (121 MHz,C_6D_6, 25°C): δ = 84.1 (d, $^{3}J_{PP}$ = 158 Hz), 96.5 (d, $^{3}J_{PP}$ = 158 Hz).

VI.3.8. Isomerization of (62b)

A diethyl ether solution of (**62b**) (204 mg, 0.27 mmol) was warmed to RT leading to the formation of rearranged germylene (**63b**), obtained as orange crystals from a cold (-20°C) concentrated solution of Et_2O (169 mg, 80%). **(63b):** ^{1}H NMR (300 MHz, C_6D_6, 25°C): δ = 1.07 (d, J_{HH} = 7.2 Hz, 1H, CH_2), 1.13 (d, $^{3}J_{HH}$ = 6.2 Hz, 3H, CH_{3iPr}), 1.15 (d, $^{3}J_{HH}$ = 6.3 Hz, 3H, CH_{3iPr}), 1.19 (d, J_{HH} = 6.4 Hz, 3H, CH_{3iPr}), 1.21 (d, J_{HH} = 6.7 Hz, 3H, CH_{3iPr}), 1.27 (d, $^{3}J_{HH}$ = 6.9 Hz, 3H, CH_{3iPr}), 1.30 (d, $^{3}J_{HH}$ = 6.9 Hz, 6H, CH_{3iPr}), 1.36 (d, J_{HH} = 6.7 Hz, 6H, CH_{3iPr}), 1.37 (d, J_{HH} = 7.8 Hz, 3H, CH_{3iPr}), 1.39 (d, $^{3}J_{HH}$ = 6.5 Hz, 6H, CH_{3iPr}), 1.41 (d, $^{3}J_{HH}$ = 5.9 Hz, 6H, CH_{3iPr}), 1.44 (d, ^{3}JHH = 6.5 Hz, 6H, CH_{3iPr}), 1.64 (d, J_{HH} = 6.3 Hz, 1H, CH2), 1.65 (m, 2H, CH2), 2.58 (b, 1H, $CH_{bridgehead}$), 2.89 (m, 3H, CH_2), 3.07 (b, 1H, $CH_{bridgehead}$), 3.12 (d, J_{HH} = 9.3 Hz, 1H, CH2), 3.39 (m, 1H, CH_{iPr}), 3.42 (m, 1H, CH*i*Pr), 3.51 (m, 1H, CH*i*Pr), 4.17 (sept, $^{3}J_{HH}$ = 7.2 Hz, 2H, CH_{iPr}), 4.21 (sept, $^{3}J_{HH}$ = 7.2 Hz, 2H, CH*i*Pr), 7.15-7.28 (m, 3H, CH_{Ar}). ^{13}C{1H} NMR (75 MHz, C_6D_6, 25°C) : δ = 21.5 (d, $^{3}J_{PC}$ = 1.7 Hz, CH_{3iPr}), 22.7 (m, 3C, CH_{3iPr}), 23.4 (s, CH_{3iPr}), 23.8 (s, CH_{3iPr}), 24.9 (d, $^{3}J_{PC}$ = 3.6 Hz, 2C, CH_{3iPr}), 25.0 (s, 2C, CH_{3iPr}), 25.2 (d, $^{3}J_{PC}$ = 5.6 Hz, 2C, CH_{3iPr}), 25.3 (s, CH_{3iPr}), 25.4 (s, CH_2), 25.4 (s, CH_{3iPr}), 25.7 (s, CH_{3iPr}), 25.9 (s, CH_{3iPr}), 28.4 (d, J_{PC} = 2.6 Hz, 2C, CH_{iPr}), 29.2 (s,

CH_2), 42.0 (dd, J_{PC} = 5.6 Hz, J_{PC} = 1.7 Hz, CH_2), 43.3 (dd, J_{PC} = 6.7 Hz, J_{PC} = 5.3 Hz, CH_2), 44.9 (dd, $^2J_{PC}$ = 7.5 Hz, J_{PC} = 3.0 Hz, CH_{iPr}), 45.0 (d, $^2J_{PC}$ = 6.5 Hz, CH_{iPr}), 46.3 (d, $^2J_{PC}$ = 5.5 Hz, CH_{iPr}), 46.8 (d, $^2J_{PC}$ = 8.5 Hz, CH_{iPr}), 47.8 (d, J_{PC} = 7.1 Hz, CH_2), 49.5 (d, $^2J_{PC}$ = 13.0 Hz, 2C, CH_{iPr}), 50.1 (d, $^2J_{PC}$ = 14.9 Hz, 2C, CH_{iPr}), 96.9 (dd, J_{PC} = 137.6Hz, $^3J_{PC}$ = 10.0 Hz, P*C*CN), 117.8 (dd, J_{PC} = 59.0 Hz, J_{PC} = 42.3 Hz, PCP), 123.4 (s, CH_{Ar}), 124.0 (s, CH_{Ar}), 126.8 (s, CH_{Ar}), 144.9 (d, $^4J_{PC}$ = 1.1 Hz, C_{Ar}), 145.6 (s, C_{Ar}), 146.8 (s, C_{Ar}), 170.8 (dd, $^2J_{PC}$ = 6.4 Hz, $^4J_{PC}$ = 1.1 Hz, N*C*CP). $^{31}P\{^1H\}$ NMR (121 MHz, C_6D_6, 25°C): δ = 30.6 (d, $^2J_{PP}$ = 158.1 Hz), 76.5 (d, $^2J_{PP}$ = 158.1 Hz).

VI.3.9. Crystallographic data

The data of the structures for compounds (**61a**), (**61b**), (**62a**), (**63a**) and (**63b**) were collected on a Bruker-AXS APEX II diffractometer using a 30 W air-cooled microfocus source (ImS) with focusing multilayer optics at a temperature of 193K, with graphite33 monochromated MoKα radiation (wavelength = 0.71073 Å) by using phi- and omega-scans. The structures were solved by direct methods, using SHELXS-97.

61a: $C_{46}H_{87}GeN_7OP_2Si$, *M*= 916.85, Triclinic, space group $P\bar{1}$, *a*= 10.4194(3) Å, *b*= 13.8223(6) Å, *c*= 20.0405(5) Å, α= 76.4920(10), β= 75.0280(10)°, γ= 82.150(2)°, *V*= 2702.18(16) $Å^3$, *Z*= 2, crystal size 0.60 x 0.50 x 0.50 mm3, 52913 reflections collected (13232 independent, Rint= 0.0257), 616 parameters, 170 restraints, *R*1 [I>2σ(I)]= 0.0361, *wR*2 [all data]= 0.1013, largest diff. peak and hole: 0.707 and -0.415 e.Å-3.

61b: $C_{40}H_{71}GeN_7P_2$, *M*= 784.57, Monoclinic, space group $P2_1/c$, *a*= 10.4194(3) Å, *b*= 17.1876(13) Å, *c*= 20.1632(15) Å, β= 96.4300(10)°, *V*= 4412.5(6) $Å^3$, *Z*=4, crystal size 0.50 x 0.40 x 0.30 mm^3, 41889 reflections collected (10866 independent, R_{int}= 0.0296), 467 parameters, *R*1 [I>2σ(I)]= 0.0329, *wR*2 [all data]= 0.0893, largest diff. peak and hole: 0.756 and -0.317 e.$Å^{-3}$.

62a: $C_{42}H_{77}GeN_5P_2Si$, *M*= 814.71, Triclinic, space group $P\bar{1}$, *a*= 10.0652(9) Å, *b*= 12.1234(11) Å, *c*= 20.7037(19) Å, α= 100.199(5)°, β= 93.700(4)°, γ= 100.552(5)°, *V*= 2432.1(4) $Å^3$, *Z*= 2, crystal size 0.40 x 0.24 x 0.22 mm^3, 45412 reflections collected (6765

independent, R_{int}= 0.0516), 480 parameters, *R*1 [I>2σ(I)]= 0.0524, *wR*2 [all data]= 0.1264, largest diff. peak and hole: 0.775 and -0.391 e.Å^{-3}.

63a: $C_{42}H_{77}GeN_5P_2Si$, *M*= 814.71, Monoclinic, space group $P2_1/c$, *a*= 12.0149(4) Å, *b*= 13.3330(5) Å, *c*= 28.4929(9) Å, β= 95.3190(10)°, *V*= 4544.8(3) Å^3, *Z*= 4, crystal size 0.24 x 0.14 x 0.08 mm^3, 53670 reflections collected (13204 independent, R_{int}= 0.0432), 480 parameters, *R*1 [I>2σ(I)]= 0.0370, *wR*2 [all data]= 0.0954, largest diff. peak and hole: 0.459 and -0.260 e.Å^{-3}.

63b: $C_{40}H_{71}GeN_5P_2$, *M*= 756.55, Triclinic, space group $P\bar{1}$, *a*= 9.8517(4) Å, *b*= 10.3538(4) Å, *c*= 22.4488(10) Å, α= 85.4800(10), β= 81.329(2)°, γ= 70.6260(10)°, *V*= 2134.46(15) Å^3, *Z*= 2, crystal size 0.62 x 0.40 x 0.36 mm^3, 38146 reflections collected (10483 independent, Rint= 0.0248), 449 parameters, *R*1 [I>2σ(I)]= 0.0317, *wR*2 [all data]= 0.0838, largest diff. peak and hole: 0.670 and -0.346 e.Å^{-3}.

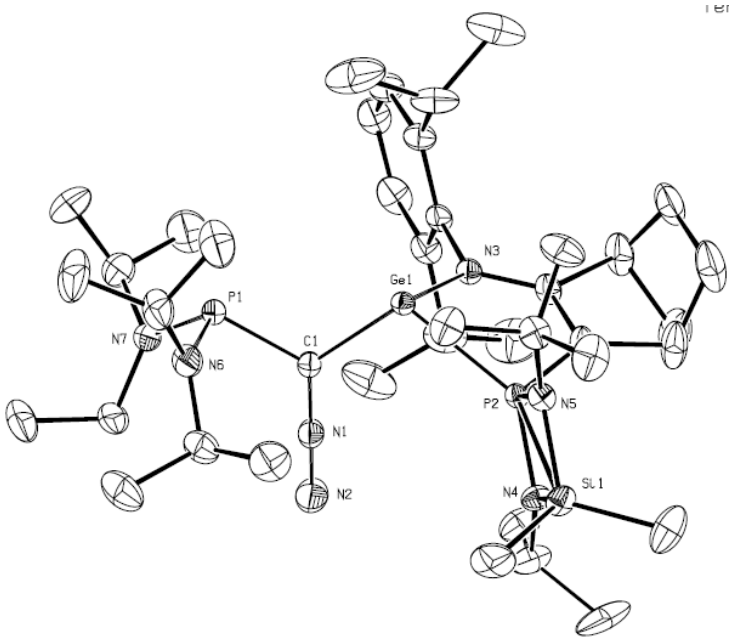

Figure VI.11. Molecular structure of (**61a**). H atoms are omitted for clarity. Selected bond lengths (Å), and angles (deg): C1-Ge1 1.9977(16), C1-P1 1.8295(16), Ge1-N3 1.9992(12), Ge-P2 2.4429(4), P1-N6 1.6852(17), P1-N7 1.7098(17), C1-N1 1.282(2), N1-N2 1.151(2), C1-Ge1-N3 103.46(6), C1-Ge1-P2 110.49(5), N3-Ge1-P2 84.22(4), N6-P1-N7 109.51(9), N7-P1-C1 106.05(8), N6-P1-C1 100.92(8), N1-C1-P1 122.63(12), N1-C1-Ge1 127.64(12), P1-C1-Ge1 109.46(8), N2-N1-C1 179.30(18). $\sum P_{2\alpha}$ = 316.48°, $\sum Ge_{\alpha}$ = 298.17°.

VI.3.10. Theoretical data

Table VI.4. Total electronic energies [a](E, in a.u.), thermal corrections to free energies [b](TCGFE, in a.u.) and number of imaginary frequencies (NIMAG) of **62a-III**, **62b-II** and **62b-III**.

Structure	E	TCGFE	NIMAG(v)
62a-III	-4947.939984	1.079847	0
62b-II	-4580.024701	1.012544	0
62b-III	-4580.040625	1.012379	0

[a] Computed at the bHandH(Si)/6-31G* [161] level of theory as implemented in Gaussian09.[162] [b] Computed at 298 K at the bHandH/6-31G* level of theory.

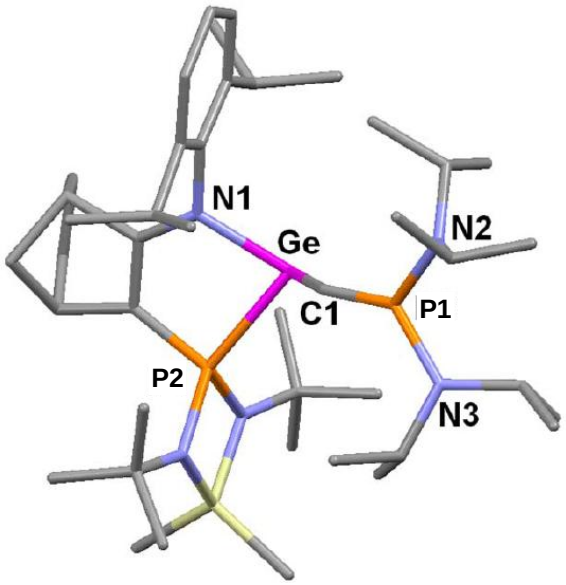

Figure VI.12. Calculated molecular structure of **62a** (BHandH/6-31G*). H atoms are omitted for clarity. Selected bond lengths (Å), and angles (deg): C1-Ge 1.838, C1-P1 1.552, Ge-N1 1.937, Ge-P2 2.384, P1-N3 1.666, P1-N2 1.657, C1-Ge-N1 105.48, C1-Ge-P2 112.18, N1-Ge-P2 83.97, C1-P1-N3 129.43, C1-P1-N2 127.58, N2-P1-N3 102.83, Ge-C1-P1 145.83. Torsion angles (deg): N2-P1-C1-Ge -84.89, N3-P1-C1-Ge 100.45.

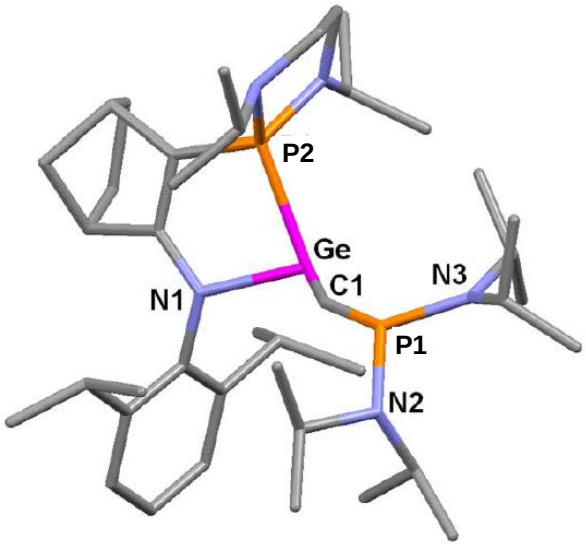

Figure VI.13. Calculated molecular structure of **62b** (BHandH/6-31G*). H atoms are omitted for clarity. Selected bond lengths (Å), and angles (deg): C1-Ge 1.833, C1-P1 1.555, Ge-N1 1.973, Ge-P2 2.328, P1-N3 1.661, P1-N2 1.689, C1-Ge-N1 110.19, C1-Ge-P2 105.21, N1-Ge-P2 84.95, C1-P1-N3 129.19, C1-P1-N2 123.93, N2-P1-N3 102.76, Ge-C1-P1 150.55. Torsion angles (deg): N2-P1-C1-Ge 26.28, N3-P1-C1-Ge -126.80.

VI.4. Conclusions

The precursors phosphino(germyl)diazomethanes (**61a-b**) were prepared by reaction of the phosphine-stabilized germylenes (**38a-b**) with the lithiated phosphinediazomethane (**60**). Phosphino(germyl)diazomethanes (**61a-b**) were obtained as a mixture of two diastereomers owing to the chiral norbonadiene fragment and to the pyramidalized chiral germanium (II) center.

Photolysis of phosphino(germyl) diazomethanes (**61a-b**) (λ = 300 nm) at -60°C in THF led to the formation of compounds (**62a**) and (**62b**) respectively. In the case of (**62a**), an X-ray diffraction analysis indicates a quite long GeC-bond length for a triple bond, but consistent whit theoretically predicted values for germynes bearing electron-withdrawing and π-donating substituents, as well as a short PC-bond length.

X-ray diffraction analysis and theoretical calculations reveal that derivatives (**62a-b**) have a bis-carbenoid structure with a strongly π-interaction from the exocyclic phosphine moiety to carbenic center.

Compounds (**62a-b**) are thermally unstable and they undergo an isomerization reaction above -30°C. The isomerization of (**62b**) led to the formation of cyclic germylene (**63b**). Meanwhile, the isomerization of (**62a**) affords a mixture of phosphaalkene (**64a**) and cyclic germylene derivative (**63a**). Cyclic germylenes (**63a-b**) can be considered new stable *N*-heterocyclic germylenes.

The results demonstrate the significant differences not only on the structure of (**62a**) but also on its chemical behavior from those of the silicon analogue (**55**).[137]

General Conclusions

In the course of this work, we have studied the ligating properties of a series of diallylphosphines, as well as, we have synthesized divalent germanium species stabilized by coordination of a phosphine. On the other hand, the reactivity of these germanium(II) species have been studied on base to reactions with organic compounds and transition metal complexes.

Cationic rhodium complexes [Rh(COD){κ^3(P,C,C)RP($CH_2CH=CH_2$)$_2$}][BF_4] [R= ^{i}Pr$_2$N (**22a**), ^{t}Bu (**22b**) and Ph (**22c**)] have been synthesized starting from the dimer complex [$Rh_2(\mu\text{-}Cl)_2(COD)_2$]. X-ray diffraction analysis showed the coordination of only one allyl moiety to rhodium centre, while the other allyl moiety remain free, which demonstrates the bidentate character of the diallylphosphine ligands. Hemilabile properties of diallylphosphine ligands have been demonstrated by ligand exchange reactions. In solution, a dynamic equilibrium of exchange between the two allylic double bonds was detected by low temperature NMR analysis. In the same way, the reversible displacement of coordinated allylic double bond by acetonitrile could be observed.

The experimental results reveal that the displacement of acetonitrile ligand is easier in the complex (**24a**) that in the complexes (**24b**) and (**24c**). This trend has been explained on the basis of DFT calculations indicating that the electrostatic interaction between the acetonitrile ligand and the rhodium center is responsible of the experimentally observed behavior.

On the other hand, we have synthesized and fully characterized germylenes intramolecularly stabilized by coordination of a phosphine ligand. The reactivity of these germanium(II) species have been studied on base to reactions with different organic reagent. These reactivity studies showed that phosphine-stabilized germylenes (**38-41**) are unreactive toward unsaturated compounds, such as: alkyne, alkene and carbonyl derivatives, but reactive toward 2,3-dimethylbutadiene to form [1+4] cycloadduct (**46**), typical reaction of free kinetically stabilized germylenes. The absence of reactivity with carbonyl derivatives suggests that phosphine-stabilized germylenes (**38**-**41**) do not exhibit a phosphonium ylide-like reactivity. Moreover, phosphine-stabilized germylene (**39**) reacts with BH_3·THF, as a Lewis bases, to form the corresponding germylene-borane complex (**49**). The reactivity studies indicate that phosphine-stabilized germylenes exhibit a typical reactivity for germylene.

The reactivity of phosphonium-stabilized germylenes toward transition metal complexes have been studied by reaction of germylenes (**38** and **39**) with the dimer complex $[Rh_2(\mu\text{-}Cl)_2(COD)_2]$. In this sense, phosphine-stabilized germylene (**39**) behaves as two-electron σ-donor ligands, such as the homologues carbenes and silylenes, to form neutral rhodium complex (**52**). Meanwhile, phosphine-stabilized germylene (**38**) behaves as a chelate ligand to form the metallacycle rhodium complex (**51**), which indicates that the coordination mode of theses divalent germanium species can be modified by replacing the germanium substituent. These results show that phosphine-stabilized germylenes are useful ligands with high potential in organometallic chemistry.

Photolysis of phosphino(germyl) diazomethanes (**61a-b**) (λ = 300 nm) at -60°C in THF led to the formation of compounds (**62a**) and (**62b**) respectively. X-ray diffraction analysis and theoretical calculations reveal that derivatives (**62a-b**) have a bis-carbenoid structure with a strongly π-interaction from the exocyclic phosphine moiety to carbenic center. The isomerization of (**62a-b**) at RT affording the new stable N-heterocyclic germylenes (**63a-b**).[159,160] The results demonstrate the significant differences not only on the structure of (**62a**) but also on its chemical behavior from those of the silicon analogue (**55**).[137]

.

Bibliographic references

1. P. Braunstein**,** *J. Organometal. Chem*., **2004**, 689, 3953.
2. P. Espinet, K. Soulantica, *Coord. Chem. Rev*., **1999**, 193-195, 499.
3. S. Bischoff, A. Weigt, H. Miessner, B. Lücke**,** *Energy & Fuels*, **1996**, 10, 520.
4. A. D. Burrows**,** *Science Progress*, **2002**, 85, 199.
5. M. Diéguez, O. Pàmies, A. Ruiz, Y. Díaz, S. Castillón, C. Claver, *Coord. Chem. Rev*., **2004**, 248, 2165.
6. H. M. Lee, C.-C, Lee, P.-Y. Cheng, *Current Org. Chem*., **2007**, 11, 1491.
7. M. Sauthier, P. Zinck, A. Mortreux, *C. R. Chimie*, **2010**, 13, 304.
8. A. Bader, E. Lindner, *Coord. Chem. Rev*., **1991**, 108, 27.
9. C. S. Slone, D. A. Weiberger, C. A. Mirkin, *Prog. Inorg. Chem*., **1999**, 48, 233.
10. P. Braunstein, F. Naud, *Angew. Chem. Int. Ed*., **2001**, 40, 680.
11. J. C. Jeffrey, T. B. Rauchfuss, *Inorg. Chem*., **1979**, 18, 2658.
12. P. Braunstein, D. Matt, F. Mathey, D. Thavard, *J. Chem. Res*., **1978**, 232, 3041 (S) (M).
13. M. Bassetti, *Eur. J. Inorg. Chem*., **2006**, 4473.
14. P. Braunstein, M. Knorr, C. Stern, *Coord. Chem. Rev*., **1998**, 178-180, 903.
15. N. Lugan, F. Laurent, G. Lavigne, T. P. Newcomb, E. W. Liimatta, J. J. Bonnet, *J. Am. Chem. Soc*., **1990**, 112, 8607.
16. N. Lungan, F. Laurent, G. Lavigne, T. P. Newcomb, E. W. Liimatta, J. J. Bonnet, *Organometallics*, **1992**, 11, 1351.
17. I. Bertini, P. Dapporto, G. Fallani, L. Sacconi, *Inorg. Chem*., **1971**, 10, 1703.
18. E. W. Abel, K. Kite, P. S. Perkins, *Polyhedron*., **1986**, 5, 1459.
19. E. W. Abel, K. Kite, P. S. Perkins, *Polyhedron*., **1987**, 6, 549.
20. R. Jaouhari, P. G. Edwards, *Recl. Trav. Chim. Pays-Bas*., **1988**, 107, 511.
21. C. Vaccher, A. Mortreux, F. Petit, J. P. Picavet, H. Sliwa, N. W. Murrall, A. J. Welch, *Inorg. Chem*., **1984**, 23, 3613.
22. M. C. Bonnet, B. Stitou, I. Tkatchenko, *J. Organomet. Chem*., **1985**, 279, C1.
23. P. Braunstein, F. Naud, S. J. Retting, *New J. Chem*., **2001**, 25, 32.
24. K. G. Orrell, A. G. Osborne, V. Sick, M. W. Da Silva, *Polyhedron*., **1995**, 14, 2797.
25. E. W. Abel, J. C. Dormer, D. Ellis, K. G. Orrell, V. Sick, M. B. Hursthouse, M. A. Mawid, *J. Chem. Soc., Dalton Trans*., **1992**. 1073.
26. A. Gelling, K. G. Orrell, A. G. Osborne, V. Sick, *J. Chem. Soc., Daton Trans*., **1996**. 3371.

27. A. Gelling, D. R. Noble, K. G. Orrell, A. G. Osborne, V. Sick, *J. Chem. Soc., Dalton Trans*., **1996**, 3065.
28. S. E. Bouaoud, P. Braunstein, D. Grandjean, D. Matt, D. Nobel, *J. Chem. Soc. Chem. Commun*., **1987**, 488.
29. H. Werner, A. Hampp, B. Windmüller, *J. Organomet. Chem*., **1992**, 435, 169.
30. N. W. Alcock. A. W. W. Platt, P. Pringle, *J. Chem. Soc., Dalton Trans*., **1987**. 2273.
31. J. Andrieu, B. R. Steele, C. G. Screttas, C. J. Cardin, J. Fornies, *Organometallics*, **1998**, 17, 839.
32. J. I. Dulebohn, S. C. Haefner, K. A. Berglund, K. R. Dumbar, *Chem. Mater*., **1992**, 4, 506.
33. R. W. Wegman, A. G. Abatjoglou, A. M. Harrison, *J. Chem. Soc. Chem. Commun*., **1987**, 1891.
34. P. Jutzi, U. Siemeling, *J. Organomet. Chem*., **1995**, 500, 175.
35. M. Draganjac, C. J. Ruffing, T. B. Rauchfuss, *Organometallics*., **1985**, 4, 1909.
36. J. Amerasekera, T. B. Rauchfuss, *Inorg. Chem*., **1989**, 28, 3875.
37. J. andrieu, P. Braunstein, A. Tiripicchio, F. Ugozzoli, *Inorg. Chem*., **1996**, 35, 5975.
38. C. S. Slone, C. A. Mirkin, G. P. A. Yap, I. A. Guzei, A. L. Rheingold, *J. Am . Chem Soc*., **1997**, 119, 10743.
39. A. M. Allgerier, C. A. Mirkinm, *Angew. Chem. Int. Ed*., **1998**, 37, 894.
40. D. A. Weinberger, T. B. Higgins, C. A. Mirkin, L. M. Liable-Sands, A. L. Rheingold, *Angew. Chem. Int. Ed*., **1999**, 38, 2565.
41. E. Ocando-Mavarez, M. Rosales, N. Silva, *Heteroatom Chem*., **1998**, 9(2), 253.
42. S. Hietkamp, D. J. Stufkens, K. Vrieze, *J. Organomet. Chem*., **1976**, 122, 419.
43. S. Hietkamp, D. J. Stufkens, K. Vrieze, *J. organomet. Chem*., **1977**, 134, 95.
44. L. P. Barthel-Rosa, K. Maitra, J. H. Nelson, *Inorg. Chem*., **1998**, 37, 633.
45. P. Alvarez, E. Lastra, J. Gimeno, J. A. Sordo, J. Gomez, L. R. Falvello, M. Bassetti, *Organometallics*., **2004**, 23, 2956.
46. I. Hyder, M. Jimenéz-Tenorio, M. C. Puerta, P. Valerga, *Dalton Trans*., **2007**. 3000.
47. J. R. Ascenso. A. R. Dias, P. T. Gomes, C. C. Roñao, I. Tkatchenko, A. Revillon, Q. T. Pham, *Macromolecules*., **1996**, 29, 4172.
48. D. Gareau, C. Sui-Seng, L. F. Groux, F. Brisse, D. Zargarian, *Organometallics*., **2005**, 24, 4003.
49. A. Thapper, E. Sparr, B. F. G. Johnson, J. Lewis, P. R. Raithby, E. Nordlander, *Inorg. Chem. Commun*., **2004**, 7, 443.

50. H.-L. Ji, J. H. Nelson, A. De Cian, Fischer, J. y L. Solujic´, E. B. Milosavljevic´, *Organometallics*, **1992**, 11, 401.
51. L. P. Barthel-Rosa, K. Maitra, J. Fisher, J. H. Nelson, *Organometallics*, **1997**, 16, 1714.
52. P. Alvarez, E. Lastra, J. Gimeno, M. Bassetti, L. R. Falvello, *J. Am. Chem. Soc*., **2003**, 125, 2386.
53. M. A. Esteruelas, A. I. González, A. M. López, E. Oñate, *Organometallics*, **2004**, 23, 4858.
54. M. Bassetti, P. Alvarez, J. Gimeno, E. Lastra, *Organometallics*, **2004**, 23, 5127.
55. J. Díez, M. P. Gamasa, J. Gimeno, E. Lastra, A. Villar, *Organometallics*, **2005**, 24, 1410.
56. J. Díez, M. P. Gamasa, E. Lastra, A. Villar, E. Pérez-Carreño, *Organometallics*, **2007**, 26, 5315.
57. M. Bernechea, J. R. Berenguer, E. Lalinde, J. Torroba, *Organometallics*, **2009**, 28, 312.
58. B. R. James, R. H. Morris, K. J. Reimer, *Can. J. Chem*., **1977**, 55, 2353.
59. V. R. Landaeta, M. Peruzzini, V. Herrera, C. Bianchini, A. Sánchez-Delgado, A. E. Goeta, F. Zanobini, *J. Organometal. Chem*., **2006**, 691, 1039.
60. **P. E. Garrou.** Chem. Rev : s.n., 1981, Vol. 81. 229.
61. L. P. Barther-Rosam V. J. Catalano, K. Maitra, J. H. Nelson, *Organometallics*., **1996**, 15, 3924.
62. G. Martín, E. Ocando-Mavarez, A. Osorio, M. Laya, M. Canestrari, *Hetereatom Chem*., **1992**, 3, 395.
63. E. Ocando-Mavarez, G. Martín, A. Andrade, *Heteroatom Chem*., **1997**, 8, 97.
64. R. F. W. Bader, *Atomos in molecules: A quantum theory*, Oxford University press, New York, **1990**.
65. R. J. Gillespie, P. L. A. Popelier, *Chemical bonding and molecular geometry: From Lewis to electron densities*, Oxford University press, **2001**.
66. $DMol^3$ is available as part of Material Studio. Accelrys Inc. San Diego. USA. **2010**.
67. B. Delley, *J. Chem. Phys*., **1990**, 92, 508.
68. B. Delley, *J. Chem. Phys*., **2000**, 113, 7756.
69. J. P. Perdew, Y. Wang, *Phys. Rev*., **1992**, B 45, 13244.

70. H. Jonsson, G. Mills, K. W. Jacobsen, B. J. Berne, G. Ciccotti, D. F. Coker, *Classical and Quantum Dynamics in Condensed Phase Simulations*, World Scientific, Singapore, **1998**, 385.
71. G. Henkelman, H. Jónsson, *J. Chem. Phys*., **2000**, 113, 9978.
72. Y. Mizuhata, T. Sasamori, N. Tokitoh, *Chem. Rev*., **2009**, 109, 3479
73. W. P. Neumann, *Chem. Rev*., **1991**, 91, 311.
74. W. P. Leung, K. W. Kan, K. H. Chong, *Coord.Chem. Rev*., **2007**, 251, 2253.
75. J. Barrau, G. Rima, *Chem. Rev*., **1998**, 178-180, 593.
76. W. W. Schoeller, A. Sundermann, M. Reiher, A. Harrington, *Eur. J. Inorg. Chem*., **1999**, 1155.
77. P. Jutzi, S. Keitemeyer, B. Neumann, H.-G. Stammler, *Organometallics*, **1999**, 18, 4778.
78. R. S. Foley, Y. Zhou, G. P. A. Yap, D. R. Richeson, *Inorg. Chem*., **2000**, 39, 924.
79. Y. Ding, H. W. Roesky, M. Noltemeyer, H.G.Schmidt, P. P. P. Power, *Organometallics*., **2001**, 20, 1190.
80. P. Jutzi, S. Keitemeyer, B. Neumann, A. Stammler, H.-G. Stammler. *Organimetallics*., **2001**, 20, 42.
81. A. Akkari, J. J. Bryrne, I. Sour, G. Rima, H. Gornitzka, J. Barrau, *J. Organometallic Chem*., **2001**, 600, 190.
82. Y. Ding, A. Ma, H. W. Roesky, R. Herbst-Irmer, I. Usón, M. Noltemeyer, H.-G. Schmidt, *Organometallics*., **2002**, 21, 5216.
83. K. Izod, W. McFarlene, B. Allen, W. Clegg, R. W. Harrington, *Organometallics*., **2005**, 24. 2157.
84. A. C. Tomasik, N. J. Hill, R. West, *J. Organometal. Chem*., **2009**, 694, 2122.
85. S.-H. Zhang, Ch.-W. So, *Organometallics*., **2011**, 30, 2099.
86. J. Barrau, G. Rima, T. El Amraoui, *Organometallics*., **1998**, 17, 607.
87. S. Yao, C. Wüllen, M. Driess, *Chem. Comm*., **2008**, 2393.
88. N. Bruncks, W. W. du Mont, J. Pickardt, G. Rudolph, *Chem. Ber*., **1981**, 114, 3572.
89. W. W. du Mont, G. Rudolph, *Inorg. Chim. Acta*., **1979**, 35, L341.
90. D. Gau, T. Kato, N. Saffon-Merceron, F. P. Cossío, A. Baceiredo, *J. Am. Chem. Soc*., **2009**, 131, 8762.
91. D. Gau, R. Rodriguez, T. Kato, N. Saffon-Merceron, F. P. Cossío, A. Baceiredo, *Chem. Eur. J*., **2010**, 16, 8255.

92. D. Gau, R. Rodriguez, T. Kato, N. Saffon-Merceron, A. Baceiredo, *J. Am. Chem. Soc*., **2010**, 132, 12841.
93. I. Ganzer, M. Hartmann, G. Frenking, *The Chemistry of Organic Germanium, Tin and Lead Compounds.* New York : Jhon Wiley & Sons, 2002 , Vol. 2, 171.
94. W. W. Schöeller, R. Schneider, *Chem. Ber*., **1997**, 130, 1013.
95. L. Nyulászi, T. Veszprémi, J.Réffy, *J. Phys. Chem*., **1995**, 99, 10142.
96. M. Draeger, J. Escudie, C. Couret, H. Ranaivonjatovo, J. Satge, *Organometallics*., **1988**, 7(4), 1010.
97. K. Izod, W. McFarlane, B. Allen, W. Clegg, R. W. Harrington, *Organometallics*., **2005**, 24(9), 2157.
98. S. Hanessian, T. Focken, R.l Oza, *Organic Letters*., **2010**, 12(14), 3172.
99. W. J. Leigh, F. Lollmahomed, C. R. Harrington, J. M. McDonald, *Organometallics*., **2006**, 25, 5424.
100. U. N. Alexander, K. D. King, W. D. Lawrance, *Phys. Chem. Chem. Phys*., **2003**, 5, 1557.
101. P. A. Rupar, M. C. Jennings, P. J. Ragogna, K. M. Baines, *Organometallics*., **2007**, 26, 4109.
102. K. C. Thimer, S. M. I. Al-Rafia, M. J. Ferguson, R. McDonald, *Chem. Commun*., **2009**, 7119.
103. S. M. Ibrahim Al-Rafia, A. C. Malcolm, S. K. Liew, M. J. Ferguson, E. Rivard, *J. Am. Chem Soc*., **2011**, 133, 777.
104. Z. Guan, W. J. Marshall, *Organometallics*., **2002**, 21, 3580.
105. T. J. Marck, *J. Am. Chem. Soc*., **1971**, 93, 7090.
106. W. Petz, *Chem. Rev*., **1986**, 86, 1019.
107. M. F. Lappert, R. S. Rowe, *Coord. Chem. Rev*., **1990**, 100, 267.
108. P. Jutzim, C. Leue, *Organometallics*., **1994**, 13, 2898.
109. K. E. Litz, K. Henderson, R.W. Gourley, M. M. Banaszak Holl, *Organometallics*., **1995**, 14, 5008.
110. K. E. Litz, J. E. Bender IV, J. W. Kampf, J. W. Banaszak Holl, *Angw. Chem. Int. Ed. Engl*., **1997**, 36, 496.
111. D. Agustin, G. Rima, H. Gornitzka, J. Barrau, *Inorg. Chem*., **2000**, 39, 5492.
112. D. Agustin, G. Rima, H. Gornitzka, J. Barrau, *Eur. J. Inorg. Chem*., 2000, 693.
113. C. Bibal, Stéphane Mazières, H: Gornitzka, C. Couret, *Organometallics*., **2002**, 21, 2940.

114. Z. T. Cygan, J. W. Kampf, M. M. Banaszak Holl, *Inorg. Chem*., 2003, 42, 7219.
115. I. Saur, G. Rima, K. Miqueu, H. Gornitzka, J. Barrau, *J. Organomet. Chem*., **2003**, 672, 77.
116. Y.Usui, S. Hosotani, A. Ogawa, M. Nanjo, K. Mochida, *Organometallics*., **2005**, 24, 4337.
117. O. Kühl, K. Lifson,W. Langel, *Eur. J. Org. Chem*., **2006**, 2336.
118. A. V. Zabula, F. E. Hahn, T. Pape, A. Hepp, *Organometallics*., **2007**, 26, 1972.
119. F. Ullah, O. Kühl, G. Bajor, T. Veszprémi, P. G. Jones, J. Heinike, *Eur. J. Inorg. Chem*., **2009**, 221.
120. C. M. Crudden, D. P. Allen. *Coord. Chem. Rev*., **2004**, 248, 2247.
121. A. C. Filippou, J. G. Winter, G. Kociok-Köhn, I. J. Hinz, *J. Organomet. Chem*., **1997**, 544, 225.
122. A. C. Filippou, J. G. Winter, G. Kociok-Köhn, C. Troll, I. Hinz, *Organometallics*., **1999**, 18, 2649.
123. A. C. Filippou, P. Portius, J. G. Winter, G. Kociok-Köhn, *J. Organomet. Chem*., **2001**, 628, 11.
124. Y. Morino, Y. Nakamura, T. Iijima, *J. Chem. Phys*., **1960**, 32, 643.
125. R. D. Adams, E.Trufan, *Inorg. Chem*., **2010**, 49, 3029.
126. I. Sour, S. García alonso, J. Barrau, *Appl. Organomet. Chem*., **2005**, 19, 414.
127. R. C. Fischer, P. P. Power, *Chem. Rev*., **2010**, 110, 3877.
128. E. Ploshnik, D. Danovisch, P. C. Hiberty, S. Shaik, *J. Chem. Theory Comput*., 2011, 7, 955.
129. Q. Sekiguchi, R. Kinjo, M. Ichinohe, Science., **2004**, 305, 1755.
130. T. Sasamori, K. Hironaka, T. Sugiyama, N. Takagi, S. Nagase, Y. Hosoi, Y. Furukawa, N. Tokitoh, *J. Am. Chem. Soc*., **2008**, 130, 13856.
131. Y. Sugiyama, T. Sasamori, Y. Hosoi, Y. Furukawa, N. Takagi, S. Nagase, N. Tokitoh, *J. Am. Chem. Soc*., **2006**, 128, 1023.
132. G. H. Spikes, P. P. Power. *Chem. Commun*., **2007**, 85.
133. A. D. Phillips, R. J. Wright, M. M. Olmstead, P. P. Power, *J. Am. Chem. Soc*., 2002, 124, 5930.
134. L. Pu, B. Twamley, P. P. Power, *J. Am. Chem. Soc*., **2000**, 122, 3524.
135. D. Danovich, F. Ogliaro, M. Karni, Y. Apeloig, D. Cooper, S. Shaik, *Angew. Chem. Int. Ed*., **2001**, 40, 4023.
136. P.-C. Wu, M.-D. Su, *Organometallics*., **2011**, 30, 3293.

137. D. Gau, T. Kato, N. Saffon-Merceron, A. D. Cózar, F. P. Cossío, A. Baceiredo, *Angew. Chem. Int. Ed*., 2010, Vol. 49. 6589.
138. N. Lühmann, T. Müller, *Angew. Chem. Int. Ed*., **2010**, 49, 2.
139. C. Bibal, S. Mazières, H. Gornitzka, C. Couret, *Angew. Chem. Int. Ed*., **2001**, 40(5), 952.
140. E. Bonnefille, E. Mazières, N. Saffon, C. Couret, *J. Organometal. Chem*., **2009**, 694, 2246.
141. W. Sataka, K. Hirai, H. Tomioka, K. Sakamoto, K. Kira, *J. Am. Chem. Soc*., **2004**, 126, 2696.
142. W. Sataka, K. Hirai, H. Tomioka, K. Sakamoto, M. Kira, *Chem. Commun*., **2008**, 6558.
143. S. M. Stonger, R. S. Grev, *J. Chem. Phys*., **1998**, 108, 5458.
144. H.-Y. Liao, M.-D. Su, S.-Y. Chu, *Inorg.Chem*., **2000**, 39, 3522.
145. H.-Y. Liao, m.-D. Su, S.-Y. Chu, *Chem. Phys. Lett*., **2001**, 341, 122.
146. M.-J. Cheng, H.-M. Cheng, S.-Y. Chu, *J. Phys. Chem. A*., **2006**, 110, 10495.
147. P.-C. Wu, M.-D. Su, *Dalton Trans*., **2011**, 40, 4253.
148. A. Baceiredo, G. Bertrand, G. Sicard, *J. Am. Chem. Soc*., **1985**, 107, 4781.
149. A. Baceiredo, A. Igau, G. Bertrand, M. J. Menu, Y. Dartiguenave, J. J. Bonnet, *J. Am. Chem. Soc*., **1986**, 108, 7868.
150. K. M. Baines, W. G. Stibbs, *Coord. Chem. Rev*., **1995**, 145, 157.
151. J. Vignolle, X. Cattoën, D. Bourissou, *Chem. Rev*., **2009**, 109, 3333.
152. M. Regitz, *Chem. Rev*., **1990**, 90, 191.
153. A. Igau, A. Baceiredo, H. Grützmacher, H. Pritzkow, G. Bertrand, *J. Am. Chem. Soc*., **1989**, 111, 6853.
154. O.Guerret, G. Bertrand, *Acc. Chem. Res*., **1997**, 30, 486.
155. J. E. Jackson, M. S. Platz, *Advances in Carbenes Chemistry*, Ed. U. Brinker, **1994**, Vol. 1.
156. M. Stender, A. D. Phillips, P. P. Power, *Inorg. Chem*., **2001**, 40, 5314.
157. S. Yao, X. Zhang, Y. Xiong, H. Schwarz, M. Driess, *Organometallics*., **2010**, 29, 5353.
158. A. Streitweiser, A. Rajca,R. S. McDowel,R. Glaser, *J. Am. Chem. Soc*., **1987**, 109, 4184.
159. O. Kühl, *Coord. Chem. Rev*., **2004**, 248, 411.
160. M. Asay, C. Jones, M. Driess, *Chem. Rev*., **2011**, 111, 354.

161. W. J. Hehre, L. Radom, P. R. Schleyer, J. A. Pople, *Ab Initio Molecular Orbital Theory*, Wiley, New York, **1986**, 65-88 and references therein.
162. Gaussian 09, Revision A.1, M. J. Frisch, G. W. Trucks, H. B. Schlegel, G. E. Scuseria, M. A. Robb, J. R. Cheeseman, G. Scalmani, V. Barone, B. Mennucci, G. A. Petersson, H. Nakatsuji, M. Caricato, X. Li, H. P. Hratchian, A. F. Izmaylov, J. Bloino, G. Zheng, J. L. Sonnenberg, M. Hada, M. Ehara, K. Toyota, R. Fukuda, J. Hasegawa, M. Ishida, T. Nakajima, Y. Honda, O. Kitao, H. Nakai, T. Vreven, J. A. Montgomery, Jr., J. E. Peralta, F. Ogliaro, M. Bearpark, J. J. Heyd, E. Brothers, K. N. Kudin, V. N. Staroverov, R. Kobayashi, J. Normand, K. Raghavachari, A. Rendell, J. C. Burant, S. S. Iyengar, J. Tomasi, M. Cossi, N. Rega, J. M. Millam, M. Klene, J. E. Knox, J. B. Cross, V. Bakken, C. Adamo, J. Jaramillo, R. Gomperts, R. E. Stratmann, O. Yazyev, A. J. Austin, R. Cammi, C. Pomelli, J. W. Ochterski, R. L. Martin, K. Morokuma, V. G. Zakrzewski, G. A. Voth, P. Salvador, J. J. Dannenberg, S. Dapprich, A. D. Daniels, Ö. Farkas, J. B. Foresman, J. V. Ortiz, J. Cioslowski, and D. J. Fox, Gaussian, Inc., Wallingford CT, 2009.

Résumé

La conception de ligands hybrides devient un secteur d'activité croissante en chimie organométallique. Dans cette thèse, nous avons étudié la chimie de coordination de diallylphosphines et germyléne phosphine-stabilisés. En particulier, les germyléne phosphine-stabilisés ont non seulement été étudiées pour leur potentielle utilisation comme ligand pour complexes de métaux de transition, mais aussi comme un possible outil de synthèse en chimie organique.

Diallylphosphines se comportent comme des ligands bidentées pour stabiliser l'espèces type [Rh(COD){η^3(P,C,C)RP($CH_2CH=CH_2)_2$}][BF_4] [R= $^{i}Pr_2N$, ^{t}Bu and Ph]. Les propriétés hémilabiles des ligands diallylphosphines ont été démontrées par des réactions d'échange de ligands. En solution, un équilibre dynamique généré par l'échange entre les doubles liaisons allyliques a été détectée par RMN à basse température. Également, le déplacement réversible de la double liaison allylique coordonnée en présence d'acétonitrile a été observé. Des calculs théoriques ont été réalisées pour expliquer les résultats expérimentaux pour l'ordre de réactivité de l'élimination de l'acétonitrile sous vide.

Germylènes stabilisés par la coordination d'un ligand phosphine ont été synthétisés et entièrement caractérisés. Des études de réactivité ont montré que les germylènes phosphine-stabilisés ne sont pas réactifs vis a vis des composés insaturés, tels que les alcynes, alcènes et dérivés carbonylés, mais réagissent avec le 2,3-diméthylbutadiène. La réactivité des germylènes phosphine-stabilisés avec des complexes de métaux de transition a été étudiée par réaction avec le complexe dimère [$Rh_2(\mu\text{-}Cl_2)(COD)_2$], démontrant qu'ils sont des ligands utiles avec un grand potentiel en chimie organométallique. Des germynes, composés du germanium analogue aux alcynes, stabilisés par la coordination d'un ligand phosphine ont été synthétisés et entièrement caractérisés. Les germynes synthétisés se réarrangent à température ambiante donnant une phosphaalcène y un germylène N-hétérocyclique stable.

Mots clés: Ligands hybrides, propriétés hémilabiles, chimie de coordination, diallylphosphines, germylènes phosphine-stabilisés, germynes.